The University Of Sheffield.

Regulation of Endogenous Interleukin-36 Activity

Ali Adnan Jaafar

A thesis submitted for the degree of Doctor of Philosophy

June 2019

Department of Infection, Immunity and Cardiovascular disease

University of Sheffield

Summary

IL-36 is a pro-inflammatory cytokine that consists of three agonists IL-36α, IL-36β and IL-36γ and one antagonist, IL-36Ra. In addition to their receptor (IL-36R), IL-36 cytokines require IL-1RAcP as a co-receptor for their signalling. IL-36 cytokines and their receptor are members of the IL-1 family of proteins. IL-36 has been shown to play important roles in activation of NF-κB and MAPK pathways. Activated IL-36 induces expression of inflammatory mediators such as CXCL8 and recruits inflammatory cells such as neutrophils into the site of infection. Uncontrolled signalling of IL-36 cytokines can lead to excessive inflammation and potentially chronic inflammatory diseases such as psoriasis. Previous studies that were used to assess the biological activity of recombinant, fully active IL-36 cytokines have either used exogenous transfected IL-36R or endogenous IL-36R for 24 h. Here in this thesis I used HT-29 cells, which express endogenous IL-36R. They have been stably transfected with an NF-κB reporter gene and cloned. I confirmed by gene editing, that *IL1LR2* is the only gene that encodes IL-36R in HT-29 cells. Our results showed that the EC_{50} values of the active forms of n^5-IL-36β and n^{18}-IL-36γ, which I prepared, and previously prepared n^6-IL-36α in our laboratory was considerably greater than previously had been reported. The duration of the response of the NF-κB reporter gene to n^6-IL-36α and n^5-IL-36β is between 3 and 9 h. Our data also showed that replacing of n^6 amino acid lysine of IL-36α with either glycine or serine leads to increase EC_{50} of the IL-36α protein. Finally, limited in vitro digestion of n^1-IL-36α by chymotrypsin leads to cleavage of n^1-IL-36α in four different sites. Reporter gene data showed that the mixed digested protein has similar activity to n^6-IL-36α.

Proteolytic processing of endogenous IL-36 proteins is still largely unexplored, but an in vitro study showed that specific truncation of their N-termini activates them. Another study showed that serine proteases enzymes derived from neutrophils can cleave pro-IL-36 proteins but not necessarily at the same sites suggested by the previous in vitro study. The last section of this thesis focuses on expression of endogenous IL-36 cytokines at the level of mRNA and protein and my attempts to induce proteolytic processing of endogenous IL-36γ. RT-PCR and RT-qPCR data presented here showed that the expression of IL-36β and IL-36γ mRNAs but not IL-36α is induced in

response to IL-1α, TNF, PMA, flagellin, TNF and PMA or TNF and flagellin in both human epithelial cell lines (HaCaT and A-431). IL-36γ is the most abundant IL-36 mRNA that is regulated by these stimuli. Furthermore, IL-36α was not found to induce expression either of itself or other IL-36 agonists in HaCaT cells. Our research within this thesis shows that the synergistic action of PMA or flagellin with TNF in HaCaT and A-431 or *Staphylococcus aureus* in HaCAT induces endogenous IL-36γ protein. However, processing of endogenous IL-36γ protein was not induced in response to these stimuli. The apoptotic stimuli, cycloheximide and staurosporine but not calcium ionophore induced a mobility change of endogenous IL-36γ suggesting a processing at a site before n^{18} of IL-36γ. The same effect was not seen in primary keratinocytes the significance of this processing has not yet been investigated.

Acknowledgment

I would like to express my special appreciation and thanks Dr. Martin Nicklin for his support, useful discussion and guidance. You have been a tremendous mentor for me. I would like to thank you for encouraging my research and for allowing me to grow as a research scientist. Your advice on research has been priceless.

I would also like to thank (in particular order) my student advisor, professor Jon Sayers, professor Peter Monk for generously providing me A-431 cell line and Dr Luke Green for generously providing *S. aureus*.

Beyond these, my gratitude to all staff of Department of Infection, Immunity and Cardiovascular disease who either directly or indirectly made my time a unique and pleasant experience.

I dedicate this thesis to my wife, Mrs Zinah Majid for her constant support, encouragement and understanding through the hard times. To my daughter Narjis, who never cease to amaze me. My mother and my father who have been my own powerful which was empathised with my desire for a constant learning process and my ambitious vision for a prospective research career. My mother in low, father in low, my sisters and my brother for supporting me spiritually throughout the writing of this thesis and my life in general.

ABBREVIATIONS

ATP	Adenosine triphosphate
ACD	Allergic contact dermatitis
AP-1	Activator protein 1
BMDC	Bone marrow derived dendritic cells
BACF	Bronchoalveolar lavage fluid
CXCL	Chemokine (C-X-C motif) ligand
COPD	Chronic obstructive pulmonary disease
DC	Dendritic cell
DAMPs	Danger-associated molecular patterns
DNA	Deoxyribonucleic acid
DMSO	Dimethyl sulfoxide
DTT	Dithiothreitol
dDC	Dermal dendritic cell
ELISA	Enzyme linked immunosorbent assay
EDTA	Ethylenediaminetetraacetic acid
EC	Epithelial cell
FPLC	Fast Protein Liquid Chromatography
FBS	Foetal bovine serum
GPP	Generalised pustular psoriasis
HSV	Herpes simplex virus
HS	Hidradenitis suppurativa
HSM	High serum medium
IL	Interleukin
IFN	Interferon
IBD	Inflammatory bowel disease
IRAK	Interleukin-1 receptor associated kinase
IKK	IκB kinase
iNOS	Inducible nitric oxide synthase
IκB	Inhibitory NF-κB
JNK	c-Jun N-terminal kinase

KC	Keratinocyte
LC	Langerhans cells
LPS	Lipopolysaccharide
MAPK	Mitogen activated protein kinase
MYD	Myeloid differentiation primary response
MHC	Major Histocompatibility complex
NF-κB	Nuclear factor-κB
NEMO	NF-κB essential modulator
NLR	Nod-like receptor
PCR/qPCR	Polymerase chain reaction/quantitative real time PCR
PAMp	Pathogen associated molecular pattern
pDC	Plasmacytoid DC
PBS	Phosphate-buffered saline
PMA	Phorbol ester
PMSF	Phenylmethylsulfonyl fluoride
RNA/mRNA	Ribonucleic acid/messenger RNA
RT	Reverse transcription
SEMF	Subepithelial myofibroblasts
SD	Standard deviation
SDS	Sodium dodecyl sulphate
SDS-PAGE	SDS-polyacrylamide-gel electrophoresis
TLR	Toll-like receptor
TNF	Tumour necrosis factor
TRAF6	TNF receptor-associated factor 6
Treg cell	Regulatory T cell
UV	Ultraviolet
v/v	Volume to volume ratio (%)
v/w	Volume to weight ratio (%)

Contents

List of Tables

List of figures

Chapter 1 – Introduction

Chapter 2 – Material and methods

Chapter 3 – Results

Chapter 4 – Results

Scientific appendix

Chapter 1
Introduction

1.1 IL-36 receptors and signals

Interleukin-36 (IL-36) is a family of pro-inflammatory cytokine that includes three agonists and one signalling inhibitor. It plays an important role in the innate immunity through activation of NF-κB and MAPK after binding to its receptor (IL-36R) and co-receptor (IL-1RAcP). IL-36 cytokines are expressed mainly by epithelial cells. Keratinocytes are an example of these cells. Only one receptor has been reported and I will refer to it in this work as IL-36R, through the official gene name is *IL1RL2*, which predates the discovery of its function. IL-36 cytokines are members of family of proteins known as the IL-1 family. The enzymatic processing of IL-36 to produce mature active proteins has not been completely studied. Although signalling of IL-36 can organise immune response to pathogens through activation of NF-κB and MAPK to produce chemokines and cytokines thus recruiting of innate immune cells into the site of inflammation, IL-36 signalling is also connected negatively with pathogenic immune responses in the skin. For example, over-activity of IL-36 in mice causes a skin disease similar to pustular psoriasis. In humans, various mutations in the natural antagonist of IL-36, IL-36Ra lead to generalised pustular psoriasis disease. IL-36 also has been shown to regulate immunity in the airway system and the gut against both bacterial and viral infection. The presence of three agonists for IL-36 in humans potentially gives diversity to the immune system to control many of pathogens threats.

The members of IL-36 system, IL-36α, IL-36β, IL-36γ and IL-36Ra are members of the IL-1 family that were principally identified from searching anonymous cDNA data (Dunn et al., 2001). The genes that encode IL-36α, IL-36β, IL-36γ, and IL-36Ra reside in a ~ 87-kb genomic segment on chromosome 2. The *IL1A, IL1B*, and *IL1RN* genes surround them as in shown in figure 1.1 and together constitute the IL-1 cluster that includes the IL-1 family members except IL-18 and IL-33 (Nicklin et al., 2002).

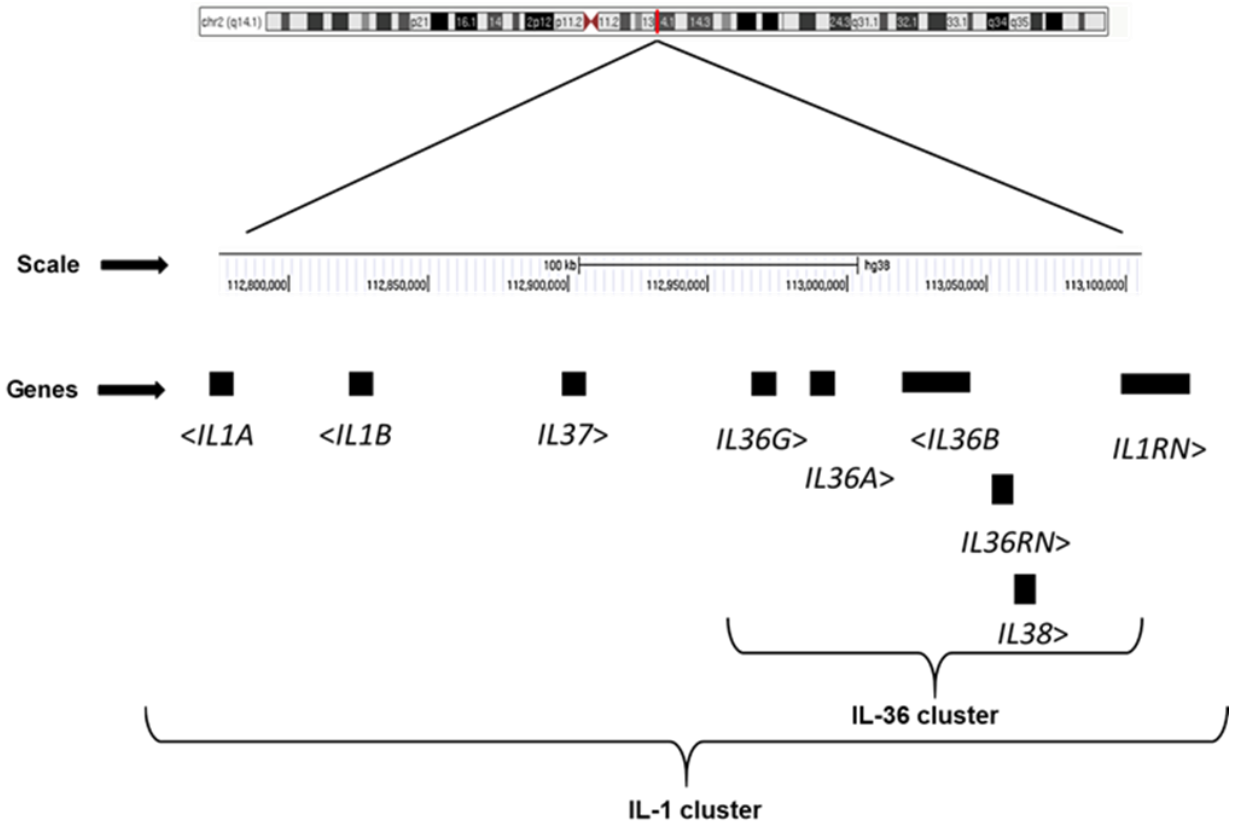

Figure 1.1 Chromosomal locations and orientation (arrows) of genes encoding the human IL-36 agonists. IL36 genes are located on chromosome 2 (Nicklin et al., 2002), and they are surrounded by *IL1* genes. *IL1A* encodes IL-1α, *IL1B* encodes IL-1β, *IL1RN* encodes IL-1Ra, *IL36A* encodes IL-36α, *IL36B* encodes IL-36β, *IL36G* encodes IL-36γ, *IL36RN* encodes IL-36Ra, *IL37* encodes IL-37 and *IL38* encodes IL-38 (Kent et al., 2002).

The IL-1 family contains eleven different ligands, which are IL-1α, IL-1β, IL-1Ra (IL-1 receptor antagonist), IL-18, IL-33, IL-36α, IL-36β, IL-36γ, IL-36Ra, IL-37, and IL-38. IL-1Ra, IL-36Ra, IL-37, and IL-38 are antagonists. All the agonists of the IL-1 family can activate NF-κB and MAPK pathways. IL-1 was one of the first two interleukins that were recognized in 1979 and has consistently been recognised as an important immunomodulator. The observation that the other family members share the same signalling pathways suggests a role in the immune system for all members of the family. IL-1 receptor antagonist (IL-1Ra) and IL-36Ra are also members of IL-1 family but they act as competitive inhibitors of IL-1 and IL-36 by engaging unproductivitly with IL-1R and IL-36R respectively. In this way they prevent agonists from binding to the receptors and prevent IL-1RAcP from interacting with ligand receptor-complex as in figure 1.2 (Arend, 1993, Arend et al., 2008).

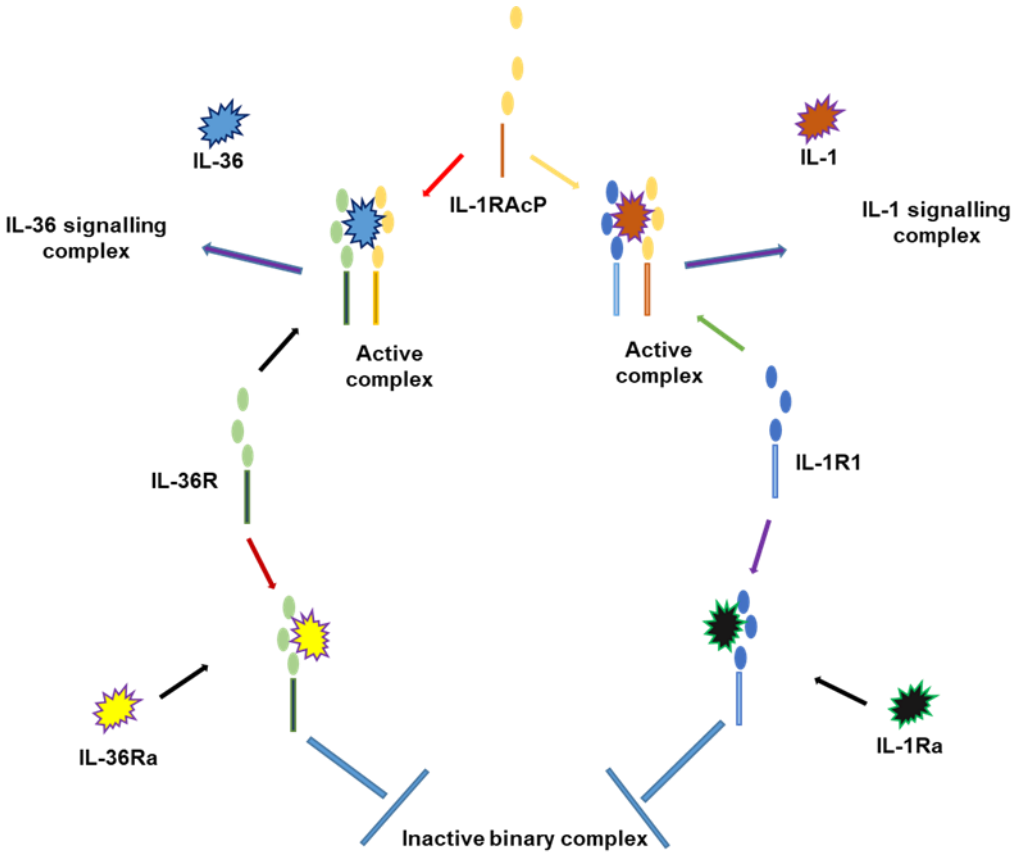

Figure 1.2 The Inhibitory role of IL-36Ra and IL-1Ra. Adapted from Nicklin, 2011. IL-36Ra and IL-1Ra act as natural inhibitors to the IL-36α, IL-36β and IL-36γ and IL-α and IL-1β respectively by binding to their receptors (IL-36R and IL-1R1) to block their signalling pathways.

The signalling pathway of IL-1 cytokines (IL-1α and IL-1β) includes a cascade of intracellular signals. The first step in the activation pathway of IL-1 cytokine is to bind to their cell surface receptor IL-1R1. The binary complex recruits the coreceptor IL-1RAcP (Greenfeder et al., 1995, Wesche et al., 1997, Korherr et al., 1997). Data from EL-4 subline D6/76 cell line, which expresses IL-1R1 but lacks expression of constitutive IL-1RAcP, showed that these cells did not respond to IL-1. However, transfection of these cells with IL-1RAcP cDNA was enough to make cells respond to IL-1 and activate IL1R1 associated kinases (Wesche et al., 1997). This observation suggests that the IL-1RAcP has a role in signalling of IL-1. Equilibrium binding assay data showed that IL-1R1 engages with IL-1β with relatively low affinity, and IL-1RAcP does not engage with IL-1R1 but acts with IL-1R1/IL-1 complex, increasing affinity ~5 fold (Greenfeder et al., 1995). This suggests that IL-1RAcP alone cannot bind directly to IL-1R. This heterotrimer complex recruits the adaptor protein MyD88 as well as IL1R associated kinases 1 and 2 (IRAK1 and IRAK2) and activates them (Huang et al., 1997, Cao et al., 1996a, Croston et al., 1995, Volpe et al., 1997, Muzio et al., 1997, Suzuki et al., 2002). In antigen pull-down experiments, human embryonic kidney cell line (HEK293) transfected to stably express Myc-epitope–tagged IL-1RI and Flag-epitope– tagged IL-1RAcP was used to identify the association of IRAK protein with IL-1R1/IL-1/IL-1RAcP complex. HEK293 cells IL-1R/IL-1RAcP were labelled with (^{35}S) methionine and cysteine, then cells were treated for 3 min with IL-1β. IRAK protein was detected in the cell lysate of treated cells by immunoprecipitation with anti-myc and anti-Flag but not in the untreated cells, while MyD88 association with IL-1R/IL-1RAcP complex was detected after 5 min stimulation with IL-1β (Wesche et al., 1997).

The recruitment of TRAF6 after complex formation between IRAKs and IL-1R1 (IL-R1/IL-1 with IL-1RAcP) complex results in the disassociation of IRAKs to react with recruited TRAF6, which is essential for IL-1 activation of the NF-κB pathway (Cao et al., 1996b).

This suggests a signal transducer role of TRAF6 in IL-1R signalling. Firstly, the formation of a complex between IRAKs and TRAF6 leads to activation of TAK1. Activation of TAK1 results in phosphorylation and activation of IκB kinases (IKKβ) in an IKKγ dependent manner as well as dissociation of nuclear factor-κB inhibitor (IκB) from NF-κB which allows to NF-κB (P50/P65 subunits) to be released and to relocate

into the nucleus (Carmody and Chen, 2007), where NF-κB functions as a sequence specific transcriptional activator incubation of protein extract from a mouse pre-B lymphocyte cell line with recombinant TRAF6 in vitro in the presence and absence of IKKγ showed that endogenous IκBα is phosphorylated in the presence of IKKγ but not in its absence (Deng et al., 2000). This suggests that phosphorylation of IκB to activate the NF-κB pathway is IKKγ dependent. A purified IKK complex extracted from Hela cells was not activated by TRAF6, but activation of IKK was detected in the crude 293 cells protein extract. This suggests that other factors are needed to activate the IKK by TRAF6. Two further factors purified from Hela cell extract TRIKA1 and TRIKA2, TRAF6-regulated factors are required to activate the IKK complex in a TRAF6 dependent manner (Deng et al., 2000). TAK1, TAB1 and TAB2 protein kinases are forms of TRIKA2 (Ninomiya-Tsuji et al., 1999, Takaesu et al., 2000). The NF-κB pathway is not alone in being activated by IL-1 signalling. MAPK is also activated through TAK1, which activates p38, c-Jun N-terminal kinase (JNKs) (Shirakabe et al., 1997). and extracellular signal regulated kinase (ERKs) via MKK3/6, MKK4/7, MEK1/2, respectively, so activating the transcriptional factor AP-1 (Yao et al., 2007, Sanz et al., 2000, Ninomiya-Tsuji et al., 1999).

To activate NF-κB and MAPK, IL-36α, IL-36β and IL-36γ require to interact with IL-36R. They also require IL-1RAcP as a co receptor for their signalling (Towne et al., 2004). This suggests that IL-36 cytokines share the same signalling pathway of IL-1 as shown in figure 1.3 which shows signalling pathways of IL-1 and IL-36. The activation of signalling by IL-36α, IL-3β, IL-36γ through endogenous IL-36R was first reported in a human ovarian tumuor cell line (NCI/ADR-RES) (Towne et al., 2004). A response to IL-36 was shown later in a mouse macrophage cell line RAW264.7 (Ramadas et al., 2011), and in primary human cells, including bronchial epithelial cells (Chustz et al., 2011) articular chondrocytes, synovial fibroblasts (Magne et al., 2006), and colonic sub-epithelial myofibroblasts (Kanda et al., 2015).

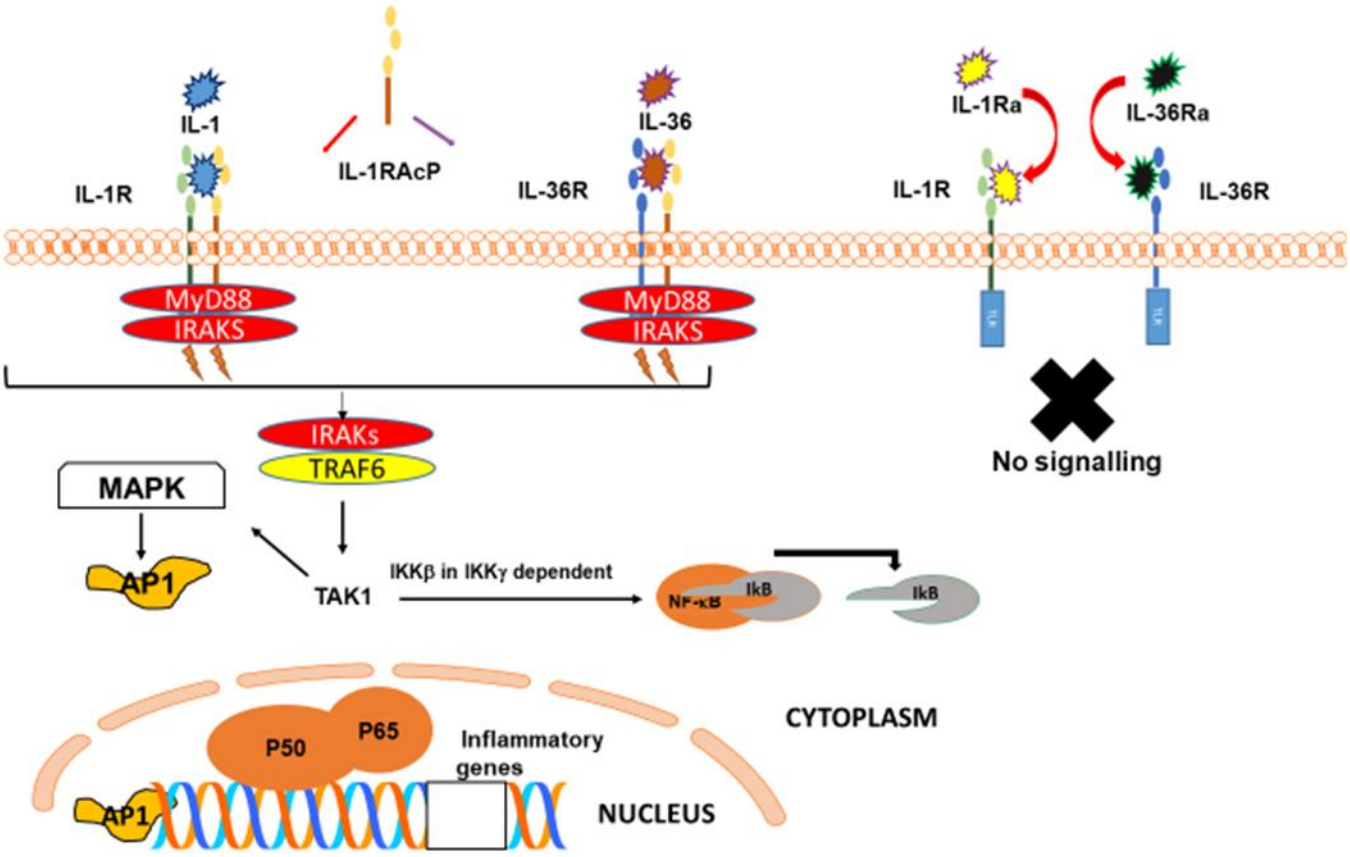

Figure 1.3 Comparison of the signalling pathway of IL-1 and IL-36. After binding of IL-1α and IL-1β or IL-36α, IL-36β and IL-36γ to their receptors, which are IL-1R1 and IL-36R respectively, IL-1RAcP binds to the complex and increase binding affinity between agonists and their receptors. MyD88 and IRAKs (IRAK1 and IRAK2) proteins are recruited. IRAKs then dissociate from the receptor complex to react with TRAF6, which is necessary to activate NF-κB (p50 dependent) and MAPK inflammatory pathways, which result in the production of chemokine and cytokine mRNAs and recruitment of inflammatory cells (Huang et al., 1997, Cao et al., 1996a, Croston et al., 1995, Volpe et al., 1997, Muzio et al., 1997, Suzuki et al., 2002, Cao et al., 1996b, Yao et al., 2007, Sanz et al., 2000).

1.2 Evolution of IL-1 family

Nine IL-1 family genes, in order, *IL1A, IL1B, IL37, IL36A, IL36B, IL36G, IL36RN, IL38* and *IL1RN* are located on human chromosome 2q13 clustered within 430 kb (Nicklin et al., 2002). They encode, respectively, IL-1α, IL-1β, IL-37, IL36α, IL-36β, IL-36γ, IL-36Ra, IL-38 and IL-36Ra. The remaining two superfamily members, *IL18* and *IL33*, are located on chromosome 11 and chromosome 9, respectively. The close proximity of *IL-1* family genes in the IL-1 cluster on chromosome 2 suggests that they probably originated from a common ancestral gene that underwent multiple gene duplications (Dunn et al., 2001).

Predicted IL-1 cluster genes thus appear to have arisen from a common IL-1-like ancestor **(**Rivers-Auty et al., 2018). The IL-1 cluster genes also show conservation of protein structure, which is a 12-strand beta-trefoil (12SBT), similar immunomodulatory activity and a similar mode of receptor binding **(**Rivers-Auty et al., 2018). Rivers-Auty et al. derived a phylogenetic tree of IL-1 superfamily ligand members from 155 predicted protein-coding sequences from across the animal kingdom and showed that an IL-1β homologue gene exists in all vertebrate species. There is also functional evidence for IL-1β activity in cartilaginous fish, hence the function seems to have arisen in the ancestor of sharks and all vertebrates ~425 million years ago. In modern bony fish there has been parallel radiation of IL-1-like genes that do not appear to have direct orthologues in mammals (Zou and Secombes, 2016). *IL1B* consistently maps close to the unrelated gene *SLC20A1* in vertebrate lineages and shares near-neighbours *PSD4* in mammals and reptiles and *OGDH* in birds and reptiles. This functionally irrelevant association between *IL1B* and specific genes supports the identification of the *IL1B* genes in all vertebrates as true homologues (Rivers-Auty et al., 2018). An early form of *IL1B* gene seems to have come to rest near *SLC20A1* before the divergence of all vertebrates.

Rivers-Auty et al. identify an IL-1 family, which includes all nine genes of the IL-1 cluster but suggest that IL-18 and IL-33 proteins are not true homologues of the IL-1 family. These authors suggest that IL-18 and IL-33 may have arisen by convergent evolution that selected similarly folded proteins to fit similar receptors. Rivers-Auty et al. argue that this is not unlikely, on the basis of the simplicity of the 12-strand beta-trefoil protein (12SBTP) structure. They argue that IL-18 and IL-33 lack sequence

similarity with the IL-1 family and point out that there is no evidence of ancestral gene clustering which would provide additional evidence for their diversification from a common IL-1-like gene. They note that there are other 12SBTPs that do not share function with IL-1 and that appear to have arisen independently from all the 12SBTPs. They also argue that IL-18 and IL-33 are no more similar to the IL-1 family than to the fibroblast growth factor (FGF) family, which are also cytokines and 12SBTPs. This would not exclude the possibility that there is a single ancestor for all such 12SBTP cytokines.

12SBTPs have pseudo 3-fold symmetry, so might be expected to have a arisen from triplication of a repetitive three unit structure. To test this, Nicklin et al, 2002 aligned available IL-1-family protein structures with the exon coding content of the IL-1-family genes and showed that almost the entire 12SBT fold of IL-1α, I-1β, IL-1Ra and IL-36Ra is indeed encoded in three conserved exons (which they named CEI, CEII, CEIII), but the boundaries bear no relation to the structural repeat. The boundary between CEI and CEII is in reading frame 3 with respect to CEII and locates to the loop between beta-sheets 3 and 4, while the boundary between CEII and CEIII is in reading frame 1 and locates to within beta-sheet 7. There is no relationship between the pseudo 3-fold repeat within the structure and the position of the exon boundaries. All IL-1 family structures that have been obtained since publication of that paper have confirmed this relationship between protein structure and exon boundaries, suggesting that they have all diverged from a common ancestor, on the grounds that there is no plausible reason for exon structure to converge in this way. Nicklin et al., 2002 predicted the same relationship between gene and protein structure for IL-18, which has been demonstrated experimentally (Tsutsumi et al., 2014). We conclude that this is evidence that IL-18 and the IL-1 family are homologous and that the 12-strand beta-trefoil was not achieved by convergent evolution. However, inspection of the structure of FGF-1 (DiGabriele et al., 1999; Nicklin, unpublished) shows the *same* relationship in FGF-1 between exons CEI, CEII and CEIII and their phase and protein structure. We therefore agree with Rivers-Auty et al. that there are no grounds to discriminate between an IL-1-like or an FGF-like origin for IL-18, but we argue that all of these cytokines are homologues. Like IL-1β, IL-18 has also been identified in sharks and all vertebrate lineages, so seems to have evolved before ~425 million years ago, before the divergence of modern sharks and bony fish.

The IL-33 gene also has intron boundaries between beta-sheets 3 and 4 at the 5'-end of an exon that starts in reading frame 3, and another within beta-sheet 7, in reading frame 1, at the start of the final coding exon. In the case of IL-33, though, the ancestral CEII appears to have been invaded by an extra intron (between beta-sheets 4 and 5). It therefore appears that IL-33 too is derived from a gene with the same structure as IL-1 or FGF. The divergence of IL-33 is difficult to explain. IL-33 seems to be specific to mammals (Rivers-Auty et al., 2018) but is encoded in all complete mammalian genomes. Hence, IL-33 seems to have arisen after ~325 million years ago when the sauropsid lineage (birds, turtles, reptiles), which lack IL-33, diverged from the synapsid lineage (now represented only by the mammals) and the subsequent radiation of mammals, ~160 million years ago. As mentioned before, IL-33 does not have an obvious ancestor because it is highly divergent yet seems to be derived from the same common ancestor as FGFs or the IL-1 family. One possibility that was not explicitly considered by Rivers-Auty et al. is that IL-33 may have been *present* in the common, extinct ancestor of the sauropsids and synapsids but may have been *lost* from the extant sauropsid lineage. This could account for its extreme divergence from all other 12SBT cytokines.

IL-1α and the IL-36 agonists, IL-36α, IL-36β and IL-36γ, and IL-37 and IL-38 also only appear to be present in mammals but presumably evolved during the period between the sauropsid-synapsid split and the radiation of modern mammals, that is, between ~325 and ~160 million years ago. IL-1α appears to be derived from the IL-1 family; the adjacent positions of *IL1A* and *IL1B* in the genome suggest gene duplication, yet IL-1α seems to have diverged rapidly from IL-1β, while retaining its core activity of activating the IL-1 receptor, IL-1R1. Rivers-Auty et al. have reasoned that the divergence has been driven by additional known or suspected non-cytokine functions of IL-1α, that are not shared with IL-1β (Rivers-Auty et al., 2018).

Because IL-1 itself has diverged into various genes in the bony fish, it is not possible to place IL-1Ra with any certainty as distinct from any other IL-1, and it may be present in sharks. Functional IL-1Ra has been identified in bony fish (Zou and Secombes, 2016) and chicken (Gibson et al., 2012).

IL-36α, IL-36β, IL-36γ, IL-37 and IL-38 seem to be present only in the modern marsupial and placental mammals and are most related to IL-1Ra and IL-36Ra. It is

not yet clear what might have driven the evolution of this novel branch of the IL-1 family. Rivers-Auty have identified IL-36Ra orthologues in birds, which lack IL-36 agonists, placing the evolution of IL-36Ra to between the divergence of the land vertebrates from the bony fish ~425 million years ago and the separation of the sauropsid and synapsid lineages ~325 million years ago. Because the IL-36 agonists are absent from modern sauropsids (such as birds), and by implication from the common ancestor of the land vertebrates, yet the IL-36Ra orthologue has been retained, IL-36Ra in birds must have a different function, which is currently unknown, from its role in mammals as an antagonist to IL-36α, IL-36β and IL-36γ. It is worth noting in general that the genomic identification of homologues has only rarely been tested experimentally. Most genes in most sequenced eukaryote species have only been annotated by homology with known genomes.

The apparently paradox of receptor antagonists existing in some species where there is no agonist is repeated in the family of IL-1 receptor-like molecules that seem to lack agonists. Six IL-1 receptors-related genes cluster together in the human genome (Dale & Nicklin, 1999). Rivers-Auty et al. identify physically linked homologues in all vertebrates and have identified orthologues of IL-1R1, IL-18R, IL-18RAcP, IL-36R and IL-33R in all species as well as the co-receptor IL-1RAcP, which seems to have derived from an IL18RAcP-like gene and is now separated from the cluster of receptors. Except in mammals, the orthologues of IL33R and IL-36R seem to exist in the absence of their expected ligand orthologues. It is tempting to speculate that the 'IL-1Ra' and 'IL-36Ra' genes from non-mammals might be agonists, or that divergent IL-1-like proteins might be the missing agonists, or that the apparent orphan receptors have functions that do not involve IL-1-like ligands, as has been suggested by Rivers-Auty et al.

1.3 Processing of IL-36

IL-36α, IL-36β and IL-36γ are produced in many cell types, including bronchial epithelium, keratinocytes (KCs), dendritic cells (DCs), macrophages and glial cells (Towne and Sims, 2012, Blumberg et al., 2007, van de Veerdonk and Netea, 2013).

This suggests a major role of IL-36 cytokines in homoeostasis and inflammation of related tissues. To be biologically active, IL-36 cytokines require proteolytic processing. The biological activity of IL-36α, IL-36β, and IL-36γ increases at least ~3000, ~8000 and ~1500-fold respectively after deletion of a small number of residues from their N-termini (Towne et al., 2011). Recently, neutrophil granule-derived proteases enzymes (cathepsin G, elastase, and proteinase-3) have been shown to be capable of activating IL-36. Cathepsin G and elastase cleaved IL-36α, cathepsin G and proteinase-3 cleaved IL-36β while elastase and proteinase-3 processed IL-36γ in vitro. The biological activity of IL-36β and IL-36γ agonists were increased ~500 fold by these enzymes which are producing by infiltrating neutrophils in tissues where IL-36 is activated, the processed products of the digestion of pro-IL-36 by these enzymes were the active forms identified by deletion analysis of the N-termini of IL-36 agonists by Towne et al., (2011) (Henry et al., 2016). This is illustrated in figure 1.4. Incubation of full- length IL-36γ or SUMO-tagged IL-36γ full-length with recombinant caspase-1 enzyme did not show any cleavage (Ainscough et al., 2017), although IL-1β which is in a same family of IL-36γ, can be activated by caspase-1 proteolytic enzyme (Thornberry et al., 1992). The sequence of the IL-36 protein that surrounds the cleavage sites do not resemble caspase 1 site. Recently, it was shown that IL-36γ produced by barrier tissues could be activated because of cleavage by endogenous cathepsin S, which is cysteine proteases, at the same site that was identified by Towne et al., (2011). Moreover, IL-36γ and cathepsin S expression were actively upregulated in psoriatic inflammation (Ainscough et al., 2017). Expression of CXCL8 (IL-8) in a keratinocytes cell line (HaCaT) was significantly upregulated after incubation of full-length IL-36γ and a cell lysate from adenocarcinoma human alveolar basal epithelial cells (A549 cells), compared with cells incubated only with full length IL-36γ. Expression of CXCL8 in the HaCaT cells, incubated with full length IL-36γ and cell lysate from A549 cells, was reduced when a cysteine protease enzymes inhibitor but not serine proteases enzymes inhibitor was added (Ainscough et al., 2017). This suggests that IL-36γ cleavage site is cysteine proteases dependent.

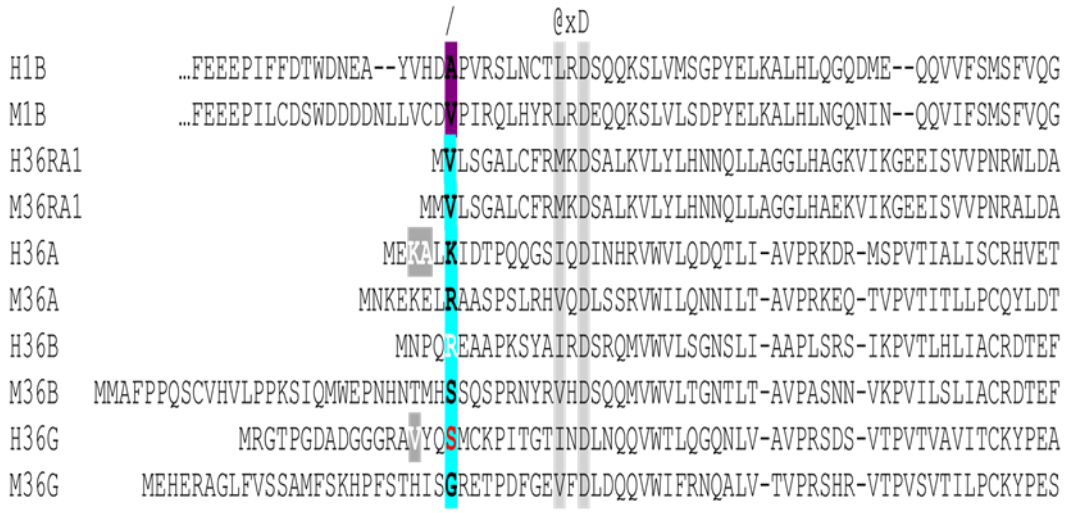

Figure 1.4 Extracted N-terminal of a manual sequence alignment of mouse (M) and human (H) pro-IL-1β proteins, IL-36Ra and the three IL-36 agonists from mouse and human. The aliphatic-X-aspartate motif is highlighted in grey (Towne et al., 2011). Purple highlighting shows the experimental validated N-terminus of the mature IL-1β protein. Cyan highlighting indicates the N-termini for the IL-36 precursors that lead to maximum activation compared with neighbouring processing sites, representing activity enhancement of >1000 over other cleaved products or the unprocessed precursor (Towne et al., 2011). Processing of IL-36 agonists by neutrophil proteases (Henry et al., 2016) created the new N-termini indicated in white characters which are counter-shaded with grey where they do not coincide with the cyan highlighting. Processing of human recombinant pro-IL-36γ by cathepsin S, which is an endogenous enzyme, is indicated in red (Ainscough et al., 2017).

1.4 IL-36 secretion

Because IL-36α, IL-36β and IL-36γ do not have signal sequences, they cannot be secreted directly into the endoplasmic reticulum by the conventional pathway of signal recognition. Another route is needed for their release from cells. The first investigation of the pathway for the release of IL-36α examined secretion from mouse bone marrow derived macrophages (BMDMs) that were transduced with retrovirus to overexpress IL-36α. IL-36α was released from cells after stimulation by liposaccharide (LPS) followed by ATP-induced activation of the $P2X_7$ receptor. IL-1β was also discharged. Although the release of IL-36α does not require caspase-1 activity, caspase-1 may have a role in the lysosome activation through destroying the integrity of the plasma membrane (Martin et al., 2009). This suggests that coupled stimuli required to release of IL-36α protein. Keratinocyte cells incubated with the Toll-like receptor-3 ligand polyinosinic-polycytidylic acid (poly I:C), which is a model of double strand RNA present in some viruses, for 24 h released IL-36γ through activation of caspase-3/7 and death and lysis of the cells (Lian et al., 2012). Inhibition of caspases 1 and 3/7 in KC treated with poly (I:C) led to the blocking of IL-36γ release (Lian et al., 2012). Depending on dose and time, TLR3 activator (poly I:C) has been reported to induce keratinocytes cells to produce and release IL-36γ protein (Rana et al., 2015). These findings suggest that IL-36γ protein may be released in response to viral infection.

1.5 Structure of the skin

Skin represents 1.8 m^2 of the human body, so it can be considered as the largest organ and most exposed surface that is directly in contact with biological, physical and chemical factor (Di Meglio et al., 2011). The structure of the skin consists of three layers, which are epidermis (outer layer), composed mainly of impervious keratinocyte squamae, dermis (inner layer) composed of adipose tissue, coonective tissue, mast cells and vessels, and the basement membrane (separating the epidermis and dermis) (Kanitakis, 2002). Depending on the morphology of keratinocytes and their location, the epidermis can be subdivided into four layers, which are, from outer part inwards, the stratum corneum that is composed of corneocytes (dead

keratinocytes), the stratum granulosum, the stratum spinosum and the stratum basale (James, 2006, Murphy, 1997), as illustrated in the figure 1.5. Mitotically active cells that provide cells to the outer epidermal layers are in the stratum basale (Jones, 1996, Lavker and Sun, 1982). At the stratum basale/stratum spinosum layer, transcription, morphology and functional changes of keratinocytes take place while at the granular/stratum corneum, the nucleus is lost before being it is filled with cables of keratin filaments covered by a γ-glutamyl-ε-lysine cross-linked the cell cornified envelope of proteins (Fuchs, 2008). In the human, stratum basale cells require 30 days to migrate from basale layer to epidermis in order to renew themselves (Chu, 2008).

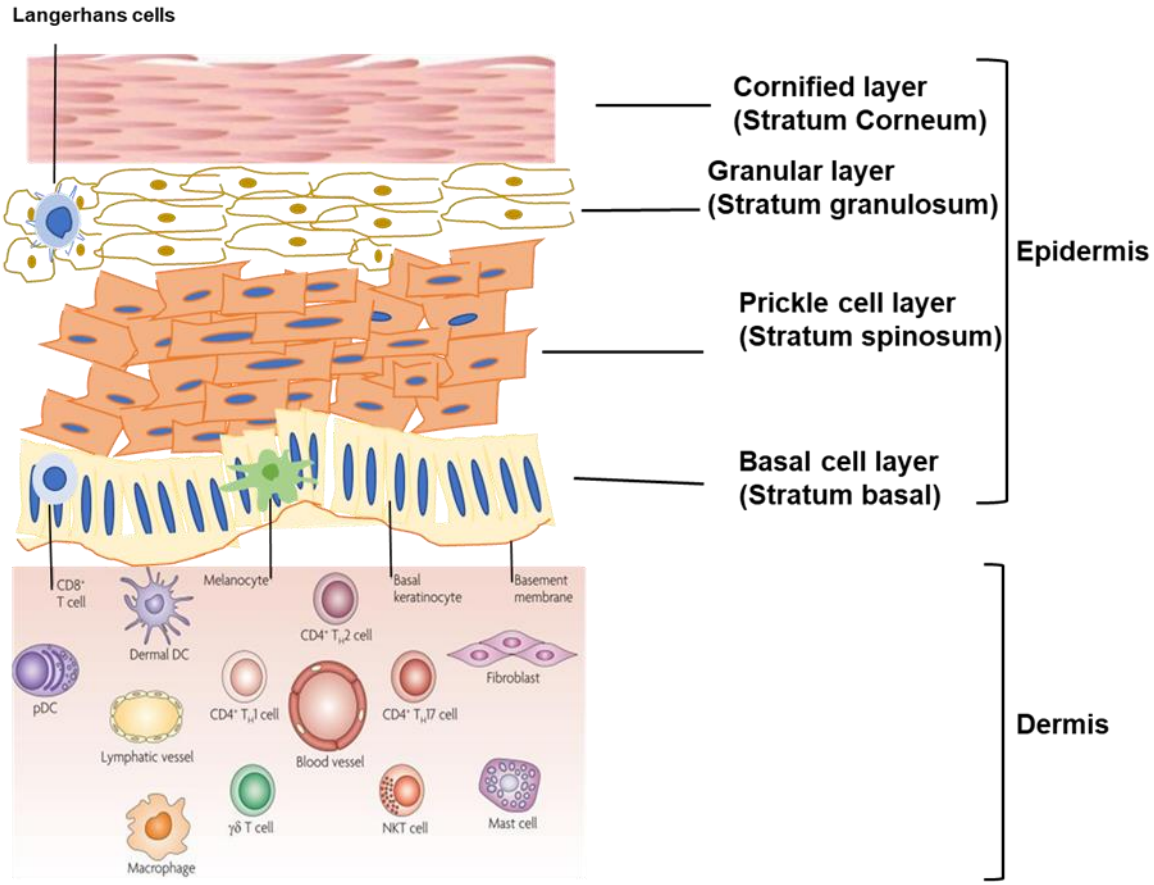

Figure 1.5 Structure of human skin. Human skin consists of three layers, which are the epidermis (upper layer), the basal lamina, the dermis (lower layer) (Kanitakis, 2002). The epidermis can be divided into four layers, which are the stratum corneum that is composed of cornyocytes (dead keratinocytes), the stratum granulosum, the stratum spinosum and the stratum basale. Dividing stem cells reside in the stratum basale (Jones, 1996, Lavker and Sun, 1982). Dermis contains many specialist immune cells such as macrophages, dermal DC, $CD8^+$ T cells, $CD4^+$ T cells and Th17 cells (Nestle et al., 2009).

1.6 Activation of keratinocytes

Keratinocytes can be considered as the first line of defence that protects the skin from external pathogens, and they are the main occupant of the outer layer of the skin (epidermis) (Matejuk, 2018). As in the epithelial cells of the gut, keratinocytes can recognise harmful microorganisms, and induce immune responses to eliminate non-pathogenic and pathogenic organisms (Nestle et al., 2009). Immune cells in eukaryotes can recognise pathogens by using receptors that sense various constituents of pathogens known as pathogen-associated molecular patterns (PAMPs) (Janeway, 1989). Several PAMP receptors, termed Toll-like receptors (TLR) are expressed on keratinocyte cells. TLR1, TLR2, TLR4, TLR5 and TLR6 are expressed on the cell surface while TLR3 and TLR9 are expressed in the endosomes (Lebre et al., 2007). Expression of TLR7 is induced by double strand RNA after 36 h engaging with TLR3, which leads keratinocytes to respond to the TLR7 ligand gardiquimod, a member of the imidazoquinoline antiviral immune response modifier family (Kalali et al., 2008). Expression of TLRs by keratinocytes is expected to be important in triggering an immune response in the skin. When TLRs are activated on human keratinocytes cells, activation results in a predominantly Th1 type immune response, which leads to type 1 IFN production (Miller and Modlin, 2007). In addition to the role of TLRs in sensing external microbes and in inducing cell signalling cascades, a family of intracellular molecules that contain nucleotide-binding domains, and leucine-rich repeats, known as the NLR gene family, can sense PAMPs and endogenous danger-associated molecular patterns (DAMPs), such as, toxins or irritants (Martinon et al., 2009). When these receptors are activated, proinflammatory signalling pathways are activated by inflammasomes, which are large cytoplasmic multiprotein complexes formed by an NLR, the adaptor protein ASC (apoptosis-associated speck-like protein containing a caspase recruitment domain) and pro-caspase 1 (Martinon et al., 2009). Inflammasome assembly results in the processing and activation of pro-IL-1β and pro-IL-18 by caspase 1(Martinon et al., 2009). Inflammasomes in the human keratinocytes can also be activated by UV radiation induced damage (Feldmeyer et al., 2007, Keller et al., 2008). Moreover, proteolytic activation of IL-1β and IL-18 can be induced in keratinocytes by trinitro-chlorobenzene, which induces eczema or contact hypersensitivity (CHS) through activation of

inflammasome formation (Watanabe et al., 2007), as illustrates in the figure 1.6. These findings suggest that expression of all these receptors on the surface of keratinocytes allow these cells to have a role in the skin protection from different chemical or biological challenges.

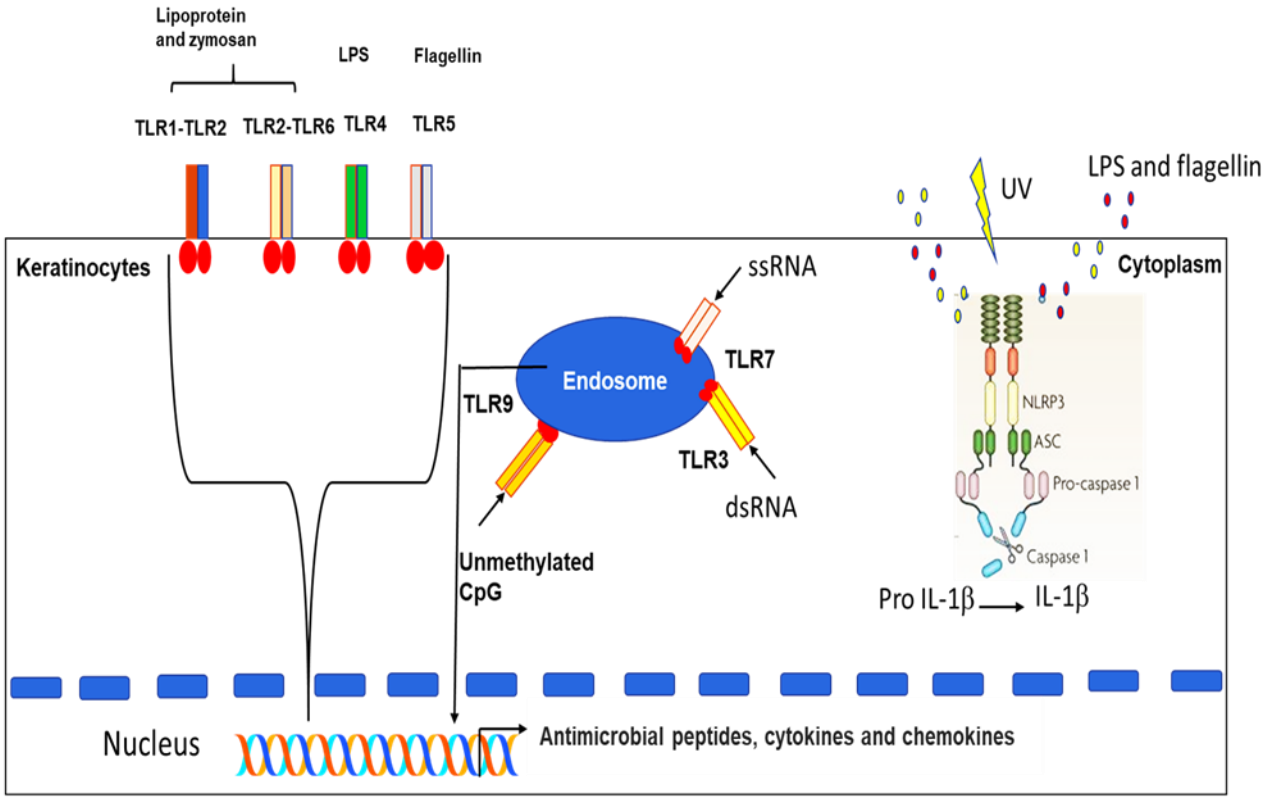

Figure 1.6 The role of keratinocytes in the skin immune responses. Adapted from (Martinon et al., 2009). Keratinocytes use different TLR that are either expressed on their surface (TLR1, TLR2, TLR4, TLR5 and TLR7) or in their endosomes (TLR3, TLR7 and TLR8) to recognise pathogens and activate signalling pathways (Lebre et al., 2007). Keratinocytes also express the NLR protein, which is sensitive to pathogens in the cytoplasm such as lipopolysaccharide (LPS) and flagellin, in addition to UV light, toxins or irritants (Martinon et al., 2009).

1.6.1 Immune mediators from keratinocytes.

The main mechanism of innate defence of eukaryotic cells against pathogen threats is the production of antimicrobial peptides (AMP). AMP are produced on the surface of damaged epithelial cells and protect the host from colonisation by microorganisms through different mechanisms, for example, AMP kill some pathogens directly but also act as signalling molecules to immune cells (Gilliet and Lande, 2008, Lai and Gallo, 2009). In the skin, keratinocytes are the main source of cationic AMPs, which are the β-defensins and the cathelicidins. During infections, T helper 17 (Th-17) cells produce IL-17A and IL-22, which can induce keratinocytes to increase production of AMP (Liang et al., 2006). This suggests that AMP can be regulated indirectly. In the skin with psoriasis, AMPs are upregulated, so they may be responsible for reducing skin infections (Harder et al., 1997). After injury, keratinocytes increase expression of TLR2, LL37 and 25-hydroxyvitamin $D_3$1α hydroxylase. 25-hydroxyvitamin $D_3$1α hydroxylase converts inactive 25-hydroxyvitamin D_3 to active form 1,25-dihydroxyvitamin D_3 (Schauber et al., 2007). The latter can synergistically act with IL-17A to regulate LL37 positively (Peric et al., 2008). Keratinocytes also provide inflammatory cytokines, which have activities at a distance. For instance, keratinocytes can secrete IL-1, IL-6, IL-8, IL-10 and TNF (Albanesi et al., 2005). IL-1α and IL-β mRNAs are produced by human keratinocytes in culture (Kupper et al., 1986). IL-1α activation is negatively regulated by caspase 8 in apoptosis. The active form of IL-1α is produced in epidermal caspase 8 deficient mice (Lee et al., 2009). The skin of genetically modified mice, which are induced to overexpress IL-1α by inserting vector carrying the IL-1α gene, showed inflammatory conditions (Groves et al., 1995). Keratinocytes can mediate activation of immune cells through production of chemokines and the expression of chemokine receptors, which results in the recruitment of various immune cells into skin. During diseases, for example, activated keratinocytes express chemokines CCL20, CXCL9, CXCL10 and CXCL11 and selectively recruit effector T cells. Moreover, by producing CXCL1 and CXCL8, neutrophils are recruited into the inflamed epidermis of patients with psoriasis (Albanesi et al., 2005). In atopic dermatitis, keratinocytes express high level of thymic stromal lymphopoietin (TSLP) (Soumelis al., 2002). TSLP can activate CD11c (+) dendritic cells (DC) and stimulate these cells to produce Th2 attracting chemokines (CCL17 and CCL20) (Soumelis et al., 2002). These findings illustrate that KCs can

regulate immunity of the skin indirectly through secretion of different inflammatory mediators that recruit various immune cells into site of inflammation, as well as directly through the production of AMP.

1.6.2 Induction of inflammation by keratinocytes in vivo

Analysis of the reaction of the skin with the topical sensitizer poison ivy showed the immunological role of keratinocytes before T cells enter the skin (Griffiths and Nickoloff, 1989). By using fluorescent dye and fluorescent microscopy, it has been shown that mice that are genetically modified to overexpress CD40 ligand in the basal keratinocytes, greater than 90% of Langerhans cells from the epidermis of ear of mice migrated from epidermis toward dermis on challenge with dermatitis. Moreover, spontaneous dermatitis on the face, ears, tail, and/or paws developed because of the overexpression of CD40L in these mice (Mehling et al., 2001). This suggests that LC in epidermis can migrate into lymph nodes.

Specific deletion of IKKβ in the epidermis of mice led to the development of a severe inflammatory skin disease as a result of TNF mediated and $\alpha\beta$ T cell independent inflammatory response that begins in the skin of mice soon after birth (Pasparakis et al., 2002). Skin samples from human psoriatic plaques show elevation of signal transducing molecule STAT3 in KC where it is mainly in nuclei. KC from transgenic mice with constitutive expression of STAT3 show human psoriatic plaque like disease in the mice after 2 weeks of birth. This suggests a role for STAT3 signals in human psoriatic plaques (Sano et al., 2005).

1.7. Langerhans cells in the epidermis

Dendritic cells (DC) in skin are classified according to their location as well as their phenotypes. For example, Langerhans cells occupy the epidermis while dermal DCs (dDC) are found in dermis (Nestle et al., 2009). A specific feature of LC is the Birbeck granule, which is formed around of langerin (CD207). Human LC express the lipid-antigen presenting MHC I-like molecule CD1a (Romani et al., 2006). In vitro studies showed that the non peptide antigen of *M. leprae* was presented to human

effector T cells by freshly isolated LCs in a CD1a-restricted and langerin-dependent manner (Hunger et al., 2004). Allogenic CD4+ and CD8+ were primed more efficiently by epidermal LCs than dermal CD14+ DCs (Klechevsky et al., 2008). This suggests that LCs have a role in the adaptive immune regulation. Additional types of LCs can be recognised in the epidermis of patients with inflammatory diseases. For example., inflammatory dendritic cells (CD1a(+)/CD206(++)) population, which can be recognised by expression of CD206 on their surface, and Langerhans cells (CD1a(+++)/CD206(-)) population were detected in the epidermal cell suspensions from psoriasis and atopic dermatitis (Wollenberg et al., 2002).

1.7.1 Immune cells in the dermis

Dermal DCs (dDC) emigrate rapidly to the lymph nodes and occupy microanatomical areas in the paracortex of lymph nodes (Kissenpfennig et al., 2005). Data from normal mice treated with 2,4-dinitrofluorobenzene (DNFB), which is hapten, showed that LC and dDC migrate to lymph node in a ratio of 1:10, but only dDC are responsible for the activation of T cells proliferation (Fukunaga et al., 2008). Again, suggests that DC are involved in adaptive immunity. Data from mice that were infected with herpes simplex virus (HSV) showed that langerin positive (CD207+) CD 103 (+) dermal subset DC can process and present HSV to $CD8^+$ T cells but LC and classical dDC cannot (Bedoui et al., 2009). Self-DNA coupled with LL-37 induces human plasmacytoid dendritic cells (pDC) in culture to produce IFNα through TLR9 (Lande et al., 2007). Flow cytometry data showed that in healthy human skin CD14 (+) dDCs express TLR2, TLR4, CD206 and CD209 on their surface while CD1a+ dDCs express only TLR4. Moreover, CD83 which is a marker of maturation, is expressed at a high level on CD1a+ dDC surface and, and at low level on CD14 (+) dDCs (Angel et al., 2007). In atopic dermatitis (AD), CCL17 and CCL18 protein were produced by CD11c1 myeloid DCs while CCL22 seemed to be produced by plasmacytoid (pDC) (Guttman-Yassky et al., 2007). CCL22 seemed to be produced by plasmacytoid (pDC) (Guttman-Yassky et al., 2007). $CD11c^+$ DCs, which are known as TIP DCs, are found to produce inducible nitric oxide synthase (iNOS) and TNF in psoriasis patient samples (Lowes et al., 2005). In systematic lupus erythematosus (SLE), which is an autoimmune disease, and psoriasis, pDC play a role through producing IFNα (Blanco et al., 2001, Nestle et

al., 2005). Macrophages are mainly immobile immune cells in the dermis but under inflammation condition, macrophages can migrate to lymph node (van Furth et al., 1985). A study that characterised immune cells in the dermis of normal human skin, using monoclonal antibodies showed that dDCs and poorly stimulatory macrophages are marked by CD163 (Zaba et al., 2007).

1.7.2 IL-36 and dendritic cells

Mouse bone marrow derived dendritic cells (BMDCs) carry IL-36R and IL-36 triggers maturation of BMDCs and stimulates the release of pro-inflammatory cytokines including IL-1β, IL-6, IL-12, IL-23 and TNF. The effect is stronger than is seen with IL-1 cytokines (Vigne et al., 2011). Mouse myeloid dendritic cells and monocyte derived DC (MO-DC) also express IL-36R on their cell surface and they respond to IL-36 (Foster et al., 2014). MO-DC treated with IL-36α enhance the proliferation of CD4+ T cells, showing that IL-36 activates DC and controls proliferation of T cells (Foster et al., 2014). These are examples of regulation of both innate and adaptive immunity by IL-36.

Quantitative reverse transcription PCR was used to measure IL-36α expression. IL-36α mRNA was activated in GM-CSF–induced dendritic cells (GM-DCs) in response to the cytoplasmic PAMP Dectin-1/-2 and TLR2 activation by zymosan, TLR4 activation by LPS and imiquimod activation of TLR7 or TLR8, but not in response to ODN D19, which is a TLR9 activator or Poly (I:C), a TLR3 activator. In mouse bone marrow derived Langerhans cells (BM-LC), the data showed that zymosan and imiquimod, but not LPS, ODN D19 and poly (I:C) induced the expression of IL-36α (Hashiguchi et al., 2018). These suggest that different pathogen associated molecular patterns (PAMPs) can regulate expression of IL-36 in different types of DC.

1.8 Function of T cells in the skin

The majority of γδT cells (2 x 10^{10}) are present in normal human skin, which is more than double the number in the circulation (Clark et al., 2006). $CD8^+$ αβ T cells can be found in the normal human epidermis, and the basal suprabasal keratinocyte layer are shared by both epidermal T cells and Langerhans cells (Foster et al., 1990). Downregulation of TNF secretion by macrophages causes deterioration of dermal blood vessels in elderly people. Deterioration of dermal blood leads vessels to reduce a number of infiltrating $CD3^+$ T cells and $CD4^+$ T cells into the skin after secondary challenge with Candin from *Candida albicans* (Agius et al., 2009). Th17 cells play an important role in skin diseases, such as atopic dermatitis and psoriasis (Di Cesare et al., 2008, Di Cesare et al., 2009). Data from the skin of mice infected with yeast and filamentous *C. albicans* showed that Th17 responses are induced by the yeast form. This is dependent on Dectin-1 mediated expression of IL-6 by LC, while the filamentous form induces a Th1 response but not a Th17 response because of the absence of Dectin-1 mediated expression of IL-6 by LC. Moreover, data for *C. albicans* showed that Th1 cells are responsible for protection against systematic infection, while Th17 cells are responsible for protection against cutaneous infection (Kashem et al., 2015). Regulatory T cells (Treg) that comprise 5-10% of all skin resident cells control immune responses in the skin (Clark et al., 2006). The number of memory T cells ($CD4^+Foxp3^–$) and putative nTreg ($CD4^+Foxp3^+$) T cells are increased by tuberculin purified protein derivative (PPD) in the human skin (Vukmanovic-Stejic et al., 2008). When mice were genetically modified to express Kaede protein, which is a photoconvertible fluorescent protein that changes from green to red under UV light conditions, it was seen that both $CD4^+Foxp3^+$ Tregs cells and memory $CD4^+Foxp3^-$ (non Treg) T cells continually migrated from the skin to draining lymph node in the uninfected condition (Tomura et al., 2010). Moreover, $CD4^+Foxp3^+$ Treg cells can regulate not only T cells responses, but also regulate antigen presenting cell functions. For instance, DC co-incubated with Tregs changed their activity from stimulatory into a regulatory function through downregulation of MHCII and B7-2 molecules and inducing or increasing negative the regulatory molecules B7-H3 (CD276) and B7-H4 on the DC surface (Schwarz and Schwarz, 2010). Co-incubation of $CD4^+Foxp3^+$ Treg cells with monocytes results in differentiation of monocytes to alternatively activated

macrophages (AAM), which have strong anti-inflammatory potential involved in immune regulation, tissue remodelling, parasite killing, and tumour promotion, as well as enhanced phagocytic capacity (Tiemessen et al., 2007). Treg cells also reduced the accumulation of neutrophils in a Fas ligand (B16FasL) expressing mouse melanoma cell line, which produces an inflammatory response following subcutaneous injection of mice, through downregulation of neutrophil CXCL1 and CXCL2 (Richards et al., 2010). Treg cells are also found in primary and metastatic human melanoma (Ahmadzadeh et al., 2008). The number of $FOXP3^+$ (Treg) T cells is 50% in the human squamous cell carcinoma of the skin (Clark et al., 2008).

Topical treatment of the human squamous cell carcinoma with imiquimod (TLR7 agonist) leads to reduced function and plethora of Treg and upregulated expression of E-selectin (Clark et al., 2008). Both splenocyte and T cell (CD4+) can produce IL-17, IL-4 and IFN-γ after stimulation with IL-36 (Vigne et al., 2011). The expression level of IL-36R mRNA in naïve T cells is higher than Th1, Th2 or Th17 (Vigne et al., 2012). Naïve T cells in mice predominantly express IL-36R. Proliferation and IL-2 production naïve by activated CD4+ T cell are stimulated by IL-36. Moreover, polarisation of naïve CD4+ T cells into activated Th1 cells is stimulated by synergistic action of IL-36 with IL-12. IL-36β can induce IFNγ in CD4+ T cells (Vigne et al., 2012). Mice with a deletion of *Myd88* in T cells show decreased the skin inflammation after epicutaneous infection of their skin with *S. aureus* compared with wild type (Liu et al., 2017). Mice with knocked out IL-36R, but not mice with knocked out IL-1α, IL-1β, IL-18R1 or IL-33 show a decrease in skin inflammation after epicutaneous infection of their skin with *S aureus*, compared with wild type mice (Liu et al., 2017). This suggests that MYD88 in the T cells is responsible for inflammation, and activation of MYD88 in T cells is mediated by IL-36 signal.

1.9 Expression and association arthritis disease association of IL-36

IL-36 mRNAs are expressed in the synovial tissue of patients with arthritis. Moreover, expression of proinflammatory cytokines and activation of NF-κB and MAPK pathways are induced by IL-36α in human synovial fibroblasts (Derer et al., 2014). This suggests either a direct or an indirect inflammatory role of IL-36.

Expression of IL-36α is notably upregulated in synovial infiltrating plasma cells from patients with psoriatic arthritis and rheumatoid arthritis but not in osteoarthritis synovium, increasing the connection of plasma cells to inflammatory cytokine production (Frey et al., 2013). IL-36α regulates expression of IL-6 and CXCL8 by synovial fibroblasts in vitro via p38 and NF-κB activation (Frey et al., 2013).

1.10 IL-36 and skin diseases

Psoriasis is a type of skin lesion. It is seen in 2% of the North American and European population (Nestle et al., 2009). It was shown that all three IL-36 agonists are upregulated in psoriasis (Debets et al., 2001, Blumberg et al., 2007). IL-36 cytokines are expressed in KC, and disorders of the skin have been shown to be connected with these cytokines. Expression of IL-36γ and IL-36Ra is altered in psoriatic skin (Debets et al., 2001). This suggests that targeting of IL-36 signals could lead to therapy of inflammatory skin diseases. To understand the role of IL-36 in the skin inflammation, genetically modified mice that produce a large quantity of IL-36α in basal cells (basal keratinocytes) were used. The skin of genetically modified mice showed abnormalities distinguished by thickening of the stratum basale and stratum spinosum the skin (acanthosis) and thickening of the outer layer of the skin (hyperkeratosis). Human epidermis skin models treated with IL-36γ that was processed at n^{18} by cathepsin S showed epidermal cornification and changes in stratum corneum (hyperkeratosis) (Ainscough et al., 2017).

Moreover, maintenance of the inflammation characteristic of psoriasis in human skin transplanted into immunodeficient mice was dependent on the presence of the mouse IL-36R gene and could be blocked by an antibody to mouse IL-36R (Blumberg et al., 2007). Again, this suggests an inflammatory role of IL-36R signalling in the skin. IL-36γ mRNA expression was synergistically induced by a combination of IL-17/TNF in primary keratinocytes (Chiricozzi et al., 2011). Psoriasis is connected with expression of Th17 cytokines IL-22, IL-17 and TNF through the upregulation expression of IL-36 cytokines, and the interaction between these cytokines and IL-36 cytokines is

consistent with the role for IL-36 cytokines in skin psoriasis (Carrier et al., 2011). As in figure 1.7. In mouse experimental skin inflammation and human psoriasis, initiation and enhancement of inflammatory responses result from IL-36 stimulation (Debets et al., 2001, Carrier et al., 2011).

The phenotype is similar to psoriasis, and its resolution is blocked by removing one or both copies of the IL-36Ra gene (Blumberg et al., 2010). Treated IL-36α transgenic mice with normal skin with phorbol ester led to develop an inflammatory condition. Inhibition of the IL-12/23p40, IL-23p19 and TNF pathways by giving antagonist to these pathways, which are related to inflammatory conditions, were positively effective in blocking skin lesions in IL-36α overexpressing mice (Blumberg et al., 2010). Absence of IL-36R also rescued mice from expansion of dermal IL-17–producing $\gamma\delta$T cells and psoriasiform dermatitis that results from TLR7 agonist imiquimod treatment (Tortola et al., 2012). IL-17, IL-22 and IL-23 deficient mice were not protected as much as IL-36R$^{-/-}$ (Tortola et al., 2012). These results suggest that in this model, at least, IL-36 indicates inflammation through multiple pathways. mRNAs expression of Th17 associated cytokines and chemokines (IL-1α, IL-1β, IL-6, IL-17C, IL-17F, CXCL2 and S100A9) were downregulated in IL-36$\alpha^{-/-}$ mice after treatment their ears with imiquimod cream compared with wild type mice. (Hashiguchi et al., 2018). This experiment suggests that IL-36α has a specific role in the model that cannot be filled by IL-36β, IL-36γ or any other cytokines.

Generalised pustular psoriasis (GPP) of humans is a severe form of psoriasis. Mutation of amino acid 27 from leucine to proline in IL-36Ra was seen in a Tunisian family with GPP. This leads to the production of a less potent or possibly inactive IL-36Ra protein (Marrakchi et al., 2011). These data clearly show that IL-36 has a pathogenic role in GPP in this family. In cultured keratinocytes, expression of IL-36α, IL-36β and IL-36γ was positively regulated by TNF and IL-17A (Carrier et al., 2011). Blood derived CD14^{+} monocytes/ macrophages express IL-36R on their surface. IL-23 and TNF were produced from psoriasis macrophages in response to IL-36γ stimulation (Bridgewood et al., 2018). IL-36 has been implicated in other skin diseases. In allergic contact dermatitis (ACD), the level of IL-36 cytokines transcripts but not IL-36Ra was increased. Immunohistochemistry data showed that IL-36 cytokines were detectable in the epidermal layer (Mattii et al., 2013). In hidradenitis suppurativa (HS),

which is an inflammatory skin disease that causes tenderness, swelling and redness in parts of skin having apocrine sweat glands, increased expression of IL-36α, IL-36β and IL-36γ at both mRNA and protein levels were observed compared with healthy control (Thomi et al., 2017). IL-36 agonists mRNAs were notably induced in the lesional HS skin in comparison with healthy controls, while in the perilesional HS only IL-36β but not IL-36α or IL-36γ was induced, compared with healthy controls (Hessam et al., 2018). IL-36α and IL-36γ mRNAs are highly expressed in human pustular psoriasis and plaque psoriasis. Moreover, the level of expression in pustular psoriasis is higher than plaque psoriasis (Johnston et al., 2017). IL-36α and IL-36γ mRNAs and IL-36Ra mRNAs were expressed more strongly in psoriasis than compared with lesional atopic dermatitis (Suarez-Farinas et al., 2015). IL-36α protein is upregulated in the KC of mouse skin after 7 days of epicutaneous infection with *S. aureus* compared with wild type mouse. Immunofluorescent labelling showed that protein is localised in the cytoplasm of cells (Liu et al., 2017). The infection was only seen in epicutaneous infection. Deep intradermal cutaneous infection led to induction of IL-1β rather than IL-36.

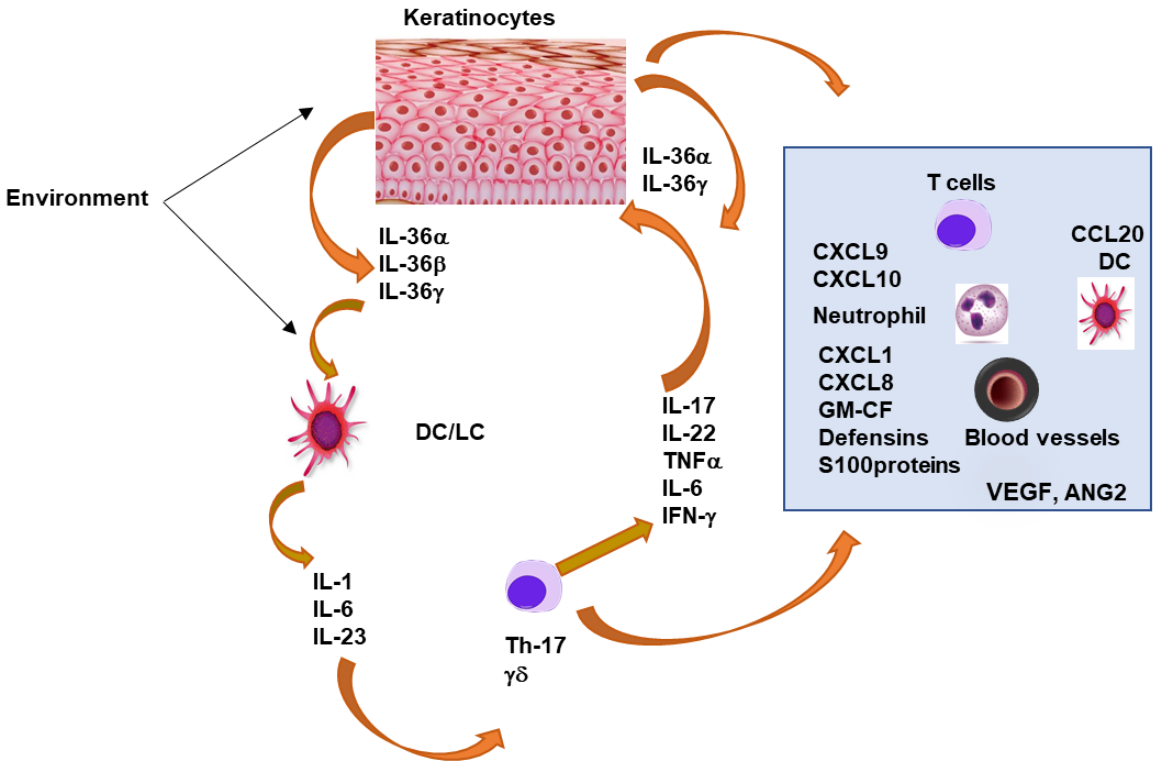

Figure 1.7 Role of IL-36 cytokine in psoriasis and inflammatory skin diseases. Adapted from (Gabay and Towne, 2015). Biological or chemical factors can induce IL-36 in KC and/ or DC or LC. KC and DC/LC in an autocrine or paracrine manner is stimulated by IL-6. Secretion of IL-1, IL-6 and IL-23 by activated DC/LC leads to stimulation of Th17 activity. Activated Th17 can react with KC through secretion of IL-17, IL-22, TNF, IL-6 or INFγ. Psoriasis involves recruitment of DC, T cells and neutrophils, in addition to KC proliferation caused by chemokine and abundant cytokine production.

1.11 Antimicrobial peptide production

IL-36 promotes production of many antimicrobial peptides such as LL-37, lipocalin 2, peptidase inhibitor 3, B-defensin 4, B-defensin103 and S100 calcium binding protein A7 in cultured keratinocytes (Nguyen et al., 2012, Johnston et al., 2011) while, B-defensin DEFB4A (human B-defensin-2 and DEFB104) were secreted in vaginal and endocervical epithelial cells IL-36 stimulation (Winkle et al., 2016). These suggest a regulatory role of IL-36 in immune defence.

1.12 Induction of IL-36 by microorganisms

IL-36α mRNA and protein are up-regulated in proliferating keratinocytes of mouse skin after infection with herpes simplex virus (HSV-1) (Kumar et al., 2000). This suggests a role of IL-36α in response to HSV-1. Activation of human monocytes with LPS led to increased expression of IL-36β mRNA (Smith et al., 2000). This suggests a role of IL-36β against bacterial infection. The level of mRNAs and proteins of IL-36 agonists were increased in immune and epithelial cells because of pathogen associated molecular patterns, microbial agents, and inflammatory mediators. IL-36 activating agents, such as flagellin, zymosan, LPS and *Mycoplasma fermentans* synthetic lipopeptide (FSL-1), induced expression of IL-36 agonists in either skin KC, bronchial epithelial cells or female reproductive tract epithelial cells (a human endocervical and a human vaginal epithelial cells) (Chustz et al., 2011, Winkle et al., 2016). This suggests that IL-36 is involved in the response to many pathogens.

TIGK cells, which are a transformed cell line derived from oral epithelial cells, express an antimicrobial protein peptidoglycan amidase 2 in response to IL-36α or IL-36γ (Scholz et al., 2018a). In the same cells, IL-23p19 and Epstein-Barr Virus-Induced gene 3 (EBI3), which is a viral mimic of the IL-12 family, were expressed in response to IL-36γ (Scholz et al., 2018b). This suggests a regulatory role of IL-36 in the immune response. During oropharyngeal candidiasis in the tongue tissue of wild type mice, IL-36α, IL-36β and IL-36γ mRNAs were induced. Moreover, candidalysin, which is a toxin secreted by hypha of *C. albicans*, is responsible for inducing IL-36α and IL-36γ mRNAs

in the human buccal epithelial cell lines (TR146) through p38-MAPK/c-Fos, NF-kB, and PI3K signalling pathways (Verma et al., 2018). This suggests a role of IL-36 cytokines against fungal infections.

Heat inactivated *Aspergillus fumigatus* hyphae and heat-killed conidia significantly induce expression of IL-36α and IL-36β mRNAs, respectively in human peripheral blood derived monocytes, while expression level of IL-36γ mRNA is significantly induced after 8 h incubation with heat inactivated *Aspergillus fumigatus* hyphae or 24 h incubation with live conidia (Gresnigt et al., 2013). Again, this suggests a role of IL-36 cytokines against fungi. A recent study showed that IL-36α production is increased in mouse macrophage cell lines by *Burkholderia* species (Chiang et al., 2015). A high level of IL-36α has been noticed in the peritoneal cavity, lungs, and blood as a result of caecal ligation and puncture in mice, but responsible cells were not indicated (Tao et al., 2017). However, the source of IL-36α could be macrophages and monocytes because mRNA expression of IL-36α is increased in these cells when they are treated with bacteria or LPS (Smith et al., 2000, Chiang et al., 2015, Nerlich et al., 2015). This suggests that bacteria or bacterial products can induce IL-36α during infection.

Inflammatory mediators also activate expression of IL-36 cytokines (Jensen, 2017). Tumour necrosis factor (TNF), IL-1, IL-17, IL-18 and IL-22, as well as IL-36 cytokines themselves can induce expression of IL-36 mRNAs in synovial fibroblasts, skin keratinocytes, bronchial epithelial cells, colonic myofibroblasts, articular chondrocytes and myeloid cells (Magne et al., 2006, Takahashi et al., 2015, Bachmann et al., 2012). IL-36β is the only IL-36 that can be induced in normal human keratinocytes (NHK) by interferon-gamma (IFN-γ) in vitro (Carrier et al., 2011, Chustz et al., 2011). TNF and IL-1α stimulate expression of IL-36 (α, β and γ) as well as IL-36Ra mRNAs in primary human keratinocytes (Johnston et al., 2011).

1.13 Role of IL-36 in the recruitment of immune cells

Expression of CXCL1 and CXCL2, which are neutrophil chemokines, but not CCL11 and CCL24 (eosinophil chemokines) is regulated positively in the lung of mouse after intratracheal administration of IL-36γ (Ramadas et al., 2011). IL-36 cytokines upregulate the expression of neutrophil chemokines (CXCL8, CCL20 and CXCL1) T lymphocytes attractant chemokines (CCL20, CCL5, CCL2, CCL17, and CCL22), as well as macrophages attractant chemokines (CCL3, CCL4, CCL5, CCL2, CCL17, and CCL22) in human KC (Foster et al., 2014). Intradermal administration of IL-36α in the mouse skin leads to expression of chemokine infiltration of leukocytes and acanthosis of mouse skin (Foster et al., 2014). In primary human synovial fibroblasts (hSFs) and human articular chondrocytes (hACs), expression of CXCL8 and IL-6 is induced in response to IL-36β (Magne et al., 2006). The expression of TNF mRNA and protein is induced in KC after incubation with IL-36α or IL-36β (Carrier et al., 2011). Expression level of IL-6, CXCL1, CXCL2 and CXCL8 mRNAs is significantly increased in primary colonic human colonic subepithelial myofibroblasts in response to IL-36α or IL-36γ (Kanda et al., 2015).

1.14 Function of IL-36 in immune cell activation

$CD4^+$ and $CD8^+$ T cells and $CD19^+$ B lymphocytes in the human blood, as well as CD4+ T lymphocytes in the intestinal lamina express IL-36R on their surface. Moreover, the proliferation of circulating $CD4^+$ T cells is induced significantly and rapidly after incubation with IL-36β compared with untreated cells (Penha et al., 2016). This suggests a role of IL-36β in regulation of T cells. Normal mice treated with antiviral drug imiquimod to induce inflammation showed Th1 related skin disease activation because of in vivo cross communication between DCs and KCs (Tortola et al., 2012). The numbers of T helper 1 and T cytotoxic cell and their activation and IFNγ production can be promoted by IL-36 cytokines. The IFNγ level in the cells isolated from $Il36r^{-/-}$ knocked out mice was less than wild type mice after infection with vaccine strain *Mycobacterium bovis Bacillus Calmette Guerin* (BCG) (Vigne et al., 2012). The phagocytic activity of mouse peritoneal macrophages against *E. coli* was enhanced by pre-treatment with IL-36α (Tao et al., 2017).

1.15 Role of IL-36 in the airway system

During inhalation of about 10,000 litres of air in the day, the lungs of humans are exposed to many potential and toxic environmental pollutants transported by air (Bals and Hiemstra, 2004). The mucosa protects the airways from dangerous factors that enter the lungs by inhalation Bals (Bals and Hiemstra, 2004). Bronchial epithelial cells produce IL-36 in the lungs as a result of several stimuli. Epithelial cells and fibroblasts express IL-36R on their surface and respond to IL-36. Moreover, NF-κB and MAPK pathways can be activated by IL-36γ in primary normal human lung fibroblasts and the neutrophil chemokines CXCL3 and CXCL8 and Th17 chemokine CCL20 (Chustz et al., 2011). CD11c+ alveolar macrophages, which are principle macrophages (95%) in the naïve mouse lung, also express IL-36R on their surface (Ramadas et al., 2012). IL-1α, IL-1β, IL-36γ and TNF expression, as well as neutrophil chemokines (CXCL1 and CXCL2), are upregulated in CD11c+ macrophages from the spleen in response to IL-36α in vitro (Ramadas et al., 2012).

IL-1β, IL-17 and TNF significantly enhanced mRNA expression of IL-36α and IL-36γ, but not IL-36β in primary human bronchial epithelial cells (Chustz et al., 2011). IL-36γ protein was detected immunologically by ELISA in the cell supernatant after stimulation with poly I:C or a combination of poly I:C and IL-17 while IL-36α protein was detected only in the cell lysate (Chustz et al., 2011). Infectious agents, for instance, *Pseudomonas aeruginosa* and rhinovirus induce human primary bronchial epithelial cells (PBECs) to produce IL-36γ. Moreover, IL-36γ induction level was stronger in PBECs from asthmatic donors in response to rhinovirus than normal controls (Bochkov et al., 2010, Vos et al., 2005). Expression of IL-36α and IL-36γ was increased in the lungs of mice that infected with flagellated *Pseudomonas aeruginosa* via intratracheal administration (Aoyagi et al., 2017b). Pulmonary macrophages and alveolar epithelial cells expressed IL-36α and IL-36γ in vitro following *Pseudomonas aeruginosa* challenge. The death rate in mice following bacterial infection in *IL36r* $^{-/-}$ mice and *Il36g*$^{-/-}$ mice but not *Il36a*$^{-/-}$ mice was notably lower than wild type mice. Furthermore, expression of prostaglandin E2 (PGE2) was enhanced by IL-36γ both in vitro and in vivo (Aoyagi et al., 2017b). IL-36γ mRNA was induced in the lungs of mice

challenged with intranasally administrated, purified bacterial flagellin (Kovach et al., 2017)**.** LPS and flagellin but not poly I:C induced IL-36γ mRNA in pulmonary macrophages (Kovach et al., 2017). IL-36γ mRNA was induced in mouse pulmonary macrophages after 6 hr in stimulation with live *S. pneumoniae* or 18 h with killed *S. pneumoniae* bacteria (Kovach et al., 2017). IL-36γ induction was detected in the lungs of mice challenged with *Streptococcus pneumonia* infection, and an active IL-36γ protein was detected mainly in micro particles by flow cytometry. Administration of *S. pneumoniae* to Il36g$^{-/-}$ mice led to increasing mortality compared with wild type because reduced clearance of bacteria in the lungs and increased dissemination of bacteria as well as reduction of the Th1 response and increased polarization of lung macrophages (Kovach et al., 2017).

Administration of *Legionella pneumophila* intratracheally in wild type mice led upregulation of mRNA and protein of both IL-36α and IL-36γ in the lungs of mice compared with untreated animals. The survival rate of mice for 3 weeks in response to challenging with *L. pneumophila* was assessed in *Il36a*$^{-/-}$, *Il36g*$^{-/-}$ and *Il36r*$^{-/-}$ compared with treated wild type. Data showed that the survival rate of *Il36r*$^{-/-}$ was decreased but not in *Il36a*$^{-/-}$ or *Il36g*$^{-/-}$ mice in contrast with wild type. That suggests that IL-36R signalling is important in the airway system (Nanjo et al., 2019). Data from the lungs of IL-36R$^{-/-}$ mice treated with *L. pneumophila* were collected in different time points (2, 4 and 6 days) showed that numbers of bacteria in the lungs of IL-36R$^{-/-}$ mice are higher than controls. Furthermore, the accumulation rate of alveolar leukocytes was decreased in the lung of *Il36r*$^{-/-}$ mice but not polymorph nuclear leukocytes (PMN), monocytes/macrophages Broncho alveolar fluid (BAL) cells in contrast with wild type treated mice. (Nanjo et al., 2019).

Expression of IL-36γ mRNA positively was increased in mice challenged with influenza H1N1 and H5N1 virus. Morbidity and mortality were increased in the *Il36g*$^{-/-}$ mice after challenge them with influenza virus compared with wild type mice (Wein et al., 2018). The expression level of IL-36γ was increased in biopsy samples in recurrent respiratory papilloma's (DeVoti et al., 2008). This suggests the role of IL-36γ in the lungs against viruses. Figure 1.8 illustrates the role of IL-36 in the airway system. The level of IL-36α and IL-36γ mRNAs, but not IL-36β, was increased in the lungs of mice following a pro-inflammatory administration of influenza virus after 2 and 6 days

respectively. The level of IL-36α protein but not IL-36γ protein was elevated in BAL compared with untreated controls (Aoyagi et al., 2017a). In vitro data showed that influenza virus induces alveolar epithelial cells (AECs) to produce IL-36α but not IL-36γ via activation of both caspase-1 and caspase 3/7. Inhibition of caspase-1 suppresses level of IL-36α mRNA and protein while inhibition of caspase 3/7 does not change the level of IL-36α mRNA, but the secretion level is dropped in AECs treated with influenza virus (Aoyagi et al., 2017a). These findings suggest that IL-36α is the important IL-36 product of alveolar epithelial cells.

In healthy mouse lungs, expression of IL-36γ was increased in response to a house dust mite challenge, and in A/J mice challenged with ovalbumin (OVA) (Ramadas et al., 2011, Ramadas et al., 2006). These suggest the role of IL-36γ in allergy. Normal mouse lungs became significantly infiltrated. Mucus production and epithelial cell hypertrophy were seen after a challenge with IL-36γ (Ramadas et al., 2011).

The induction of IL-36γ in macrophages was regulated in two stages during infection with *Mycobacterium tuberculosis*. In the early stage, the expression of IL-36γ results from the triggering of MyD88 dependent pathway. A knockdown of MYD88 in the human monocytes cell line (THP-1) by siRNA reduced expression and secretion of IL-36γ compared with control. Moreover, IL-36γ mRNA failed to be induced in BMDMs derived from MyD88$^{-/-}$ mice compared with wild type mice. This suggests that regulation of IL-36γ is under control MYD88 pathway. TLR2 ligands (FSL1, Pam3CSK4 and HKLM) and TLR4 (LPS derived from *E. coli*) regulate expression of IL-36γ in THP-1 cells. In the later stage, production of IL-36γ is further amplified by endogenous IL-1β and IL-18. Knockdown and blocking of IL-1R and IL-18R in THP-1 challenged with *M. tuberculosis* show reduction in the level of IL-36γ mRNA expression (Ahsan et al., 2016). That suggests that IL-1R and IL-18R signals can induce expression of IL-36.

Uracil uptake and a colony-forming unit (CFU) numbers show elevation of *M. tuberculosis* number in 2 days and 5 days after infection in both *IL36R* and *IL1R1* knockdown macrophages (Ahsan et al., 2016). This suggests that IL-36 as well as IL-1, are required to control *M. tuberculosis*.

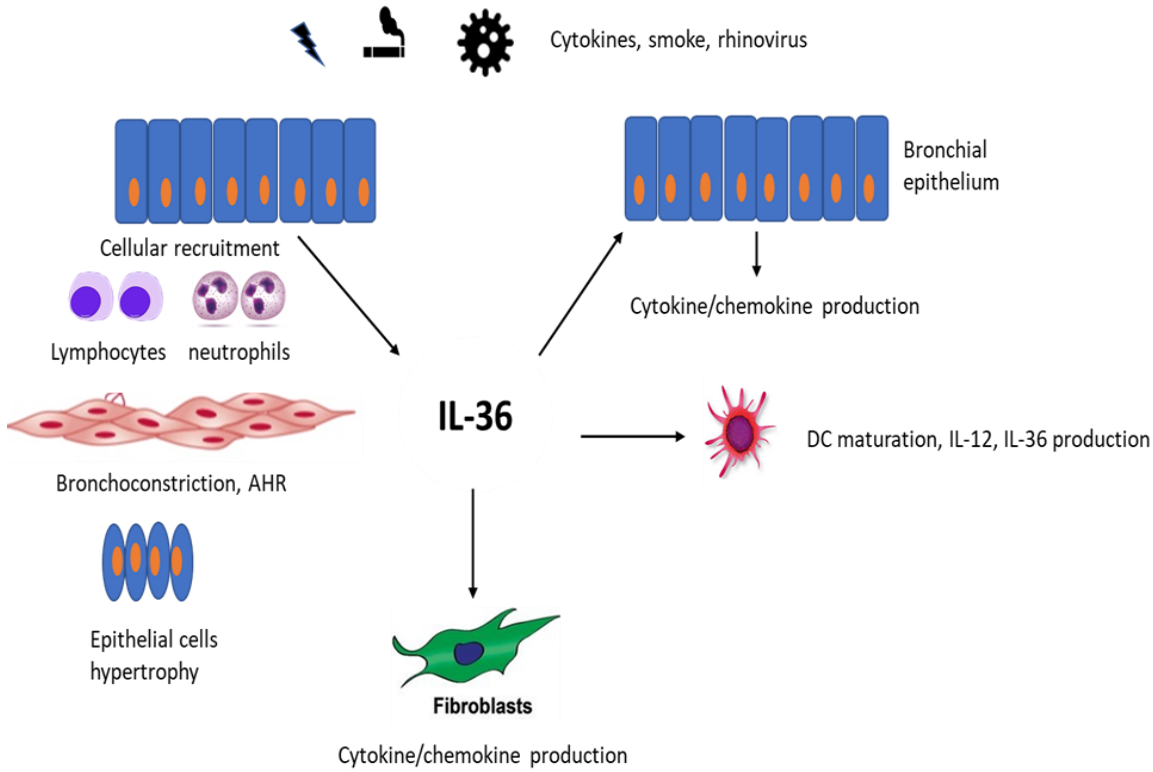

Figure 1.8 The role of IL-36 in the lungs. Adapted from (Gabay and Towne, 2015). In response to cytokines, smoking or viruses, IL-36 cytokines are produced by epithelial cells. IL-36 cytokines stimulate chemokines and production other cytokines, mucus production and immune cells recruitment via acting on the bronchial epithelia cells and adjoining fibroblast and alveolar microphages.

Quantitative-RT-PCR data demonstrated that human lung fibroblasts and bronchial epithelial cells have IL-36R on their surface. Moreover, IL-36α, IL-36β or IL-36γ positively stimulate expression of IL-6 cytokine and CXCL8 chemokine in human lung fibroblasts and bronchial epithelial cells (Zhang et al., 2017). The intratracheal administration of IL-36α or IL-36γ stimulates large number of neutrophils to migrate into bronchoalveolar lavage fluid (BACF) in mice (Ramadas et al., 2011, Ramadas et al., 2012). Accumulation of neutrophil in the airway system has a role in the pathogeneses of pulmonary diseases as well as asthma. These diseases include chronic obstructive pulmonary disease (COPD), cystic fibrosis and acute respiratory distress. Smoking causes COPD, challenging healthy human epithelial cells with cigarette smoke condensate (CSC) increases expression of IL-36 agonists in bronchial epithelial cells (Parsanejad et al., 2008).

1.16 Role of IL-36 in intestine

IL-36α and IL-36γ mRNAs but not IL-36β, are increased in colonic biopsies from patient with inflammatory bowel disease (IBD). Immunohistochemical data analysis indicate that the sources of IL-36α and IL-36γ in the colonic mucosa are T cells, monocytes, and plasma cells (Nishida et al., 2016). This suggests the proinflammatory roles of IL-36α and IL-36γ in bowel inflammatory disease. CXCL1, CXCL2, CXCL3, CXCL6 and CXCL8 chemokines are upregulated by IL-36α and IL-36γ in the human colon carcinoma cell lines (HT-29 and Widr) in vitro (Nishida et al., 2016). The expression of IL-36α and IL-36γ was raised in mucosal biopsies from the colon of patients with IBD with active inflammation in comparison with healthy individual. Also, IL-36β was not detected in the human colon (Scheibe et al., 2017). Again, this suggests that IL-36α and IL-36γ but not IL-36β have pro-inflammatory roles in bowel inflammatory disease. Moreover, secretion of CXCL1, CXCL2, and CXCL8 chemokines was enhanced by IL-36α and IL-36γ in the cultured human colonic subepithelial myofibroblasts (SEMFs). The stimulation of IL-6 and CXC chemokines was affected by a synergistic effect of either IL-36α or IL-36γ and IL-17A or IL-36α or IL-36γ and TNF (Kanda et al., 2015).

At low levels and in combination with IL-1β and IL-17A, IL-36α, IL-36γ was stimulated in the colon of mice that gave dextran sulphate sodium-induced colitis (DSS) (Boutet et al., 2016) Germ free mice treated with DSS failed to express IL-36γ while *Il36r*$^{-/-}$ mice that treated with DSS failed to recover from colitis because of reduction in IL-22 expression specially by colonic neutrophils. Moreover, weakened wound repairing in Il36r$^{-/-}$ mice resulted from a deficiency in neutrophil migration into the wound bed. (Medina-Contreras et al., 2016). This suggests the role of IL-36 signal during intestine repair. Moreover, IL-36 activation related to DSS concentration (Scheibe et al., 2017). Increased colonisation of bacteria and reduced inflammation in the colon of IL-36R$^{-/-}$ mice was seen during infection with *Citrobacter rodentium*. Moreover, IL-36R$^{-/-}$ mice also displayed elevated Th17 but decreased responses of Th1 (Russell et al., 2016). This suggests that signalling through IL-36R also controls intestinal mucosal T cells responses.

IL-22, IL-23 and AMPs levels are reduced in the *Il36r*$^{-/-}$ and *Il36g*$^{-/-}$ mice after treatment with DSS compared with wild type mice, in addition to failing to repair acute intestinal damage (Ngo et al., 2018). This suggests that IL-36R/IL-36γ signals have a role in immune defence and repairing of intestine.

1.17 Summary

To summarise, interleukin-36 belongs to the IL-1 family. IL-36 cytokines comprise of three agonists IL-36α, IL36β, IL-36γ. IL-36 agonists are specific to mammals and present in all mammals, but it is not clear what specific function they have evolved to fill. IL-36Ra is a natural antagonist for these agonists. IL-36 cytokines employ a receptor (IL-36R), and IL-1RAcP for their signaling. IL-36 plays an important role in innate and adaptive immunity through the activation of NF-κB and MAPK pathways.

Keratinocytes play a crucial role in the immune system of skin through expression of various Toll like receptors. Different cytokines can be secreted by KCs in response to biological, chemical or physical threats to skin, but LCs are no less important than KCs in epidermis. LCs with different CD markers are presented in epidermis, and these cells can initiate adaptive immunity through migration into lymph nodes to activate T lymphocytes cells. LCs are absent in dermis. Epithelial cells and particularly KC are the known principle source of IL-36. Expression of IL-36 is connected with skin diseases such as psoriasis, atopic dermatitis and allergic contact dermatitis. After binding to its receptor, IL-36 has a role in regulation of innate immunity through activation chemokines, cytokines and recruitment of immune cells into the site of infection and adaptive immunity through induction of proliferation and differentiation of CD4+ T cells. Th17 cells in skin are usually connected with skin diseases such as psoriasis, atopic dermatitis through the secretion of pro-inflammatory cytokines and the recruitment of immune cells into the site of infection, after being activated by dendritic cells. IL-36, dendritic cells and Th17 orchestrate psoriasis disease in skin. IL-36 agonists are produced as pro-proteins that require proteolytic processing to become active, but this processing is not fully understood, and it is not known how the IL-36 receptor distinguishes so strongly between slightly different molecules. One study showed that truncation of a small number of amino acids from their N-termini can lead to activation of IL-36 agonists. Recently, in vitro studies have shown that IL-36α, IL-36β and IL-36γ can be cleaved by cathepsin G, elastase and proteinase 3, which are derived from neutrophils, but the cleavage sites are not the same as these suggested in the truncation experiments. Another study showed that IL-36γ could be cleaved by cathepsin S at the expected site. We do not yet understand fully the

secretion the processing and site of processing of different IL-36 species in the tissue. These processes are likely to be closely related to the function of IL-36 in health and disease. Controlling the processing of IL-36 has been suggested as a target for therapeutic interaction (Ainscough et al., 2017). Previous studies have shown that inflammatory cytokines and pathogen associated molecular patterns such as LPS, flagellin or poly I:C induce the expression of IL-36 cytokines at the level of mRNAs and proteins. N-terminal clipping is required to generate active IL-36 proteins. I hypothesized that transcription and translation of IL-36 cytokines are activated in response to pro-inflammatory stimuli. To generate active cytokines, the translation products must be proteolytically cleaved. I have investigated ways to optimize the detection and expression of IL-36 mRNAs and their protein products in established cell lines and I have tested a number of different stimuli that might be expected to trigger processing.

Chapter 2
Material and Methods

2. Materials

2.1. Sources of material

Tissue culture plasticware was from Costar. Microfuge tubes were from Starlabs. 384-well plates for qPCR were from Thermo Fisher. Pipette tips were from Starlabs or Thermo Fisher.

All laboratory chemicals were from Thermo Fisher except where noted. High melting agarose was from Thistle. Trizol reagent was from Life Technologies. SYBR green qPCR kits were from Qiagen. Recombinant human (rh) TNFα and full length rhIL-36γ R&D systems antibodies (primary & secondary). rhIL-1α was from Glaxo and all IL36α derivates (rh-n^{6}-IL-36α, rh-n^{6}-K^{6}S- IL-36α, rh-n^{6}-K^{6}G- IL-36α, rh-n^{1}-IL-36 and rh-n^{2}-IL-36Ra) were produced in the laboratory in an *E. coli* host and were finally purified by ion-exchange chromatography before verification by mass spectrometry (M.Nicklin, unpublished). poly I:C and staurosporine were a gift from Dr Liza Parker (Department of Infections, Immunity and Cardiovascular Disease).

Molecular biology reagents (AMV reverse transcriptase, RT buffer, deoxynucleotides, RNase inhibitor, random hexamer and oligo-dT primers) were from Promega. All primer oligonucleotides were from Sigma. Primary human keratinocytes, HaCaT and A-431 cell lines were obtained Professors Sheila McNeil (Department of Materials Science and Engineering) and Peter Monk (Department of Infections, Immunity and Cardiovascular Disease). HT-29, HaCaT and A-431 cell lines were verified by microsatellite analysis in the Genetics Facility of the Medical School. THP-1 cells were from Mr Jon Kilby and were originally from ATCC. A-431, HaCaT, HT-29 and 3T3L1 cell lines were cultured in Dulbecco's modified Eagle medium (DMEM Lonza) which contains of 4 g/l glucose, 2 mM glutamine and was supplemented with 10% fetal bovine serum and 100 u/ml penicillin and streptomycin. THP-1 were grown in RPMI1640. Fetal bovine serum was from Bio sera and Lonza.

2.1.1 General Buffers

DNA Loading Buffer (1X): was 12 mM EDTA (pH 8)/ 10% glycerol/ 0.1% bromophenol blue and was prepared at various concentrations depending on its final use.

2.1.2 Culture media

All bacterial growth media were sterilised by autoclave and were supplemented with sodium ampicillin (100 μg/ml) to sterile media when needed.

2.1.2.1 LB media

LB medium contained 10 g/l bacto tryptone, 5 g/l yeast extract 10 g/l sodium chloride. LB agar contained 15 g bacto agar and was aliquoted at 25 ml per 10 cm petri dish.

2.1.2.2 MDG media

MDG media contained 2 mM $MgSO_4$/, 0.2x trace metals/, 0.5%glucose/, 0.25% sodium aspartate/ 25 mM Na_2HPO_4/ 25 mM KH_2PO_4/ 50 mM NH_4Cl/ 5 mM Na_2SO_4 (Studier, 2005). MDAG-11 medium contained, 2 mM $MgSO_4$, 2.8 mM glucose, 7.5 mM sodium aspartate, 25 mM Na_2HPO_4/ 25 mM KH_2PO_4/ 50 mM NH_4Cl/ 5 mM Na_2SO_4/ 2 mM $MgSO_4$/ 0.5% glycerol/0.05% glucose/ 0.2% lactose/ 10 μM $FeCl_3$/ 4 μM $CaCl_2$/ 2 μM $ZnSO_4$/ 0.4 μM $CoCl_2$/ , 0.4 μM $NiCl_2$/ 0.4 μM Na_2SeO_3/ 0.4 μM boric acid, 1% 18 amino acids, 100 mg sodium ampicillin.

2.1.2.3 ZYM-5052 media

ZYM-5052 contained 1% N-Z-amine, 0.5% yeast extract, 25 mM Na_2HPO_4/ 25 mM KH_2PO_4/ 50 mM NH_4Cl/ 5 mM Na_2SO_4/ 2 mM $MgSO_4$/ 0.5% glycerol/0.05% glucose/ 0.2% lactose/ 10 μM $FeCl_3$/ 4 μM $CaCl_2$/ 2 μM $ZnSO_4$/ 0.4 μM $CoCl_2$/ , 0.4 μM $NiCl_2$/ 0.4 μM Na_2SeO_3/ 0.4 μM boric acid/ ampicillin (Studier, 2005).

2.1.3 General buffers

2.1.3.1 Protein loading buffer (1x)

The final concentration of protein loading buffer was 1% SDS/ 6% glycerol/ 10 mM dithiothreitol (DTT)/ 31 mM Tris/HCl pH 6.8.

All buffers used in Ni-chelate chromatography contained 0.5 M Cl^- and 0.5 M total cation, which include 42 mM $TrisH^+$, various concentrations of imidazole H^+ and the balance was Na^+. The pH of buffers was set with 8 mM Tris base at pH 7.5. 1 M imidazole was adjusted with 0.3 M HCl also give pH 7.5 when diluted. Buffers were named 'B' to indicate the 50 mM Tris/HCl 0.5 M Cl^- composition.

The numeral in the name of buffers indicates the concentration of Imidazole/HCl in pH 7.5 and 'G^+' when included the presence of 10 % glycerol to allow freezing of the solutions without damage to the protein.

For denaturation Ni-chelate chromatography and renaturation of IL-36γ while bound to the column, bound protein was first applied in B20 supplemented with 3 M guanidine hydrochloride. For IL-36γ renaturation, buffers were based on 0.2 M ammonium acetate/ 0.5 M NaCl/ 20 mM imidazole /HCl/ 1 mM DTT which were supplemented with zero, 2 M, 4 M, 6 M or 8 M urea. Elution buffers for IL-36γ contained 0.2 M NH_4 acetate/0.5 M NaCl/ 200 mM imidazole/HCl pH7.5. 1 mM DTT. This was finally supplemented with 8 M urea to elute residual denatured protein.

2.1.3.2 Dialysis buffer

10 mM Tris/ 10 mM Tris HCl/ 10 % glycerol/ 1mM DTT/ pH8.2

2.2.1 Thawing of human cell line stocks

For long-term storage, cells lines used in this study (Table 2.1) were stored in liquid nitrogen in DMEM/25% FBS/ 10% DMSO in 1 ml aliquots of ~ 5 million cells. To begin a culture, the frozen cells were thawed by placing the vial in 15 ml of water at room temperature in a closed tube. The cell suspension was quickly thawed by rocking with gentle mixing. The suspension was pipetted into a new 15 ml conical tube and 9

ml of high serum medium (HSM) was added at first dropwise, to limit the rate of change of osmotic pressure. Cells were recovered by centrifugation at 1000 rpm (80 x *g*) and resuspended in the growth medium. Adherent cells (HaCAT, A-431, HT-29 and 3T3L1) were usually cultivated in a T75 tissue culture flask in 15 ml medium.

Table 2.1. Cell lines used in this study. The cell lines that used in this study are shown. Their origin is described by American type culture collection (ATCC).

Cell line	Information	Passaging
A-431	Human epidermoid carcinoma adherent	1/3 every 3.5 days
HaCaT	Human keratinocyte adherent	1/3 every 5 days
HT-29	Human colon cancer adherent	1/3 every 3.5 days
THP-1	Human monocytic non-adherent	1/3 every 3.5 days
3T3L1	Fibroblast Mouse adherent	1/3 every 3.5 days

2.3.1 Maintenance of cell lines

The adherent cell lines that were used in this study were routinely cultured in T75 bottles in 15 ml DMEM supplemented with 10% foetal bovine serum (FBS) except THP-1, which was grown in RPMI 1640 with 10% FBS. All cells were maintained in a humidified incubator at 37 °C in a 5% CO_2 atmosphere. I refer to DMEM + 10% FBS as high serum medium (HSM). Cells were passaged need from T75 flasks. Adherent cells were washed with 10 ml phosphate buffered saline (PBS) or PBS supplemented with 1 mM EDTA for adherent HaCaT cells (to leach calcium from their strong intercellular contacts) and were incubated for 2-3 minutes at room temperature and drained. After that 1.5 ml of trypsin/ EDTA was used to digest the extracellular matrix during incubation at 37 °C for 15 min for HaCaT and A-431, or 8 min for HT-29 and 3T3L1. For HaCaT, HT-29 and A-431, a 5-ml pipette was used to pull cells quickly up and down to produce a single cell suspension, and this was confirmed on an inverted microscope. HSM 7.5 ml was added with resuspension. HSM, 12 ml was added to

each of three new T75 flasks and 3 ml of the cell suspension was added to each. Cells were thus split 1:3 (area/area) into the appropriate medium.

Primary human keratinocytes were provided for this study through a collaboration with Prof Sheila MacNeil. Keratinocytes were cultured from skin removed for elective surgery procedures and not required for patient's treatment and obtained through a collaboration with the NHS department burns plastics and reconstructive surgery, Sheffield Teaching Hospitals. All patients signed written consent forms for skin not required for the treatment to be used for research purposes. All work related to wound healing in trauma using donated skin is covered by ethical procedure number 15/YH/0177 approved by the regional ethics committee of Sheffield and Humberside.

2.4 Cell stimulation

2.4.1 Stimulation of HaCaT for mRNA analysis

To induce expression of IL-36 mRNAs, confluent HaCaT cells were removed from two T75 flasks as described in section 2.3.1. In stimulation experiments, 16 T25 flasks were used, each was populated with 1 ml (1/9 of a confluent T75 flask, as described) added to 4 ml HSM. Cells were cultured for four days. To turn off growth dependent and serum-stimulated transcription after 4 days, HSM was replaced with low serum media (LSM) (supplemented DMEM containing 0.5% serum). After 18-24 h, cells were treated with inflammatory cytokines or control medium (LSM) in 2.5 ml. Cells were incubated at 37 °C between

4 and 7 h respectively. After stimulation, the cells were washed briefly with 5 ml PBS/EDTA and drained with a pipette. Cells were then lysed in 2 ml of Trizol reagent per flask. The Trizol is proprietary mixtures containing buffer, phenol and guanidine thiocyanate. Cells were gathered by using sterile disposable scrapers. The suspension was divided into two and transferred to 1.5 ml microfuge tubes. Samples were stored at -20 °C for later analysis.

2.4.2. RNA extraction and precipitation from human cell lines

To extract RNA from the samples, RNA was purified from the Trizol extracts by phase separation, achieved by adding 0.2 ml of chloroform per 1 ml of Trizol suspension. Samples were incubated for 3 min at room temperature before centrifugation at 12,000 *x g* for 15 minutes at 4 °C. The aqueous (upper) phase was transferred to another 1.5 ml tube and glycogen (10 μg) (Sigma), as a carrier, was added to aid recovery of RNA pellets. RNA was precipitated by adding 0.5 ml of cold isopropyl alcohol per 1 ml of Trizol suspension. The mixture was then incubated at room temperature for 10 min and then centrifuged at 12,000 x *g* for 10 minutes at 4 °C. The supernatant was discarded, and the pellet containing RNA was washed with at least 1 ml of 75% v/v ethanol per 1 ml of Trizol suspension. Samples were mixed on a vortex mixer and centrifuged 7,500 x *g* for 5 minutes. Finally, ethanol was removed by brief air drying. The RNA/glycogen pellet was resuspended with 50 μl RNAase free water. A NanoDrop spectrophotometer (Thermo Scientific) was used to determine the final A_{260} and A_{280} of the RNA solutions, to assess concentration and purity; the absorbance of 1 μg/ml RNA was assumed to be 0.025 and an A_{260}/A_{280} ratio >1.8 was accepted as sufficiently pure.

2.4.3 Synthesis of cDNA and PCR (RT-PCR)

To make cDNA to be used for RT-PCR after extraction and purification of RNA from HaCaT as described in section 2.3.1. cDNA was synthesised. Reverse transcription to prepare cDNA was primed with a mixture of oligo-dT and random primers. Reactions were mixed in 0.6 ml microfuge tubes on wet ice. A 72 μl of aliquot 5X RT buffer and 36 μl of 10 mM dNTP were mixed with 9 μl of (400 units) RNasin and 14.4 μl of (300 units) of AMV reverse transcriptase before being added quickly to 20 μl oligo-dT (5 μg) and 20 μl random primers (5 μg) which was mixed thoroughly and a 22 μl of aliquot of the mixture was added to 2 μg RNA (20 μl) before being incubated at room temperature for 15 minutes, then 42 °C for 30 minutes. The reaction was stopped by heating at 95 °C for 5 minutes, briefly centrifuged and then placed on wet ice. At this stage, first-strand reverse transcription could be stored at -20 °C. For

non-quantitative polymerase chain reactions (PCR), for detection of mRNA, reactions were prepared by mixing on ice in 1.5 ml microfuge tube, 990 μl water then 275 μl 5x GoTaq Green buffer. Next, 27.5 μl 10mM (50X) dNTPs and 5.5 μl GoTaq (5 u/μl) were added. Six (0.6 ml) tubes were labeled according to the target pairs of primers. Then, 1 μl of each primer pairs (5 μM) (as described below) were added before aliquoting 274 μl of master mix into each primer mix tube. 0.5 μl of the relevant cDNA was added to each tube then 24.5 μl of master mix/primer mixtures was pipetted to each relevant tube. Amplification consisted of 35 cycles as following: initial PCR activation step: 5 m 96 °C, denaturation: 30 s 94 °C, annealing 30s 56°C, extension: 30 s 72 °C, and data acquisition 5 m 72 °C.

2.4.4. RT-PCR primers

Five primers pairs were used successfully to detect mRNA expression of IL-36 agonists, antagonist and receptor in HaCaT and THP-1. They are shown in Table 2.2

Table 2.2. Primer pairs and conditions. RT-PCR primer pairs in this study are indicated along with oligonucleotide sequences, size of the PCR product and conditions of PCR. β–Actin was used a positive control.

Gene	**Oligonucleotide Sequences**	**Size of product (bp)**	cDNA Ref-sequence	Exon number
β–Actin	AGCACTGTGTTGGCGTACAG AGAGCTACGAGCTGCCTGAC	184	NM_001101.4	4 to 5
IL-36α	CGGTTAAACTGTGGCTTGGG AGAACCCACACCCGATGATT	175	NM_014440.2	1 to 2
IL-36β	GGCAGCACCCAAATCCTATG TGCCCTGAATTTCTGCACAG	224	NM_173178.2.	3 to 4
IL-36γ	ATCAGCAAGTGTGGACCCTT TTTAGCTGCAATGTGGGCTG	208	NM_019618.3	3 to 4
IL-36R	CATGTCATCTGCACTTCCCG GTATGGCTTGACACGCGTAG	166	NM_003854.2.	4 to 5
IL36Ra	AAGGACTCGGCATTGAAGGT GGCACCAAGATAGAGCTCCA	243	NM_012275.2	3 to 4

β–Actin= control

2.4.5 Gel Electrophoresis

Gel electrophoresis was used to assess the RT-PCR products. Gels were 8 mm thick x 100 x 100 and contained 2% w/v agarose in 0.2 μg/ml ethidium bromide in 1x TAE (50 mM Tris base) 20 mM acetic acid/ 0.1 $EDTANa_3$) buffer. PCR samples (12.5 μl) were loaded directly. A 100 bp interval ladder was used as a marker. Samples were run at 200 V and visualised by UV-induced fluorescence. DNA bands were visualised by UV-induced fluorescence recorded in a Bio-Rad gel Doc system.

2.4.6 Sequence analysis

Sequence analysis was used to confirm that PCR products represented specific mRNA. Amplified cDNA IL-36α, IL-36β, IL-36γ, IL-36R and IL-36Ra **as described in section (2.4.3)** was run on low melting point agarose gels. Gel slices containing the DNA of interests were cut from gel with a scalpel blade. Gel slices were melted at 99 °C for 5 minutes in a heat block. DNA solutions were diluted by adding 5 μl of sample to 95 μl distilled water. Samples were re-amplified as follows by preparing a master mix which consists of 243 μl of water, 66 μl of 5x Go Taq colourless buffer, 6.6 μl of 10x dNTPs and 1.5 ml of Go Taq. Relevant primer pairs (1 μl of 100 μM) were added to 0.6 μl tube before 48 μl of master mix being added. Relevant diluted PCR product (1 μl) was added to 0.6 ml tube, then 48 μl of master mix/ primer pairs was added. PCR reaction processed for 20 cycles.

2.4.7. Quantification of CXCL8 (IL-8) secretion by HaCaT

To assess CXCL8 secretion in response to inflammatory stimuli, HaCaT cells were seeded onto two 24 well plates. Each well was assumed to be 1.9 cm^2 and cells were plated in 1.0 ml of HSM and were grown to confluence over 4 days. Cells were deprived of serum in 0.5 ml LSM for 18-24 h then treated with NF-κB activator for 7 h. Experiments were done in 5-fold replicates. Supernatants were tested for CXCL8 secretion by ELISA (Peprotech) as described in figure 2.1. Samples were diluted 1/5

and 1/15 and measured in triplicate to get a mean and standard deviation, and a 96-well plate was used to carry out ELISA. Absorbance from each sample was measured and compared to the mean of triplicates of CXCL8 standard curve.

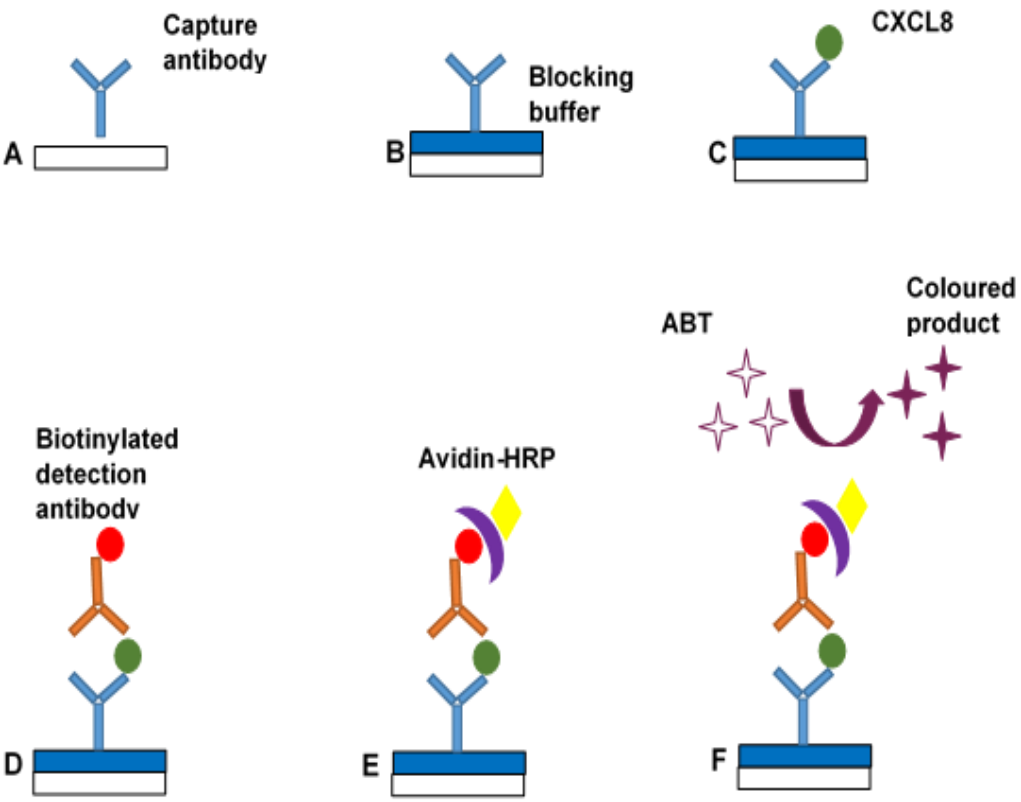

Figure 2.1 CXCL8 ELISA procedure. Plates was washed 4 times with washing buffer between each step to remove unbound protein. **(a)** A 96- well plate ELISA plate was coated with capture antibody 100 μl at 1 μg/ml in 1x PBS overnight. **(b)** To block the well from binding proteins, the plate surface was blocked with a 1% solution of bovine serum albumin (BSA). **(c)** Samples and standards containing IL-8 were loaded to allow the IL-8 to bind to the capture antibody. **(d)** Detection antibody (biotinylated antibody) was added. **(e)** Avidin-horse radish peroxidase (HRP) conjugate was bound to the biotin complex. **(f)** ABTS reagent mix (Sigma) was converted into visible coloured by HRP, whose A_{405} was measured with 5 min intervals for 35 min.

2.4.8 Quantitative PCR (qPCR) of mRNA from cultured cells

To assess the induction level of mRNAs in response to inflammatory stimuli, RT-qPCR was used, RNA was extracted as described in section (2.4.2). The first strand cDNA was synthesized by mixing on the ice 288 μl of 5X RT buffer then 144 μl of 10 mM dNTP mixture. After that 40 μl of (400 units) RNasin and 48 μl of (300 units) of AMV reverse transcriptase were added and 80 μl of oligo-dT primers and 80 μl random primers were added and mixed thoroughly. The mixture (42.5 μl) was added to 5 μg RNA (47.5 μl) and incubated at room temperature for 15 minutes, then 42°C for 30 minutes in a thermocycler block. The reaction was stopped by heating at 95°C for 5 minutes, centrifuging. The samples were held on wet ice. cDNA was stored at -80°C. Real-time PCR was performed with an SYBR Green (Qiagen) method. Amplification was monitored in real time in an Applied Biosystems 7900 Detection System (Applied Biosystems). The amplification consisted of 45 cycles as follows. PCR initial activation step: 15 m 95 °C, denaturation: 15 s 94 °C, annealing: 30 s 58 °C, extension: 30 s 72 °C and Data acquisition: 15 s 64 °C in 10 μl reactions, 100 nM each primer, 1 μl of cDNA. Primers were used as table below.

Table 2. 3 RT-qPCR primer pairs. RT-qPCR primer pairs that were used through the whole of study are illustrated, along with oligonucleotide sequences, size of the PCR product.

Primers name	Oligonucleotide Sequences	Size of product (bp)	RefSeq cDNA	Exon number
IL-36α	TCTACCTGGGCCTGAATGGA AAAGGACTTCACAGGCTCGG	128	NM_014440.2	3 to 4
IL-36β	TGTGCAGAAATTCAGGGCAAG GCCAGGGTAAGAGACTGAC	150	NM_173178.2	4 to 5
IL-36γ	TGGAGGAAGGGCCGTCTATC GTGACTGGGGTCACACTGTC	135	NM_019618.3	2 to 3
IL-36R	CATGTCATCTGCACTTCCCG GTATGGCTTGACACGCGTAG	162	NM_003854.2	4 to5
M2	AGATGAGTATGCCTGCCGTG TCATCCAATCCAAATGCGGC	120	NM_004048.2	3 to 4
H1	AATGACCAGTCAACAGGGGAC GCCTGACCAAGGAAAGCAAAG	136	NM_000194.2	4 to 6
P1	ATACGGGTCCTGGCATCTTG GCCTCCACAATATTCATGCCT	148	NM_021130.4	4 to 5
L1	AATCCAAGAAGGGGCTGTCC GGGTCCAGCGAGAAGGTTTT	140	NM_005157.5	1 to 2

M2= β2 microglobulin, H1= hypoxanthine phosphoribosyltransferase, P1= peptidyl proline isomerase (PPIA), L= ABL kinase (ABL1).

2.4.9. Standard of qPCR2.4.10 A-431 or HaCaT cells stimulation for mRNA analysis

To induce expression of IL-36 mRNAs in HaCAT or A-431 cells, A-431 or HaCaT cells were routinely cultured as described in 2.3.1. Confluent A431 or HaCat cells were resuspended from T75 (75 cm^2) flasks. In stimulation experiments, T25 (25 cm^2) flasks were used. Each was populated with 5 ml from the suspension of A-431 or HaCaT cells and were incubated at 37 °C for four days. To repress growth dependent and serum-stimulated transcription after 4 days, HSM was replaced with LSM. After 18-24 h, inflammatory stimuli were added in 2.5 ml LSM (in addition to the 2.5 ml of LSM that was used as control during comparison with the stimulant. After stimulation, T25 flasks were washed with 5 ml PBS and drained. After draining, cells were scraped off in the 2 ml of Trizol and RNA prepared as described in section 2.4.2.

2.5 Creation of expression constructs for IL-36β and IL-36γ

2.5.1 Preparation of inserts

To prepare insert, the IL-36β (pEXA2-AXn5F8) and the IL-36γ (pEXA2-ATn18F9) were designed by Dr Martin Nicklin and prepared by gene synthesis (Eurofins). Plasmids were digested with *Xho*I and *Acc65*I restriction endonucleases to excise the inserts. Digestion of 5 μg of plasmids with 20 units *Xho*I and 30 units of *Acc65*I was performed at 37 °C for 2 h in 50 μl of their recommended buffer. Gel electrophoresis was used to check digestion progress of 10% of the samples. Digested inserts were recovered from high melting agarose after electrophoresis.

The analytical gel: The gel contained 1% agarose/ 40 mM Tris acetic acid pH 8.3/ 0.1 mM $EDTANa_3$ /0.2 μg/ml ethidium bromide. The samples were supplemented with DNA loading buffer and electrophoresed alongside a DNA ladder at 100 V. The remaining digested samples were loaded into 4 cm x 10 cm 1% high melting agarose gel containing 40 mM Tris acetic acid pH 8.3/0.1 mM $EDTANa_3$/0.2 μg/ml ethidium bromide.

2.5.2 Digestion of pET3a plasmid with restriction enzymes

Plasmids were created by removing a pre-existing insert from a pET-3 derived plasmid that contained convenient restriction sites (Martin Nicklin unpublished). Sticky ends were generated by digesting pET-H3.2 plasmid with *Xho*I and *Acc65*I. This was carried out by digesting pET3 with 20 units of *Xho*I and 30 units of *Acc65*I for 2 h at 37 °C in 50 μl of their recommended buffer. 10% of digested sample was checked by a 1% agarose gel, while nuclease in the remaining digested sample was inactivated with an excess of 0.5 M $EDTAHNa_3$. Proteins were extracted by adding 30 μl of 3 M sodium acetate, 70 μl water and 200 μl phenol/chloroform buffer, vortexing for 20 s. The aqueous phase containing the DNA was transferred into 1.5 ml tube that contained 400 μl 100% ethanol and was incubated at -80 °C for 5 min before centrifuging at 17,000 x *g* for 5 min. The vector was washed with 1 ml of 70% ethanol, dried on heated block at 37 °C for 15 min and dissolved in 10 μl TE.

2.5.3. Ligation

To ligate inserts with pET3a plasmid, DNA fragments were excised from agarose gels and transferred to a 1.5 ml tube. Agarose were dissolved to recover DNA bands by using 4 volume of gel dissolving buffer (Monarch) and incubated samples at 50 °C until the gel slice completely dissolve. Then samples were loaded onto columns before spinning for 1 min. Columns were reinserted into the collection tube and 200 μl of DNA wash buffer was added and spin for 1 min this step were repeated twice. Next, to elute DNA, columns were transferred into a clean 1.5 ml tube and 6 μl of DNA elution buffer were added to the centre of mixture. Each insert DNA was ligated with the vector in a 10 μl ligation reaction in the buffer supplied (Promega) with 0.5 units T4 ligase (Promega) and was incubated overnight at 15 °C.

2.5.4 Transformation of *E. coli* DH5α

pET vectors were constructed to place the open reading frame of the precursors of IL-36β and IL-36γ under control of T7 promoter. The completed pET3 vector plasmids were transferred first into competent *E. coli* DH5α (a non-expressing bacteria strain) by using heat shock. To so this, frozen competent DH5α cells were thawed by using wet ice. Cells were gently mixed and widened pipette tip was used to transfer 100 μl of cells suspension to 1.5 ml tube that contains 10 μl of ligation mixtures and gently mixed. Then, they were incubated on wet ice for 1 h before being shocked by heating at 42 °C for 20 s, and then tubes were quickly returned into wet ice. To recover cells, 200 μl Soc media were added and incubated at 37 °C in a shaker at 225 rpm for 40 min, before being spread cells on LB plate containing 100 μg/ml ampicillin. pET3 (10 ng) was also transformed as a positive control, as well as two negative controls of ligation containing no inserts and no ligase. For each tube, a sample of recovered bacteria (50 μl) was spread on plate. The plates were incubated overnight at 37 °C and checked for colonies the next day.

2.5.5. Screening transformants

To identify pET-IL-36β and pET-IL-36γ transformed clones, sterile pipet tips were used to pick labelled transformed colonies. Colonies were grown in 3 ml of LB media and re-cultured on LB agar plates both containing 10 μg/ml ampicillin. Cultures were incubated overnight at 37 °C with stirring. Gel Elute plasmid miniprep kit (Sigma-Adrich) was used to isolate plasmid DNA. *XhoI* (20 units) and *Acc65I* (30 units) restriction endonucleases were used to screen for the presence of pET-IL-36β or pET-IL-36γ DNA fractions by overnight incubation at 37 °C.

2.5.6. Transformation into *E. coli* BL21 (DE3) cells

E. coli BL21 (DE3) was used to express target proteins because these cells carry a T7 RNA polymerase transgene controlled by a lacUV5 promoter (Studier, 2005). pET3-IL-36β or PET3-IL-36γ plasmids (10 ng) were extracted from DH5α and transformed into BL21 (DE3) as in section 2.5.4. Empty pET3 plasmid was used as a negative control. As with *E. coli* (DH5α), BL21 (DE3) transformation was carried out as in section 2.5.4 except the repression medium (MDG) supplemented with 200 μg/ ml 18 amino acids mixture was used as recovery medium and transformed bacteria were plated on MDAG-11/ amp. MDAG-11 is a super repressive medium that helps to stabilise the pET plasmid within BL21 (DE3) (Studier, 2005).

2.5.7 Growth of transformants in repression media and generation of stock cultures

Colonies of Amp^R BL21 (DE3) containing pET expression plasmids were picked with a sterile loop and cultured in 2 ml MDG + 0.1 mg/ml ampicillin repression medium in capped 10 ml polypropylene tubes, before being incubated at 37 °C on the shaker at 320 rpm. Good oxygenation is needed for repression. To store transformed bacteria at -80 °C, glycerol was added to yield 8% w/v.

2.5.8 Proteins expression by auto-induction

To induce expression of targeted proteins in *E. coli* bacteria BL21 (DE3), a buffered rich medium ZYM-5052 media was used (Studier, 2005). This medium is buffered with phosphate and contains aspartate, glucose, lactose, and glycerol. Expression of T7 RNA polymerase, which is located under control of l*acUV5* is repressed efficiently until the glucose is exhausted or oxygen becomes deficient. When glucose is used up in the medium, bacteria activate on lactose metabolism, but they mainly metabolise glycerol and sodium aspartate as a nutrient and that activates expression of transgene *lac*UV5-T7 RNA polymerase in DE3 (BL21). Activation of *lac*UV5-T7 RNA polymerase leads to subsequent expression of target protein from the T7 promoter in the pET3 expression vector.

2.5.9 Large scale protein expression by auto-induction

For the large-scale expression of targeted proteins, 400 ml of ZYM-5052/amp medium was inoculated with 100 μl of transformed BL21 (DE3) culture stock. Sterile baffled flasks were used. Cultures were incubated at 25 °C in a shaker at 320 rpm after the addition of 100 μl of Anti-Foam 240 (Sigma). After 18 h, growth was monitored continuously by measuring A_{600} every 2 hours to determine the time needed to approach the stationary phase. For A_{600} reading, samples of cultures were diluted to give readings in the range 0.100-0.300. To harvest, the cultures were rapidly chilled by swirling the flasks surrounded by wet ice. Bacteria were harvested by centrifuging at 4 °C in a Beckman J26 centrifuge at (5000 x *g*) for 10 min and were washed by re-suspending in the 400 ml of 42 mM Tris-HCl/8 mM Tris/0.1 M NaCl pH 7.5 (L7.5) which had been chilled to 0 °C, followed by centrifugation for 10 min at 4 °C. The pellet was re-suspended to 20 ml in L7.5 supplemented with 10 % w/v glycerol in a polypropylene tube for storage at -80 °C.

2.5.10 Small scale expression test for target proteins

To test expression of targeted proteins, 1 ml of the 400 ml culture of auto-induced BL21 (DE3) was thawed, and the bacteria were collected by centrifugation for 1 min at 4°C and resuspended in 1 ml cold water to remove glycerol. The suspension was centrifuged again and resuspended in 50 μl of water. Protein loading buffer (50 μl of 2X) was added to each sample immediately before being transferred into a boiling water bath for 5 min. Then samples were ultra-centrifuged at 560,000 x *g* for 5 min and the supernatant was collected, which contained solubilised total cell proteins. 1 μl of Bromophenol blue (BPB) stain (0.02%) was added into each sample. SDS-PAGE gel electrophoresis was used for analysis.

2.5.11. SDS- PAGE analysis

To analyse protein samples, SDS PAGE gel was used. SDS electrophoresis was performed in a 14% (29:1) polyacrylamide gels, which contained in 375 mM Tris HCl/ 0.1% SDS pH 8.8 buffer. The gel was 0.7 mm x10 cm x 7 cm with 1.5 cm 5% acrylamide/0.12% methylene bisacrylamide. The stacking gel contained 0.1% SDS /125 mM Tris/HCl pH 6.8. The electrophoresis tank buffer was 25mM Tris/192mM glycine/0.1% SDS pH 8.8. Ammonium persulphate and N,N,N',N'-tetramethyl-diaminoethane (TEMED) were used to polymerise gels. Samples were heated to 100 °C in 1X loading buffer containing 20 mM DTT for 5 min. The gel was run at 20 mA until the bromophenol dye left the running gel, then the gel was stained with staining solution (0.1% Brilliant Blue R/30% methanol/20% acetic acid) at 55 °C for 20 min. Excess stain was removed in de-staining solution (30% methanol/1% formic acid). Gels were washed with formic acid (1%), then water, and were stored in re-sealable bags.

2.5.12. Large scale protein extraction

To extract expressed targeted proteins from *E. coli* BL21 (DE3), half of the concentrated stock of bacteria (12.5 ml) for each 400 ml culture were washed to remove glycerol by mixing after being thawed with 200 ml of 50 mM Tris/HCl/0.1 NaCl buffer. Bacteria were centrifuged at 5000 *rpm* at 2 °C, and the pellet was resuspended to 12 ml with the same buffer. The suspension was collected in a universal tube and supplemented with 120 μl of 100 mM PMSF and 12 μl of 1 M dithiothreitol (DTT). Sonication was carried out with 15 s bursts at 45 s intervals with 20% amplitude using a medium sized probe. Samples were taken before and after sonication to measure A_{600}. The sonicated suspension was ultra-centrifuged at 560,000 *g* for 20 min at 2 °C. The supernatant that contained the soluble protein fraction was transferred to a universal vial and held on wet ice.

2.5.13. Protein purification by Ni-chelate chromatography

To purify proteins after their extraction from bacteria, Ni-chelate chromatography was used. The precursor of IL-36β as it was expressed from *E. coli* was substantially soluble under these conditions. Nickel chelate chromatography was used to purify the cleavable N-terminal His_6-tagged n^5-IL-36β protein. A column tube 16 mm was packed with 5 ml of NTA nickel II Sepharose. A flow rate of ~ 2.2 ml/min was created. Before starting, the column was washed with 10 ml of BA buffer to elute weakly bound nickel from the matrix before re-equilibrating with 30 ml of B20G. The protein sample was supplemented with 1 M Imidazole/ HCl/pH 7.5 and NaCl to yield a final concentration of 0.45 M NaCl and 20 mM imidazole and loaded in ~10 ml. Weakly associated proteins were eluted in a mixture in buffer B20G. Buffer B35G was used to elute low affinity protein. To elute target protein, B200G was used. A NanoDrop spectrophotometer was used to quantify protein in these fractions by A_{280} by reference to the extinction coefficients.

2.5.14 IL-36γ purification

IL-36γ was found to be an insoluble protein as expressed in BL21 (DE3) (12.5 ml) containing the auto-induced ET-IL-36γ plasmid. After they were thawed bacteria were washed to remove glycerol by mixing with 200 ml of 50 mM Tris/HCl/0.1 NaCl buffer. Bacteria were centrifuged at 5000 x *rpm* at 2 °C, and the pellet was resuspended to 12 ml with the same buffer. The suspension was collected in a universal tube and supplemented with 120 μl of 100 mM PMSF and 12 μl of 1 M dithiothreitol (DTT). Sonication was carried out in 15 s bursts at 45 s intervals with 20% amplitude using a medium sized probe. Samples were taken before and after sonication to measure A_{600}. A mixture of 1.5 ml of 5 M NaCl and 1.5 ml of 10% w/v Triton X-100 in water was mixed with lysate into lysate to remove lipids from the pellet, which contained insoluble IL-36γ protein. The supernatant was mixed for 30 s in a vortex mixer before being transferred into 50 ml centrifuge tube and centrifuged at 20,000 x *g* in the J-26 centrifuge for 10 min at 4 °C to collect the washed pellet for further processing.

2.5.15. Dialysis

To remove low molecular weight contaminants including imidazole and NaCl, present in the elution buffer through protein purification chromatography. Fraction containing pooled IL-36β protein dialysed in dialysis tubing (SpectraPor). Pooled protein was loaded into the dialysis tube, sealed and dialysed against two changes of 500 ml of low salt buffer (10 mM Tris/ 10 mM Tris-HCl/ 10% glycerol/1 mM DTT) at 4 °C with continue stirring overnight.

2.5.16. Concentration of IL-36γ protein

A 2-ml tangential concentrator (Sartorius) with polyethersulfone (PES) membrane and a molecular size cut-off (MWCO) 5 kDa was used. Pooled protein was transferred into the concentrator tube and centrifuged at 4000 x g for 15-20 min until

the volume was reduced to 500 μl. Then, low salt buffer (1.5 ml) was added into concentrated protein and centrifuged until the volume was reduced to 500 μl. This process was repeated three times. Finally, the concentrated protein was recovered and washed out from concentrate pocket with 1.5 ml of low salt buffer. The protein concentration was measured spectrophotometrically.

2.5.17 Preparation of active IL-36β and IL-36γ

To remove His_6-tagged, purified proteins were digested with chymotrypsin and thrombin (Sigma). To test the procedure, a range of enzyme concentrations were tested. To terminate chymotrypsin and thrombin digestion, 1 mM PMSF was added by adding 1% volume of 100 mM PMSF in dry ethanol.

2.5.18 Capturing His-tagged contaminants

To remove the His_6-tag peptide and undigested precursor from the protein mixture, a 2 ml glass chromatography column tube was washed out thoroughly with deionised water. The tube was washed with 10 ml 1 M NaOH, and the whole apparatus, including caps, was soaked for 1 hr in 1 M NaOH. All parts were rinsed thoroughly with four changes of ultrapure water. The column tube was clamped into a stand and 1 ml of resin added. The column was washed with 10 ml of buffer D (10 mM Tris base/ 10 mM Tris-HCl/ 10% glycerol) by filling the reservoir. The protein samples were added, and the eluate drained into a universal tube. The collected samples were reloaded twice to ensure that all His_6-tagged peptide was bound, and protein was eluted twice with 1 ml of Buffer D and collected. A small sample (~20 μl) was taken for SDS-PAGE gel analysis from each elution. To visualise the rejected bound material, it was removed. Buffer D (2.4 ml) was mixed with 0.6 ml of 1 M imidazole (pH7.5) to yield a 0.2 M imidazole solution. Bound protein was eluted with this mixture and a sample was taken.

2.5.18 Fast Protein Liquid Chromatography

2.5.18.1 FPLC of n^5-IL-36β

To produce highly purified n^5-IL-36β protein, Fast Protein Liquid Chromatography (FPLC, GE technology) was used. IL-36β has a predicted isoelectric point of pH 9.14 and was therefore purified on Mono S, a cation exchanger. Before loading the sample of n^5-IL-36β, S column HR5/5 was washed, connected to a Pharmacia/LKB (now GE-Healthcare) Äkta system. The column volume is 1 ml. IL-36β is expected to have a strong positive charge at neutral pH. The Mono S column consists of monodisperse beds that have diameters of 10 μm, carrying sulphonic acid groups (RSO_3^-) as a strong cation exchanger. The pH of the protein pool was adjusted to 6.2 with 0.5 M morpholino ethane sulphonic acid (MES). The sample was purified in 1.5-2 ml loadings (2 mg). IL-36β was retained on the column and eluted with a linear gradient (20 mM MES/10 mM NaOH/0-0.5 M NaCl). The gradient was 25 ml, and the flow rate was 1 ml/min. The size of fractions was adjusted at 0.6 ml, which corresponds to the dead-volume between UV monitor and fraction collector. Depending on A_{280} and SDS PAGE analysis, fractions that contain a substantial amount of IL-36β were pooled.

2.5.18.2 FPLC of n^{18}-IL-36γ

A column of Resource Q material (1 ml) was used and was pumped by an Äkta system (as above). The column material is made from 15 μm polystyrene/divinylbenzene beads substituted with quaternary ammonium as a strong anion exchanger. The pH of the protein pool was adjusted to 8.8 with 40 mM Tris base. The sample was loaded into the system in 1.5-2 ml doses. The protein has an isoelectric point of 4.99 and so possesses a substantial negative charge at pH 8.8. It was retained on the column and eluted with a linear gradient (40 mM Tris base/10 mM Tris/HCl) of increasing Cl^- concentration 0-0.25 M over 10 min then 0.25-0.5 M over 5 min. Fractions of 0.6 ml fractions were collected, which corresponds to the dead-volume between UV monitor and fraction collector. Protein concentration was determined spectrophotometrically from A_{280} (NanoDrop/Thermo Scientific) and SDS

PAGE was used to characterise fractions that contained a substantial amount of IL-36γ.

2.6. High sensitivity detection of endogenous IL-36γ in western blots

2.6.1 Protein extraction from adherent cells

To extract protein from cells lysates, cells were washed twice with cold 10 ml 1X PBS (Lonza) and gathered by scraping cells in cold 7 ml for T75 (75 cm^2) flasks or 3 ml for T25 (25 cm^2) of TBS (45 mM Tris-HCl, 5 mM Tris base and 150 mM NaCl).

Cells were scraped up and pipetted into a 15 ml conical tube and collected by centrifugation at 4°C for 2 min at 100 x *g* (1000 *rpm*). Supernatants were removed, and cells were resuspended in 1 ml of TBS/ 25 mM DTT and immediately lysed by adding 1 ml of 2% SDS/20% glycerol and immediately heating to 95-100 °C for 5 min to denature the protein and endogenous proteases. The extracts were put into a clean ultracentrifuge tube and ultracentrifuged at 22 °C (for 30 min). The supernatants were collected. Spectrophotometry was used to estimate protein concentration and TBS/DTT was used as a blank.

2.6.2 Western Blotting

To detect specific protein in the samples, western blot was used. Proteins were transferred from the gel onto a nitrocellulose membrane after being separated by SDS-PAGE as in section 2.5.11. To allow detection of IL-36γ as sensitively as possible and to reduce background, I used nonmetal tools to handle the blots. The western blotting procedure was used as follows. Gels were soaked without fixing for 30 min in the CAPS transfer buffer in clean containers (cleaned by using 1% SDS and boiled in a microwave oven for 2 min). The transfer sandwich cassette contained: a mesh, 2 pieces of Whatman 3 MM blotting paper, the nitrocellulose membrane (Bio-Rad), the SDS PAGE gel, 2 pieces Whatman blotting 3 MM paper and a mesh. All the equipment were pre-immersed in transfer buffer containing 200 mM CAPS/NaOH/pH11, 10% v/v methanol. The transfer cassette sandwich was then placed in a transfer tank and

proteins were transferred electrophoretically for 1 h at 100 mA. After transferring protein, the nitrocellulose membrane was soaked in a clean container for 1 min in a 4 % w/v solution of trichloroacetic acid, to fix the transferred proteins, then the membrane was moved to a clean container that contained 20 ml of neutralising buffer (50 mM Tris/HCl/1 mM EDTA/ 150 mM NaCl/pH7.5). Further, direct binding by proteins was blocked by shaking the membranes in a solution of 5% dried skimmed milk (Marvel) dissolved in 1 x PBS, which had been filtered through Whatman No 1 filter paper to remove particles. The membrane was rocked overnight at 4 °C in the primary antibody solution in 5% dried milk solution in PBS. The primary antibody used at 0.9 μg/ml and was an antigen purified goat anti-human IL-36γ (AF2320 R&D systems). Following incubation with primary antibodies, the membrane was washed in PBS + 0.02% Tween-20 (PBST) 3 times for 5 minutes each time. The membrane was then incubated with the secondary, which is goat IgG HRP-conjugated Antibody (HAF017 R&D systems), diluted in PBS + 0.02% Tween-20 (PBST) for 1 h (1 μg/1 ml) at 4 °C. The membrane was again washed in PBST 3 times for 5 min. The membrane was drained, and proteins were then visualised by washing the membrane in Enhanced Chemiluminescence (Bio-Rad) reagent (Bio-Rad) for 5 min. The membranes arrayed on a washed, folded sheet of polythene. Luminescence was quantified in a Bio-Rad imager.

2.6.3 A-431 or HaCaT cells protein extraction

To induce expression of IL-36γ protein, confluent A-431 or HaCaT cells were resuspended from T75 flask (75 cm^2) as in section 2.3.1. In stimulation experiments, T25 flask (25 cm^2) was used, each was populated with 5 ml from the suspension, and were incubated at 37 °C for four days. To turn off growth dependent and serum-stimulated transcription after 4 days, HSM was replaced with LSM. After 18-24 h inflammatory stimuli were added in 2.5 ml LSM (in addition to the 2.5 ml of LSM that was used as control during comparison with the stimuli. Protein was extracted as in section 2.6.1.

2.6.4 TLR7, TLR8 and necroptosis activation to induce IL-36γ protein expression

To induce processing of IL-36γ protein, confluent A-431 cells were resuspended from two T75 flasks (75 cm^2) as in section 2.3.1. As usual, cells were grown for four days in HSM before being turned off growth with LSM. After 18-24 h, cells were treated with PMA and TNF for 6 h followed by TLR7 agonist, TLR8 agonist or Leu-Leu methyl ester hydrobromide (Leu-Leu-OMe) for 2 h. Protein was extracted from samples as in section 2.6.1.

2.6.5 Attempted induction of IL-36γ protein processing in A-431 cells after treatment with cycloheximide, staurosporine or A23187 (calcium ionophore) drugs.

To induce apoptosis in A-431 cells, A-431 cells were grown in 6-well plate as in section 2.3.1. HSM was replaced with LSM for 18 h. Cells were treated with PMA and TNF for 6 h then cells were washed with serum free medium and drained before treating with cycloheximide, staurosporine, A23187 or mixture of cycloheximide, staurosporine and A23187 in serum free medium for 24 h in total volume 0.2 ml , in addition to cycloheximide, staurosporine or A23187 only in serum free medium for 24 has a negative control. Plates were covered with parafilm to prevent drying. Supernatants and cell lysate were harvested and prepared in sample buffer containing 2% SDS, 20% glycerol and 2.5 mM DTT. Samples were prepared as in section 2.6.1.

2.6.6 Time course of processing of IL-36γ after treatment with staurosporine

To assess duration of IL-36γ protein processing by staurosporine, A-431 cells were grown on 6-well plate as in section 2.3.1. HSM was replaced with LSM for 18 h. Cells were treated with PMA and TNF for 6 h then cells were washed with serum free medium and drained before treatment with staurosporine (0, 6, 12 and 24 h) in total volume of 0.2 ml. Plates were covered with parafilm to prevent drying. Supernatants and cell lysate were harvested and prepared in sample buffer containing 2% SDS, 20% glycerol and 2.5 mM DTT. Samples were prepared as in section 2.6.1.

2.6.7 Expression of IL-36γ protein in primary human keratinocytes cells by PMA and TNF and attempted induction of endogenous processing.

To induce expression and processing of IL-36γ protein in primary human keratinocytes, primary human keratinocytes cells were grown on 6-well plate. High serum Green's medium was replaced with LSM for 18 h. Cells were treated with PMA and TNF for 6 h, then cells were washed with serum free Green's medium and drained before treating with staurosporine or were left untreated for 24 h in a total volume 0.2 ml. Plates were covered with parafilm to prevent drying. Supernatants and cell lysate were harvested and prepared in sample buffer containing 2% SDS, 20% glycerol and 10 mM DTT. Samples were prepared as in section 2.6.1.

2.6.8 Infection of HaCaT cells with bacteria

To attempt to induce expression of IL-36γ protein in response to bacterial infection, HaCaT cells were grown on 6-well plate for 3 days. HSM was replaced with LSM for 18 h. Cells were infected with *Staphylococcus aureus* or untreated for 6 h in total volume 1 ml. Supernatants and cell lysate were harvested by using scraper and prepared in sample buffer containing 2% SDS and 2.5 mM DTT and immediately heating to 95-100 °C for 5 min to denature the protein and endogenous proteases. Samples were concentrated into 200 μl by a 2-ml tangential concentrator (Sartorius) with polyethersulfone (PES) membrane and a molecular size cut-off (MWCO) 5 kDa. Then extracts were put into a clean ultra-centrifuge tube and ultra-centrifuged at 22 °C (for 30 min). The supernatants were collected. Spectrophotometry was used to estimate protein concentration and serum free medium/DTT was used as a blank. 20% of glycerol was added into each sample before being loaded into the SDS-PAGE.

2.7. Isolation of clonal κB reporter HT-29 cell line

2.7.1 Cloning of HT-29 cell lines

HT-29 had been stably transfected with plasmid pGL 4.32 κB-*luc2*p-Hygro (Promega). The population ms5 showed strongly inducible luciferase expression. To clone HT-29 cells, a confluent monolayer of HT-29 κB-*luc* (ms5) were removed from a T75 flask. Cells were counted in a heamocytometer.

Cells were adjusted at 10^6/ml by dilution with HSM. Then 10 μl, containing 10^4 cells, was added to 10 ml of HSM to achieve 10^3 cells/ml. After that, 100 μl of the last dilution was added into 30 ml of HSM on a petri dish to yield 3.3 cells/ml and cells were continuously mixed. By using a multichannel pipette, 100 μl (predicted 0.33 cells) were added to each well of plate, and 100 μl of HSM was added into each well. Cells were incubated at 37 °C. After 19 days of incubation, colonies were examined with an inverting microscope to check which wells contained cells. I obtained 21 colonies. Medium was removed from wells that contained colonies, and wells were rinsed with 200 μl of PBS for 2 minutes and drained, then 50 μl of trypsin/EDTA was added. The cells were incubated at 37 °C for 15 minutes. Then, 100 μl of HSM were added to resuspend colonies from the wells. Colonies were transferred into a 24-well plate, and 1 ml of HSM was added to each well. Plate was incubated at 37 °C to allow clonal cells to replicate. To check the ability of clonal cells to express luciferase, confluent HT-29 clonal cells from 24-well plate were used. In the experiment, 2 plates 24-well plates were used. Clonal cells (21 clones) were washed with 1 ml PBS for 2 minutes and drained. Then 100 μl of trypsin/EDTA were added and cells incubated at 37 °C for 10 minutes. After that 800 μl of HSM were added and resuspended. Cells suspension (300 μl) were added into a single well on a 24-well plate with 700 μl of HSM. Plates were incubated at 37 °C for 3 days. After 3 days, medium was changed with serum in 0.5 ml of LSM for 18-24 h, then cells were treated with a pro-inflammatory cytokine LSM for 6 h. After 6 h, the medium and treatment were removed by inverting and stapping to remove any excess medium. 1 x lysis buffer (0.25 ml) was added per well. The plate was swirled and frozen at -80 °C. The luciferase output was measured as in section 2.5.19.1.

2.7.2 Determination of Puromycin sensitivity of HT-29

To determine the effective concentration of puromycin that can kill cells, a killing curve was made. HT-29 cells were treated with different concentrations of puromycin to determine the lowest concentration of antibiotic that can kill all cells within 7 days. HT29-κB-luc (D7) were grown to near confluence on a T75 flask and were removed and converted into a single cell suspension.

Approximately, 60 x 10^5 cells in 200 μl were plated in each well of two six-well plates (9.5 cm^2). Cells were washed and split, as in section 2.3.1. Duplicated wells were used for each concentration. Cells were treated with (1, 1.8, 3.5, 6.5 and 10 μg/ml) of puromycin in the total volume 2.5 ml in each well and were incubated at 37 °C for 7 days. Medium containing floating cells and debris was removed by washing with PBS. The viability of cells was assessed qualitatively by examining the base of the well for adherent cells.

2.7.3 *IL1RL2* gene disruption sublines in HT29-κB-luc cells

To distrust the *IL1RL2* gene, a CRISPR plasmid was used. HT-29 clone-κB-*luc* D7 were transiently transfected with derivatives of pSpcas9n (BB)-2A-Puro (also known as pX 489) (Ran et al., 2013) that were designed to express RNA guides that targeted exon 5 of IL-1RL2. The plasmid also carries a puromycin resistance marker, and transient expression of puromycin resistance was used for selection of transfected clones. In this experiment, I transfected both knockout vectors (CRISPR1 and CRISPR2) and I co-transfected with a plasmid that drives strong expression of eGFP as a positive control for transfection. A liposome-based transfection reagent (Mirus reagent, Mirus Bio) was used over a range (6, 7.5 and 9.4 μg) of concentrations with cells in suspension and 2.5 μg of DNA per well of two six-well plates. One million cells were transfected in each well. The first plate received only eGFP expression plasmid. These served as a 24 h transfection control and then a puromycin toxicity control. In two separate 1.5 ml tubes, 10 μg of pX-eGFP was added to the first tube as control, and 5 μg of pX-eGFP, 2.5 μg of pX489-36R-CRISPR1 and 2.5 μg of pX489-36R-CRISPR2 were added to the second tube. To each tube, 1 x TE to 200 μl and 50 μl 3

M sodium acetate were added and mixed before being added 500 µl of 100% ethanol. Tubes were frozen on solid CO_2 twice then thawed before being centrifuged at 17,000 x *g* for 5 minutes at 4°C. The supernatant was discarded, and the pellet was washed with at least 1 ml of 70% v/v ethanol. Samples were then mixed on a vortex mixer and centrifuged 17,000 x *g* for 5 minutes. Finally, ethanol was removed by brief air drying. The DNA samples were dissolved in 20 µl water at 37 °C. A Nanodrop spectrophotometer was used to determine the final A_{260} and A_{280} of the DNA solutions.

The cell line HT29-κB-luc (D7) was grown to near confluence. Cells were resuspended and counted with a hemocytometer. A volume that contains 12 million cells was diluted with medium to a final volume of 30 ml. An aliquot of 2.5 ml of the cell suspension was plated per well in two six-well plates. The first six-well plate contained only the control eGFP expression plasmid, the second contained the eGFP and both Cas9/CRISPR plasmids. Mirus Reagent was warmed to room temperature before being used. 0.25 ml of RPMI medium (without foetal bovine serum and antibiotic) was added into twelve tubes. Then 2.5 µg (2.5 µl of a 1 µg/µl stock) of the plasmid DNA mixtures were added to each tube and mixed each gently with a 1 ml plugged tip. Transfection reagent was added (6 µl, 7.5 µl or 9.4 µl) in duplicate to each diluted DNA and mixed completely. Each six-well plate had a pair of similarly treated wells. Tubes were incubated at room temperature for 20 min to allow the DNA –reagent complexes to form. The mixtures were added dropwise to cells across the well. After each addition, the plate was gently rocked back-and-forth and from side-to-side to distribute the complexes evenly. Cells were allowed to adhere to the plate for 24 h in the absence of puromycin. After 24 h, to break intercellular contacts that would allow expressed puromycin acetyltransferase to rescue non-transfected cells, cells from each well were re-suspended in 1.0 ml complete medium, to which 1.5 ml of 3 µg/ml puromycin was added (final 1.8 µg/ml). Cells were observed again at 24 and 48 h. At 72 h, cells were washed twice with PBS to remove puromycin and as many non-adherent, dead cells as possible. The adherent cells were treated with 0.1 ml trypsin/EDTA. Cells from each well were re-suspended in 7.5 ml of full medium (without puromycin) and plated in 3 wells (2.5 ml each) of six-well plates. After a further 48 hours, the density of the surviving cells was estimated in each well. The cells were allowed to divide until each of the groups of three wells that

were transfected with pX489 derivatives reached confluence. The adherent cells were washed with PBS to remove puromycin and cells were removed with 0.1 ml trypsin/EDTA per well and resuspended with a further 1.4 ml medium in a universal vial. The three wells from each transfection treatment were pooled and the cell suspension was placed on wet ice to inhibit membrane remodelling and thus to prevent adhesion. Samples of resuspended cells were counted in a haemocytometer. A sample of this suspension was diluted to yield 10-20 ml of suspension at 1000 cells/ml (1 cell/μl). The cells were resuspended thoroughly and 150 μl of the suspension was pipetted (~150 cells) in a 50 ml conical tube in 50 ml medium (333-fold, yielding expected three cells/ ml). An eight-channel pipette was used to dispense 100 μl (0.3 cells) into each well of three 96 well plates. Extra medium (100 μl) was added to each well. 96-well plates (three plates) were placed in a clean open box in an incubator for 19 days. Plates were examined on an inverting microscope to check which wells contained colonies. Eight clones were recovered. To pick up colonies into a 24 well plate, medium was removed from wells that contained colonies, and wells were rinsed with 200 μl of PBS for 2 minutes and drained, then 50 μl of trypsin/EDTA was added. The plate was incubated at 37 °C for 15 minutes and then 100 μl of HSM were added and cells re-suspended. Cells were transferred into a well of a 24-well plate, and 1 ml of HSM was added to each well. The plate was incubated at 37 °C to allow clonal cells to be grown up. Once cell lines were confluent, they were tested for IL-36 response by using luciferase assay to check whether *IL1RL2* gene had lost its function out or not. In the experiment, two plates of a 24-well were used. Clonal cells (8 clones) were re-plated after trypsin/EDTA into three wells on separate plates in 1 ml (final) HSM. Plates were incubated at 37 °C for 3 days. After 3 days, cells were serum starved in 0.5 ml of LSM for 18-24 h, and then cells were treated with inflammatory stimuli as a positive control, in addition to LSM as a negative control for 6 h. Four replicates were used for each treatment. Luciferase activity was determined as described in section 2.5.19.

2.7.4 Genomic DNA preparation from *IL-1RL2* deficient cells

To identify the distribution in the *IL-1RL2* gene, DNA was extracted from transfected cells that failed to respond to IL-36. Genomic DNA was extracted from a sample of three IL-36 non-responsive lines (A6, E3 and G4), and IL-36 responsive parent D7 clone as a positive control. A6, E3, G4 and D7 were grown on a T75 (75 cm^2) bottles until they were confluent. Cells were washed with 10 ml PBS for 2 minutes and drained. Cells were trypsinised and were washed in 5 ml cold PBS and collected by centrifugation at 2,000 x *rpm* for 5 min, 4 °C in benchtop centrifuge each time. The supernatant was discarded, and cells were digested with 0.3 ml of digestion buffer (100 mM NaCl, 6 mM Tris-HCl, 4 mM Tris base, 25 mM Na_3ETDA, 5% SDS and 0.1 mg/ml proteinase K) before being transferred into a microfuge tubes and mixed vigorously. The samples were gently shaken in an oven at 55 °C overnight. To extract residual protein and to fragment very long DNA, 0.3 ml of phenol/chloroform/isopentyl alcohol buffer (0.3 ml) was added to each tube and the tube was vortexed vigorously for 30 s. The tubes were centrifuged at 17,000 x *g* for 2 min and the aqueous phase of each tube was collected into a fresh microfuge tube and the volume of aqueous phase was estimated. To each tube was added 0.15 ml of 7.5 M ammonium acetate per 0.3 ml of aqueous phase and 2 x the combined volume (0.9 ml) of 100 % ethanol. Tubes were centrifuged at 17,000 x *g* for 2 minutes at room temperature. The supernatants were discarded, and samples were vortexed and centrifuged at 17,000 x *g* for 5 minutes. Finally, traces of ethanol were removed by brief air drying in a desiccator. The genomic DNA was dissolved in 50 μl of TE (6 mM Tris-HCl, 4 mM Tris base, and 1 mM EDTA) with rocking for two hours at 65 °C. A NanoDrop spectrophotometer (Thermo Scientific) was used to measure the A_{260} and A_{280} in triplicate of each sample.

2.7.5 Amplification of exon 5 of IL-1RL2 for sequencing

To optimise RT-PCR, different concentrations of standard HT-29 D7 DNA (500, 150, 50, 15 and 5ng) and ranges of annealing temperature (52 °C, 56 °C and 58 °C) were used. The master mix was made by mixing on ice in 1.5 ml microfuge tube 666 μl water, 200 μl 5x GoTaq Green buffer. Next, 20 μl 10 mM (50X) dNTPs, 60 μl $MgCl_2$

and 5 μl GoTaq (5 u/ μl) were added. The primer pair to amplify exon 5 was AGCTATCTGTTGTCTTCCAG (e5IL-36R/forward) GTCTGAGAGCCTACTAGCCT (e5IL-36Rr1/reverse). A 2 μl (100 μM) of each primer was added into mixture. The relevant DNA dilutions (1 μl) were added to each tube then 24 μl of master mix/primer mixtures was pipetted to each relevant tube. PCR products were visualized by agarose gel electrophoresis in TAE buffer in 0.02% ethidium bromide.

2.7.6 Test of all IL-36 and IL-36 mutant forms on the standard HT29-κB-*luc* (D7) and IL-36R knocked out cells (A6)

To determine the effective dose for IL-36R, HT-29/κB-*luc*2P (clone D7) and the (*IL1RL2*$^{-/-}$) subline A6 were grown as described in section 2.7. As usual, the cells were grown for three days and then medium was drained and replaced with 0.5 ml of LSM for 18 h. The cytokine dilution in 0.6 ml as in Table 2.4 was added for 6 h. Replicates were loaded on the plates along diagonals to prevent clustering at the plate edges. Five replicates were used for each concentration. The luciferase output was measured as in section 2.5.19.1.

Table 2.4 Tested proteins and their dilutions.

Agent	start	1st dilution	2nd dilution	3rd dilution	4th dilution	5th dilution	6th dilution
n[1]-IL-36α	300 nM	100 nM	30 nM	10 nM	3 nM		
n[4]-IL-36α	300 nM	100 nM	30 nM	10 nM	3 nM		
n[6](Lys)-IL-36α	10 nM	3 nM	1 nM	0.3 nM	0.1 nM		
n[6]-K6S-IL-36α	100 nM	30 nM	10 nM	3 nM	1 nM		
n[6]-K6G-IL-36α	100nM	30 nM	10 nM	3 nM	1 nM	0.3 nM	
n[5]-(Arg)- IL36β	10 nM	3nM	1nM	0.3 nM	0.1nM	0.3 nM	0.01 nM
n[18]-IL-36γ	30 nM	60 nM	18 nM	6.0 nM	1.8 nM		
IL-1α	3 nM	1 nM	0.3 nM	0.1 nM	0.03nM		
TNF	10 ng/ml	3 ng/ml	1 ng/ml	0.03 ng/ml	0.1 ng/ml		
IL-36Ra	100 nM						
IL-36β	100 nM IL-36Ra + 0.3 nM IL-36β						
Control	LSM						

2.7.7 HT29-κB-luc time course stimulation with IL-36α, IL-36β and TNF

To determine induction time of NF-κB in response to cytokines confluent HT29-κB-luc cells were used and trypsinised as in section 2.3.1. Treatments were performed in quadruplicates in 0.6 ml. Cells were treated with inflammatory cytokines for 3, 6, 9, 12, 18, and 24 h. Luciferase assay was performed as usual by using 5 μl of lysate as in section 2.5.19.1.

2.7.8 Downregulation of TNF and IL-36 responses and to test for the expected specificity

To check if luciferase expression can be re-activated by cytokines after it had been down regulated, confluent HT29-κB-luc cells were used and trypsinised as in section 2.3.1. Treatments were performed in 16 wells for each stimulus in 0.6 ml for 6 h. Luciferase assay was proceeded as usual by suing 5 μl of lysate as in section 2.5.19.1.

2.7.9 Digestion of n^1-IL-36α with chymotrypsin and test the biological activity of the digested protein

To confirm that n^1-IL-36α precursor can be activated, n^1-IL-36α protein that prepared in our lab was digested with chymotrypsin at different time points. PMSF in a final concentration 1 mM was used to terminate chymotrypsin digestion. To test the biological activity, as usual, the cells were grown for three days and then medium was drained and replaced with 0.5 ml of LSM for 18 h. Digested protein at different time points was added to cells for 6 h. Three replicates were used for each concentration. The luciferase output was measured as in section 2.5.19.1.

2.7.10 Data analysis

Statistical significance of ELISA data was determined using one-way ANOVA. The luciferase data were normalised to the response to 100 ng/ml TNF in each set of experiments and were analysed to fit a non-linear regression curve (four parameters) in which the Hill coefficient was fixed at 1.5 and the background luminescence was fixed at zero. The 95% confidence limits of the EC_{50} were used to judge the statistical significance of the differences between the different dose-response curves.

Statistical significance of RT-qPCR data differences between groups was determined using Wilcoxon test**.** All statistical analyses were performed using GraphPad Prism 8. Significant differences are illustrated by * =P≤0.05, ** =P≤0.01 *** =P≤0.001, **** =P≤0.0001.

Chapter 3

Results

3.1 Introduction

Understanding the proteolytic processing of IL-36α, IL-36β and IL-36γ has been the subject of several papers. An in vitro study showed that N-terminal truncation of pro-IL-36α, pro-IL-36β, pro-IL-36γ and pro-IL-36Ra proteins at specific sites, which are n^6, n^5, n^{18} and n^2 respectively, elevated their biological activity compared with full-length IL-36 proteins (Towne et al., 2011). Endogenous proteolytic enzymes that can clip IL-36α, IL-36β, IL-36γ proteins to provide fully active proteins have not yet been identified, but an in vitro study by Henry et al., 2016 showed that cathepsin G, elastase and proteinase-3, which are neutrophil derived enzymes, can cleave IL-36α, IL-36β and IL-36γ proteins. These serine proteases can cleave IL-36 proteins but not at the same truncation sites that were suggested by Towne et al. Moreover, the biological activity of cleaved IL-36α, IL-36β, IL-36γ proteins by these neutrophil derived enzymes is less than has been reported by Towne et al. Another in vitro study by Ainscough et al., 2017 showed that cathepsin S, which is a cysteine protease, can cleave IL-36γ protein at the same site that was identified by Towne et al., and the cleaved protein is fully active. Most of the research that assessed the biological activity of truncated IL-36 proteins either used cells that were transfected with exogenous IL-36R or that contained endogenous IL-36R but were treated for 24 h. For example., Towne et al., used Jurkat cells with transfected IL-36R to measure the biological activity of truncated IL-36α, IL-36β, IL-36γ and IL-36Ra proteins while Foster et al., 2014 and Zhou et al., 2018 used cells that have endogenous IL-36R, but they treated their cells for 24 h with IL-36 proteins. In this study, HT-29 cells that have endogenous IL-36R and stably transfected with a luciferase reporter gene were used. I used these cells to measure the dose response to IL-36 species and to determine its time course. I will present evidence that confirms that *IL1RL2* is the only gene that encodes an IL-36R in HT-29 cells. I compare the kinetics of n^6-IL-36α, n^5-IL-36β and n^{18}-IL-36γ. I will investigate the relationship between N-terminal structure of IL-36α and its activity. Given that, I found that EC_{50} values of our recombinant proteins were all higher than reported by others I have assessed the duration of response of cell line to n^6-IL-36α and n^5-IL-36β proteins. Finally, I have tested whether the almost inactive n^1-IL-36α can be activated by chymotrypsin thus showing its activity is latent rather than missing.

3.2 Construction of plasmids for expression IL-36β and IL-36γ in *E. coli*

Active IL-36α, IL-36α precursors and variants have been produced over several years in our laboratory, but I had not previously attempted to express IL-36β or IL-36γ. Moreover, sequences were cloned to create IL-36β and IL-36γ proteins that could be used in the purification of polyclonal antibodies and as standard proteins for electrophoresis. These proteins and the derivatives of IL-36α were used in studying their interactions with endogenous IL-36R. Coding regions of IL-36β and IL-36γ were transformed into *E. coli* to produce these proteins.

pET-IL-36β and pET-IL-36γ plasmids were designed to encode proteins that contain cleavage sites for recombinant chymotrypsin and thrombin, which are serine proteolytic enzymes, which were used to process chimeric recombinant precursors of IL-36β and IL-36γ respectively. The coding sequences of the processing sites and the final IL-36β and IL-36γ encoding sequence in these plasmids are located between restriction sites, Acc65I and XhoI. As shown in figure 3.1 and 3.2**.** The coding sequences of both plasmids (between the green “ATG” and the red “TAA”) were read at least once in both directions, except for the three bases of pET-IL-36β and one from pET-IL-36γ.

Figure 3.1 DNA sequence alignment of raw base calls from an ABI capillary sequencer of the pET-IL36β plasmid used in this work (clone 3). The alignment was prepared from the output of the MUSCLE server on the EBI bioinformatics website (www.ebi.ac.uk). Line pETIL36B contains the designed sequence, including the T7 promoter (yellow) and the entire open reading frame (bright green ATG until red TAA). The magenta and dark green hexanucleotides correspond to the Acc65I and XhoI sites, respectively. Raw sequence from the pETL1 primer and pETL2 primers are shown in lines sL1beta3 and sL2beta3. The implied complementary sequence from the pETR1 primer and pETR2 primers are shown in lines cR1beta3 and cR2beta3. When lines of sequence are absent, there is no valid sequence from that primer. In the bottom line * indicate bases confirmed by all four sequence runs. + indicates bases that have been sequenced at least once in both directions.

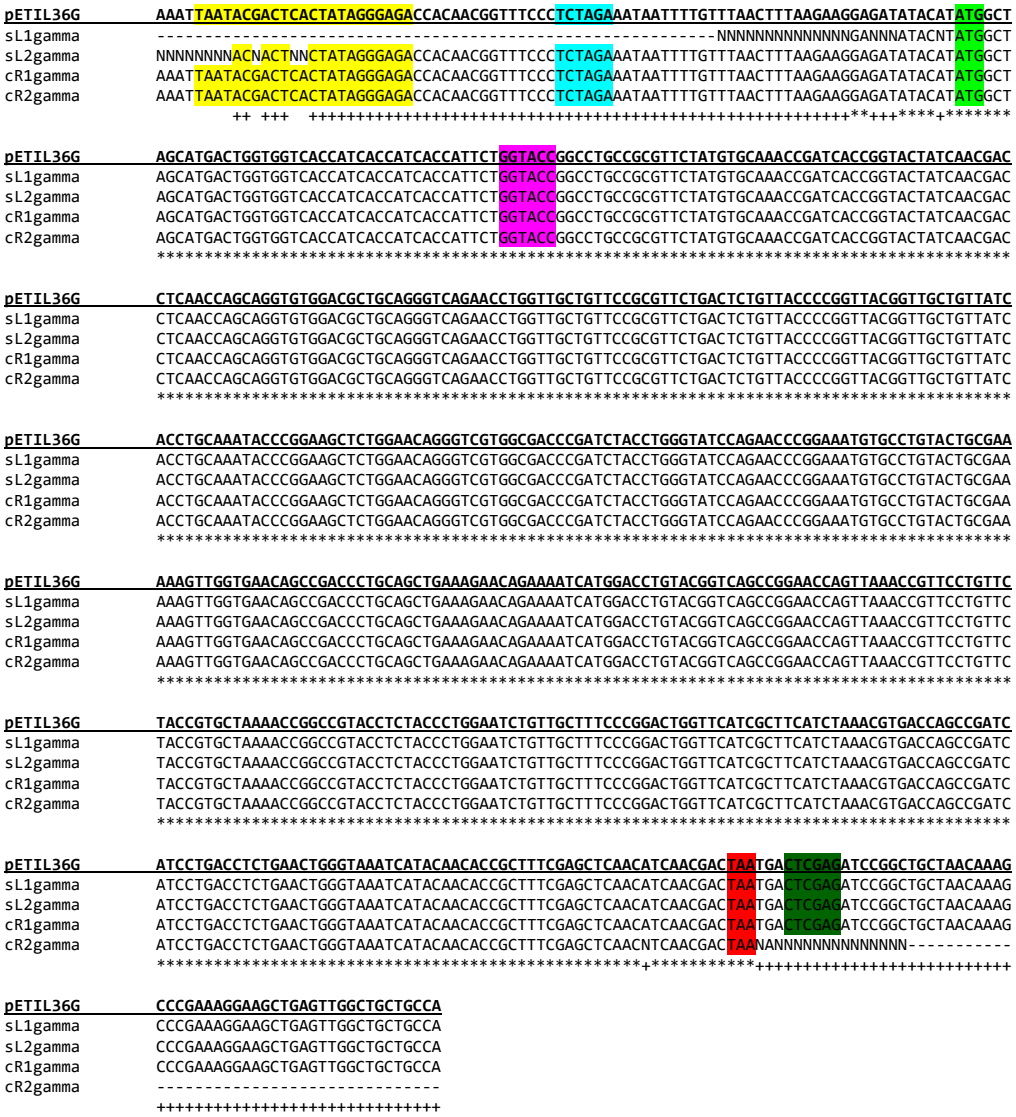

Figure 3.2 DNA sequence alignment of raw base calls from an ABI capillary sequencer of the pET-IL36γ plasmid used in this work (clone 1). The alignment was prepared from the output of the MUSCLE server on the EBI bioinformatics website (www.ebi.ac.uk). Line pETIL36G contains the designed sequence., including the T7 promoter (yellow) and the entire open reading frame (bright green ATG until red TAA). The magenta and dark green hexanucleotides correspond to the Acc65I and XhoI sites, respectively. Raw sequence from the pETL1 primer and pETL2 primers are shown in lines sL1gamma and sL2gamma. The implied complementary sequence from the pETR1 primer and pETR2 primers are shown in lines cR1gamma and cR2gamma. In the bottom line * indicate bases confirmed by all four sequence runs. + indicates bases that have been sequenced at least once in both directions.

The complete sequence of pET-IL1RN plasmid is shown in figure (A.1) in the appendix.

pET-IL1RN was designed by Dr. Martin Nicklin to express a His_6-tagged IL-1 family member IL-1Ra. It was chosen as basis for these constructions because it had suitable restrictions sites for Acc65I and XhoI restriction enzymes as in figure (A.1) in the appendix. The Acc65I is located on the His_6-encoding sequence and XhoI is located after the stop codon before T7 transcriptional termination. The plasmid carries the ampicillin resistance marker (AMP^R).

Synthetic recombinant human IL-36β and IL-36γ protein sequences were designed to be located between Acc65I and XhoI to replace the analogous fragments of pET-IL1RN and were synthesised by Eurofins. The DNA fragments were provided in pEX2. The sequences were optimised by Dr Martin Nicklin for expression in *E coli*, except where the placing of convenient restriction sites demanded changes.

pEXA2-IL36β, pEXA2-IL36γ as well as the pET-IL1RN vector were digested with Acc65I and XhoI as described in section 2.5.2. Bands of vector (pET-IL1RN), pEXA2-IL36β, pEXA2-IL36γ, which are 4650, 483 and 483 bp respectively, were isolated by gel electrophoresis and as described in 2.5.3.

Fragments were ligated and the ligation mixtures were transformed into *E. coli* DH5α as described in 2.5.4. Ampicillin resistant colonies were screened for the presence of inserts, and positive clones were sequenced with the primers shown in Table 3.1.

Table 3.1 Primer sequence of pETIL1RN vector

Primer	sequence
pETL1	CCACAACGGTTTCCCTCTAG
pETL2	CGGCGTAGAGGATCGAGAT
pETR1	ACCCCTCAAGACCCGTTTAG
pETR2	CAACTCAGCTTCCTTTCGGG

Both the open reading frames of IL-36β and IL-36γ were constructed to be under control of T7 promoter. Competent *E. coli* BL21 (DE3) were used because BL21 (DE3) carry T7 polymerase transgene under control of a lac promoter. The autoinduction method was used as described by (Studier, 2005) to produce proteins on a ten milligram scale.

The protein product as a result of pET-IL36β expression is a His_6-tagged mature soluble n^5-IL-36β protein that can be released from its His_6-tag by digestion with chymotrypsin, as will be described in this chapter. The protein product as a result of pET-IL-36γ expression is a His_6-tagged mature n^{18} -IL-36γ protein. n^{18}-IL-36γ protein product proved to be insoluble and was re-solubilised by guanidine hydrochloride and urea denaturation followed by renaturation. The activated protein was then produced by removing the His_6-tag through digestion with thrombin.

pET IL-36β or pET IL-36γ transformed BL21 (DE3) were grown on MDG medium supplemented with ampicillin as described in section 2.5.6. MDG strongly represses the *lac* promoter. MDG/Amp was inoculated with colonies grown to low density and stocked with 8% glycerol at -80 °C. Autoinduction medium (ZYM-5052/amp) section 2.5.9 was inoculated with these cultures. Recombinant His_6-tagged-n^5IL-36β and His_6-tagged-n^{18}IL-36γ precursor proteins were expressed in *E.coli* BL21 (DE3) (Studier, 2005) as described in section 2.5.9. High levels of precursor proteins were expressed by auto-induction according to the protocol of Studier (2005). Cultures were grown at 25 °C for 30 h at 320 rpm. The growth rate of pET-IL-36β and pET-IL-36γ cultures were followed with time at 25 °C by measuring culture density at A_{600} every ~2 has shown in figure 3.3. To check the expression of proteins, cell lysates were tested as described in section 2.5.10. Analysis was based on the SDS-PAGE electrophoresis as in figure 3.4.

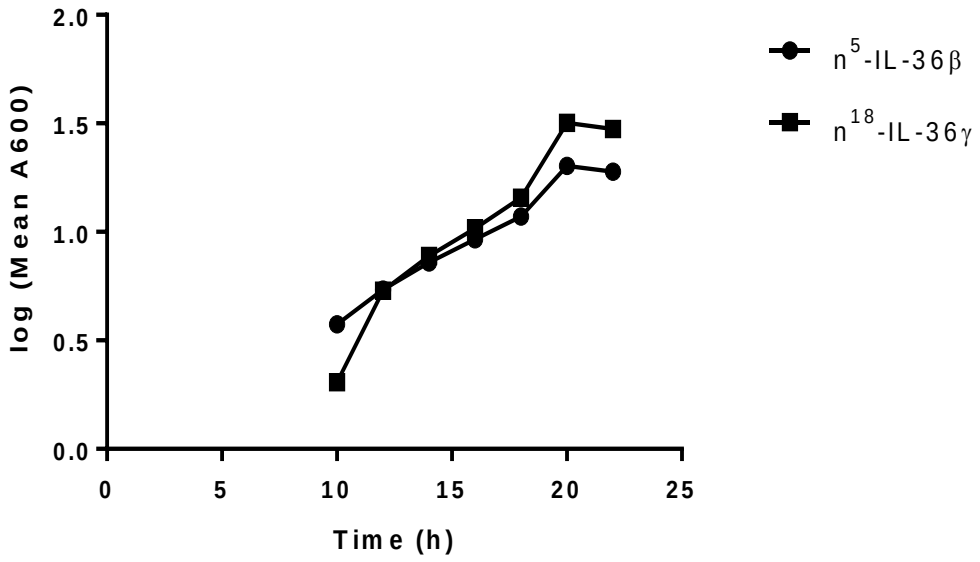

Figure 3.3 Growth curves of n^5-IL-36β and n^{18}-IL-36γ bacterial culture. The Log (mean A_{600}) was calculated from the mean A_{600} values of the in triplicate measurements. Consistent with the findings of Studier (2005), extremely high densities were observed (A_{600}>30). Time is calculated from the time of inoculation of the culture.

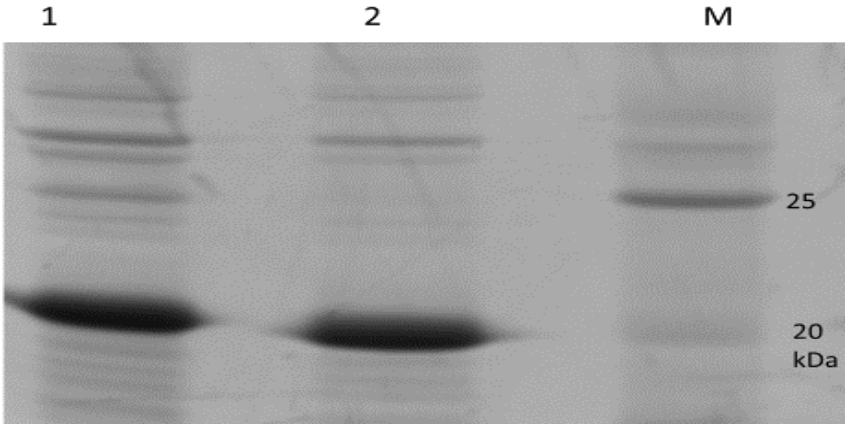

Figure 3.4 Coomassie Brilliant Blue stained SDS-PAGE analysis expression of recombinant human His_6-tagged n^5-IL-36β and n^{18}-IL-36γ proteins in large scale cultures BL21 (DE3). Total cell lysate of BL21 (DE3) carrying plasmids (Lane 1) pET-IL-36β or (Lane 2) pET- IL-36γ. M shows the molecular weight standards.

3.3 Purification of the IL-36β protein

After expression and solubility were tested, the culture of bacteria was harvested and stored at -80 °C. To prepare IL-36β, the frozen bacterial suspension (10 ml) was thawed and lysed to extract the soluble protein section 2.5.12.

A nickel-chelate Sepharose Fast Flow column was used to purify soluble His_6-tagged IL-36β recombinant protein by affinity chromatography for N-terminal His_6-tags. Cleared lysate was loaded onto a 2.5 cm x 2 cm column and washed with B20 imidazole 1 mM DTT to elute unbound and weakly associated protein, whereas a B-35G buffer was used in intermediate washing step to elute low affinity protein. His_6-tagged IL-36β protein was finally eluted in the B200G buffer figure 3.5. Protein content was quantified in these fractions by spectrophotometry at 280 nM, with a NanoDrop spectrophotometer (Thermo Scientific). A yield of 58 mg of His_6-tagged IL-36β precursor was obtained, based on the predicted A_{280} for a protein of this molecular mass and content of tyrosine and tryptophan.

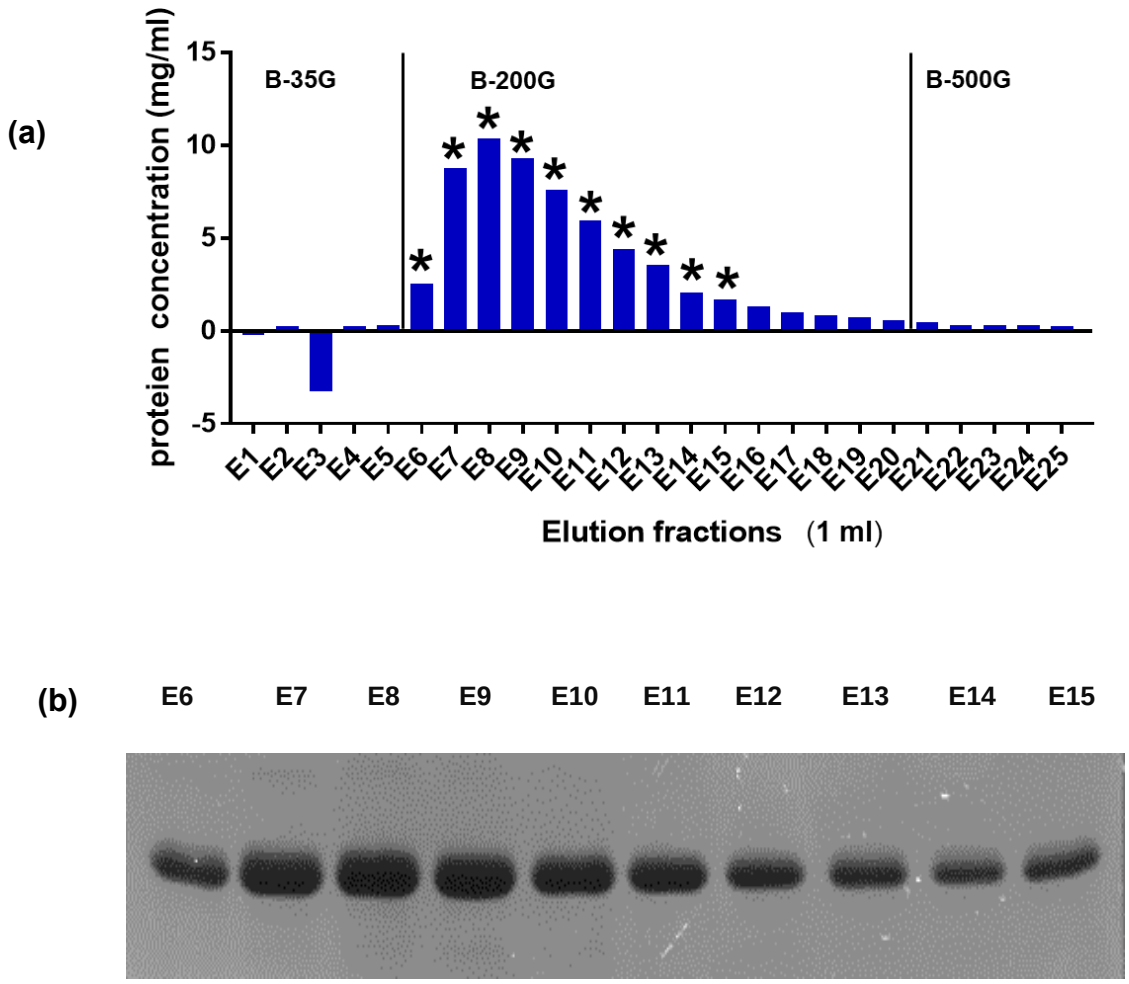

Figure 3.5 The elution profiles of His_6-tagged recombinant n^5-IL-36β from nickel chelate Sepharose. (a) Protein concentration (mg/ml) per fraction on the Y-axis is presented against the eluted fractions on the X-axis. (*****) labelled samples represent the pooled eluted fractions. B-200G buffer was used to elute the His_6-tagged n^5-IL-36β and 1 ml fractions were collected. The protein concentration was calculated from NanoDrop spectrophotometer measurements of A_{280}. **(b)** SDS-PAGE analysis of recombinant His_6-tagged-n^5-IL-36β Lanes 1-10 be composed from B-200G buffer elution fractions (E6-E15).

3.3 Affinity chromatography, purification and refolding IL-36γ protein

I first tried to purify recombinant IL-36γ protein from cleared bacterial lysate. I used the same series of imidazole containing buffers that were used to purify IL-36β. A_{280} readings showed that B200G buffer eluted fractions contained very little protein. Eluted fractions were prepared for SDS-PAGE electrophoresis. SDS-PAGE electrophoresis assessment showed that IL-36γ was not consistently or abundantly present in these fractions as shown in figure 3.6, presumably, because the protein was not in the soluble fraction of the cell lysate. Recombinant proteins sometimes are expressed in insoluble inclusion bodies in *E coli*, so urea and guanidine hydrochloride, which are solubilisation agents, are used to denature and solubilise proteins (Tsumoto et al., 2003).

I, therefore, resolubilised the insoluble cell fraction with guanidine hydrochloride and reformed chromatography of the denatured protein in urea. I chose the most robust nickel-chelate resin that I had available, as I needed to be sure it would withstand high ionic strength and strongly chaotropic conditions.

A (16 mm) Pharmacia column tube was packed to 5 ml with Amocol His-Buster resin, which is a nitrilotriacetic acid (NTA)-coupled microgranular cellulose. The NTA groups were charged with Ni^{2+}.

To denature and resolubilise protein, the supernatant was removed, insoluble pellet was resuspended in 10 ml BGdn20 (containing 3 M guanidine hydrochloride (Sigma)/ 42 mM Tris-HCl/ 8 mM Tris base/ 20 mM imidazole/HCl pH7.5/) as well as 1 mM DTT to dissolve protein. After mixing, the mixture was ultra-centrifuged at 560,000 x *g* for 20 min at 2 °C. The supernatant, which contained the solubilised target protein was collected and maintained on wet ice. The cleared solution was loaded onto the Ni-chelate column. To remove material that is not His_6-tagged, the column was first washed with 100 ml of A8U20 (8 M urea/20 mM imidazole) buffered with 0.5 M ammonium acetate to replace the ionic denaturant guanidine with non-ionic denaturant urea. The column was then washed state with 20 ml of A6U20, A4U20, A2U20 and A0U20 buffers containing (6 M, 4 M, 2 M and no urea/ 20 mM imidazole) respectively

to allow the protein to refold. After each wash, effluents were collected, and the flow was stopped for 30 min to allow slow refolding, except after the last wash when the flow was stopped for 1 h. His_6-tagged IL-36γ was then eluted with A0U200 buffer which contained (no urea/ 200 mM imidazole) (50 ml). Non-refolded protein was then eluted with a buffer containing 8 M urea and 200 mM imidazole (A8U200) buffer. A_{280} was measured by NanoDrop spectrophotometer. A yield of 27.6 mg of His_6-tagged-IL-36γ was obtained figure 3.7, as was determined, based on the predicted A_{280} for a protein of this molecular mass and content of tyrosine and tryptophan.

(a)

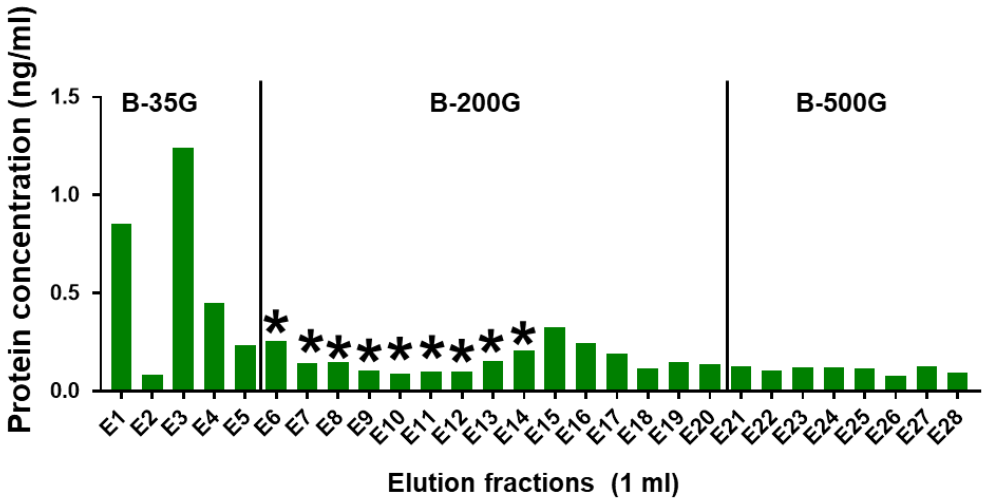

(b)

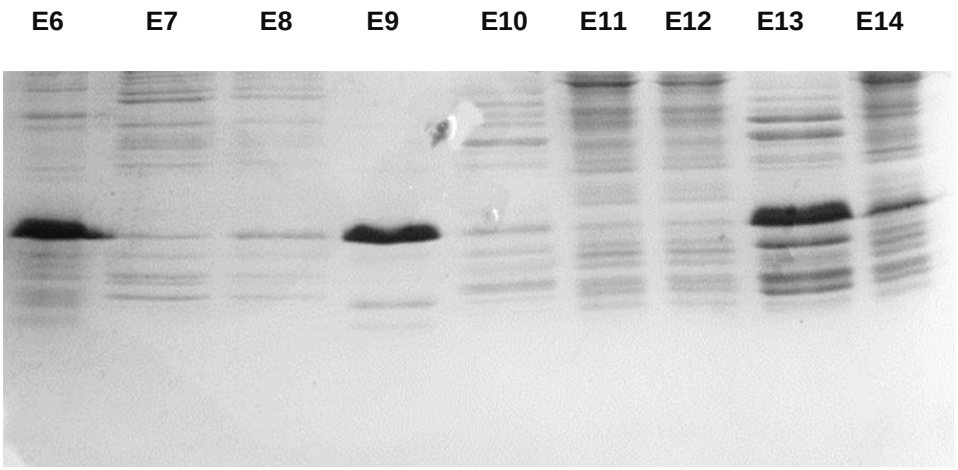

Figure 3.6 An elution pattern of His_6-tagged recombinant insoluble n^{18}-IL-36γ from nickel chelate Sepharose. (a) Protein concentration (mg/ml) per fraction on the Y-axis is presented against the eluted fractions on the X-axis. (*****) labelled samples represent the pooled eluted fractions. Imidazole buffer (B-200G) was used in an attempt to elute the His_6-tagged n^{18}-IL-36γ. Fractions (1 ml) were collected. The protein concentration was calculated from Nanodrop spectrophotometer measurements of A_{280}. **(b)** SDS-PAGE Analysis of eluted fractions. Lanes 1-9 be composed from B-200G buffer elution fractions (E6-E14).

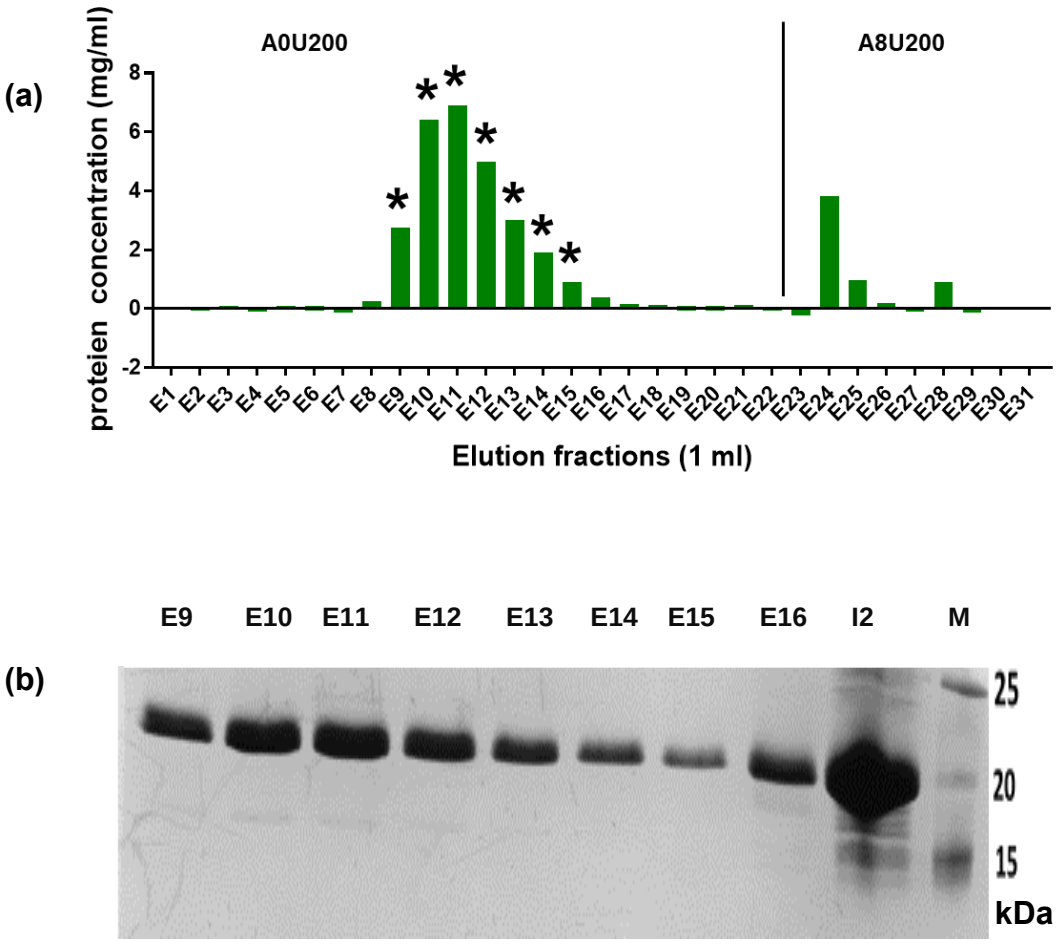

Figure 3.7 An elution pattern of His_6-tagged recombinant n^{18}-IL-36γ. (a) Protein concentration (mg/ml) per fraction on the Y-axis is presented against the eluted fractions on the X-axis. (*****) labelled samples represent the pooled fractions. No urea/ 200 mM imidazole buffer (A0U200) was used to elute the His_6-tagged n^{18}-IL-36γ and 1 ml fractions for the first 15 ml (E1-E15), then 5 ml for the remainder were collected (E16-E22). To elute failed non-refolded protein, 8 M urea/ 200 mM imidazole buffer (A8U200) was used and 5 ml fractions were collected (E23-E31). **(b)** SDS-PAGE analysis of recombinant re-folded 6xHis-tagged recombinant n^{18}-IL-36γ. Lanes (1-8) be composed from A0U200 buffer elution fractions (E9 – E16). I2: BGdn20 buffer elution fraction (of the starting material).

3.4 In vitro processing of precursor proteins

The sequence of recombinant IL-36β and IL-36γ proteins was designed to contain a His_6-tagged N-terminal that could be removed by chymotrypsin and thrombin respectively. High concentration fractions of His-tagged proteins were identified and pooled as in figures 3.5 and 3.7 and dialysed against digestion buffer.

For IL-36β precursor, the pooled fractions contained ~ 38 mg protein in 7.5 ml after being dialysed. Similarly, IL-36γ precursor, the pooled fraction contained ~ 19.2 mg protein in 4 ml after being concentrated and dialysed in a tangential concentrator.

3.4.1 Processing of His_6-tagged n^5-IL-36β by chymotrypsin

The experiment was carried out to optimise the effective chymotrypsin concentration required for IL-36β digestion. IL-36β (50 μg in 10 μl) of was digested with different masses of chymotrypsin 200, 100, 50, 25 12.5 ng and 0 for 1 hr at 30 °C. For protein processing analysis, 5 μl of the inhibitor (PMSF) was added into the protein samples before they were immersed in a boiling water bath for 5 min and 1/15th of processed denatured samples were run on the SDS page gel. Undigested protein was also run as a negative control.

SDS-PAGE electrophoresis revealed that digestion of n^5-IL-36β with 1/500 of chymotrypsin mass ratio was the most effective ratio leading figure 3.8, panel (a) Lane 2). n^5-IL-36β protein pool was digested with 1/500 of chymotrypsin mass ratio at 30 °C for 1 h. The enzyme was inhibited with 1 mM PMSF. Samples were taken before and after digestion for SDS-PAGE (see figure 3.8 b).

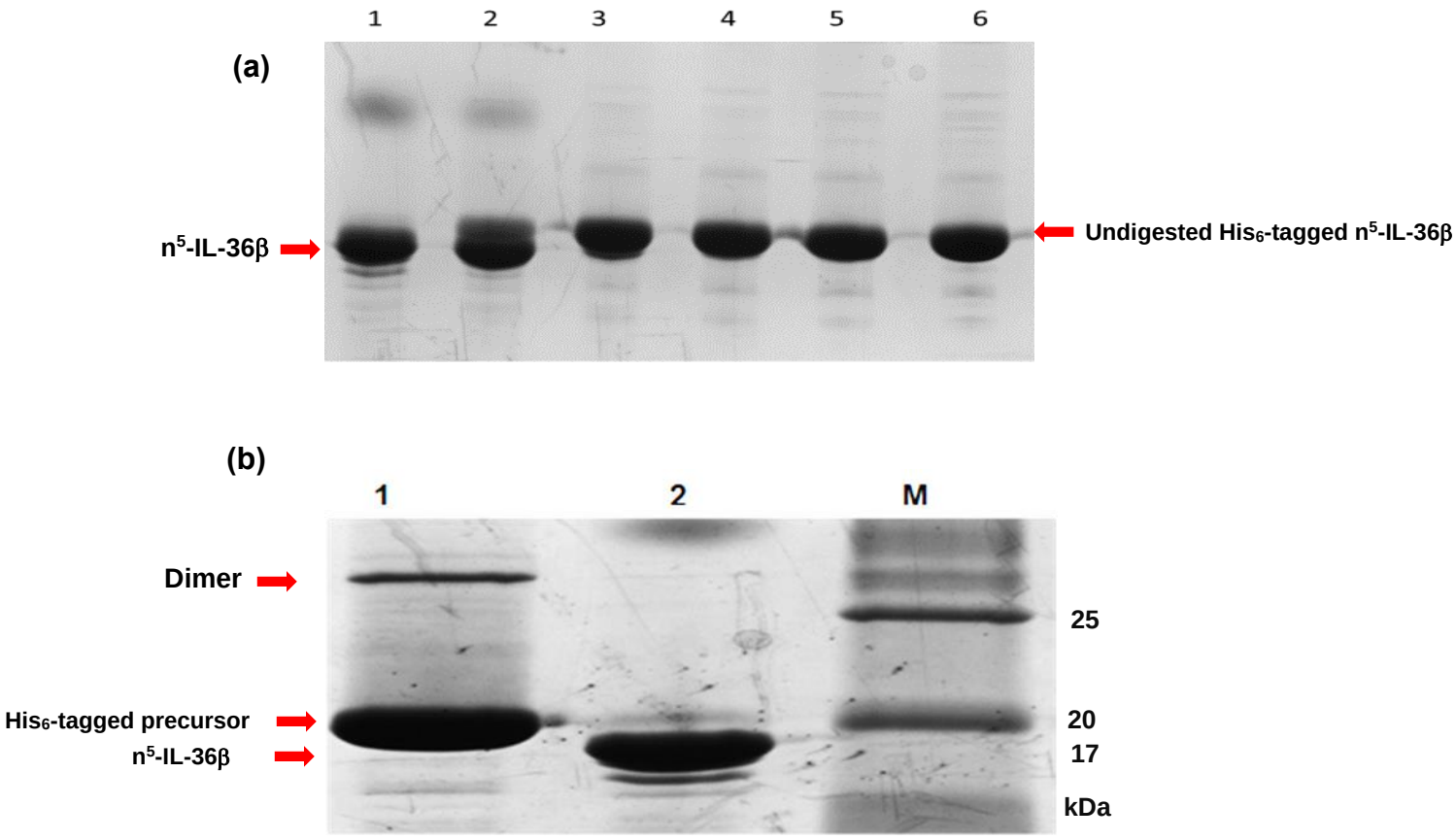

Figure 3.8 The SDS-PAGE analysis of small scale and large-scale digestion of His_6-tagged n^5-IL-36β by chymotrypsin to remove His_6-tag at 30 °C for 1 h. (a) Optimization of chymotrypsin mass ratio for His_6-tagged IL-36β digestion for 1 hr. Processing of IL-36β (50 μg in 10 μl) by a logarithmic range of chymotrypsin doses. Protein was incubated at 30 °C for 1 hr with following chymotrypsin. Lane 1: 200 ng, Lane 2: 100 ng, Lane 3: 50 ng, Lane 4: 25 ng, Lane 5: 12.5 ng and Lane 6: buffer D only. **(b)** Digestion of 5 mg/ml of His_6-tagged IL-36β with 10 μg/ml chymotrypsin. Lane 1: undigested sample of His_6-tagged IL-36β, Lane 2: Sample of the chymotrypsin digested IL-36β. M shows the molecular weight standards.

3.4.2 Processing of His_6-tagged n^{18}-IL-36γ protein by thrombin

To optimise the concentration of thrombin to achieve complete digestion of IL-36γ protein, a small volume of His_6-tagged n^{18}-IL-36γ protein fraction (5 μg in 10 μl) was tested with various concentrations ranges between 0.625 and 1 unit per 50 μg substance of the thrombin for 24 h.

SDS PAGE was used to analyse a small sample of the product (figure 3.9, a). For protein processing analysis, 1 mM PMSF was added into the protein samples before they were immersed in boiling water bath for 5 min and 1/15th of processed denatured samples were run on the SDS page gel. Undigested protein was also run as a negative control.

SDS-PAGE electrophoresis revealed that all concentrations tested were effective in converting almost all of precursor to n^{18}-IL-36γ. The identity of the product was confirmed by mass spectrometry. Because 0.0625 U thrombin/50μg precursor led to >90% processed protein, so the n^{18}-IL-36γ protein pool was digested with 0.0625 U thrombin ratio at 30 °C for 24 h, and the enzyme was inhibited with 1 mM PMSF. Samples were taken before and after digestion for SDS-PAGE (figure 3.9, b).

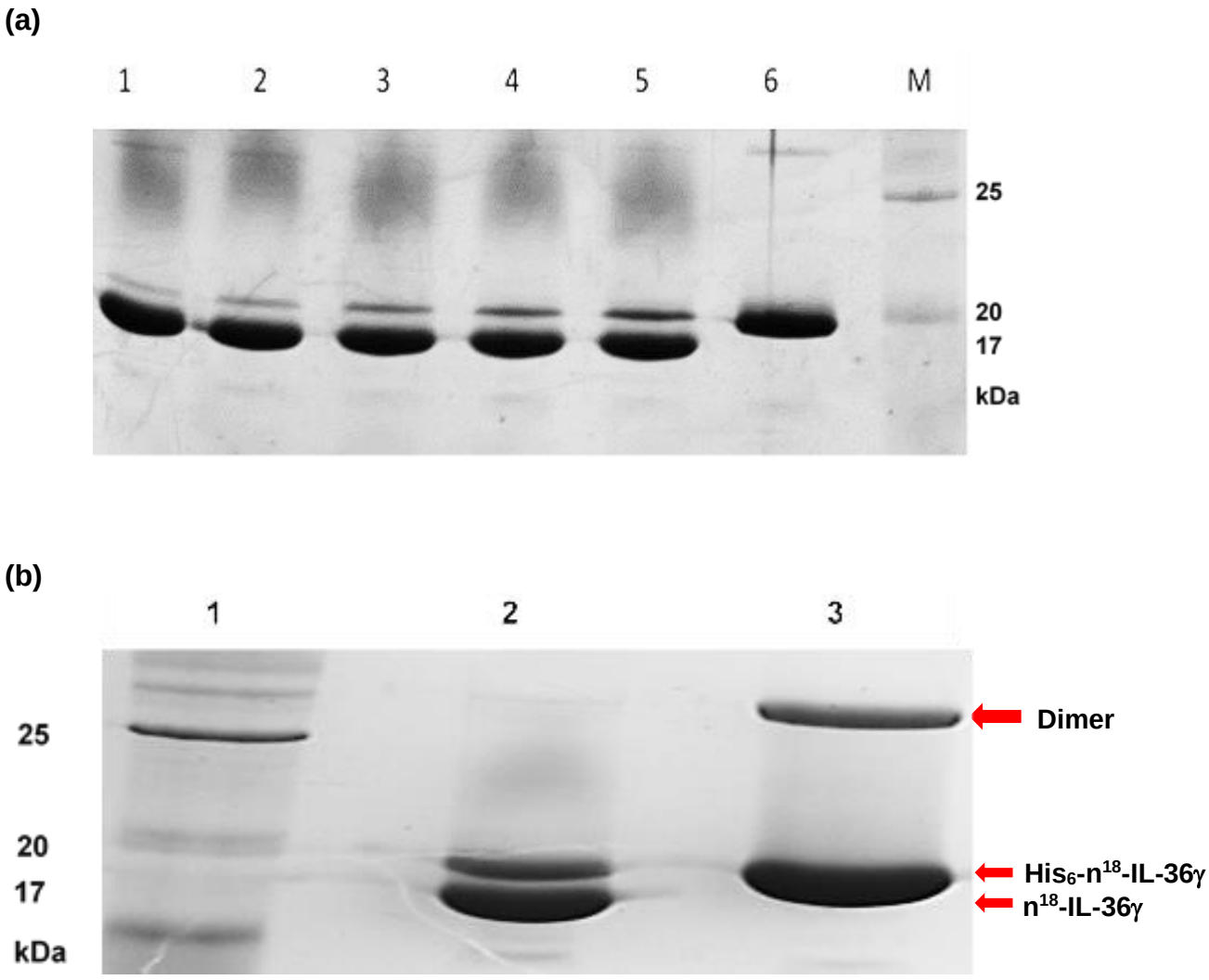

Figure 3.9 Digestion of His_6-tagged-IL-36γ digestion with thrombin. (a) Optimization of thrombin concentration for His_6-tagged-IL-36γ digestion for 24 hr at 30 °C**.** Processing of His_6- tagged-IL-36γ (50 μg in 10 μl) by a logarithmic range of thrombin doses. The protein was incubated for 30 °C for 24 hr with 1 U thrombin (Lane 1), 0.5 U (Lane 2), 0.25 U (Lane 3), 0.125 U (Lane 4), 0.0625 U (Lane 5), with buffer only (Lane 6). [1 U ~ 0.35 μg thrombin]. **(b)** Digestion of 4.8 mg/ml His_6-tagged IL-36γ with 2 μg/ml thrombin for 24 h at 30 °C. Lane 1: Standard marker, Lane 2: Digested His_6-tagged-IL-36γ and Lane 3: Undigested His_6-tagged-IL-36γ.

3.5 Removal of the residual His_6-tagged proteins by Ni-chelate affinity chromatography

To remove both the free tagged peptide and any residue of undigested protein from protein pools, a small Ni-NTA agarose resin column was used. IL-36β or IL-36γ proteins pools were loaded three times through a 2 ml Qiagen Ni-chelate agarose column, which has much lower ion-exchange capacity compared to the Ni-NTA cellulose resin matrix, and the column was washed with buffer D to elute unbound protein which was not tagged (see figure 3.10, a). SDS-PAGE electrophoresis showed that the band corresponding to the His_6-tagged protein from the elution fractions had been removed compared to the wash fractions (see figure 3.10, b).

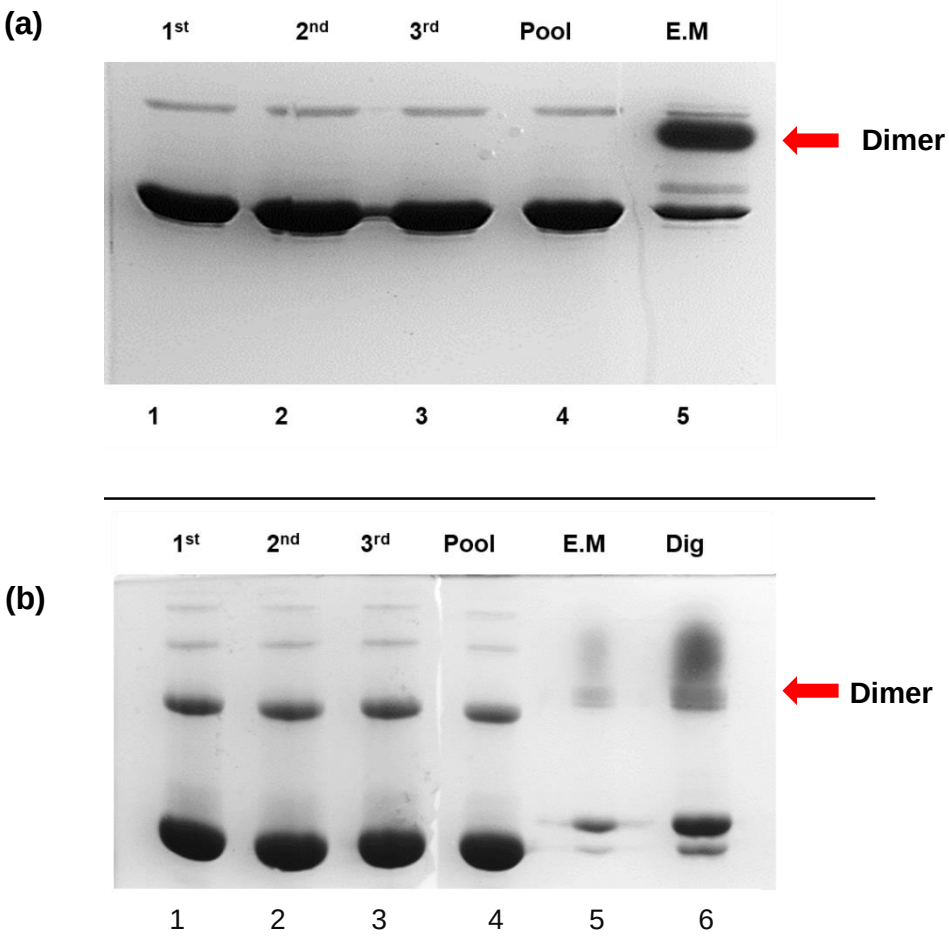

Figure 3. 10 Removal of the remaining His-tagged proteins and any residue of undigested protein from digested of His_6-tagged n^5-IL-36β and n^{18}-IL-36γ pools. (A) To remove of His-tagged material from chymotrypsin digested n^5-IL-36β protein, n^5-IL-36β protein pool was reloaded three times through nickel chelate agarose. SDS-PAGE of the effluent is shown in Lanes 1-3 for the removal of the remaining His-tagged proteins. SDS-PAGE of the pooled protein was loaded in lane 4. Eluted His-tagged molecule (E.M) is residual eluted material that binds to the matrix and are eluted by buffer D and 200 mM imidazole was performed in Lane 5. (B) Removal of His-tagged material from thrombin digested n^{18}-IL-36γ protein. n^{18}-IL-36γ protein pool was reloaded three times through the column (Lanes 1-3) for the removal of the remaining His_6-tagged proteins. Pooled fractions are shown in lane 4. Eluted His-tagged molecule (E.M) is residual eluted material that binds to the matrix and are eluted by buffer D and 200 mM imidazole was performed in Lane 5. Lane 6 shows the components of digested His_6-tagged-n^{18}-IL-36γ protein pool with thrombin.

3.6 Subsequent purification of processed IL-36β and IL-36 γ proteins purification by FPLC

3.6.1 Testing further purification of n^5-IL-36β and n^{18}-IL-36γ

n^5-IL-36β and n^{18}-IL-36γ were required to be highly purified and endotoxin free for cell biology experiments.

Processed proteins were purified entirely by repeat loading of 1 ml Resource S or Q columns which were fitted to an FPLC system for IL-36β and IL-36γ respectively. n^5-IL-36β was purified in pH 6.2 MES/NaOH buffer with NaCl on Mono-S. n^{18}-IL-36γ was purified in a pH 8.8 Tris/HCl buffer with 0-0.5 NaCl buffer on Resource Q. reloaded (2 mg per loading) into the system and eluted with a gradient of 0-0.5 M NaCl buffer. The flow rate was maintained at 1 ml/min and fraction size at 0.6 ml. NanoDrop spectrophotometer measurements (A_{280}) showed that the total protein yield in the peak fractions appeared to be <25% than the amount of protein that was initially loaded as in figure 3.11 and 3.12.

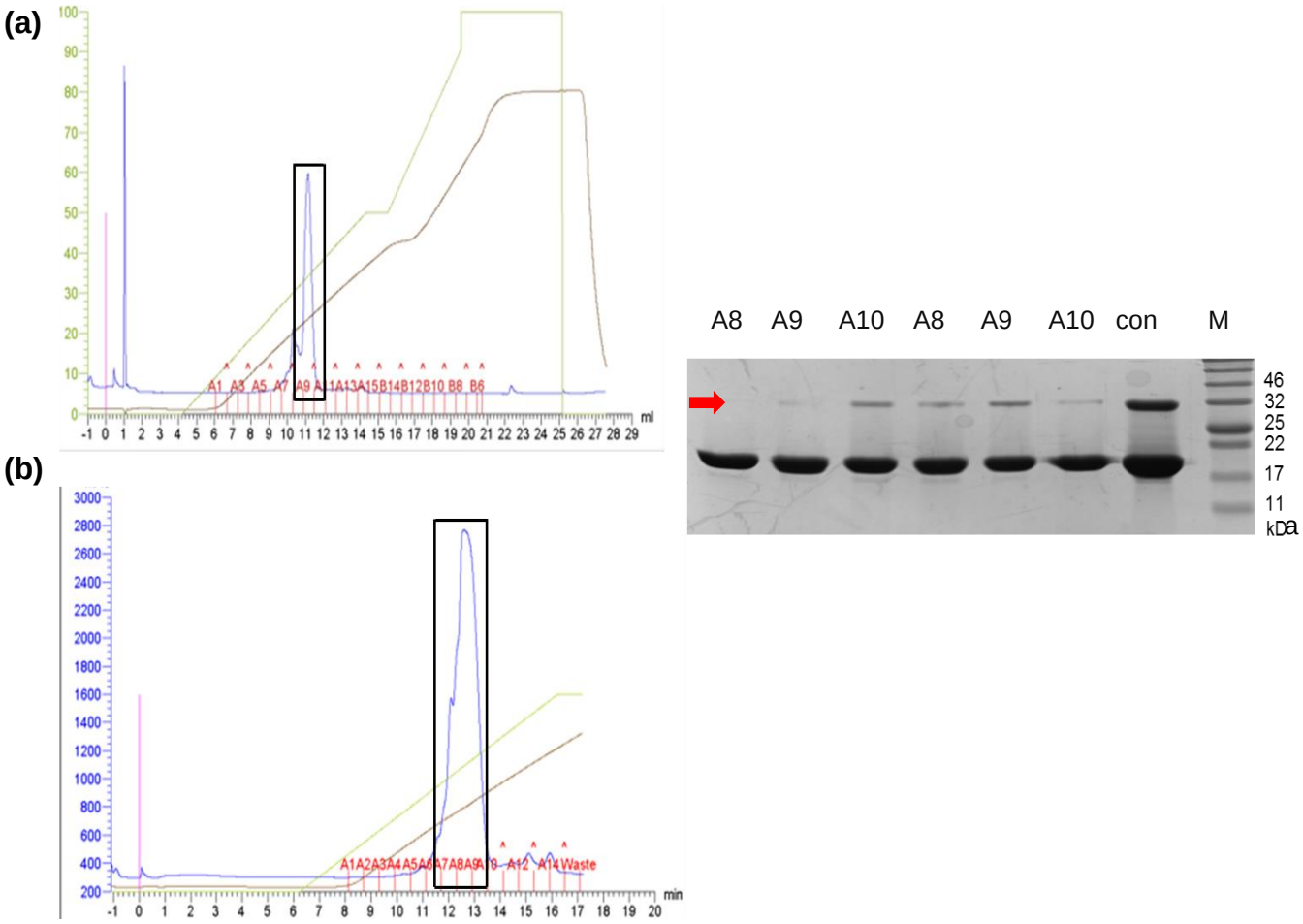

Figure 3.11 Two elution curves of 2 mg of n^5-IL-36β from a 1 ml mono S column. On Y-axis, the blue curve shows the A_{280} (mAU). The green curve shows the mixing ratio of the content of pump B with pump A and the brown curves show the conductivity recording. Pump A contained 20 mM MES, pH 6.2/ 1 mM DTT/ 10 % glycerol. Pump B contained 10 mM NaOH, pH 6.2/ 0.5 M NaCl/ 1 mM DTT/ 10 % glycerol. Chromatograph was performed at ~ 22 °C. The X-axis indicates the elution volume (ml) while the red signals show the tube numbering in which the purified protein is collected. The dead volume from the UV monitor to the fraction collector was measured in 0.6 ml, therefore the indicator for a fraction change (such as "A8" on the graph) falls at the end of the 0.6 ml of material. The black box B thus represent fractions A8, A9, and A10. Dimers are shown (red arrow). Mass spectrometry was used to determine molecular weight (See appendix figure A.2).

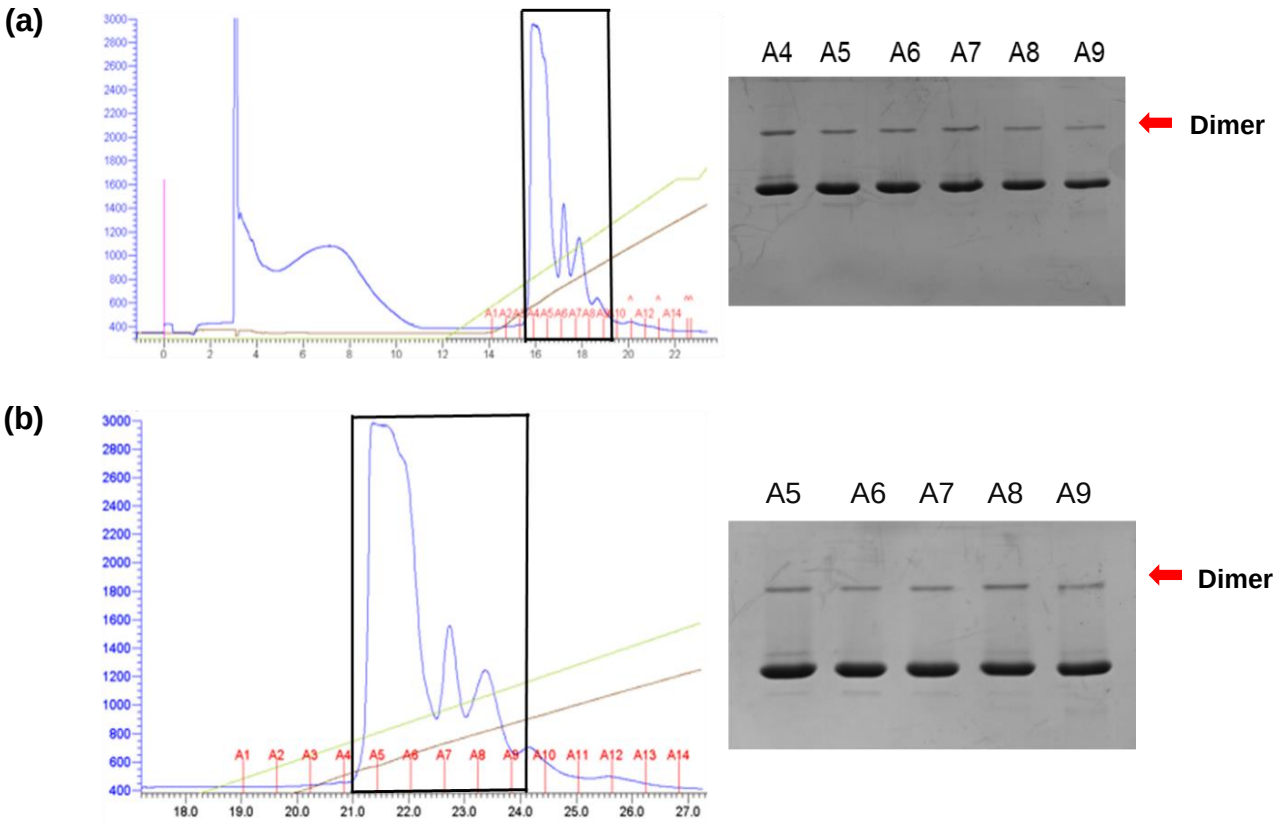

Figure 3.12 Two elution curves of 2 mg of n^{18}-IL-36γ using Resource Q column. On Y-axis, the blue curves show the A_{280} (mAU) and the brown curves show the conductivity levels. The green curve indicates the mixing ratio of the content of pump B with pump A. Pump A contained 50 mM Tris HCl, pH 8.8/ 1 mM DTT/ 10 % glycerol. Pump B contained 50 mM Tris HCl, pH 8.8/ 0.5 M NaCl/ 1 mM DTT/ 10 % glycerol. Chromatography was performed at ~ 22 °C. The x-axis indicates the elution volume (ml) while the red signals show the tube numbering in which the purified protein is collected. The black border shows absorbance of displayed fractions corresponding to the elution of IL-36γ protein taking into account the 0.6 ml delay from the UV monitor to the fraction collector. Mass spectrometry was used to determine molecular weight (See appendix figure A.3)

3.7 HT-29 cells cloning to test mutant IL-36 proteins

To test the biological activity of the n^5-IL-36β and n^{18}-IL-36γ that I prepared, in addition to IL-36α forms that are prepared in our lab, HT-29 cells were used. These cells are carrying a stable pGL4.32 *luc2p*-NFκB-Hygro plasmid. I cloned these cells before being used. Twenty-one clones of cells were obtained as described in section 2.7.1. All obtained clones were tested for luciferase output after being treated with 5 nM IL-36α or being left unstimulated for 6 hr. The D7 clone showed high expression and ~ 500-fold increase in luciferase gene expression compared to unstimulated cells as shown in figure 3.20.

3.8 *IL1RL2* gene disruption in the HT-29 cells

To confirm that IL-36 proteins are not contaminated with other NF-κB activators, a negative control was required. Because HT-29 cells express endogenous IL-36R and they respond strongly to both IL-1α and IL-36α, I disrupted the *IL1RL2* gene, the only known IL-36R gene in the luciferase-reporter line D7 (section 3.7) by transient transfection of the cell line with two CRISPR guide plasmids. The CRISPR plasmids carried a puromycin resistant gene that was used for transient selection of plasmid transfected cells. Cells were co-transfected to allow us to confirm that DNA had been taken up. figure 3.13. I targeted used to attack exon 5 of *IL1RL2* (IL-36R) as described in section 2.7.3. Cells were selected and cloned as described in section 2.7.3. Eight Clonal lines were tested for luciferase expression in response to 5 nM IL-36α or 5 nM IL-1α compared with no cytokine for 6 h. Three selected clones that gave a strong response to IL-1α but not IL-36α were retested again with 5 nM n^6-IL-36α, 5 nM n^5-IL-36β and 10 ng /ml or 5 nM IL-1α compared with no cytokine for 6 h genomic DNA was extracted from three IL-36 non-responsive lines and exon5 of *IL1RL2* was sequenced and exon 5 of *IL1RL2* was sequenced. One of these clones that showed no response to the added IL-36α or IL-36β but did respond to TNF compared with D7 clone figure 3.14 was arbitrarily selected to be a negative control.

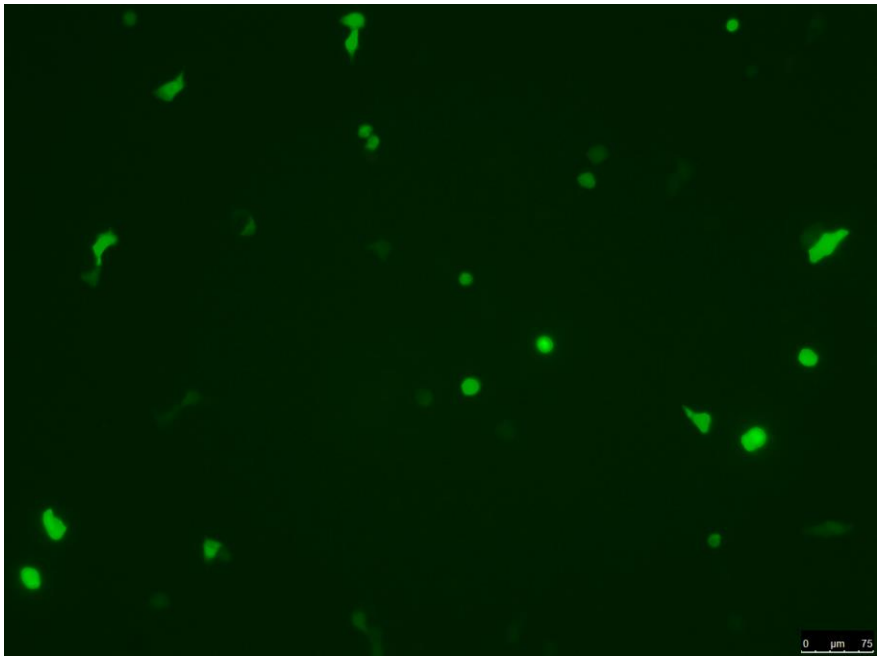

Figure 3.13 Confocal microscopical analysis after 24 hr of CRISPR1 and CRISPR2 transfected HT-29 cells. HT-29 cells were transfected with CRISPR plasmids that carry puromycin resistance marker and co-transfected with PMX-GFP plasmid which leads to green fluorescence as a positive control for transfection. Transfection was with Mirus reagent (6 μg) for 24 hr. Transfected clones were transiently selected for 48 h on a puromycin-containing medium.

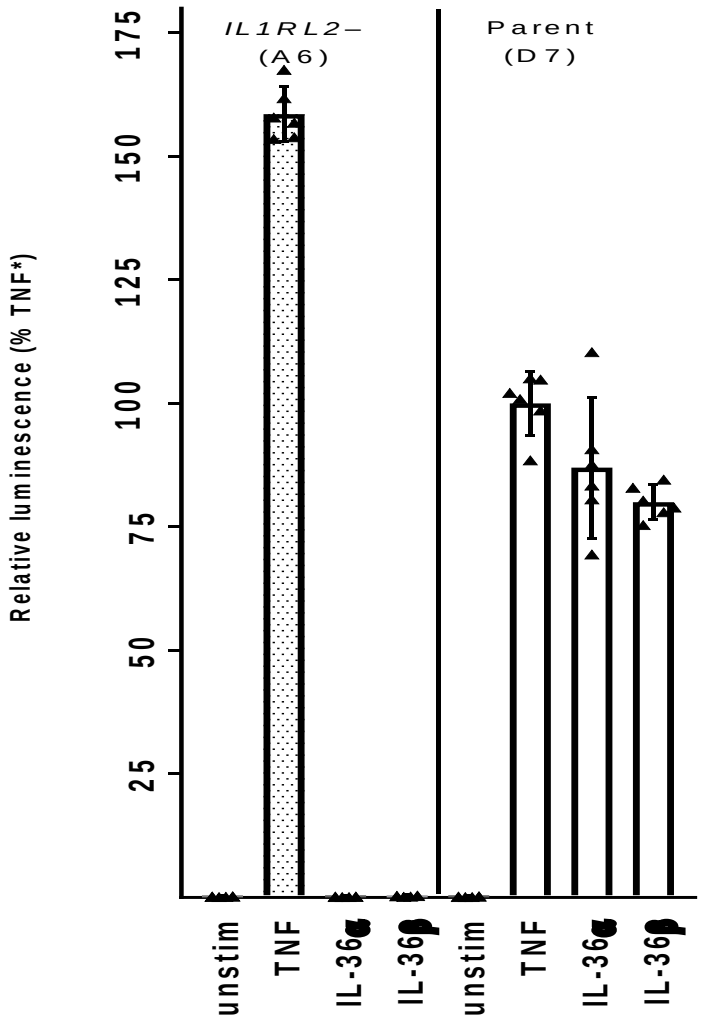

Figure 3.14 Response of cloned A6 HT-29 subline (IL1RL2-disrupted) and parent D7 to TNF and IL-36 for 6 hr. A6 and D7 were treated with 5 nM n^6-IL-36α, 2 nM n^5-IL-36β or 50 pM TNF (positive control) as well no treatment (negative control) for 6 h. (*****) labelled represents the relative luminescence is standardised to the output from TNF stimulated D7. A luciferase assay was used to measure luciferase output in response to stimuli. Data (n= 5) are the mean and 95% confidence limit of the mean of each normalised dataset from one representative experiment of at least 2 independent experiments with similar outcomes.

3.9 DNA extraction from IL-36R (*IL1RL2*)-disrupted clone and amplification of exon 5

To identify the genetic defect of the IL-36R in the clones transfected with CRISPR plasmids, DNA was extracted from IL-36R disrupted out clones (A6, E3 and G4), in addition to standard HT-29-κB-*luc* D7, as a positive control as described in the section 2.7.4. The targeted sequence was amplified from extracted DNA samples by PCR. To optimise the PCR products, different concentrations of standard HT-29 cell (D7) DNA sample 500, 150, 50, 15 and 5 ng were tested as well as different annealing temperature 52 °C, 56 °C, and 58 °C (Figure 3.15). After determining the optimum concentration and annealing temperature, exon 5 of *IL1RL2* of the IL-36 unresponsive clones were amplified using e5IL-36R primer pairs. The optimum condition of 150 ng of genomic DNA per reaction was used. Pre-measure annealed at 58 °C, as shown in figures 3.16. PCR products were sequenced with the same PCR primers. Sequences showed a deletion 36 nucleotides and 1 nucleotide in one detectable allele of the exon 5 of IL-36R (IL-1RL2) in G4 and E3 clone respectively. Cell line A6 showed two mutations, a 36 and 12 nucleotide deletion in two alleles as shown in figure 3.17.

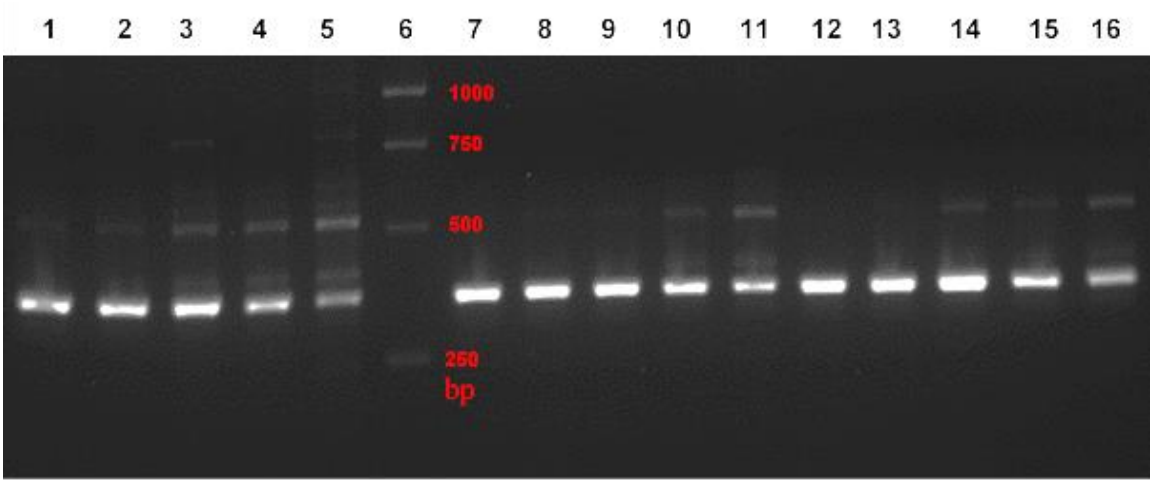

Figure 3.15 Optimisation of DNA concentration and annealing temperature of genomic PCR by using D7 clone DNA sample. HT-29 genomic DNA was extracted. Genomic PCR was performed with appropriate primers and visualised on 0.7% agarose gel. Line 1: (500 ng, 52 °C), lane 2: (150 ng ,52 °C), lane 3: (50 ng, 52 °C), lane 4: (15 ng, 52 °C), lane 5: (5 ng, 52 °C), lane 6: (1 kb ladder), lane 7: (500 ng ,56 °C), lane 8: (150 ng ,56 °C), lane 9: (50 ng, 56 °C), lane 10: (15 ng, 56 °C), lane 11: (5 ng, 56 °C), lane 12: (500 ng,58 °C), lane 13: (150 ng, 58 °C), lane 14: (50 ng, 58 °C), lane 15: (15 ng, 58 °C), lane 16: (5 ng, 58 °C).

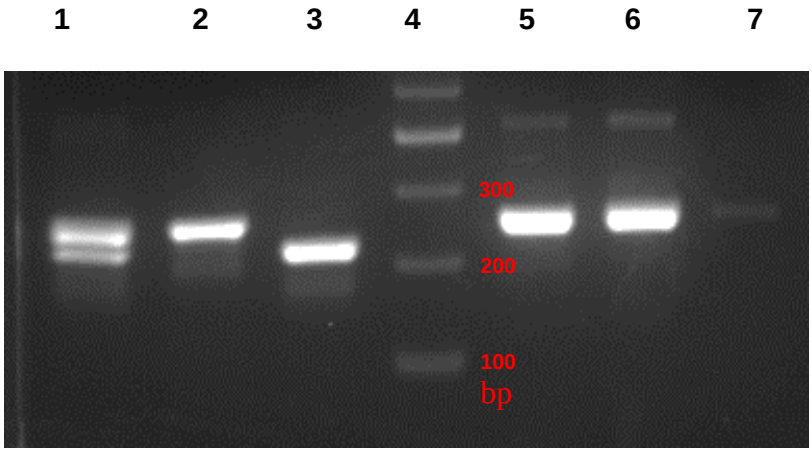

Figure 3.16 Gel electrophoresis of the genomic PCR product from exon 5 of IL-36 unresponsive cell lines and knocked out clones A6, G4 and E3 and the parent line D7. Lane 1: A6 Clone (150 ng, 58 °C). Lane 2: G4 Clone (150 ng, 58 °C). Lane 3: E3 clone (150 ng, 58 °C). Lane 4: DNA molecular weight standards. Lane 5: standard D7 clone (150 ng, 58 °C). Lane 6: Standard D7 clone (150 ng, 58 °C). Lane 7: Blank (water).

(a) *IL1RL2*$^{\Delta 12}$

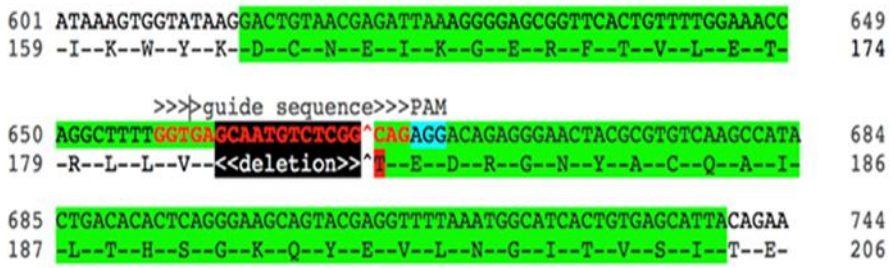

(b) *IL1RL2*$^{\Delta 36}$

Figure 3.17 Predicted open reading frame (ORF) disruption of IL-36R gene (IL1RL2) in HT-29/κB-lucP2 (D7) derived (a) G4 cell lines (b) A6 cell line. The disruption of the open reading frame, as determined by genomic sequencing, is shown here in the context of the cDNA sequence of IL-36R. The A6 clone carried two different disrupted IL1RL2 alleles**.** The plasmid encoded CRISPR guide sequences are shown in red script within exon 5 (shaded green) of IL1RL2. The identified deletions are shown in black. Mutations were created by separate Cas9/CRISPR events that targeted exon 5. The PAM motif that is required by Cas9, is highlighted with cyan. The predicted primary double strand break sites are indicated with '^'. The deleted segment of each allele is shaded with black. See appendix VIII for pSpCas9(BB)-2A-Puro (PX459) V2.0 structure and the guide oligonucleotides sequence.

3.10 Efficacy test of IL-36 mutants on standard D7 HT-29 clone (IL-1RL2^{+}/$^{+}$) and the IL-36R deficient A6 cell line

Towne et al., 2004 reported that HT-29 cells express IL-36R. Nishida et al., 2016 showed that HT-29 cells respond to stimulation with IL-36. To determine the effective dose of IL-36 receptor, A6 and D7 clones were plated at 253 x 10^3 cells per well in 1 ml of HSM/ well of 24 well plate. A total of 13 24-well plates were used for HT-29 D7 (*IL1RL2*$^{+/+}$) while 8 plates of 24-well plate were used with HT-29 A6 (*IL1RL2*$^{-/-}$) as described in section 2.7.6, IL-1RL2^{+}/$^{+}$ and IL-1RL2^{-}/$^{-}$ HT-29 cells were treated with doses of n^1-IL-36α and n^4-IL-36α, n^6-IL-36α and the two N-terminal mutations n^6-K6S-IL-36α and n^6-K6G-IL-36α, which had been purified by ion exchange chromatography by my colleagues, in addition to preparation of n^5-IL-36β or n^{18}-IL-36γ as described in this thesis. IL-1α and TNF were used as positive controls as in Table (2.4). Cells were incubated for 6 hr with these inflammatory stimuli. Five or six replicates were used for each dose. After cell lysis in 250 μl of (1x) lysis buffer, 5 μl of each sample was transferred into a 96-well plate and supplemented with D-luciferin and ATP. Data showed that the expression of the luciferase reporter gene was induced at a similar level in response to n^6-IL-36α, n^5-IL-36β and n^{18}-IL-36γ compared with TNF. n^6-IL-36α, n^5-IL-36β and n^{18}-IL-36γ seemed to reach half-saturation at 3.37 nM, 0.12 nM and 19.5 nM, respectively, and their maximum response was 6-fold higher than with IL-1α. Graphpad (Prism) was used to analysis these data (figure 3.18).

Data also showed that n^6-K6S-IL-36α and n^6-K6G-IL-36α induce NF-κB to the same level as n^6-IL-36α, but their effective concentration biological activity is less than n^6-IL-36α (figure 3.19).

Moreover, the absence of any significant signal from our IL-36 proteins in cell line A6 compatible with there being only one IL-36 receptor. These findings confirm that the active component in all IL-36 preparations is IL-36 and that there is no significant contamination with bacterial activators of NF-κB, (figure 3.20).

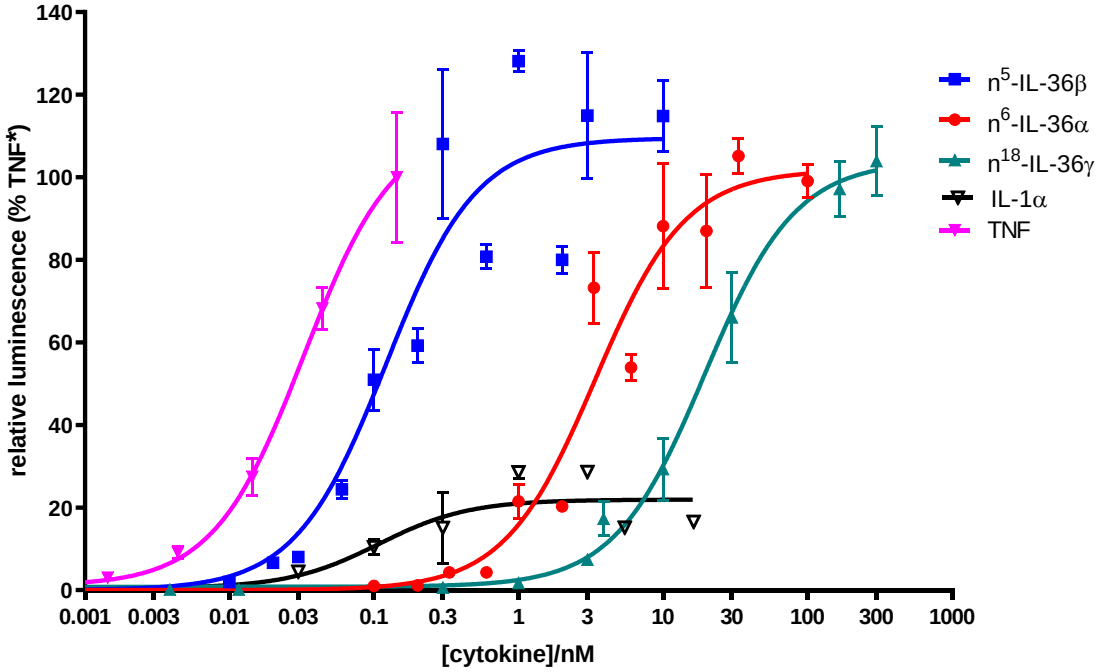

Figure 3.18 The efficacy of active IL-36β and IL-36γ proteins in activated HT-29 cells. A luciferase reporter assay was used to measure the activity of NF-κB in HT-29 cells. (*****) labelled represents the relative luminescence is standardised to the output from TNF stimulated D7. Active n^6-IL-36α forms, TNF and IL-1α were used as a positive control. Data were fitted to a 4-parameter dose response curve but with a Hill coefficient fixed at 1.5. Protein concentration of IL-36 forms were determined spectrophotometry. Each set of data (n= 5-10) represents the mean and 95% confidence limit of the mean of each normalised dataset of at least 3 independent experiments with similar outcomes. Central estimates and 95% confidence limits of EC_{50} for the three IL-36 proteins were calculated by non-linear regression with GraphPad-Prism software. Values were: IL-36α, 3.33 nM (2.68-3.99 nM); IL-36β, 0.121 nM (0.097-0.147 nM); IL-36γ, 18.2 nM (15.6-19.9 nM) and were therefore significantly different from one another.

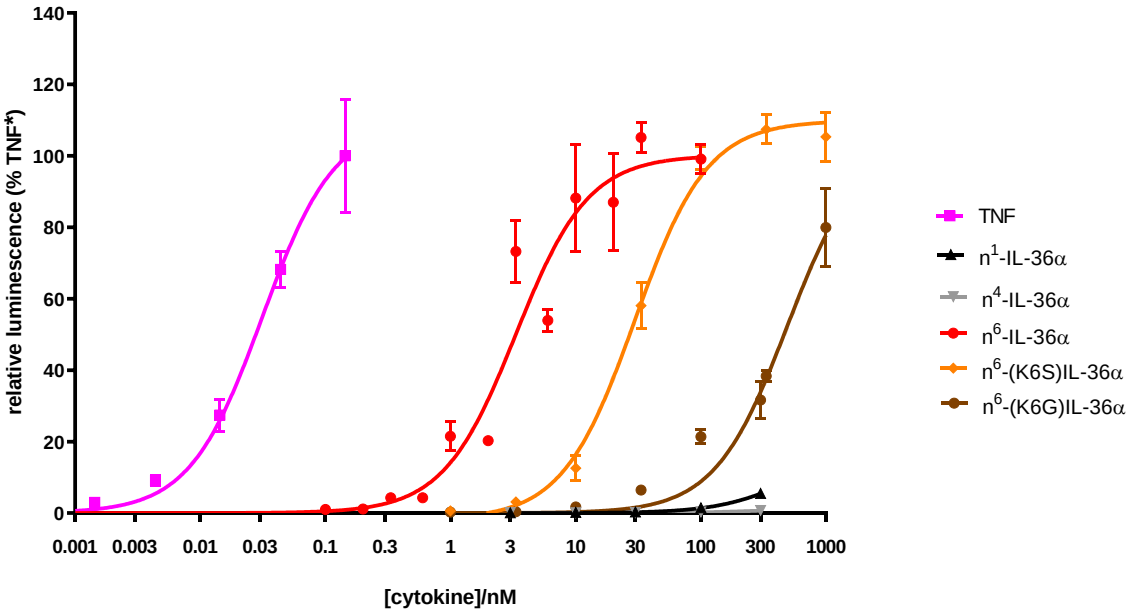

Figure 3.19 The efficacy of N-terminal-modified forms of IL-36α in stimulating the kB-dependent luciferase expression in HT29-kB-luc2P. Results are derived from a series of experiments and have been normalised to the mean response to 50 pM recombinant human TNF in each data set. TNF and n^6-IL-36α datasets are repeated from Figure 4.21. Data (n= ≥5) are the mean and 95% confidence limit of the mean of each normalised dataset from one representative experiment of at least 2 independent experiments with similar outcomes. Central estimates and 95% confidence limits of EC50 for the three n6-IL-36α derivatives were calculated by non-linear regression with GraphPad-Prism software. Values were: n^6-IL-36α, 3.33 nM (2.68-3.99 nM); n^6-(K6S) IL-36α, 29.8 nM (26.5-33.4 nM); n^6-(K6G) IL-36α, 489 nM (lower limit uncertain, upper limit 542 nM) and were therefore significantly different from one another.

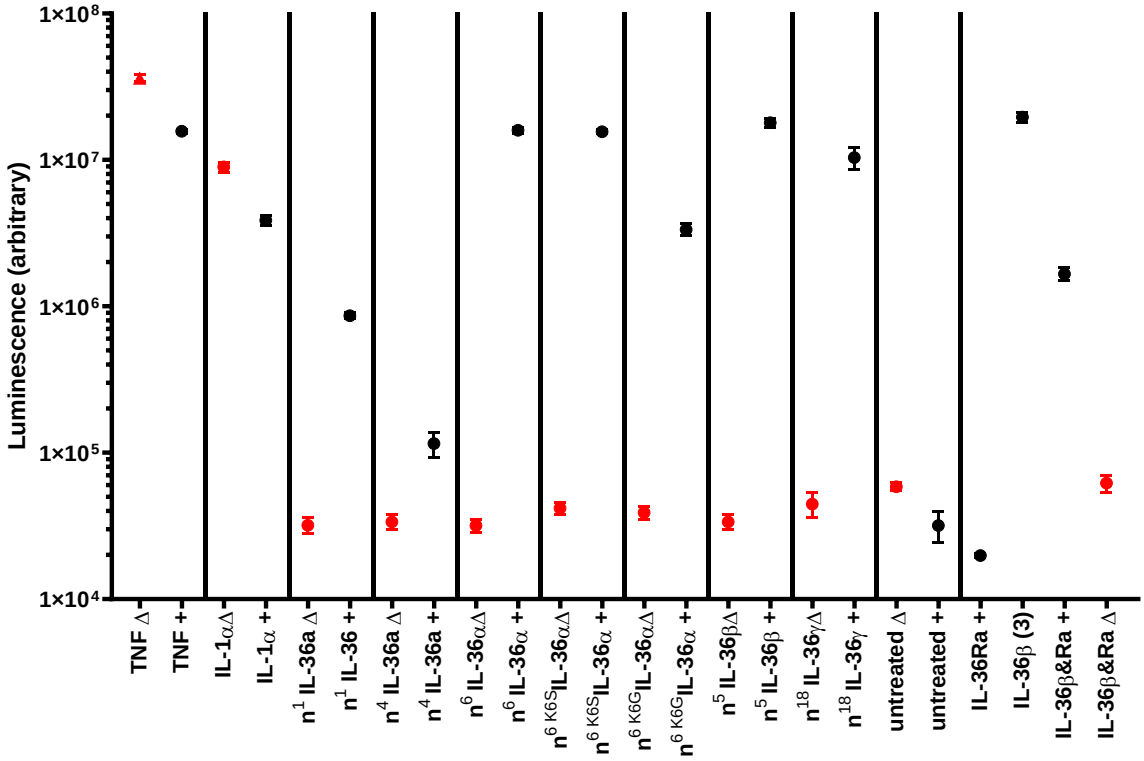

Figure 3.20 The validation of receptor specificity of our cytokine preparations in HT29 cells. *Comparison of luciferase activity in parallel activations of the IL1RL2$^{-/-}$A6 line ("Δ", red symbols) and parent D7 HT-29/κB-lucP2 ("+", black symbols) on a logarithmic scale*. Data (n= 5) are the mean and 95% confidence limit of the mean of each normalised dataset from one representative experiment of at least 2 independent experiments with similar outcomes.

3.11 Time course stimulation of HT29-kB-luc with n^6-IL-36α, n^5-IL-36β and TNF

To determine duration of NF-κB activation in response to IL-36 cytokines, HT-29 (D7 clone)/ 2.35 x 10^5 cells were grown on the 24-well plates in total volume 1 ml. As usual, the cells were grown for three days and then medium was drained and replaced with 0.5 ml of LSM for 18 hr. Cells were treated with 5 nM IL-36α, 0.2 nM IL-36β or 10 ng/ml TNF in total volume 0.6 ml for (3, 6, 9, 12, 18, and 24 hr).

Our results show that IL-36α and IL-36β gave comparable time courses to TNF. A broad peak of activity between 3 h and 9 h was shown by all three stimuli. Thereafter activity declined with a half-life of ~ 2 hr reaching a low plateau at ~ 18 h when ~ 10% of luciferase activity was present compared to the maximum figure 3.21.

Later experiments have demonstrated that the cells have become non-responsive are still viable. I, therefore, tested whether non-responsive cells could be re-stimulated.

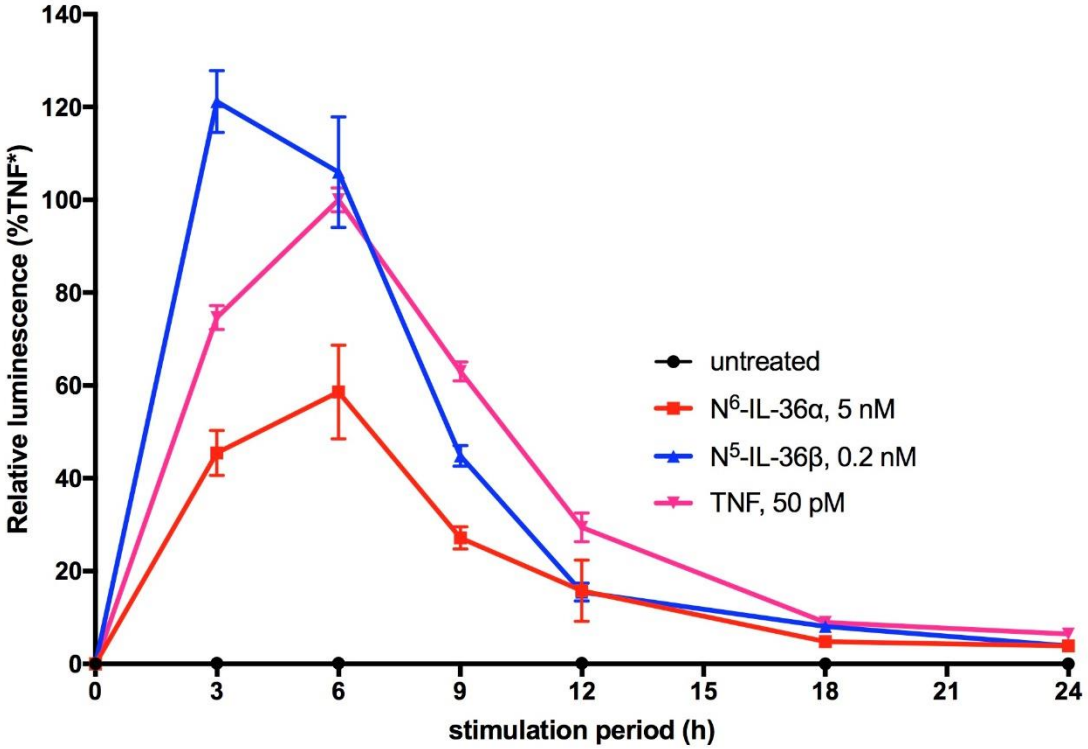

Figure 3.21 The time course of the response of the destabilised luciferase reporter of NF-κB in HT-29 derivative D7. D7 cells were incubated with n^6-IL-36α, n^5-IL-36β or TNF at different time points**.** The cytokine was continuously present during the stimulation period. Data (n= 5) are the mean and 95% confidence limit of the mean of each normalised dataset from one representative experiment of at least 2 independent experiments with similar outcomes.

3.12 Re-stimulation of non-responsive HT-29 cells with n^6-IL-36α, n^5-IL-36β or TNF

I tested whether cells could respond to a cytokine after having been treated with the dame different cytokine for 18 h, which is long enough for the response to be gradually reduced (Figure 3.22). HT-29 (D7 clone)/ 2.20 x 10^5 were grown as before in 24 well plates and serum starved, as before. Sixteen wells were used for each initial treatment, which were (a) with 10 ng/ml TNF, (b) with 10 nM n^6-IL-36α, (c) with 0.2 nM n^5-IL-36β or (d) without cytokine. The initial treatment was for 18 h. After this, supplementary medium was added so that four wells of each initial treatment then received the same set of four treatments for 6 h. Cells that had not received cytokine for the first 18 h responded very strongly to all cytokine treatments. Cells had been treated with IL-36 or TNF became poorly response to IL-36 or TNF. This result indicated that there is a general exhaustion of NF-κB signalling system. I note in these results, that cells that treated with TNF initially, show a stronger subsequent response to IL-36 than to TNF, while cells that were treated with IL-36 initially respond better to TNF as in figure 3.22.

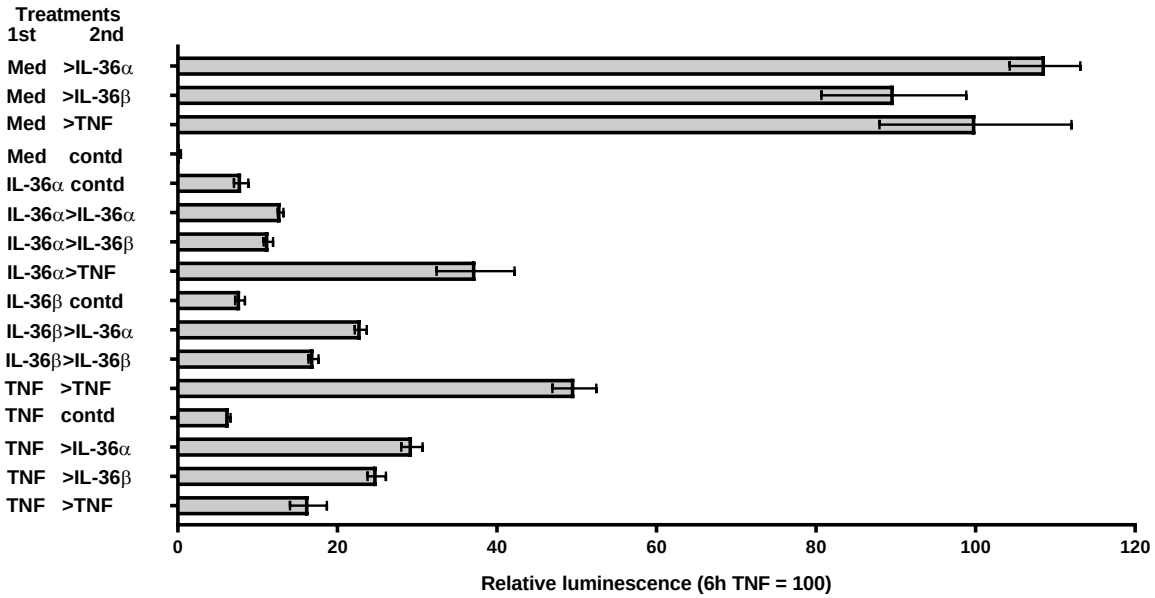

Figure 3.22 Changes in the NF-κB activation (luciferase output) in HT-29 D7 on re-stimulating after 18 h of initial treatment with the same or a different cytokine. 1st> 2nd in the labelling of the left axis represents the treatment order, where treatment A was 18 hr followed by treatment B for 6 hr. Cells were harvested after B treatment. IL-36α, IL-36β or TNF were used at 10 nM, 0.2 nM and 50 pM (10 ng/ml) respectively. Data (n= 4) are the mean and 95% confidence limit of the mean of each normalised dataset from one representative experiment of at least 2 independent experiments with similar outcomes.

3.13 Activation of n^1-IL-36α protein through digestion with chymotrypsin.

The initial translation product of IL-36α, n^1-IL-36α is very weakly active. I digested inactive 416 μg of n^1-IL-36α protein that was prepared in our laboratory with chymotrypsin in vitro to confirm that this protein can be activated. 104 μg n^1-IL-36α protein was digested with chymotrypsin at different time points (zero, 0.5,1 and 2 h). The mass spectrometry showed that n^1-IL-36α protein is cleaved at three different sites by chymotrypsin (see appendix, A.4), so the digestion process yields a mixture of protein.

The biological activity of the product was measured by stimulation of luciferase activity in HT-29. D7 and A6 cell lines were adjusted to 2.25 x 10^5 cells per well and grown on the 24-well plates in total volume of 1 ml. As usual, the cells were grown for three days and then the medium was drained and replaced with 0.5 ml of LSM for 18 h. after n^1-IL-36α had been treated with chymotrypsin, it was diluted to a concentration that corresponded to 10 nM before digestion For comparison, cells were also treated with 10 nM of n^6-IL-36α or 10 ng/ml TNF. LSM was used as a negative control. Luciferase reporter output showed that n^1-IL-36α is activated after being digested with chymotrypsin. n^1- IL-36α had been digested for 0.5 and 1 h induces luciferase at the same level as n^6-IL-36α protein. Further digestion reduced the biological activity of the mixture. Application of the same preparation to the IL-36R deficient subline, A6, showed no significant response to the chymotrypsin treated IL-36 preparations hence chymotrypsin by itself at this concentration did not defectively active an NF-κB response the results are shown in figure 3.23.

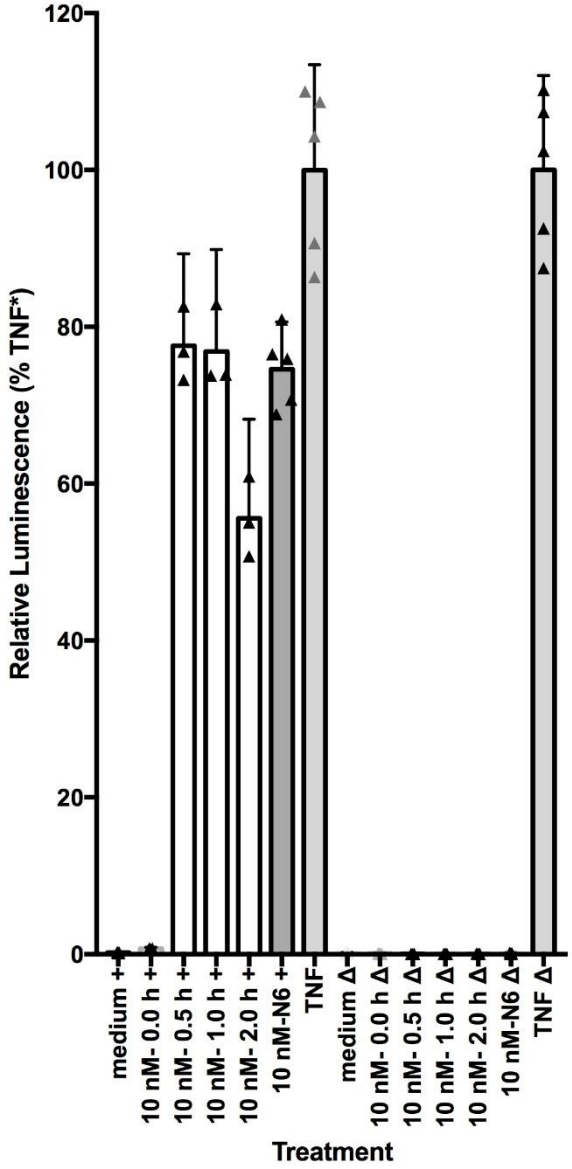

Figure 3.23 Measurement of IL-36 activity in n^1-IL-36α after digestion with chymotrypsin for different periods. 2 mg/ml of n^1-IL-36α was digested at 30 °C with 20 μg of chymotrypsin in different time points (0, 0.5, 1 or 2 h). The biological activity of the digested protein was assessed by luciferase assay. A 10 nM of digested protein after each time point, 10 nM of n^6-IL-36α or 10 ng/ml of TNF were used to assess NF-κB activation on D cell lines. A6 cell lines were used as a negative control to show that digested protein is not contaminated. Data (n= 3- 5) are the mean and 95% confidence limit of the mean of each normalised dataset from one representative experiment of at least 2 independent experiments with similar outcomes.

3.14 Discussion:

The first aim of this study was to assess the biological activity of active form of IL-36α, IL36β and IL-36γ on their receptors. Pro-IL-36 proteins are biologically inactive, and proteolytic processing is required to generate active forms. The proteolytic processing of IL-36 cytokines is not well understood, although it has been investigated. Previous studies showed that in vitro truncation of pro-proteins or clipping by neutrophil serine proteases increase the biological activity of pro-IL-36α, pro-IL-36β and pro-IL-36γ (Towne et al., 2011 and Henry et al., 2016). Towne et al (2004) reported that HT-29 cells express endogenous IL-36R. In this thesis, I used transfected HT-29 cells that contain a reporter NF-κB activity. These cells were cloned, and a subline was selected for its high signal output and low background. I used this subline to test the biological activity of active forms of IL-36. I used gene editing to create a subline of HT-29 cells with a knocked out *IL1RL2* gene.

3.14.1 Assessing biological activity of IL-36 proteins on their receptor

I conducted experiments to measure the EC_{50} values of the active forms of n^5-IL-36β and n^{18}-IL-36γ that I prepared, and the active form of n^6-IL-36α that was prepared in our laboratory. I also measured activation in response to n^6-IL-36α and n^5-IL-36β at different time points. Previous studies measured the EC_{50} values of truncated IL-36 proteins (n^6-IL-36α, n^5-IL-36β and n^{18}-IL-36γ) either used reporter cells with transfected exogenous IL-1RL2 (Towne et al., 2001) or that contained endogenous IL-36R, but where cells were treated for 24 h (Foster et al., 2014, Zhou et al., 2018). My NF-κB responsive assay data showed that the EC_{50} values of n^6-IL-36α, n^5-IL-36β and n^{18}-IL-36γ are 3.3 nM, 0.12nM and 18 nM respectively which are higher than has been measured by Towne et al., (2011) (0.06 nM, 0.015 nM and 1.22 nM), Foster et al., (2014) (0.8 nM, 0.46 nM and 1.6 nM) or Zhou et al., (2018), (2 nM for n^6-IL-36α and 1.16 nM for n^{18}-IL-36γ). The findings of the current study further indicated that n^6-IL-36α, n^5-IL-36β, n^{18}-IL-36γ have similar maximum activity in our assay to TNF. Moreover, a time course experiment showed that the peak of activity of NF-κB in

response to n^6-IL-36α, n^5-IL-36β and TNF is between 3-6 h. In contrast, there was no observed response to n^6-IL-36α, n^5-IL-36β and n^{18}-IL-36γ in IL1RL2 knocked out cell line though these cells respond to TNF and IL-1α. I therefore confirm that *IL1RL2* is the only gene that encodes an IL-36R receptor in HT-29 cells, and our n^6-IL-36α, n^5-IL-36β and n^{18}-IL-36γ preparations are free of other stimuli that might activate the NF-κB reporter such as endotoxin for example.

I tested the EC_{50} of n^4-IL-36α and n^6-IL-36α that contained a modified N-terminus, substituting lysine for n^6-glycine or n^6-serine. Neutrophil serine proteases can clip pro-IL-36α at n^4, pro-IL-36β at n^5 and n^{53} and pro-IL-36γ at n^{15}. These sites suggest that IL-36α could be activated at sites other than that reported by Towne et al (2011). My NF-κB reporter assay data showed that the n^4-IL-36α is completely inactive, and the EC_{50} values of Ser^6-IL-36α (30 nM) and Gly^6-IL-36α (435 nM) are very high compared with Lys^6-IL-36α (3.3 nM). The His-tagged pro- IL-36α precursor that was prepared was stable in solution and was used to generate pro-IL-36a and n^4- IL-36α, which was inactive. On the other hand, the pro- IL-36α was converted by chymotrypsin to a highly active mixture that contained n^6-IL-36α according to mass spectrometry. I conclude therefore that n^4-IL-36α is an inactive and is likely to be an active product of neutrophil proteases product. Mass spectrometry data showed that n^1-IL-36α was cleaved at four different sites. Reporter gene data however showed that the mixed digested protein has similar activity to a purified n^6-IL-36α.

3.15 Conclusion

To sum up, manipulation of the *IL1RL2* gene with Cas9-CRISPR data showed that this is the only gene that encodes an IL-36 receptor in HT-29. An NF-κB responsive luciferase reporter gene data showed that n^6-IL-36α, n^5-IL-36β and n^{18}-IL36γ can activate an NF-κB reporter gene to a similar extent and time range to TNF and that IL-36 is more potent than IL-1α. Moreover, n^4-IL-36α that was made in our laboratory was not biologically active. For full activity, the N-terminal lysine of mature IL-36α is required. n^1-precursor of IL-36α (inactive precursor) can be fully activated by chymotrypsin, and the cleavage site of chymotrypsin before n^6-Lys.

Chapter 4

Results

4.1 Introduction

IL-36α, IL-36β and IL-36γ proteins have been related to many diseases particularly in skin. These cytokines are expressed by epithelial cells (most predominately keratinocytes). At genetic level, individuals who are inactivating IL-36 natural antagonist of IL-36, develop generalised pustular psoriasis, which is skin disease (Marrakchi et al., 2011). An in vivo study showed that mice that (experimentally) lack expression of IL-36Ra and overexpress IL-36α develop a severe psoriasis-like disease (Blumberg et al., 2007). IL-36α, IL-36β, IL-36γ proteins do not contain an N-terminal signal, which is required for conventional secretion of newly synthesised proteins. Hence the pathway for the release of IL-36 is still unknown. Previous studies have shown that different inflammatory stimuli can regulate expression of IL-36α, IL-36β, IL-36γ at the level of mRNA and protein. For example, expression of IL-36γ mRNA in primary human keratinocytes is elevated after priming cells with TNF or PMA (Busfield et al., 2000). TNF, IL-1, IL-17A, IL-22, a combination of TNF and IL-22 or IL-17A and IL-22 all induce expression of IL-36 mRNAs in primary human keratinocytes (Carrier et al., 2011). Primary human keratinocytes can express IL-36α, IL-36β, IL-36γ and IL-36Ra mRNAs in response to TNF or IL-1α (Johnston et al., 2011). Epicutaneous infection of mice skin with *S. aureus* induces expression of IL-36α protein (Liu et al., 2017). These studies showed that expression of IL-36 cytokines is induced in response to different inflammatory inducers. We hypothesized that the processing of mRNA induction and protein expression and even processing might be observed more conveniently in established cells lines. In this chapter, I present experiment to investigate these stages in the expression of functional IL-36 in cell lines HaCaT and A-431. My PhD studies have been directed at answering four main questions. I have tested whether can IL-36α, IL36β and IL-36γ, IL-36Ra and IL-36R mRNAs are expressed in two keratinocyte cell lines. I have tested whether natural physiological agents that can stimulate the expression of IL-36α, IL36β and IL-36γ, IL-36R and IL-36Ra? I have tested whether these effects are differential. I have tested whether cell lines produce IL-36 protein, and whether the protein products can be found in whole cell lysates or whether they are released. I have investigated whether endogenously produced IL-36γ can be processed in cell culture.

4.2 RT-PCR of HaCaT cells

The first aim of my project is to investigate whether IL-36α, IL36β, IL-36γ, IL-36R and IL-36Ra mRNAs are expressed in HaCaT cell line as a model for human KC and whether the genes can be induced by cytokines. mRNA was extracted from HaCaT cells after being stimulated with 1 nM IL-1α, 1 nM IL-36α, 10 ng/ml TNF compare with cells grown in low serum medium (LSM) as a control. As will be explained later, all these doses are expected to be approaching maximum stimulation. though I understand now that the IL-36α dose is ~1/3 x EC_{50}.

First strand cDNA, 2 μg, was generated for each sample to be used in RT-PCR before it was amplified. Samples were run by using gel electrophoresis as in figure (4.1), (4.2) and (4.3). These gels were also used to evaluate the product of loaded samples by visual comparison with DNA ladder.

The results of the RT-PCR show that IL36β and IL-36γ, IL-36R and IL-36Ra are expressed in HaCaT cells. IL-36α was not detected. The product of the RT-PCR amplification of HaCaT cDNA was not the expected 175 bp (Table 2.2). The size of PCR product is compatible with the inclusion of the 92 nucleotides of intron 1 in the sequence, yielding a product of 267 bp. The obvious cause of this would be detection of contaminating *IL36A* genomic DNA in the absence of sufficient IL-36α cDNA. Therefore, it seems that HaCaT cells have a low copy number of IL-36α mRNA.

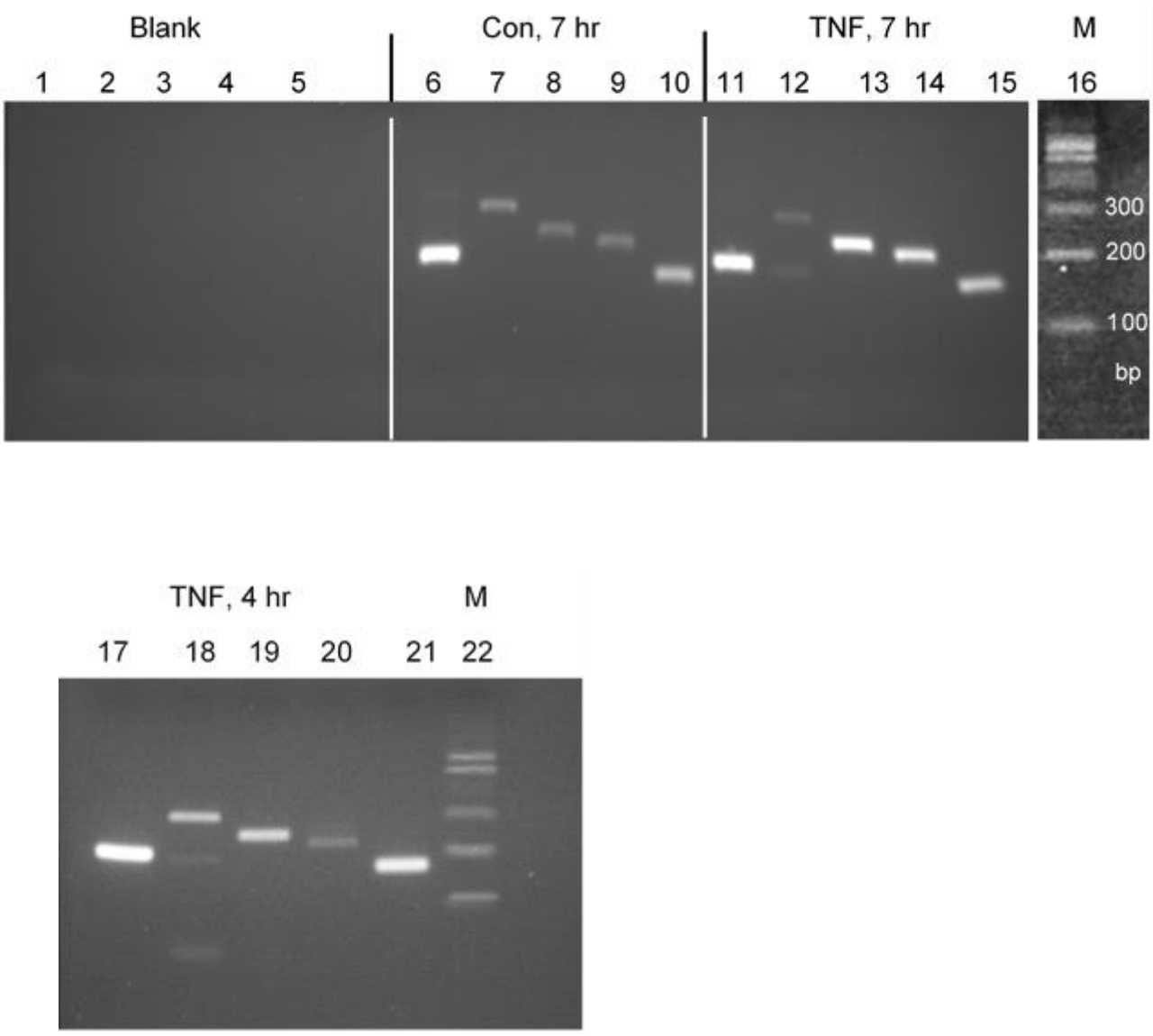

Figure 4.1 Qualitative RT-PCR of IL36 agonist and receptor cDNAs from HaCaT cells, in the absence of and after TNF treatment. The gel image shows DNA bands obtained from PCR of cDNA prepared from total mRNA. Lanes 1 to 5: PCR of water blank. Lanes 6 to 10: Control treatment (7 hr, low serum medium). Lanes 11 to 15: Stimulation with 10 ng/ml TNF (7 hr). Lanes 16: DNA size marker Lanes 17 to 21: Stimulation with 10 ng/ml TNF (4 hr). Lane 22: DNA size marker. PCR reactions with specific primers as follows. Lanes 1, 6, 11, 17: β-actin (control). Lanes 2, 7, 12, 18: IL-36α. Lanes 3, 8, 13, 19: IL-36β. Lane 4, 9, 14, 20: IL-36γ. Lane 5, 10, 15, 21: IL-36R.

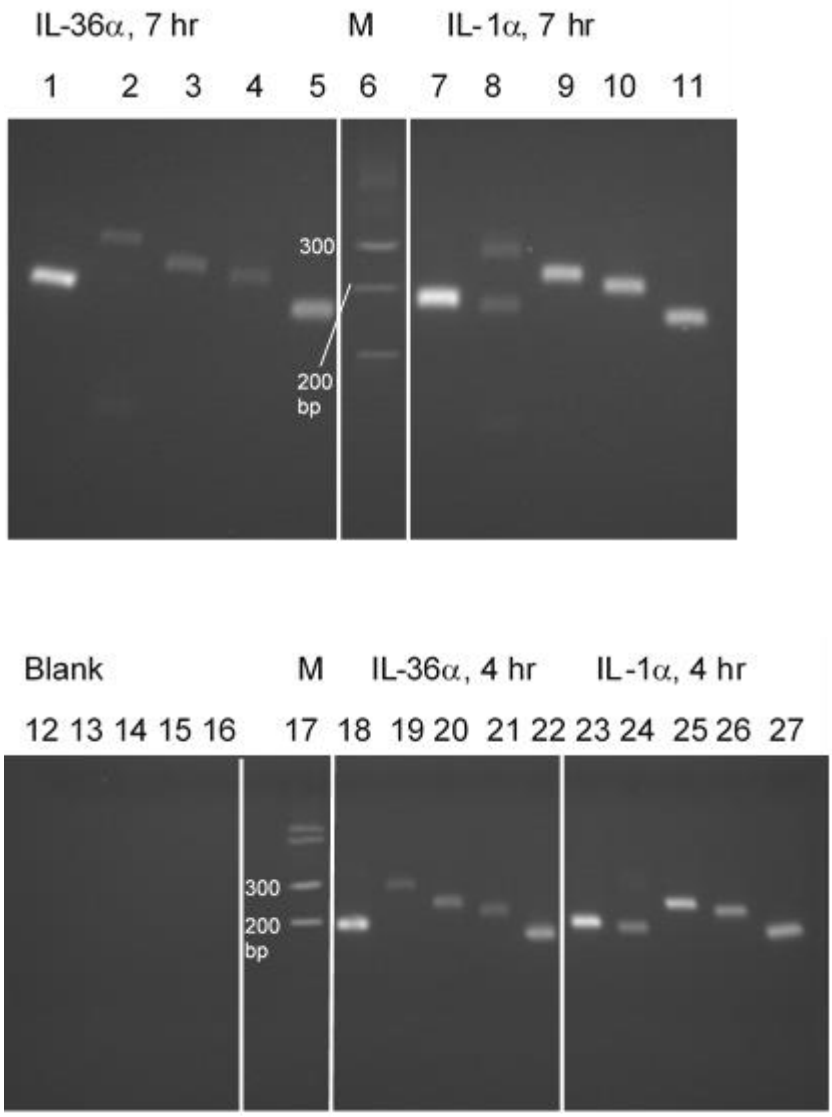

Figure 4.2 Qualitative RT-PCR of IL36 agonist and receptor cDNAs from HaCaT cells, after treatment with IL-36α or IL-1α. The gel images show DNA bands obtained from PCR of cDNA prepared from HaCaT total mRNA. Lanes 1 to 5: simulation with 1 nM IL-36α (7 hr). Lane 6: DNA size standards. Lanes 7 to 11: stimulation with 1 nM IL-1α (7 hr). Lanes 12 to 16: water blank PCR. Lanes 17 DNA size standards. Lanes 18 to 22: simulation with 1 nM IL-36α (4 hr). Lanes 23 to 27 stimulation with 1 nM IL-1α (4 hr). PCR reactions with specific primers as follows. Lanes 1, 7, 12, 18, 23: β-actin. Lanes 2, 8, 13, 19, 24: IL-36α. Lanes 3, 9, 14, 20, 25: IL-36β. Lanes 4, 10, 15, 21, 26: IL-36γ. Lanes 5, 11, 16, 22, 27: IL-36R.

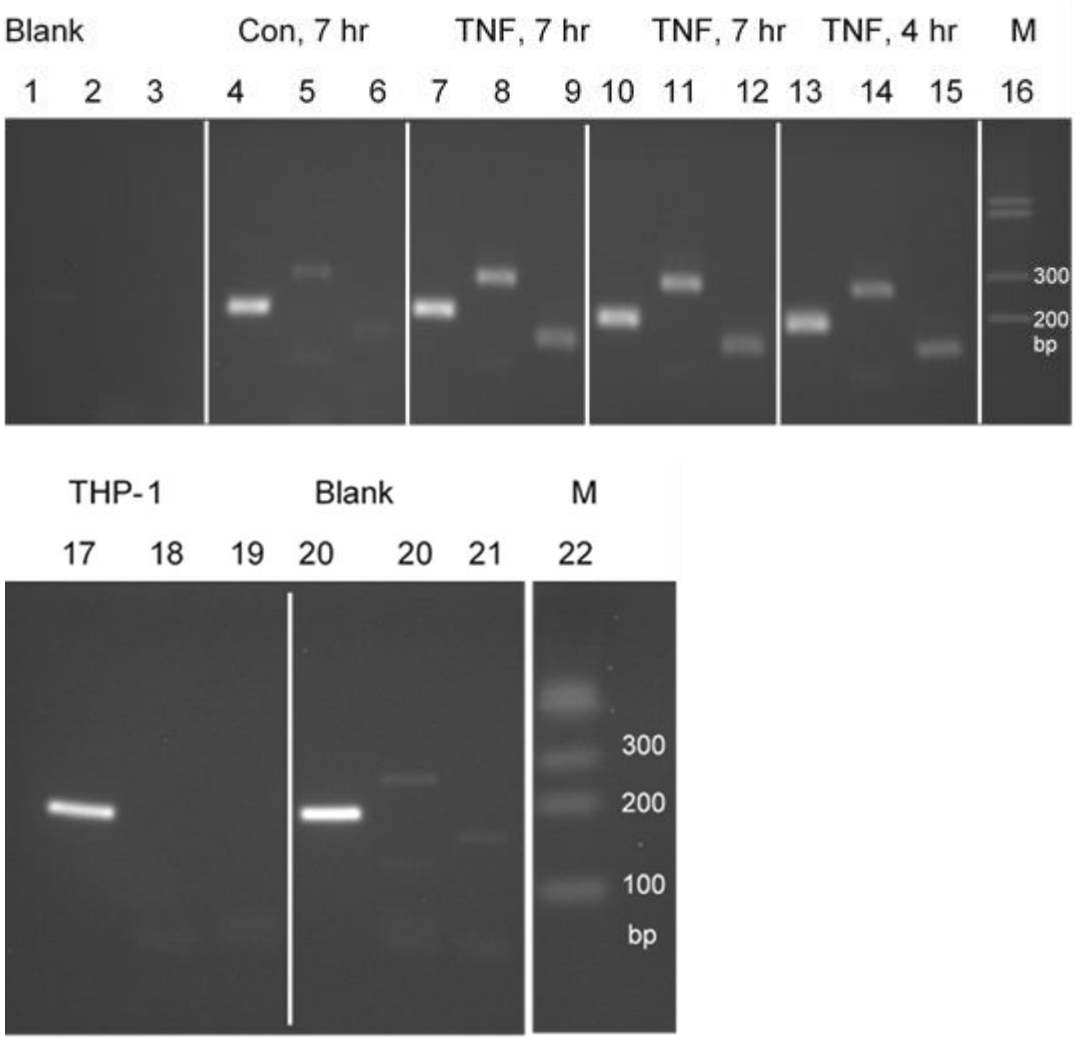

Figure 4.3 Testing primers for qualitative RT-PCR of IL-36Ra cDNA from HaCaT and THP-1, without or after treatment with TNF. The gel image shows DNA bands obtained from PCR of cDNA prepared from total mRNA. Lanes 1 to 3, water blank PCR. Lanes 4 to 6: HaCaT; 7 hr of treatment with LSM (control). Lanes 7 to 9: HaCaT; 7 hr treatment with 10 ng/ml TNF. Lanes 10 to 12: HaCaT; replicate of treatment with TNF. Lanes 13 to 15: HaCaT; 4 hr treatment with 10 ng/ml TNF. Lanes 17 to 19: continuously growing THP-1. Lanes 20 to 22: HaCaT; 4 hr treatment with LSM (control). Lanes 1, 4, 7, 10, 13, 17, 20: PCR for β-actin as internal control. Lanes 2, 5, 8, 11, 14, 18, 21 : IL-36Ra primer pair N1. Lanes 3, 6, 9, 12, 15, 19, 22 : IL-36Ra primer pair N2. Lane 16, DNA size standards.

4.2.1 RT-PCR of THP-1

The first strand cDNA that was prepared from mRNA from continuously growing THP-1 cells (a human monocytic cell line) were used as a positive control to confirm that the conditions for amplifying IL-36α from HaCaT cells were appropriate. Smith et al., 2000 has already reported that IL-36α mRNA is detectable in THP-1. mRNA was extracted from THP-1 without any stimulation. cDNA was prepared from 2 µg total RNA to be used in the RT-PCR. RT-PCR shows that IL-36α lL-36β and IL-36R are expressed in THP-1 cells line but not IL-36γ and IL-36Ra (Figures 4.3 and 4.4).

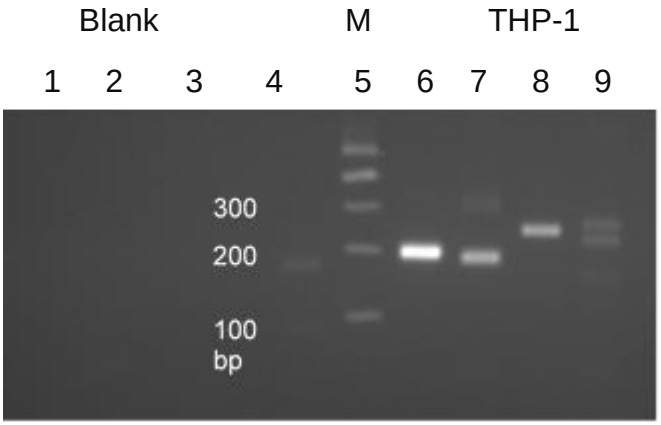

Figure 4.4 Qualitative RT PCR of THP-1 cells. The gel image shows the bands obtained from RT-PCR for mRNA extracted from THP-1 cells without any stimulation and continuously growing Lane 1 to 3: water blank. Lane 4: IL-36R. Lane 5: DNA size standards. Lane 6: IL-36R. Lane 6: β-actin. Lane 7: IL-36α. Lane 8: IL-36β. Lane 9: IL-36γ.

4.2.2 Sequencing of RT-PCR products from IL-36α, IL-36β, IL-36γ, IL-36R and IL-36Ra.

To confirm the identity of the products of PCR amplification, the PCR products were further amplified and sequenced, using the PCR primers in the sequencing reactions. The sequence of IL-36α that was expressed in THP-1 cells, and IL-36β, IL-36γ, IL-36R and IL-Ra that were expressed in HaCaT cells were determined. DNA bands of RT PCR product were extracted from a low melting agarose gel and re-amplified with 20 cycles of re-amplification. After re-amplification, RT PCR products were analyzed by direct Sanger-sequencing from the PCR primers.

Sequences from samples were aligned with NCBI reference cDNA sequences for each gene as in table 2.2. Results confirm that the PCR products are from the correct, spliced templates figure 4.5.

(A)

```
1    GGGTTAAACTGTGGCTTG>>
2    gggttaaactgtggcttgggactgactcaggtcctctcttggggtcggtctgcacataaa
3          AACTGTGGCTTGGGACTGANTCAGGTCCTNTNTTGGGGTCGGTCTGCACATAAA

1     GGANTCCTATCCTTGGCAGTTCTGAAACAACACCACCACAATGGAAAAAGCATTGAAAA
2    aggactcctatccttggcagttctgaaacaacaccaccacaatggaaaaagcattgaaaa
3    AGGACTCCTATCCTTGGCAGTTCNGAAACAACACCACCACAANNGAAAAAGCATTGAAAA

1    TTGACACACCTCANCGGGGGANCATTCAGGATATCAATCATCGGGTGTGGGT
2    ttgacacacctcagcaggggagcattcaggatatcaatcatcgggtgtgggttct
3    NNGACA                                  ||||||||||||||||||
4                                      <<TTAGTAGCCCACACCCAAGA
```

(B)

```
1    GGCAGCACCCAAATCCTATG>>                          GTGGGTCCTGAGTGG
2    ggcagcacccaaatcctatgctattcgtgattctcgacagatggtgtgggtcctgagtgg
3     GCAGCACCCAAATCCTATGCTATTCGTGATTCTCGACAGATGGTGTGGGTCCTGANTGG

1    AAATTCTTTAATAGCAGCTCCTCTTAGCCGCAGCATTAAGCCTGTCACTCTTCATTTAAT
2    aaattctttaatagcagctcctcttagccgcagcattaagcctgtcactcttcatttaat
3    AAATTCTTTAATAGCAGCTCCTCTTAGCCGCAGCATTAAGCCTGTCACTCTTCATTTAAT

1    AGCCTGTAGAGACACAGAATTCAGTGACAAGGAAAAGGGTAATATGNTTTACCNNGGAAT
2    agcctgtagagacacagaattcagtgacaaggaaaagggtaatatggtttacctgggaat
3    AGCCTGTAGAGACACAGAATTCAGTGACAAGGAAAAGGGTAATATGGTTTACCTG

1    CAAGGGAAAAGATCTCTGTCTCTTCTGTGCAGAAATTCAGG
2    caagggaaaagatctctgtctcttctgtgcagaaattcagggca
                              ||||||||||||||||||
4                          <<GACACGTCTTTAAGTCCCGT
```

Figure 4.5 Alignment of IL-36 system sequences from qualitative PCR products (part 1) (A) IL-36α from THP-1 cells with NM_014440.2. (B) IL-36β from HaCaT with NM_173178.2. Lines 1: The forward primer is shaded grey. Sequence highlighted in yellow is derived directly from readable Sanger sequence from the forward primer. Lines 2 show part of the reference cDNA sequence; a red-highlight indicates the end of an exon and green-highlight indicates the start of the next exon. Lines 3: Sequence highlighted in azure is complementary to readable Sanger sequence from the reverse primer. Lines 1 and 3: N indicates an unassigned base. Sequence runs are not included before or after runs of N occurred. Lines 4: The reverse primer is shown (3' to 5') hybridised to the reference sequence.

(C)

```
1    ATCAGCAAGTGTGGACCCTT>>                                        AGTG
2    atcagcaagtgtggacccttcagggtcagaaccttgtggcagttccacgaagtgacagtg
3       CAGCAAGTGTGGACCCTTCAGGGTCAGAACCTTGTGGCAGTNTNNNGNNGTGNCAGTG

1    TGACCCCAGTCACTGTTGCTGTTATCACATGCAAGTATCCAGAGGCTCTTGAGCAAGGCA
2    tgaccccagtcactgttgctgttatcacatgcaagtatccagaggctcttgagcaaggca
3    NGNNNCCAGTNANTGTTNNTGTTNTNACATGCAAGTAT

1    GAGGGGATCCCATTTATTTGGGAATCCAGAATCCAGAAATGTGTTTGTATTGTGAGAAGG
2    gaggggatcccatttatttgggaatccagaatccagaaatgtgtttgtattgtgagaagg
3

1    TTGGAGAACAGCCCACATTGCAGCTAAA
2    ttggagaacagcccacattgcagctaaa
                |||||||||||||||||||
4           <<GTCGGGTGTAACGTCGATTT
```

(D)

```
1    CATGTCATCTGCACTTCCCG>>
2    catgtcatctgcacttcccgaagagttgtgttttgggtccaataaagtggtataaggact
3        TCATCTGCACTTCCCGAAGAGTTGTGTTTTGGGTCCAATAAAGTGGTATAAGGACT

1    GTAACGAGNNTAAAGGGGAGCGGTTCACTGTTTTGGAAACCAGGCTTTTGGTGAGCAATG
2    gtaacgagattaaaggggagcggttcactgttttggaaaccaggctttggtgagcaatg
3    GTAACGAGATTAAAGGGGAGCGGTTCACNGTTTNNGAAACCNGGC

1    TCTCGGCAGAGGACAGAGGGACTACGCGTGTCAAGCCANA
2    tctcggcagaggacagagggactacgcgtgtcaagccatac
                           ||||||||||||||||||||
4                       <<GATGCGCACAGTTCGGTATG
```

Figure 4.5 Alignment of IL-36 system sequences from qualitative PCR products (part 2) (C) IL-36γ from HaCaT with NM_019618.3 (D) IL-36R from HaCaT with NM_003854.2. Lines 1: The forward primer is shaded grey. Sequence highlighted in yellow is derived directly from readable Sanger sequence from the forward primer. Lines 2 part of the reference cDNA sequence; a red-highlight indicates the end of an exon and green-highlight indicates the start of the next exon. Lines 3: Sequence highlighted in azure is complemetary to readable Sanger sequence from the reverse primer. Lines 1 and 3: N indicates an unassigned base. Sequence runs are not included before or after runs of N occurred. Line 4: The reverse primer is shown (3' to 5') hybridised to the reference sequence.

(E)

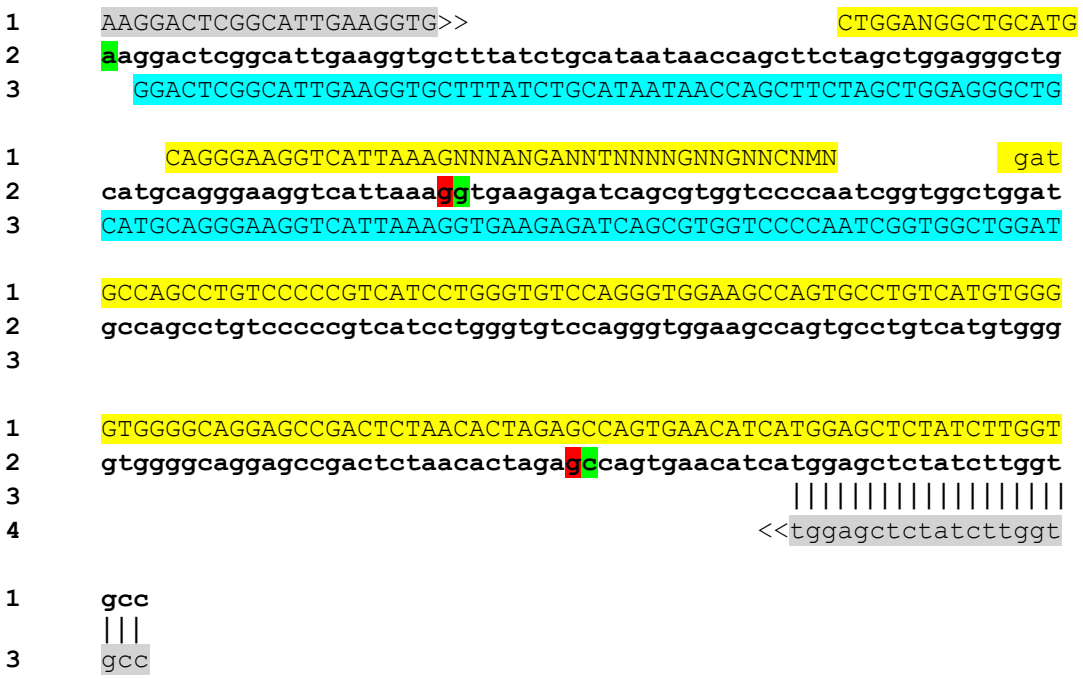

Figure 4.5 Alignment of IL-36 system sequences from qualitative PCR products (part 3) (E) IL-36Ra from HaCaT with NM_012275.2. Line 1: The forward primer is shaded grey. Sequence highlighted in yellow is derived directly from readable Sanger sequence from the forward primer. Line 2 part of the reference cDNA sequence; a red-highlight indicates the end of an exon and green-highlight indicates the start of the next exon. Line 3: Sequence highlighted in azure is complemetary to readable Sanger sequence from the reverse primer. Lines 1 and 3: N indicates an unassigned base. Sequence runs are not included before or after runs of N occurred. Line 4: The reverse primer is shown (3' to 5') hybridised to the reference sequence.

4.3 Measuring the response of the *IL36* genes and *IL36R* in HaCaT and A-431 to inflammatory stimuli.

It was because I saw data that A-431 can express a detectable amount of IL-36γ when stimulated with TNF and IFNγ. The expression of each gene under each condition was determined for at least three separate replica tissue culture plates and each value was determined three times per replica. Data for each biological replica was then processed as the mean value. In some cases, for unstimulated cells, where the expression level of the target genes is likely to be at its lowest, amplification of a particular transcript failed entirely for a particular sample. In other cases, one or more measurements in a replicate set failed. This kind of result tended to be coupled with large C_q values. (C_q is the cycle at which the product reached its detection threshold). Amplifications were judged to have failed and results were edited when the software declared a failure or where the estimated melting temperature of the product departed from the modal value by more than 1°C. Low copy number of cDNA is likely to cause both high variability between measurements and complete failure in some cases. In the raw data for unstimulated A-431 and HaCaT cells, for example, the mean C_q for IL-36α was ~31 cycles and for A-431, C_q IL-36β was 29 cycles.
It was logical and simple to express induced RNA levels for all four genes of interest as compared with uninduced, which corresponds to the conventional $\Delta\Delta C_q$ analysis. The final estimates of the degree of induction for the wealthier expressed IL-36α and IL-36β are therefore more approximate than for the more strongly expressed genes.

To calculate the expected amplification of a particular cDNA in a sample it is necessary to measure the efficiency of the reaction. I tested the efficiency of amplification for each cDNA at an annealing temperature of 58 °C. The cDNA sample was selected because it was from A-431 cells that had been treated with 67 ng/ml PMA and 20 ng/ml TNF, which was found to cause the strongest induction of IL-36γ. A dilution series was produced of the cDNA with water. Initial experiments showed that the undiluted cDNA preparation was not amplified significantly more efficiently than a sample diluted to 0.2 with water. All cDNA analysis by qRT-PCR was therefore done with a 0.2 dilution. To construct a regression line, further dilutions of 0.04, 0.008 and

0.0016 were prepared. Each dilution was tested in triplicate. In the following, *X* is the relative concentration of two cDNA samples. The data for this analysis is shown in figure 4.6.

The best fit value for the slope from the data in figure 4.6 of the linear regression of the threshold cycle value, C_q on $\log_{10}[X]$ was determined and this was used to calculate efficiency. The efficiency per cycle of a PCR reaction can be calculated as

$$E = 10^{\Delta Cq/\Delta log_{10}[X]} - 1$$

The values I obtained for efficiency were, for the test genes, 0.979 for IL-36α, 1.231 for IL-36β, 0.782 for IL-36γ, 1.070 for IL-36R, and for the control genes, 0.833 for β2-microglobulin, 0.853 for hypoxanthine phosphoribosyltransferase (HPRT), 1.023 for protein proline isomerase A (PPIA) and 1.100 for the ABL1 protein kinase. The control genes were selected for covering a range of mRNA abundances.

The derived value of *E* is an average value during the entire PCR reaction and there have been criticisms of this approach because efficiency does vary with cycle. However, this approach is commonly used for estimating efficiency. Though according to convention, the values of *E* lying outside the range 0.95-1.05 would not be used, I found that they could not be improved for these primers for these sample types. I used the efficiency estimate for the i^{th} cDNA, E_i, to estimate the amplification of each cDNA in each sample in the qPCR measurements. For constant cycle efficiency, the total amplification was calculated for all valid readings thus,

$$A_i = \frac{X_{q,i}}{X_{0,i}} = (1 + E_i)^{C_{q,i}},$$

where $X_{q,i}$ is the detectable concentration of the test cDNA, *i*, and $X_{0,i}$ is its original concentration. I then calculated $\log_{10}(\frac{X_q}{X_0})$ for all readings.

Assuming that cDNA concentrations for the four control genes would be independent of the treatment regime, I calculated a mean of $\log_{10}(\frac{X_{q,c}}{X_{0,c}})$ for the set of control genes for each biological replicate for each treatment. To correct for variations in the initial concentration of total mRNA, by analogy with a ΔC_q calculation, $\Delta\log_{10}(\frac{X_{q,i}}{X_{0,i}})$ was

calculated for each target cDNA by subtraction of the corresponding control mean for the specific biological replicate (3 for each treatment). To calculate $\Delta\Delta\log_{10}(\frac{X_{q,i}}{X_{0,i}})$ for each the target genes for each biological replicate, which is analogous to $\Delta\Delta C_q$, I subtracted the mean $\Delta\log_{10}(\frac{X_{q,i}}{X_{0,i}})$ for each target gene. These triplicate data are presented in figures 4.8, 4.9, 4.10 and 4.11.

4.4 Validation of qPCR reaction by sequence analysis

The qPCR products are short. To validate that qPCR reactions are yielding the correct products, I sequenced them directly, using The PCR primers as sequencing primers. The objective was to validate the length of the product and the product contained the expected exon junctions, thus eliminating the possibility that products are from genomic DNA. The alignment of predicted cDNA fragment and sequence data are shown in Figure B. in all cases, some sequence was obtained that bridged exon boundaries, this validate the reactions.

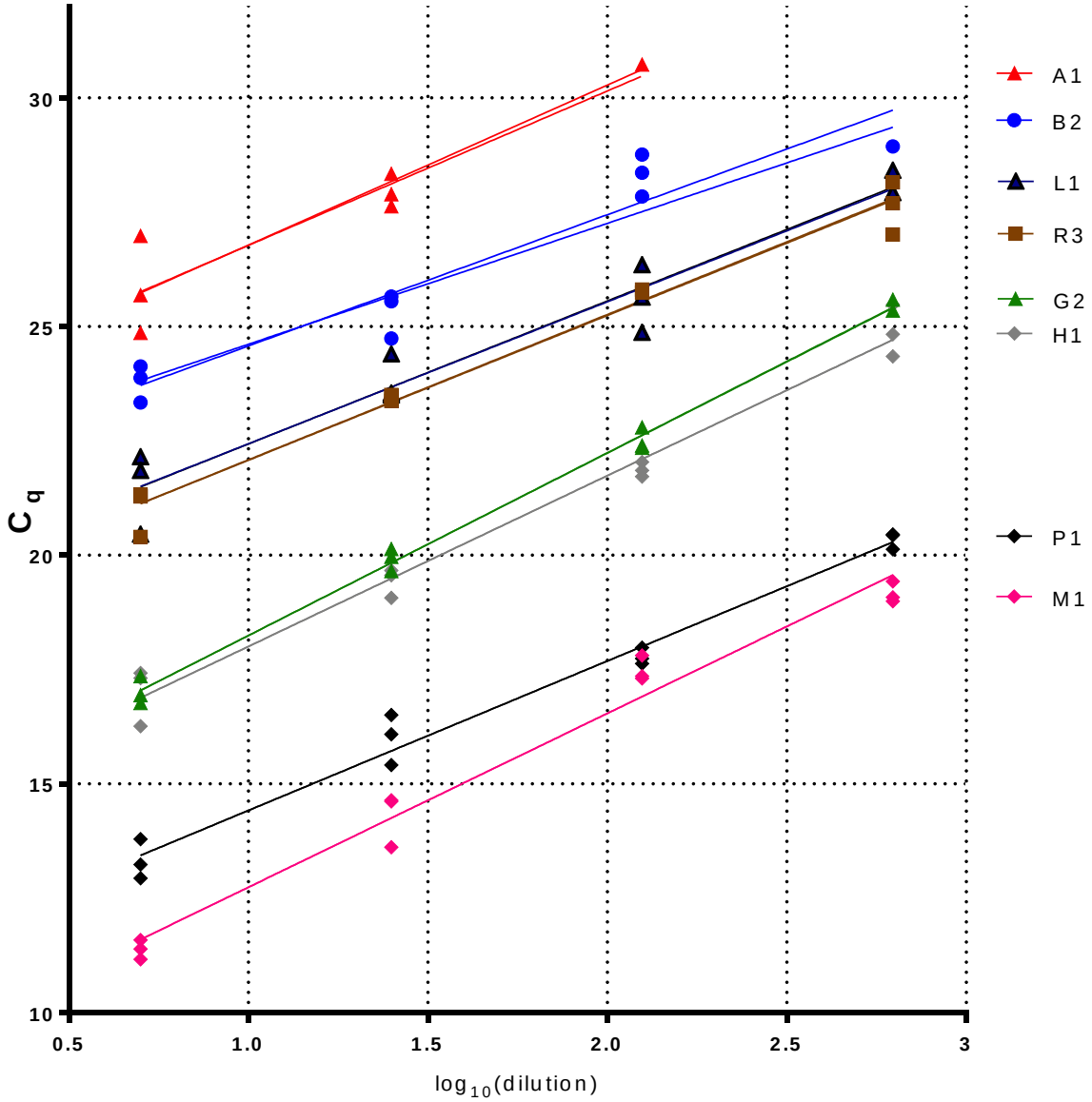

Figure 4.6 Test the amplification efficiency of the cDNAs in this study. Where is A1= IL-36α, B2= IL-36β, G2= IL-36γ, R3= IL-36R M2= β2 microglobulin, H1= hypoxanthine phosphoribosyltransferase, P1= peptidyl proline isomerase (PPIA), L= ABL kinase (ABL1). Data (n=3) represent 95% confidence units of the mean of at least 2 independent experiments with similar outcomes.

4.5 Evidence of cell signaling: Quantification of IL-8 (CXCL8) secretion by HaCaT

Inflammatory cytokines that signal through the NF-κB pathway activate the expression and secretion of the chemokine CXCL8, commonly called IL-8. I used activation of CXCL8 secretion as a positive control for inflammatory cytokine signalling in HaCaT. I tested for responses to the established activators, TNF and IL-1 and to IL-36α. CXCL8 secretion from cells was measured by the enzyme-linked immunosorbent assay (ELISA). HaCaT cells were seeded in 24 well plates at 2.5 x 10^5. HaCaT cells were stimulated with 5 nM IL-1α, different concentrations of IL-36α (0.5 nM IL-36α, 1.5 nM IL-36α, 5 nM IL-36α and 15 nM IL-36α). As a positive control, I tested 10 ng/ml TNF. LSM served as a negative control. Six-fold replicates were used for each stimulus. Cells were incubated at 37 °C for 7 h. To test for activation by cytokines, supernatants from 7 h stimulated HaCaT cells were analysed for IL-8 secretion with an ELISA kit as described in section 2.4.7. Paired one-way ANOVA was performed and p-values were shown. The results show that CXCL8 release in response to IL-36α is weaker than IL-1α and TNF figure 4.7. The highest concentration of n^6-IL-36α used here is ~ 3x EC_{50} that I report later for n^6-IL-36α on HT-29 cells and would be expected to nearly saturate the receptor.

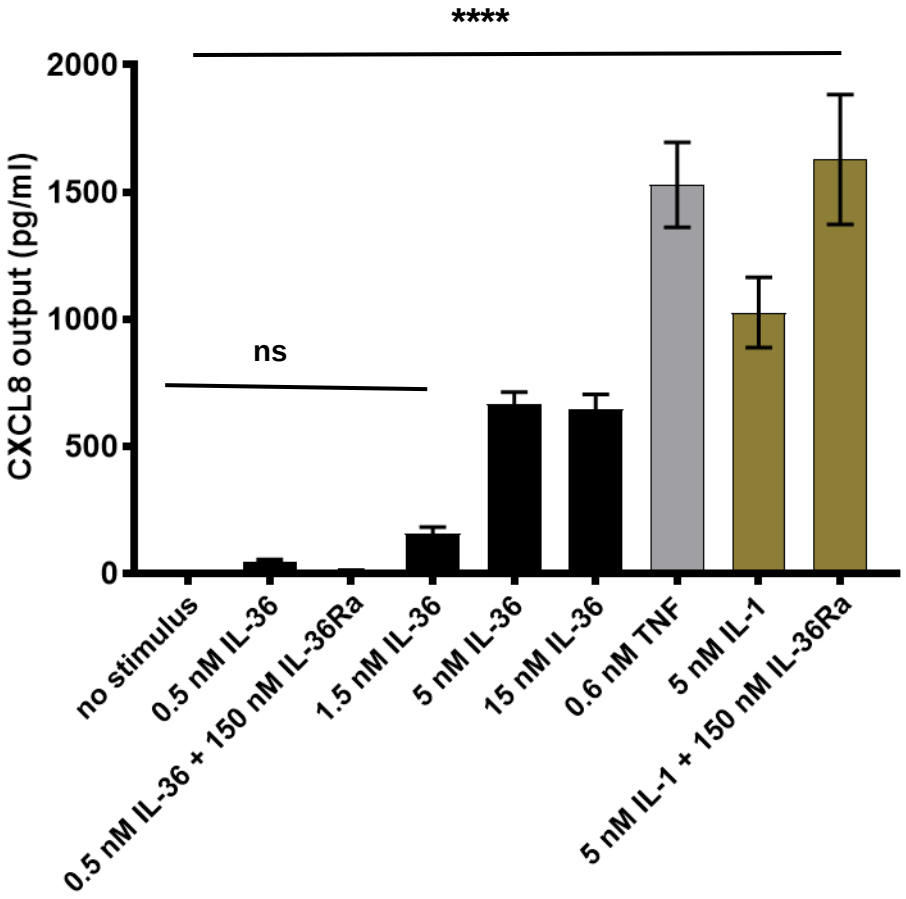

Figure 4.7 Comparative effect of IL-1α, IL-36α and TNF on NF-κB pathway activation in HaCaT cells by looking at expression of CXCL8. HaCAT cells were treated with different doses of IL-36α (0.5, 1.5, 5 or 15 nM), 5 nM of IL-1α or 10 ng/ml TNF (0.6 nM). Moreover, HaCaT cells were treated with 150 nM of IL-36Ra and 0.5 nM of IL-36α to demonstrate that the activity of the preparation of n^6-IL-36α is mediated through the IL-36R. The stimulant conditions are indicated on X-axis with the mean CXCL8 values (pg/ml). Data (n=5) represent 95% confidence units of the mean of at least 2 independent experiments with similar outcomes.

4.6 Time course and dose response of TNF to induce expression of IL-36γ mRNAs in the A-431 cells

To select optimal conditions of IL-36γ mRNA expression in A-431 cells, a time course was performed. A-431 cells were treated for 6, 9 and 12 h with 20 ng/ml TNF, in serum free medium. A negative control remained in LSM . RNA was extracted from samples as in section 2.4.2. First strand cDNA, 5 μg, was synthesized as described in section 2.4.3. In a preliminary experiment, I found that the undiluted cDNA product was not efficiently amplified by any RT-qPCR reaction and Ichose a dilution of 5-fold as the standard condition. cDNA samples were diluted 5-fold with water before being used. RT-qPCR was performed with SYBR Green (Qiagen). Primer pairs were used as in Table 2.3. The annealing temperature was 58 °C. q-RT-PCR data showed that IL-36γ induced similarly at all three times 6, 9 and 12 has showed in Figure 4.8. A dose response was also performed for TNF stimulation. A-431 cells were treated with different concentrations of TNF (10, 20, 40 ng/ml) for 6 h. qPCR data showed that all three doses induce expression of IL-36γ in a similar manner maximal ~ 20- 30-fold compared with untreated cells as shown in figure 4.9. Thus 10 ng/ml was sufficient to saturate the response of A-431. TNF alone did not strongly induce the other IL-36 genes in A-431. The expression of the receptor was not significantly changed in response to TNF.

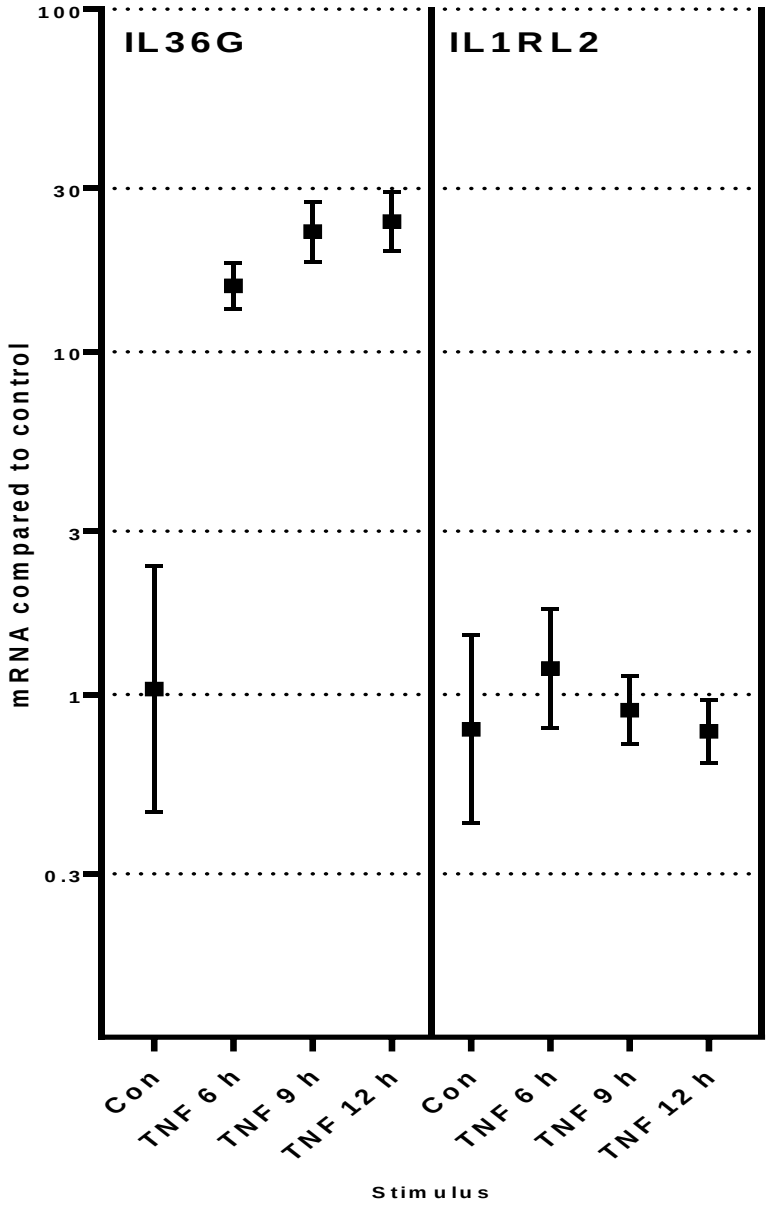

Figure 4.8 Time course expression of IL-36γ and IL-36 receptor (IL-1RL2) mRNAs in A-431 cells. A-431 cells were treated with 20 ng/ml TNF for (6, 9 and 12 hr), in addition to no treatment (control). Three biological replicate culture were used for each time point, and each Cq was determined in triplicates. Each replicate as analysed three times. The data (n=3) shown as mean and 95% confidence intervals and they are derived from the analysis shown in section 4.2.

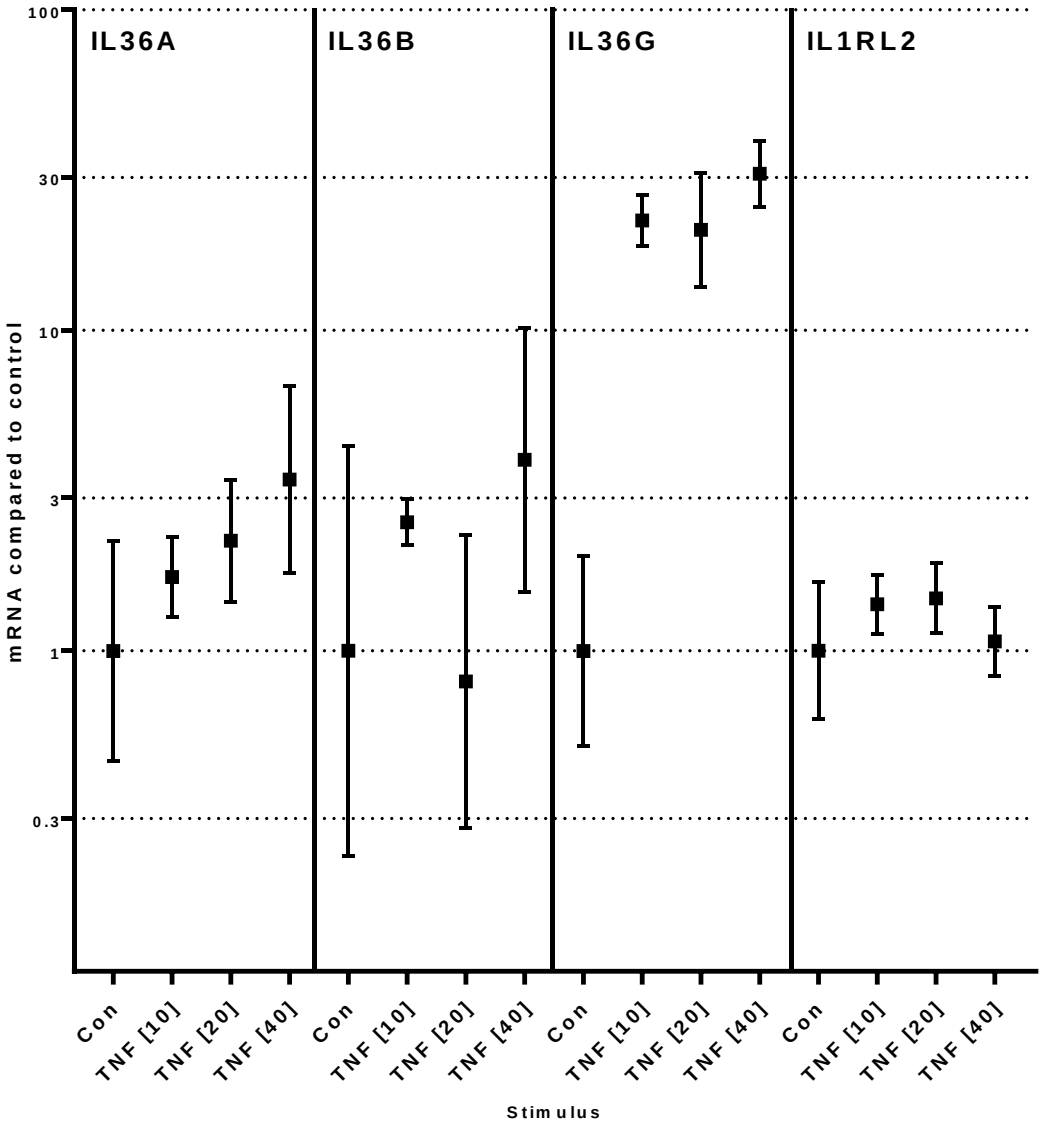

Figure 4.9 Induction of IL-36 and IL-36R gene expression in response to a range of doses of TNF dose in A-431. A-431 cells were serum deprived and then treated with (10, 20 or 40 ng/ml TNF) or not treated for 6 hr. Triplicates of Cq were made for at least three biological replicates in case 10 ng/ml and 40 ng/ml TNF. Pooled data from all experiments were combined for the control (9 replicates) and 20 ng/ml TNF treatments (11 replicates) Cq determinations were made in triplicates (see appendix VI, table 2) for the number of Cq determinations used for each treatment. The data (n=3) shown as mean and 95% confidence intervals and they are derived from the analysis shown in section 4.2.

4.7 Effect of PMA and TNF or flagellin and TNF on expression of IL-36α, IL-36β and IL-36γ mRNAs in A-431 cells.

To investigate expression of endogenous IL-36 mRNAs in A-431 in response to various inflammatory stimuli or combinations of two stimuli, A-431 cells were treated with 67 ng/ml PMA, 20 ng/ml TNF, 67 ng/ml PMA and 20 ng/ml TNF, 1 μg/ml flagellin or 1 μg/ml flagellin and 20 ng/ml TNF for 6 hr, or were not treated for 6 h. Three replicates (25 cm^2) were used for each treatment. RNA was extracted from A-431 as in section 2.4.2. First strand cDNA, 5 μg, was synthesized as described in section 2.4.3. cDNA samples were diluted 5-fold before being used.

Results are shown in figure 4.10. I found that IL-36α mRNA in A-431 cells is activated less than 2- fold by TNF, and the difference is not statistically significant. There was a strong and significant induction by PMA of ~20 -fold. Treatment with TNF does not enhance the effect of PMA. Flagellin produced a smaller but significant stimulation of ~5-fold and combination of TNF and flagellin showed some cooperativity. Flagellin or flagellin and TNF induced IL-36α mRNA ~ 7-fold and 10-fold respectively.

IL-36β mRNA was not significantly induced in response to TNF or flagellin, but with flagellin and TNF IL-36β was induced ~ 3-fold but that was not a significant increase compared with ~ 25- fold in response to PMA or PMA and TNF.

For IL-36γ mRNA, the expression was increased ~ 20-fold in response to TNF and a ~100-fold in response to PMA alone and ~ 300-fold with TNF. Flagellin or flagellin and TNF induce IL-36γ mRNA ~30 and 100-fold respectively. By contrast, there is little change in the expression of IL-36R mRNA in response to any of these stimuli.

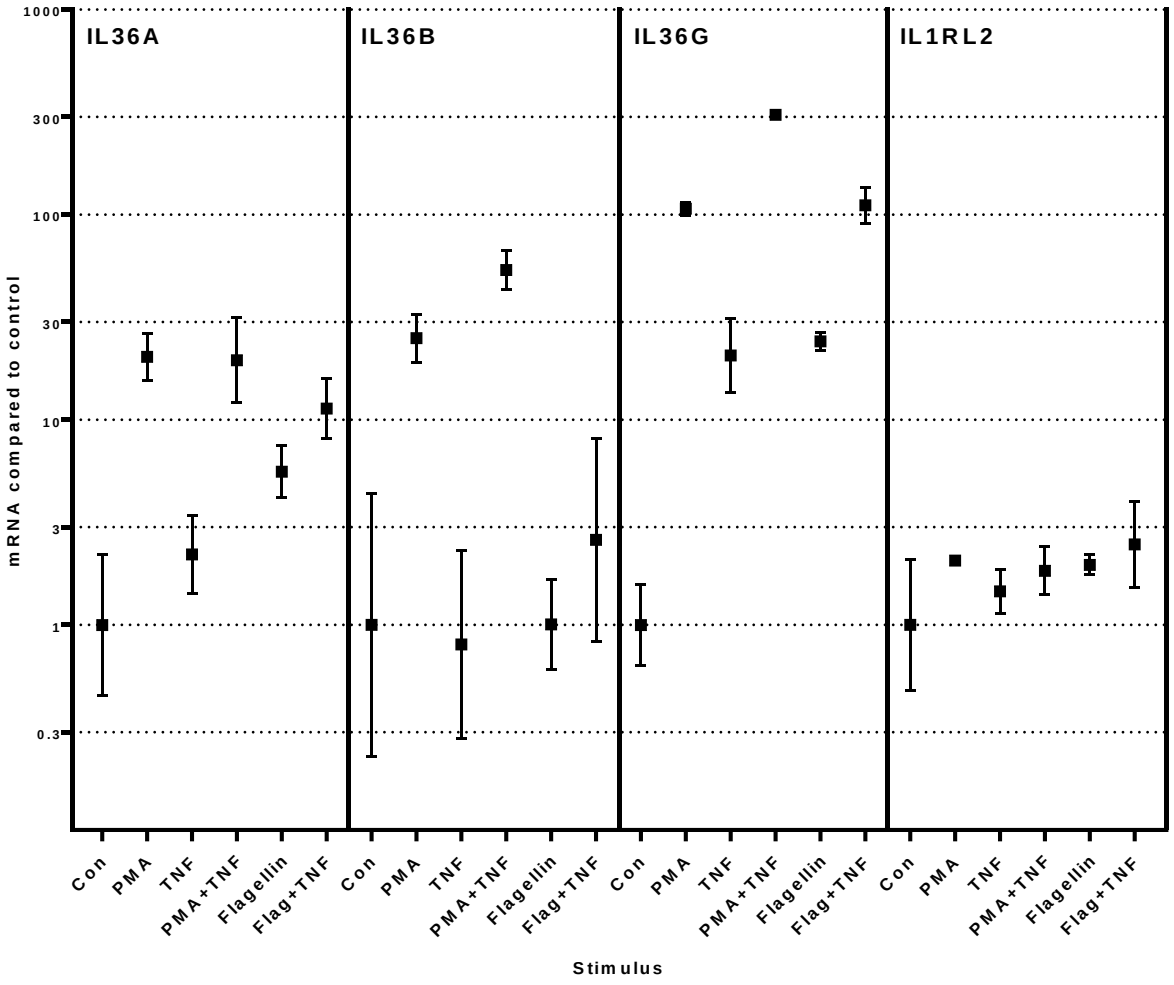

Figure 4.10 Induction of IL-36α, IL-36β, IL-36γ mRNAs. A-431 cells were serum deprived then left untreated (control) or treated with 67 ng/ml PMA, 20 ng/ml TNF, 67 ng/ml PMA and 20 ng/ml TNF, 1 μg/ml flagellin or 1 μg/ml flagellin and 20 ng/ml TNF. Triplicates measurements of Cq were made for at least three biological replicates. The analysis is described in section 4.2. The data (n=3) shown as mean and 95% confidence intervals for they are derived from the analysis shown in section 4.2. See appendix V, table A.1 for the number of Cq determinations used for each treatment.

4.8 qPCR quantification of IL-36α , IL-36β and IL-36γ mRNAs expression in HaCaT cells after co-stimulation with PMA and TNF

Our data indicate that the induction of IL-36γ in A-431 cells by TNF and PMA is synergistic. I tested whether this is true in a different cell line HaCaT. I also investigated whether IL-36 is strongly autoregulated, or it is regulated by the related cytokine IL-1α in HaCaT. HaCaT cells were treated with 5 nM IL-1α, 5 nM IL-36α, 20 ng/ml TNF, 67 ng/ml PMA or 20 ng/ml TNF and 67 ng/ml PMA, or cells were left untreated in LSM for 6 h . Three biological replicates were used for each treatment. RNA was extracted from HaCaT as in section 2.4.2. First strand cDNA, 5 μg, was synthesized as in section 2.4.3. cDNA samples were diluted 5-fold before being used. Results were illustrated in figure 4.11.

RT-qPCR data showed that added IL-36α does not significantly alter the expression of IL-36α or IL-36γ, but it induces IL-36β ~ 3-fold. IL-1α induces IL-36α, IL-36β and IL-36γ mRNAs strongly and significantly ~20, 40 and 60-fold respectively. PMA and TNF synergistically induce the expression of IL-36β by ~200-fold and IL-36γ mRNA ~ 400-fold respectively. Expression of IL-36γ mRNA seemed to respond to treatment of cells with IL-36, but the effect (3-fold) was small. TNF alone similarly induced expression of IL-36β or IL-36γ mRNAs ~ 60-fold. PMA alone induced expression of IL-36β ~ 70-fold, which is an order magnitude stronger than IL-36γ. Again, on both IL-36β and IL-36γ, the combination of TNF and PMA is synergistic. As in the A-431 cells, there is little change in the expression level of IL-36 receptor in response to any of these agents.

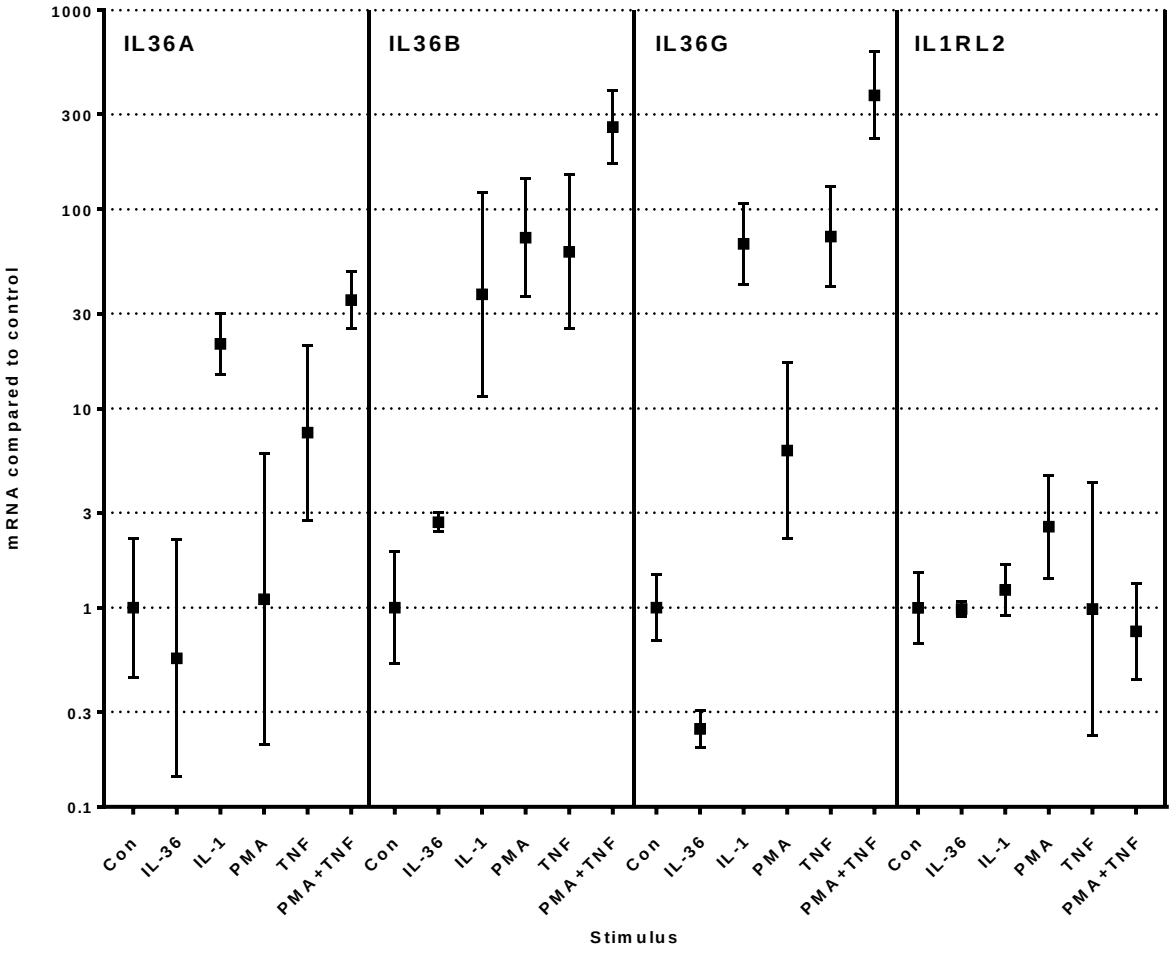

Figure 4.11 Induction of IL-36α, IL-36β, IL-36γ mRNAs. HaCaT cells were serum deprived then left untreated (control) or treated with 5 nM IL-36α, 5 nM IL-1α, 67 ng/ml PMA, 20 ng/ml TNF or 67 ng/ml PMA and 20 ng/ml TNF. Triplicates measurements of Cq were made for at least three biological replicates. The analysis is described in section 4.2. The data (n=3) shown as mean and 95% confidence intervals for they are derived from the analysis shown in section 4.2. See appendix VI, table A.1 for the number of Cq determinations used for each treatment. See Appendix VII, figure A.5 for RT-qPCR products run on gel electrophoresis.

(A)

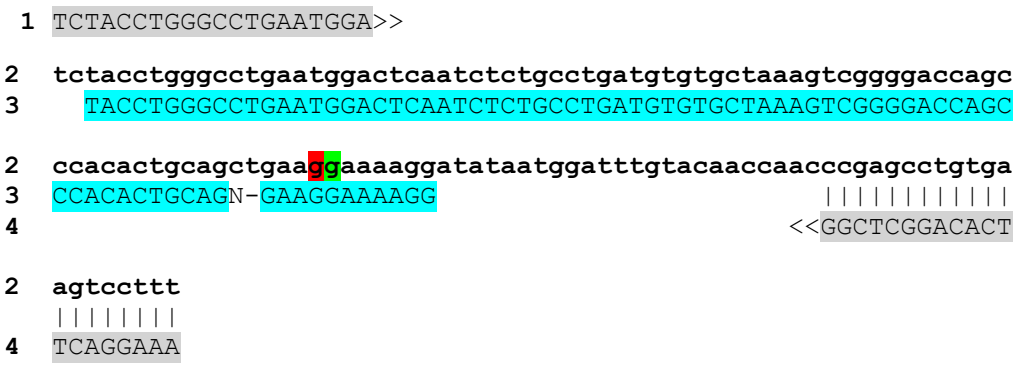

(B)

Figure 4.12 Alignment of IL-36 system sequences from quantitative PCR products (part 1) (A) Exon 3 and 4 of IL-36α from HaCaT with NM_014440.2. (B) Exon 4 and 5IL-36β from HaCaT with NM_173178.2.

Line 1: The forward primer is shaded grey. Line 2 Sequence highlighted in yellow is derived directly from readable Sanger sequence from the forward primer. Line 3 part of the reference cDNA sequence; a red-highlight indicates the end of an exon and green-highlight indicates the start of the next exon. Line 3: Sequence highlighted in azure is complementary to readable Sanger sequence from the reverse primer. Lines 1 and 3: N indicates an unassigned base. Sequence runs are not included before or after runs of N occurred. Line 4: The reverse primer is shown (3' to 5') hybridised to the reference sequence.

(C)

```
1  TGGAGGAAGGGC
2  tggaggaagggc
3  TGGAGGAAGGGC

1  cgtctatc>>          NNNNNNNNTTACTGGGANTATTAATGATTTGAATCAGCAAGT
2  cgtctatcaatcaatgtgtaaacctattactgggactattaatgatttgaatcagcaagt
3  CGTCTATCAATCAATGTGTAAACCTATTACTGGGACTATTAATGATTNGAATCAGCAAGT

1  GTGGACCCTTCAGGGTCAGAACCTTGTGGCAGTTCCACGAAGTGACAGTGTGACCCCAGT
2  gtggaccttcagggtcagaaccttgtggcagttccacgaagtgacagtgtgaccccagt
3  GTGGACNCNTCAGGGTCAGAACNT                          ||||||||||||||||
                                                    CTGTCACACTGGGGTCA

1  CAC
2  cactgttgctgttatcacatgcaagtatccagaggctcttgagcaaggcagaggggatcc
   |||
3  GTG
```

(D)

```
1  CATGTCATCTGCACTTCCCG>>
2  catgtcatctgcacttcccgaagagttgtgt
3  CATGTCATCTGCACTTCCCGAAGAGTTGTGT

1  AGTGGTATAAGGACTGTAACGAGATTAAAGGGGAGCGGTTCACTGT
2  tttgggtccaataaagtggtataaggactgtaacgagattaaaggggagcggttcactgt
3  TTTGGGTCCAATAAAGTGGTATAAGGACTGTAACGAGATTAAAGGGGAGCGGTTCACTGT

1  TTTGGAAACCNGGNTTTTGGTGAGCAATGTCTCGGCAGAGGACAGAGGGAACTACGCGTG
2  tttggaaaccaggcttttggtgagcaatgtctcggcagaggacagagggaactacgcgtg
3  TTTGGAAACCaggcttttggtgagcaatgtctcggcagaggacagagggaactacgcgtg
                                                    |||||||||
4                                                 <<GATGCGCAC

1  TCAAGCCATA
2  tcaagccata
3  tcaagccatN
   |||||||||
4  AGTTCGGTAT
```

Figure 4.12 Alignment of IL-36 system sequences from quantitative PCR products. (part 2) (C) Exon 2 and 3 of IL-36γ from HaCaT cells with NM_019618.4 (D) Exon 4 &5 of IL-36R from HaCaT cells with NM_003854.2. Line 1: The forward primer is shaded grey. Line 2 Sequence highlighted in yellow is derived directly from readable Sanger sequence from the forward primer. Line 3 part of the reference cDNA sequence; a red-highlight indicates the end of an exon and green-highlight indicates the start of the next exon. Line 3: Sequence highlighted in azure is complementary to readable Sanger sequence from the reverse primer. Lines 1 and 3: N indicates an unassigned base. Sequence runs are not included before or after runs of N occurred. Line 4 and 5: The reverse primer is shown (3' to 5') hybridised to the reference sequence.

(E)

```
1   AGATGAGTATGCCTGC
2   agatgagtatgcctgc


1   CGTG>>                        GCCCNNGATAGTTAAGTGGGATCGAGACATGTAA
2   cgtgtgaaccatgtgactttgtcacagcccaagatagttaagtgggatcgagacatgtaa

1   GCAGCATCATGGAGGTTTGAAGANGCCNCATTTGGATTGG
2   gcagcatcatggaggtttgaagatgccgcatttggattggatgaattccaaattctgctt
                              ||||||||||||||||||||
                            <<CGGCGTAAACCTAACCTACT
```

(F)

```
1     AATCCAAGAAGGGG
2     aatccaagaagggg
3     AATCCAAGAAGGGG

1     CTGTCC>>                            AGCCCTTCNGCGGCCAGTAGCATCTGAC
2     ctgtcctcgtcctccagctgttatctggaagaagcccttcagcggccagtagcatctgac
3     CTGTCCTCGTCCTCCAGCTGTTATCTGGAAGAAGCCCTTCAGCGGCCAGTAGCATCTGAC


1     TTTGAGCCTCAGGGTCTGAGTGAAGCCGCTCGTTGGAACTCCAAGGAAAACCTTCTCGCT
2     tttgagcctcagggtctgagtgaagccgctcgttggaactccaaggaaaaccttctcgct
3     NTTGAGCCTCAGGGTCNGAGNAAGCCGC                  ||||||||||||||
4                                                 <<TTTTGGAAGAGCGA

1     ggaccc
2     ||||||
3     CCTGGG
```

Figure 4.12 Alignment of IL-36 system sequences from quantitative PCR products (part 3) (E) Exon 3 and 4 of β2 microglobulin from HaCaT with NM_004048.2. (F) Exon 1 and 2 of 1ABL kinase (ABL1) from HaCaT with NM_005157.5. Line 1: The forward primer is shaded grey. Sequence highlighted in yellow is derived directly from readable Sanger sequence from the forward primer. Line 2 part of the reference cDNA sequence; a red-highlight indicates the end of an exon and green-highlight indicates the start of the next exon. Line 3: Sequence highlighted in azure is complementary to readable Sanger sequence from the reverse primer. Lines 1 and 3: N indicates an unassigned base. Sequence runs are not included before or after runs of N occurred. Line 4: The reverse primer is shown (3' to 5') hybridised to the reference sequence.

(G)

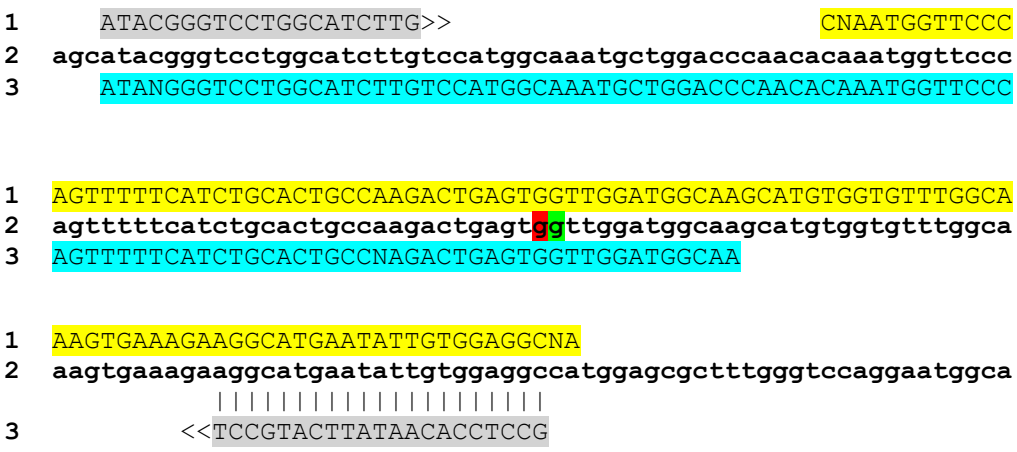

Figure 4.12 Alignment of IL-36 system sequences from quantitative PCR products (part 4) (G) Exon 1 and 2 Peptidyl proline isomerase (PPIA) from HaCaT with NM_021130.4 Line 1: The forward primer is shaded grey. Sequence highlighted in yellow is derived directly from readable Sanger sequence from the forward primer. Line 2 part of the reference cDNA sequence; a red-highlight indicates the end of an exon and green-highlight indicates the start of the next exon. Line 3: Sequence highlighted in azure is complementary to readable Sanger sequence from the reverse primer. Lines 1 and 3: N indicates an unassigned base. Sequence runs are not included before or after runs of N occurred. Line 4: The reverse primer is shown (3' to 5') hybridised to the reference sequence.

4.9 Time course of induction of expression of the IL-36γ protein in A-431

Because IL-36γ mRNA is expressed in A-431 in response to 20 ng/ml TNF, I investigated the expression of the IL-36γ protein in response to 20 ng/ml TNF at different time points. A-431 cells were treated with 20 ng/ml TNF in serum free medium over a time course (6, 9, 12 and 24 h) or left with serum free medium only as a negative control. Three biological replicates were used for each time point. Protein samples were extracted as described in section 2.6.3. SDS-PAGE gel was used to separate cell lysate proteins 10 μg/lane. n^{18}-1IL-36γ and n^{1}-IL-36γ (R&D systems) (0.25 ng) were used as positive controls. Mouse protein extracted from 3T3L1 was used as a negative control. The antibody (MAB2320, R&D systems) is specific to human IL-36γ because mouse and human IL-36γ are only 58%- 67% amino acids identical, I would not expect mouse cells to produce any specifically immunoreactive protein. In some assays, I applied a standard mixture of 5 μg of total mouse protein and 0.25 ng of each from of IL-36γ. The β-actin antibody, however, is fully cross relative between mouse and human. This enable us to approximately standardise for protein loading as measured from β-actin and IL-36γ between different immunoblots.

Inducing expression of IL-36γ protein was measured by western blotting which showed that maximum IL-36γ protein induction level in response to 20 ng/ml TNF was observed after 24 h. As shown in figure 4.13 and 4.14.

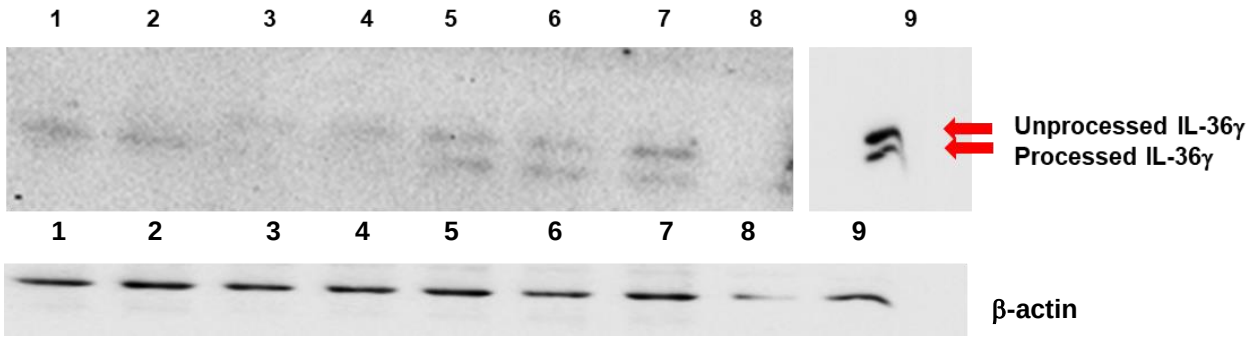

Figure 4.13 Time course of IL-36γ protein expression in A-431 cells. Lane (1-2): Control (no treatment), Lane (3-4): 6 h, Lane (5-6): 9 h, Lane 7: 12 h, Lane 8: Mouse protein (negative control), Lane 9: 0.25 ng processed and unprocessed IL-36γ protein (positive control). This experiment was performed three times and demonstrated similar results both times.

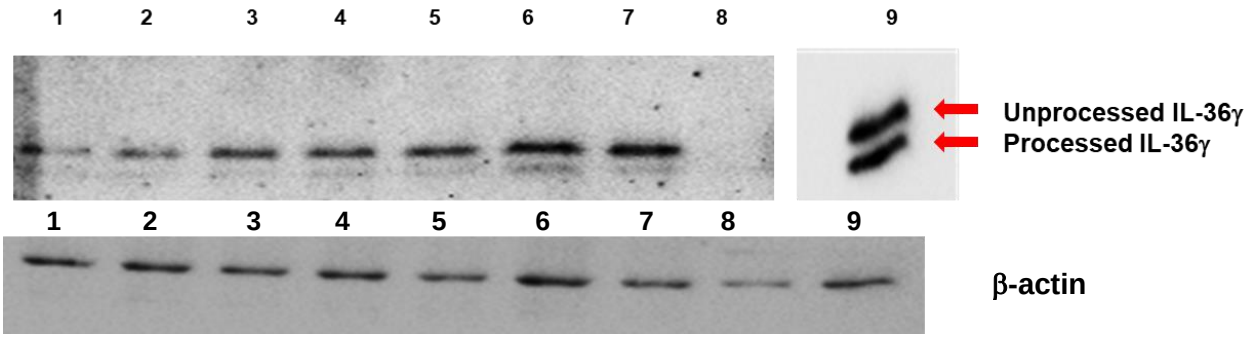

Figure 4.14 Time course of IL-36γ protein expression in A-431 cells. Lane1, 12 hr, lane 2: 6 hr, Lane 3: 9 h, lane 4: 12 h, lane 5: 24 h, Lane 6: 24 h, Lane 7: 24 h, Lane 8: Mouse protein (negative control), Lane 10: 0.25 ng processed and unprocessed IL-36γ protein (positive control). This experiment was performed three times and demonstrated similar results both times.

4.10 A first attempt to activate processing of endogenous IL-36γ in A-431 cells

I attempted to identify a signal that might cause processing of IL-36γ protein. Because I already had shown that TNF could induce IL-36γ protein in A-431 cells, I examined whether treating A-431 cells with TNF for 24 h.

After inducing expression of IL-36γ protein, I then re-stimulated with different inflammatory activators. A-431 cells were stimulated for 24 h with 20 ng/ml TNF to induce IL-36γ protein expression, then cells were re-treated with different inflammatory stimuli for 6 h. In case they might trigger the processing of the enzyme, I used 1 μg/ml flagellin, 67 ng/ml PMA, 5 μg/ml LPS, 5 nM IL-36α, 5 nM IL-1α, 3.2 μg/ml LL-37, 25 μg/ml poly I:C or ATP (19.5 mM). Protein samples were loaded at 10 μg in each lane. Recombinant processed and unprocessed IL-36γ protein (0.25 ng) were used as markers and as a positive control in a western blot. An extract of mouse 3T3L1 cells was also used as a negative control. Western blot data showed that processing of IL-36γ protein was not induced, but the combination of flagellin and TNF (see figure 4.15, lanes 1 and 2) or PMA and TNF (see figure 4.16, lanes 1 and 2) induced greater expression of IL-36γ protein than did TNF alone (see figure 4.15 and figure 4.16, lanes 6 and 7). This finding led us to use PMA and TNF treatment as our standard method for inducing IL-36γ expression. The outcomes of the experiment therefore although I did not discover a signal that would cause IL-36γ to be processed, I did find a treatment that could cause stronger expression of IL-36γ protein than has seen with TNF alone. Both flagellin and TNF or PMA and TNF produced a stronger response than TNF alone.

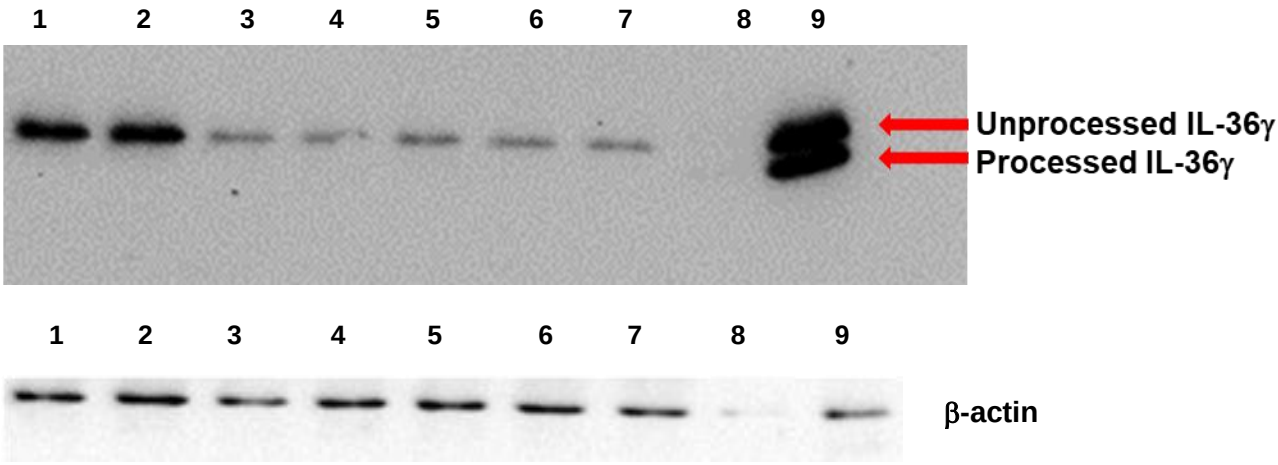

Figure 4.15 Combination of TNF and flagellin induce expression of IL-36γ protein in A-431 cells. Cells were pre-treated with 20 ng/ml TNF for 24 hto induce expression of IL-36γ then 6 hr incubated with different activators. Lane (1-2): 1 μg flagellin, Lane (3-4): 5 μg/ml LPS, Lane (5): 19.5 mM ATP, Lane (6-7): 20 ng/ml TNF for 24 h (control), Lane 8: Mouse protein (negative control), Lane 9: 0.25 ng processed and unprocessed IL-36γ protein (positive controls). This experiment was performed three times and demonstrated similar results each time.

.

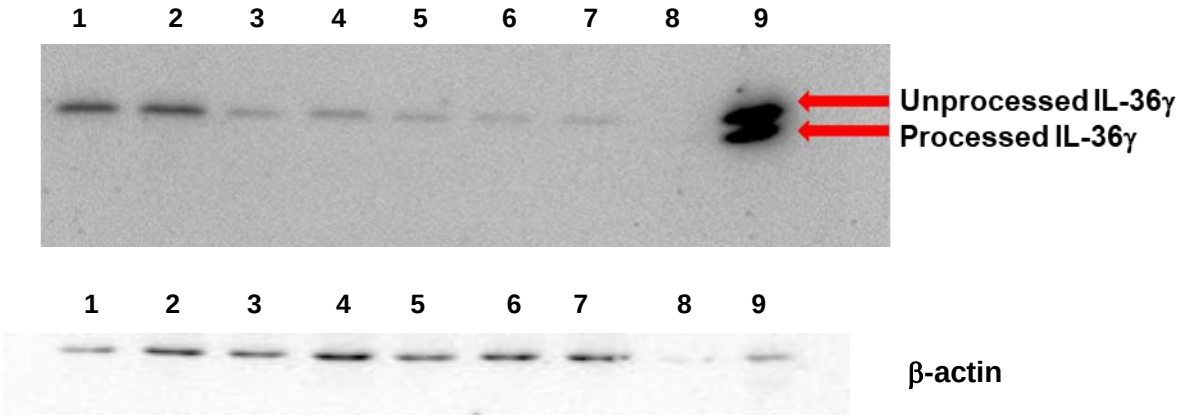

Figure 4.16 Combination of TNF and PMA induces IL-36γ protein in A-431 cells were treated with 20 ng/ml TNF for 24 h then with followed reagents for 6 h. Lane (1-2): 67 ng/ml PMA, Lane (3-4): 25 μg /ml Poly I:C, Lane 5: 95 μg/ml ATP. Lane (6-7): 20 ng/ml TNF for 24 h (control), Lane 8: Mouse protein (negative control), Lane 9: 0.25ng of processed and unprocessed IL-36γ protein (positive controls). This experiment was performed three times and demonstrated similar results each time.

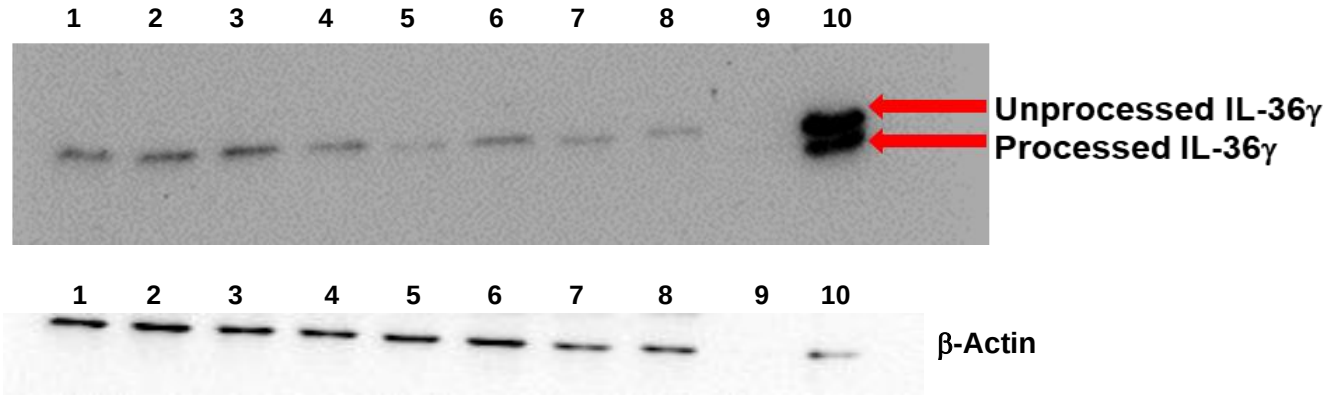

Figure 4.17 Effect of TNF with different co activators on the IL-36γ protein expression in A-431 cells. A-431 cells were treated with 20 ng/ml TNF for 24 hr then 6 hr incubated with different activators. Lane (1-2): 5 nM IL-36α, Lane (3-4): 5 nM IL-1α Lane (5-6): 3.2 μg/ml LL37, Lane (7-8): 20 ng/ml TNF for 24 h (control), Lane 9: blank (negative control), Lane 10: 0.25 ng of processed and unprocessed IL-36γ protein (positive controls). IL-36γ was incubated with primary antibody (MAB2320 R&D). This experiment was performed three times and demonstrated similar results each time.

4.11 Induction of IL-36γ protein in A-431 cells by TNF and PMA or TNF and flagellin combination.

It appeared that both PMA and flagellin activate expression of IL-36γ and possibly synergistic. I, therefore, returned to the similar protocol of 6 h of cell treatment, this time with TNF PMA and flagellin separately or PMA or flagellin in combination with TNF. To discover if PMA or flagellin could synergise with the induction of IL-36γ protein TNF, I treated A-431 cells with 20 ng/ml TNF, 67 ng/ml PMA, 20 ng/ml TNF and 67 ng/ml PMA, 1 μg/ml flagellin or 1 μg/ml flagellin and 20 ng/ml TNF for 6 hr, compared with untreated controls. 3T3L1 (mouse cell) protein extract was also used as a negative control. Protein samples were loaded at approximately 10 μg in each well. A 0.25 ng of processed and unprocessed IL-36 protein were used as positive controls. The control was combined with the IL-36γ standards, which were added at 0.25 pg per lane. This enabled us to use the β-actin content of the mouse cells to standardise between gels. I assume that the anti-β-actin antibody cross reacts completely between mouse and human proteins and that the β-actin content in all cell types. Any differences between β-actin content are expected to be a constant for the particular cell type and therefore are not expected to affect our conclusions concerning the induction of IL-36γ protein. The quantity of the IL-36γ proteins and β-actin were estimated, based on the luminescence recorded as a function of time. Calculations were done for a portion of the curves of the light recorded as a function of time when growth of the signal appeared to be linear and where analysis of the image showed the pixels were not saturated. Protein concentrations were assumed to be proportional to the rate of light emission.

Western blotting data showed that the combination of PMA and TNF (figure 4.18 lanes 5 and 6) or flagellin and TNF (figure 4.19, lanes 6, 7 and 8) positively upregulated expression of IL-36γ protein after 6 h compared with PMA, TNF or flagellin alone.

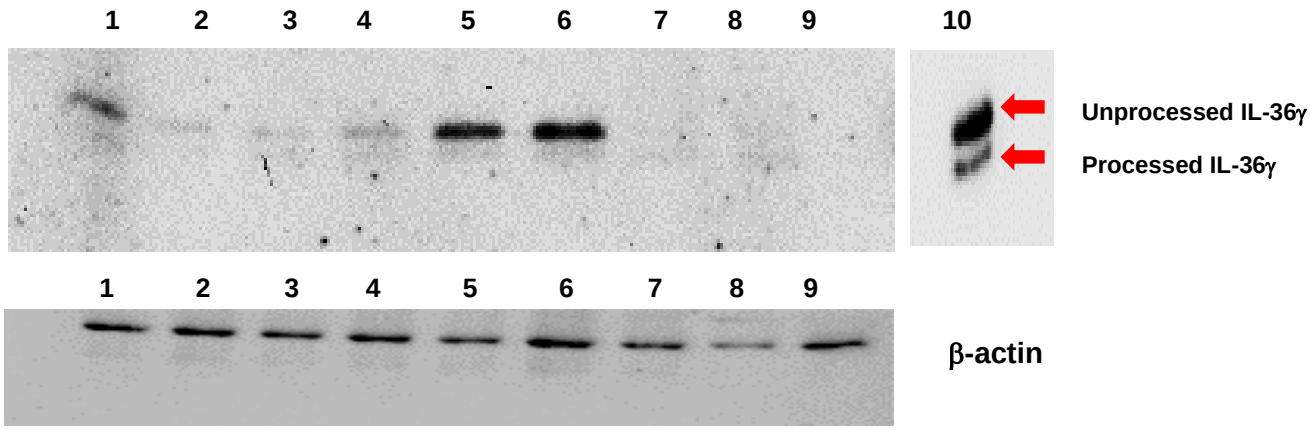

Figure 4.18 Combination of TNF and PMA for 6 hr induces IL-36γ protein activation. A-431 cells were treated with Lane (1-2): 67 ng/ml PMA, lane (3-4): 20 ng/ml TNF, Lane (5-6): 67 ng/ml PMA and 20 ng/ml TNF, Lane 7): Control (no treatment), Lane 9: Mouse protein (negative control), lane 10: 0.25 ng of processed and unprocessed IL-36γ protein (positive controls). This experiment was performed three times and demonstrated similar results each time.

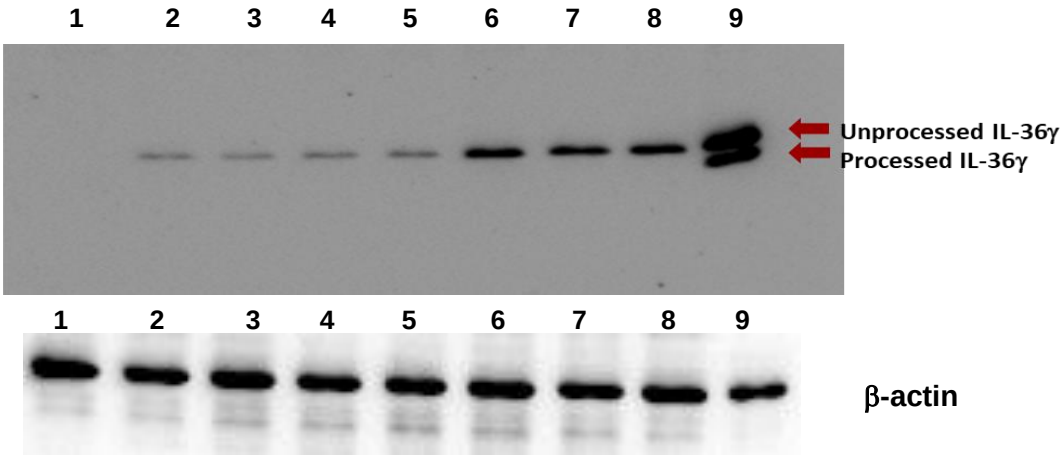

Figure 4.19 Combination of TNF and flagellin upregulated IL-36γ protein in A-431 for 6 hr. Lane 1: Control (no treatment), Lane (2-3): 20 ng/ml TNF, Lane (4-5): 1 μg/ml Flagellin, Lane (6-8): 1 μg/ml flagellin and 20 ng/ml TNF, Line 9: 0.25 ng of processed and unprocessed IL-36γ protein (positive controls). This experiment was performed three times and demonstrated similar results each time.

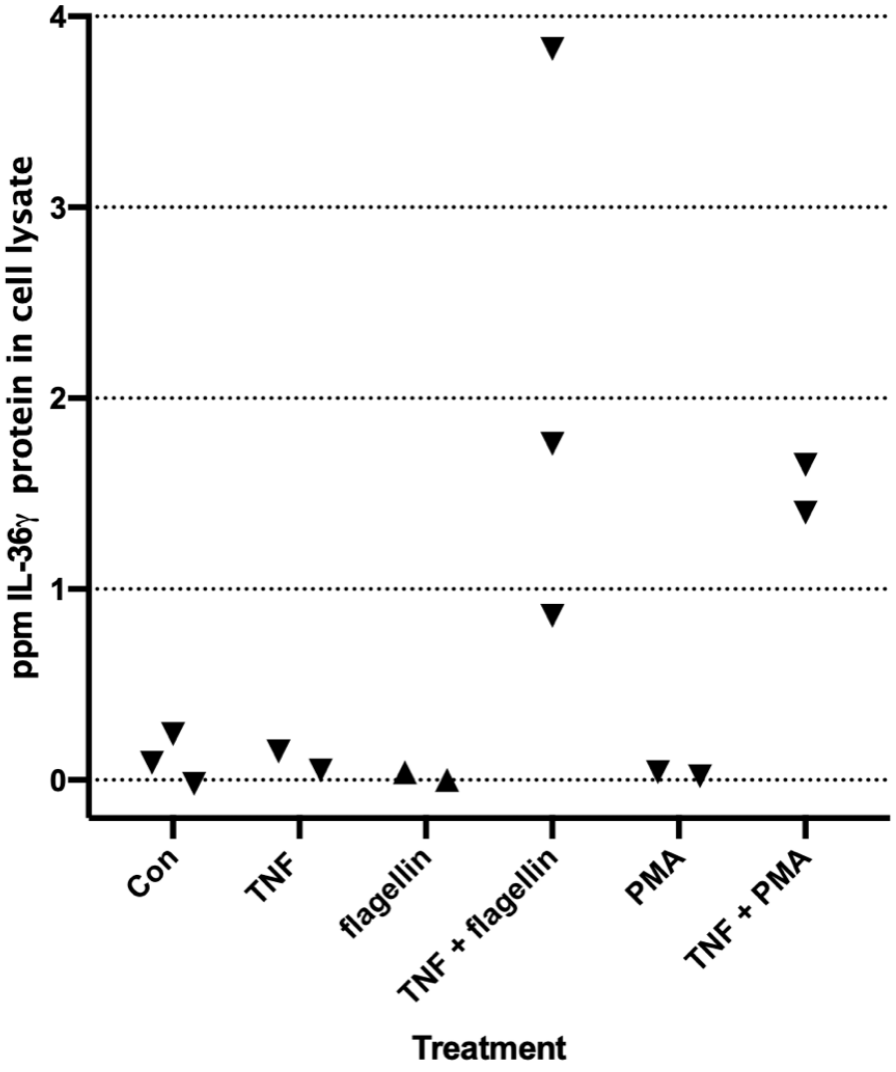

Figure 4.20 Quantity of IL-36γ protein in A-431 cells after being treated with different inflammatory stimuli. Individual data are derived as described in methods. the linear phase of growth of total luminescence output was identified for each band and a rate of luminescence was calculated. This was then related to the luminescence yield of the two 250 pg standard bands. This allows us to estimate the amount of IL-36γ on the blot. Assuming full cross reactivity for β-actin between the mouse extract control and the human cell extract, I also calibrated the relative proportion of β-actin in each lane. Given that control lane contained a known quantity of protein, it was then possible to estimate the amount of protein loaded in each lane by comparison of the quantity of β-actin. They finally allowed us to estimate the quantity of IL-36γ as a proportion (in part per million) of the total protein.

4.12 Induction of IL-36γ protein in HaCaT cells by TNF and PMA or TNF and flagellin.

Because a combination of TNF and PMA or TNF and flagellin synergistically induced expression of IL-36γ protein in A-431, I examined whether these combinations would also work on the HaCaT cells. HaCaT cells were treated with 20 ng/ml TNF, 67 ng/ml PMA, 1 μg/ml flagellin, 20 ng/ml TNF and 67 ng/ml PMA or 20 ng/ml TNF and 1 μg/ml flagellin for 6 hr. Low serum medium (no treatment) was used as a control. Mouse L3T3 extract was combined with the IL-36γ standards, which were added at 0.25 pg per lane. This enabled us to use its β-actin content to standardise between gels. I assume that the anti-b-actin antibody cross reacts completely between mouse and human proteins and that the β-actin content in all cell types is the same. Any differences between β-actin content are expected to be a constant for the particular cell type and therefore are not expected to affect our conclusions concerning the induction of IL-36γ. The quantity of the IL-36γ proteins and β-actin were estimated based on the luminescence recorded as a function of time. Calculations were done for a portion of the curves of the light recorded as a function of time when growth of the signal appeared to be linear and where analysis of the image showed the pixels were not saturated. Protein concentrations were assumed to be proportional to the rate of light emission.

Protein samples were loaded at approximately 10 μg in each well. A 0.25 ng processed and unprocessed IL-36γ protein was used as positive controls. Mouse protein was used as a negative control. Western blotting data showed again that combination of TNF and PMA (figure 4.20, lanes 5, 6 and 7) or TNF and flagellin (figure 4.21, lanes 6, 7 and 8) induced IL-36γ expression in HaCaT cells. TNF (figure 4.20, lanes 2 and 3) or flagellin (figure 4.21, lanes 4 and 5) slightly induced expression of IL-36γ, but IL-36γ protein was not detectably induced by PMA alone (figure 4.21, lanes 3 and 4).

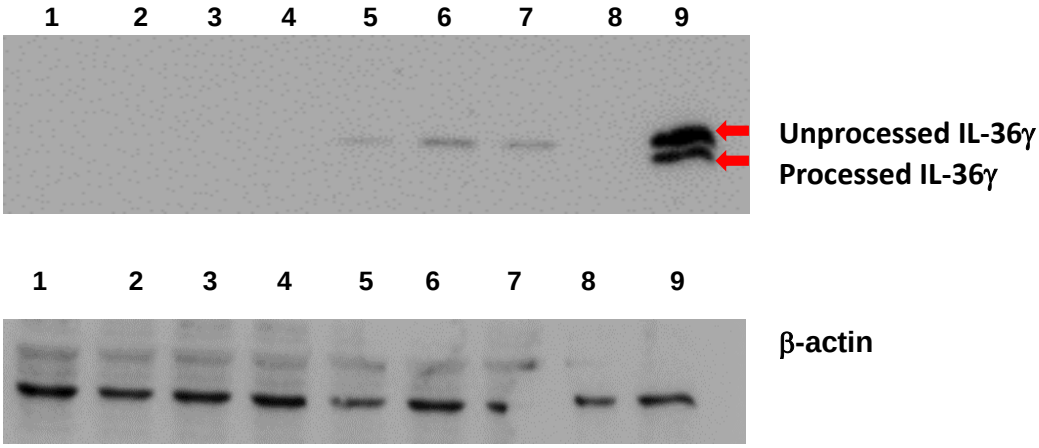

Figure 4.21 Combination of PMA and TNF upregulated IL-36γ protein expression in HaCaT cells. Lane (1-2): Control (no treatment), Lane (3-4): 67 ng/ml PMA, Lane (5-7): 20 ng/ml TNF and 67 ng/ml PMA for 6 hr, Lane 8: Mouse protein (negative control), Lane 9: 0.25 ng of processed and unprocessed IL-36γ protein (positive controls). This experiment was performed three times and demonstrated similar results each time.

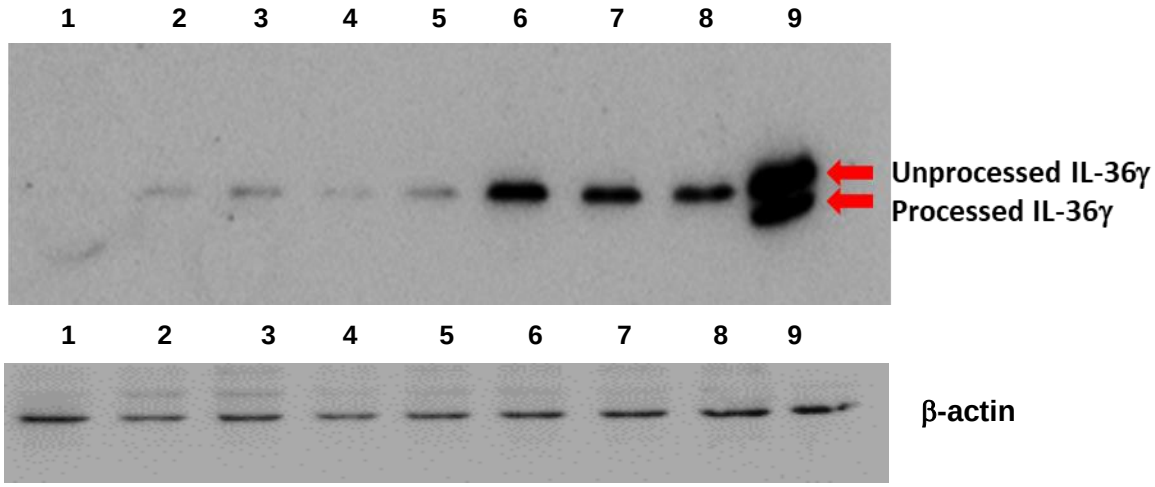

Figure 4.22 Combination of TNF and flagellin induces IL-36γ protein in HaCAT cells. Lane 1: Control (no treatment), Lane (2-3) 20 ng/ml TNF, lane (4-5): 1 μg/ml flagellin, Lane (6-8): 1 μg/ml flagellin and 20 ng/ml TNF, Lane 9: 0.25 ng of processed and unprocessed IL-36γ (positive controls). This experiment was performed three times and demonstrated similar results each time.

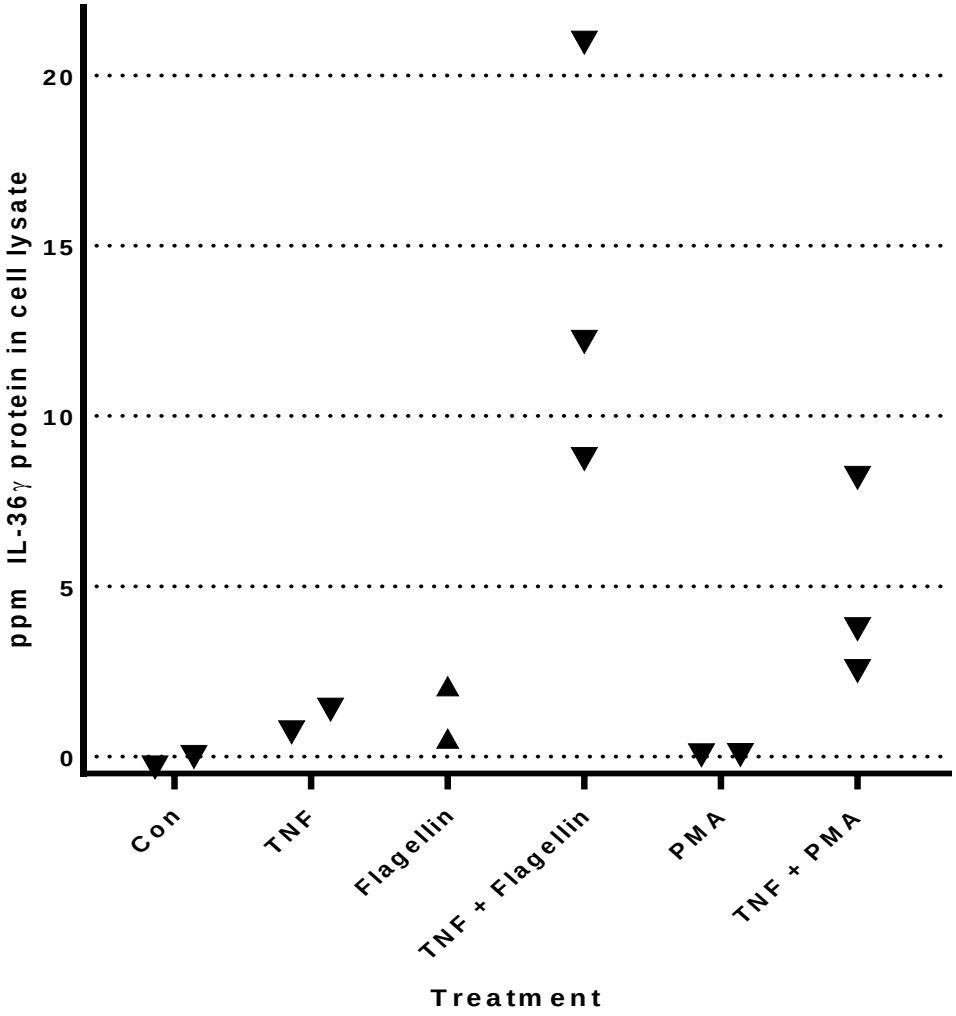

Figure 4.23 Quantity of IL-36γ protein in HaCaT cells after being treated with different inflammatory stimuli. Individual data are derived as described in methods. the linear phase of growth of total luminescence output was identified for each band and a rate of luminescence was calculated. This was then related to the luminescence yield of the two 250 pg standard bands. This allows us to estimate the amount of IL-36γ on the blot. Assuming full cross reactivity for β-actin between the mouse extract control and the human cell extract, I also calibrated the relative proportion of β-actin in each lane. Given that, control lane contained a known quantity of protein, it was then possible to estimate the amount of protein loaded in each lane by comparison of the quantity of β-actin. They finally allowed us to estimate the quantity of IL-36γ as a proportion (in part per million) of the total protein.

4.13 Attempted activation of cell autonomous processing of IL-36γ through activation of Toll-like receptors

First, I tested whether TLR7, TLR8 or activation of necroptosis could activate IL-36γ protein expression and processing in A-431. A-431 cells were treated with 20 ng/ml TNF and 67 ng/ml PMA for 8 hr or 20 ng/ml TNF and 67 ng/ml PMA for 6 hr to induce expression of endogenous IL-36γ then were further treated for 2 h with 0.1 μg/ml of CL-097, which is TLR7 activator or 1 μg/ml CL-075, which TLR8 activator as described in section 2.6.10. A western blot showed that A-431 did not respond to TLR7 or TLR8 activators and IL-36γ protein is not processed. The data are shown in the figure 4.24a and 4.24b.

The hydrotropic dipeptide ester Leu-Leu-OMe has been reported to trigger necroptosis as a result of its polymerisation by proteases inside endosomes (Odaka et al., 1995).

With the necroptosis inducer, A-431 cells were treated for 6 hr with 20 ng/ml TNF to induce IL-36γ protein expression then treated with 0.25 mM Leu-Leu methyl ester hydrobromide (Leu-Leu-OMe) for 2 h to test whether it could induce processing of the protein or 8 hr with 0.25 mM Leu-Leu-OMe drug as a control as in section 2.6.12. Three biological replicates culture were used for each treatment. Protein samples were extracted as described in section 2.6.3. SDS-PAGE gel was used to separate cells lysate proteins (10 μg/lane). IL-36γ protein was visualised and measured by western blotting. There was no detectable induction of IL-36γ protein by CL-075 or CL097 and no processing was caused by either CL-075, CL097 or Leu-Leu-OMe as shown in figure 4.25.

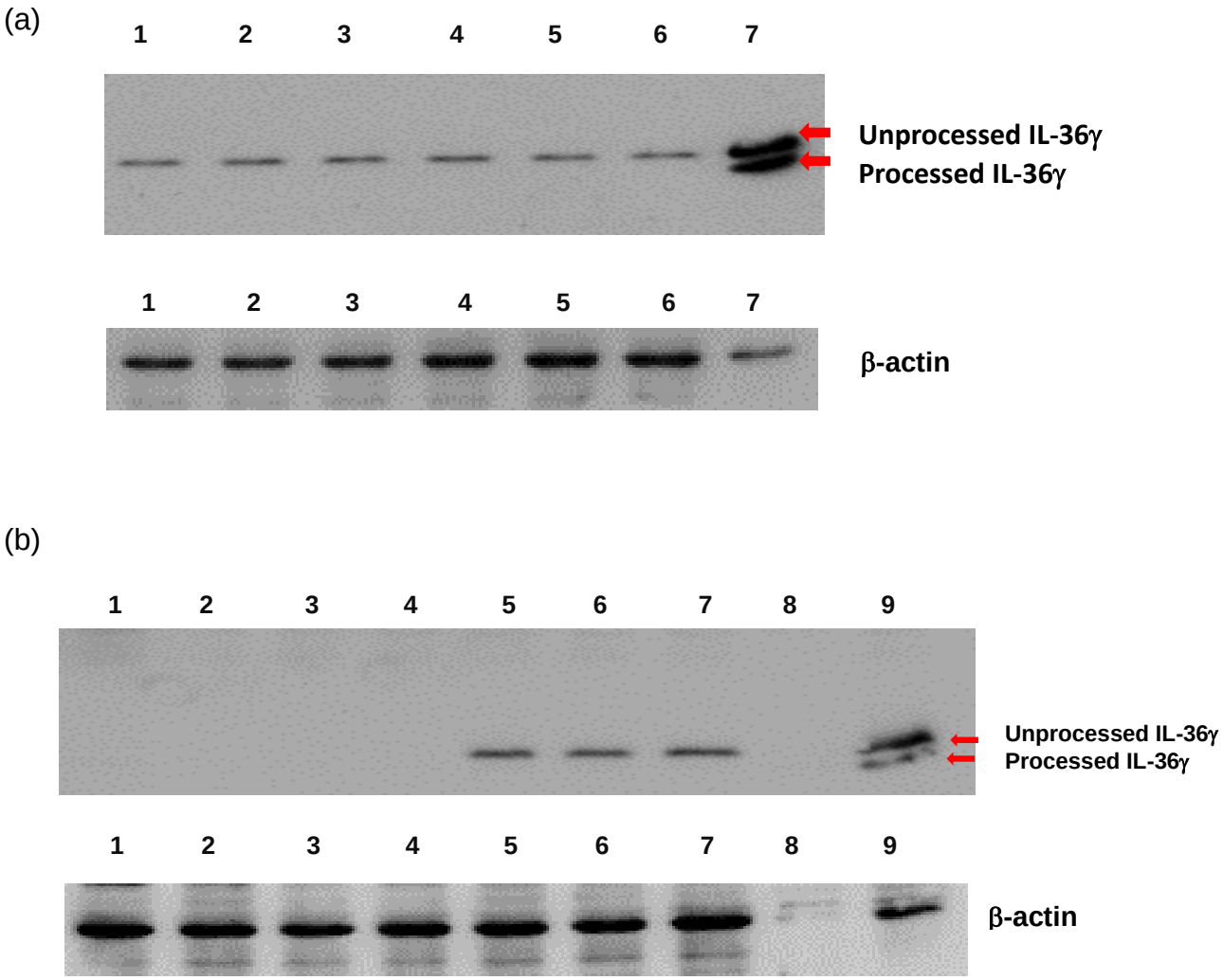

Figure 4.24 Visualisation of IL-36γ protein after toll like receptor activators treatment of TNF/PMA treated cells. (A) TLR7 activator Lane (1-3): 20 ng/ml TNF and 67 ng/ml PMA for 8 hr, lane (4-6) 20 ng/ml TNF and 67 ng/ml PMA for 6 hr TNF then 0.1 μg/ml CL-097 for 2 hr, lane 7: 0.25 ng processed and unprocessed IL-36γ protein (positive controls). **(B).** TLR8 activator**.** Lane (1-2): LSM for 6 hr then 1 μg CL-075 for 2 hr, Lane (3-4): 1 μg CL-075 for 8 hr, Lane (5-7): 20 ng/ml TNF and 67 ng/ml PMA for 6 hr then 1 μg CL-075 for 2 hr, Lane 8: blank (negative control), Lane 9: 0.25 ng of processed or unprocessed IL-36γ protein (positive controls). This experiment was performed twice and demonstrated similar results both times.

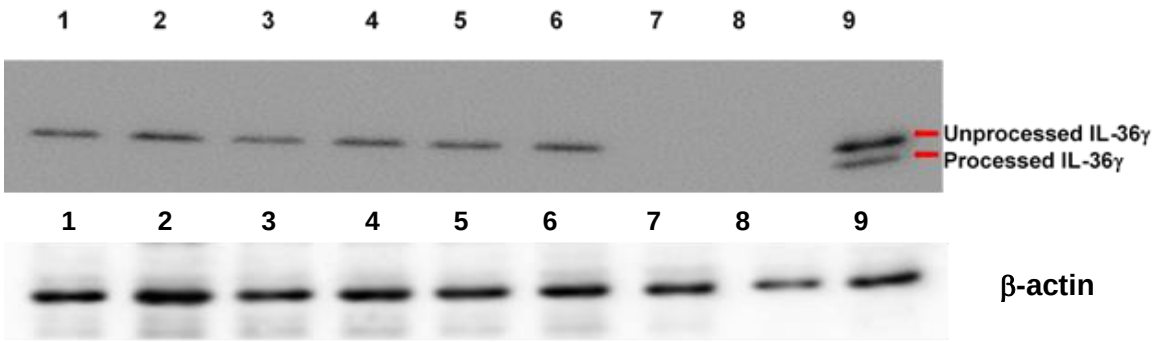

Figure 4.25 Visualisation of IL-36γ protein after treatment of A-431 cells with Leu-Leu-OMe. Lane (1-3): 67 ng/ml PMA + 20 ng/ml TNF for 8 hr, Lane (4-6): 67 ng/ml PMA + 20 ng/ml TNF for 6 hr then 2 hr with 0.25 μg Leu-Leu-Meo, Lane 7: Control (no treatment), Lane 8: Mouse protein (negative control), Lane 9: 0.25 ng of processed and unprocessed IL-36γ protein (positive controls). This experiment was performed twice and demonstrated similar results both times.

4.14 Inducing death program in A-431 through using apoptosis agents

I examined possible processing of IL-36γ in A-431 cells by apoptosis inducers cycloheximide, staurosporine and A23187 calcium ionophore. A-431 cells were treated with 20 ng/ml TNF and 67 ng/ml PMA for 6 hr to induce expression of endogenous IL-36γ before the medium was exchanged for serum free medium containing the protein synthesis inhibitor cycloheximide (100 μM/ml), protein kinase inhibitor staurosporine (0.5 mM/ml), the calcium ionophore A23187 (5 μM) or a combination of cycloheximide (100 μM), staurosporine (0.5 mM) and A23187 (5 μM) for 24 h in a total volume 200 μl on 9.5 cm^2 tissue culture well, as described in 2.6.11. SDS-PAGE gel was used to separate cell lysate proteins 20 μg/lane. Mature and immature IL-36γ protein (0.25 ng) were used as positive controls. Induction of expression endogenous IL-36γ protein was measured by western blotting. I found that a fraction of the IL-36γ protein changes to a mobile form when cells were treated with cycloheximide or staurosporine. The C^{+2}-ionophore A23187 triggers no such defect. The new band is visible in figures 4.26 and 4.27. It is less mobile than n^{18}-IL-36γ standard, so is possible cleaved at a different site. Treating A-431 cells with cycloheximide, staurosporine or A23187 alone for 24 hr did not induce IL-36γ protein synthesis as shown in figure 4.28.

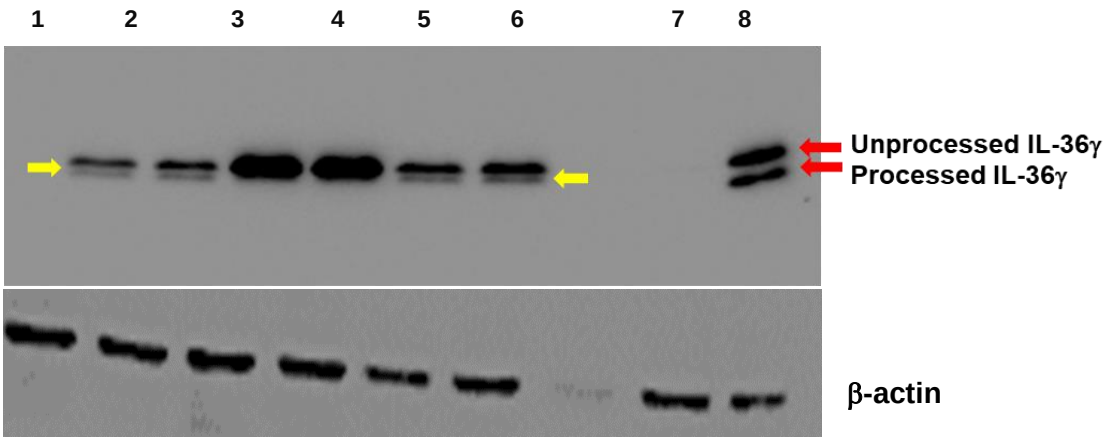

Figure 4.26 Change in mobility of IL-36γ protein in A-431 cells in response to toxic pro-apoptotic agents. A-431 cells were treated with 20 ng/ml TNF and 67 ng/ml PMA for 6 hr then re-stimulated with different apoptosis inducers for 24 hr. Lane (1-2) 100 μM cycloheximide, Lane (3-4): 5 μM A23187 (calcium ionophore), Lane (5-6): 0.5 mM staurosporine, Lane 7: mouse protein (negative controls), Lane 8: 0.25 ng processed and unprocessed IL-36γ protein (a positive controls). IL-36γ protein appeared to be processed in A-431 cells after cycloheximide or staurosporine re-stimulation (yellow arrow). This experiment was performed twice and demonstrated similar results both times.

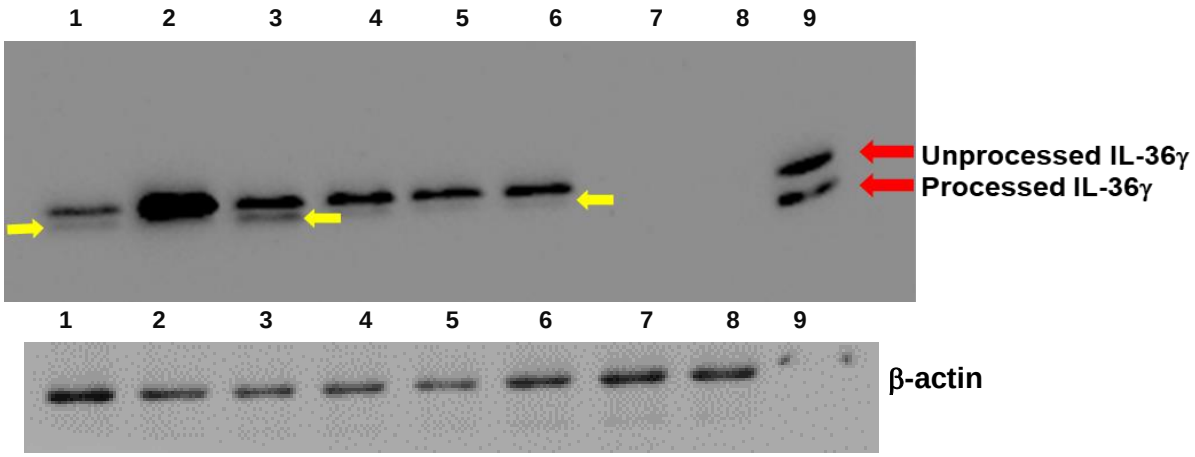

Figure 4.27 Change in mobility of IL-36γ protein in A-431 cells in response to toxic pro-apoptotic agents. A-431 cells were treated with 20 ng/ml TNF and 67 ng/ml PMA for 6 hr then re-stimulated with different apoptosis inducers for 24 hr. Lane 1: 100 μM cycloheximide, Lane 2: 5 μM A23187 (calcium ionophore), Lane 3: 0.5 mM staurosporine, Lane (4-6): 100 μM cycloheximide, 5 μM A23187 and 0.5 mM staurosporine, Lane (7-8): Mouse protein (negative controls), Lane 9: 0.25 ng processed and unprocessed IL-36γ protein (positive controls). IL-36γ protein appeared to be processed in A-431 cells after cycloheximide and staurosporine treatment (yellow arrow). This experiment was performed twice and demonstrated similar results both times.

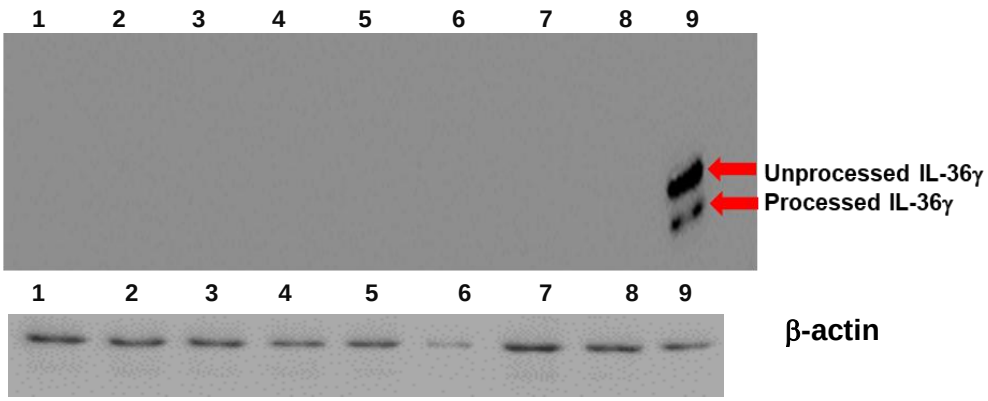

Figure 4.28 Cycloheximide, staurosporine and calcium ionophore alone do not induce IL-36γ protein synthesis in A-431 cells. A-431 cells were treated with apoptosis inducers for 24 hr (negative controls). Lane (1-2): 100 μM cycloheximide, Lane (3-4): 5 μM A23187 (calcium ionophore), Lane (5-6): 0.5 mM staurosporine, Lane (7-8): 100 μM cycloheximide, 5 μM A23187 and 0.5 mM staurosporine, Lane 9: 0.25 ng processed and unprocessed IL-36γ protein (positive controls). This experiment was performed twice and demonstrated similar results both times.

4.15 Inducing IL-36γ protein processing in A-431 cells with different time points

I sought to determine how rapidly the mobility shift in IL-36γ in response to staurosporine in A-431. A-431 cells were treated with 20 ng/ml TNF and 67 ng/ml PMA for 6 h to induce IL-36γ. The medium was changed into serum free medium and cells were incubated with 0.5 mM/ml staurosporine for 0, 6, 12 and 24 h. After each time point, cells lysate and supernatant were collected in total volume 0.2 ml as in described in section 2.6.14. SDS-PAGE gel was used to separate cells lysate proteins (20 μg) per Lane. Mature and immature IL-36γ protein (0.25 ng) were used as positive controls. Inducing expression of IL-36γ protein was visualised by western blotting. Treatment with staurosporine resulted in a change in mobility of IL-36γ in response to staurosporine in a time dependent manner as showed in figure 4.29.

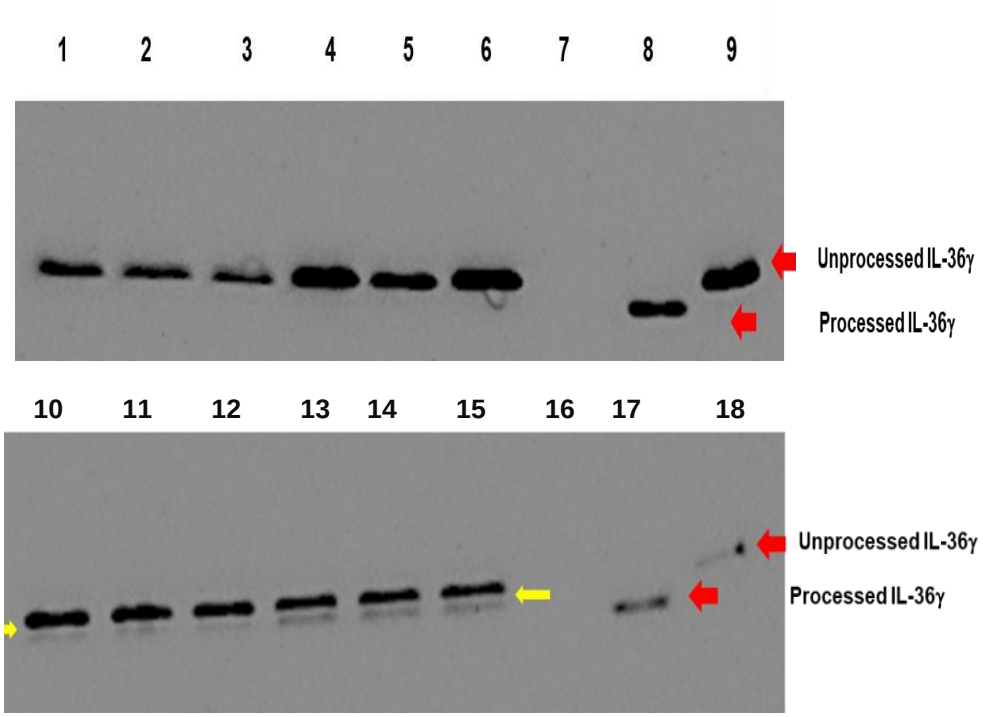

Figure 4.29 Time course of the change in mobility of theIL-36γ protein in A-431 cells in response to staurosporine. A-431 cells were treated with 20 ng /ml TNF and 67 ng/ml PMA for 6 hr then re stimulated with 0.5 mM staurosporine in different time points. Lane (1-3): 0 h, Lane (4-6) 6 h, Lane 7: Mouse protein (negative control), Lane 8: 0.25 ng processed IL-36γ protein (positive control), Lane 9: unprocessed IL-36γ protein (positive control), Lane (10-12): 12 h, Lane (13-15): 24 h, Lane 16: Mouse protein (negative control), Lane 17: 0.25 ng processed IL-36γ protein (positive control), Lane 18: unprocessed IL-36γ protein (positive control). The faster mobility from IL-36γ is indicated by the yellow arrow. This experiment was performed twice and demonstrated similar results both times.

4.16 Stimulation human primary keratinocytes with PMA and TNF then re-incubated with staurosporine

In the light of our finding, that staurosporine induced a change in mobility of IL-36γ in A-431 cells, I attempted to repeat experiment in primary human keratinocytes. Cells were cultured as described in the section 2.6.13. Human primary keratinocytes were treated with 67 ng/ml PMA and 20 ng/ml TNF for 6 hr followed by 0.5 mM staurosporine for 24 h in total volume 200 μl as in section 2.6.13. SDS-PAGE gel was used to separate cells lysate proteins (20 μg) per lane. Mature and immature IL-36γ protein (0.25 ng) were used as positive controls. The induction of expression of IL-36γ protein was demonstrated by western blotting. IL-36γ protein was induced compared with control (untreated primary cells), and I found no evidence that IL-36γ protein is truncated after treatment with staurosporine figure 4.30.

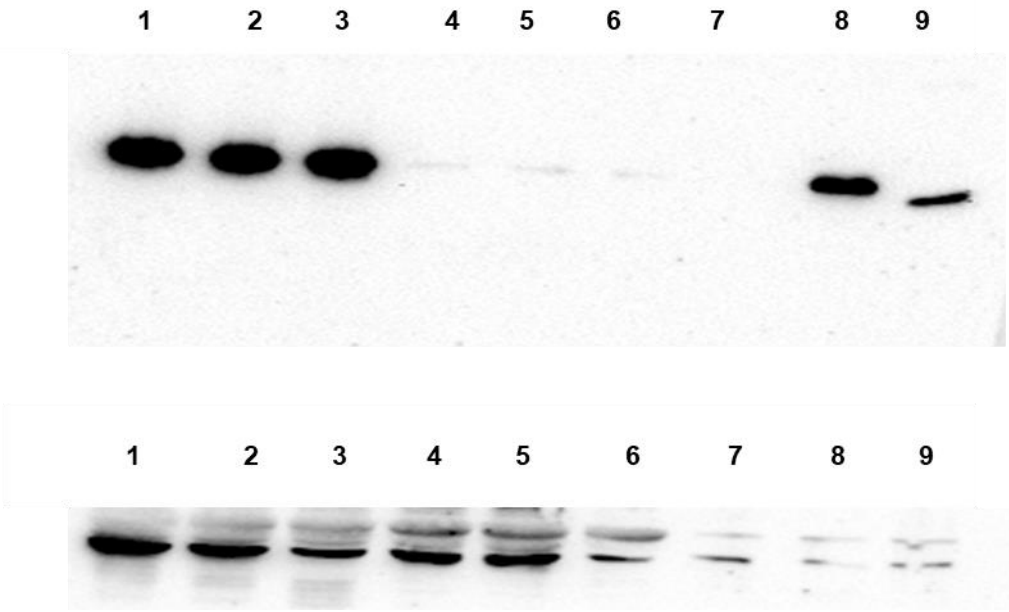

Figure 4.30 Treatment of primary human keratinocytes with PMA and TNF for 6 hr followed by staurosporine for 24 h. Lane (1-3): primary human keratinocytes were treated with 20 ng /ml TNF and 67 ng/ml PMA for 6 h then re-stimulated with 0.5 mM staurosporine for 24 h. Lane (4-6): untreated primary human keratinocytes. Lane 7: Mouse protein (negative control) Lane 8: 0.25 ng unprocessed IL-36γ protein (positive control). Lane 9: processed IL-36γ protein (positive control). This experiment was performed twice and demonstrated similar results both times.

4.17 Infection HaCaT cells with pathogenic *S. aureus* to induce IL-36γ protein.

I tested whether treatment of HaCaT cells with pathogenic *S. aureus* activates protein expression and processing in HaCaT cells I exposed 5 x 10^6 HaCaT cells to 3.6 x 10^6 *S. aureus* (SH1000) in serum free medium compared with uninfected cells. Cells were lysed a 6 h and both supernatants and cell lysate were pooled as describe in 2.6.7. Protein samples were loaded at 20 μg per lane in each well. Mouse protein was used as a negative control. Processed and unprocessed IL-36γ proteins (0.25 ng) were used as positives controls.

Western blotting data showed that IL-36γ protein is slightly induced in HaCaT cells after infection with *S. aureus* compared with uninfected cells, but induced IL-36γ protein is not processed as shown in figure 4.31.

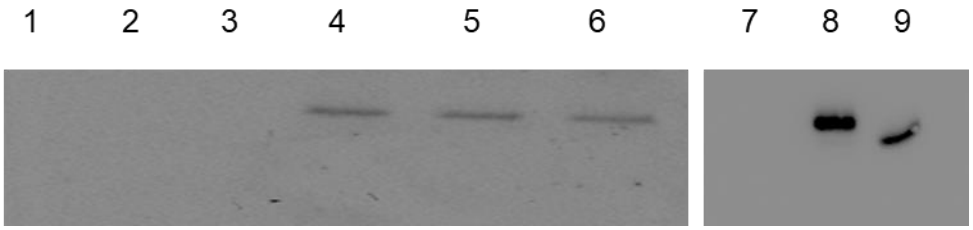

Figure 4.31 Infection HaCaT cells with *S. aureus* for 6 h. Lane (1-3): uninfected HaCaT cells. Lane (4-6): Infected HaCaT cells with S. aureus for 6 h. Lane 7: Mouse protein (negative control) Lane 8: 0.25 ng unprocessed IL-36γ protein (positive control). Lane 9: 0.25 ng processed IL-36γ protein (positive control). This experiment was performed three times and demonstrated similar results both times.

4.18 Discussion

In this chapter, I focused on the activation of IL-36 cytokines at the level of the mRNA and protein, so HaCaT and A-431 cells were used because I expect that these cells would produce IL-36 in the same way as the keratinocytes from which they are derived. The role of IL-36 signalling in host-defence and inflammation responses to injury and infection is documented. IL-36 plays an important role to protect host against infection. Epithelial cells express IL-36 particularly keratinocytes (Johnston et al., 2011). It has been demonstrated that IL-36 signalling plays an indirect role in the polarisation of Th1 cells from naive T cells (Vigne et a., 2012). Signalling of IL-36 cytokines relates to skin diseases such as psoriasis (Debets et al., 2001). Release of IL-36 that is expressed by KCs leads to binding to its receptor on DCs surface. This binding leads to the secretion of IL-23, which is needed to activate Th17 cells.

4.18.1 Inducing expression of IL-36 mRNAs

The first aim in this study was to investigate in vitro stimuli that can regulate expression of IL-36 mRNAs. HaCaT cells were treated with IL-1α, IL-36α and TNF to activate IL-36 production. In agreement with (Carrier et al., 2011) and (Johnston et al., 2011) RT-PCR results show that IL-1 α and TNF induce mRNAs (checked by sequencing of cDNA) that correspond to spliced mRNAs of IL-36β and IL-36γ. In contrast, added IL-36α was not a significant activator for expression IL-36 cytokines in HaCaT. Because IL-36α mRNA was not reliably detected in HaCaT cells, THP-1 cells were used to check IL-36α to validate the RT-PCR product.

It was necessary to test whether n^6-IL-36α (prepared in the laboratory) had activity on HaCaT. CXCL8 ELISA data showed that IL-36α was less potent than IL-1α and much less potent than TNF in the stimulation of CXCL8 expression. This finding was shown by Carrier et al., (2011) and Foster et al., (2014), who found that IL-36α is less potent than IL-1α and much less potent than TNF in activation of NF-κB through assessment of CXCL8 secretion.

RT-quantitative PCR was used to assess the induction level of IL-36 mRNAs in HaCaT cells and A-431 cells. The RT-qPCR results showed that IL-36β and IL-36γ mRNAs were very substantially and similarly induced in response to IL-1α, TNF or PMA, but

were not significantly induced by IL-36α treatment. This is particularly obvious for IL-36γ. In A-431 cells, RT-qPCR data also showed that the combination of TNF and PMA or TNF and flagellin synergistically induce expression of IL-36α and IL-36γ but not IL-36β compared with flagellin, TNF or PMA alone in A-431 cells. These results are supported by (Busfield et al., 2000), who showed that PMA or TNF can regulate the expression of IL-36γ mRNA in the human primary keratinocytes. Moreover, the role of synergistic action of two inflammatory stimuli in the regulation of IL-36 gene expression was shown before. For instance, Carrier et al., 2011 showed that IL-36 genes are significantly induced in primary keratinocytes in response to a combination of IL-17A with IL-36α, IL-36β or IL-36γ proteins. Furthermore, IL-36α, IL-36β and IL-36γ mRNAs in the primary human keratinocytes were positively regulated in response to the combination of IL-22 with IL-17A or TNF (Carrier et al., 2011 and Johnston et al., 2011).

4.18.2 Induction of expression of IL-36γ protein

I investigated the role of TNF in regulation expression of IL-36γ protein at different time points in A-431 cells and to check whether TNF can regulate proteolytic processing of IL-36γ. Western blot data showed that IL-36γ protein was induced in response to TNF in a time dependent manner. However, the proteolytic processing was not observed. To induce proteolytic pressing, A-431 cells were treated for 24 h within TNF then re-incubated for 6 h with different inflammatory stimuli. Western blot data showed that the combination of TNF with PMA or flagellin induced IL-36γ protein, but again proteolytic processing was not observed. These data were confirmed in HaCaT and A-431cells after incubation with TNF and PMA or TNF and flagellin for 6 h compared with TNF, PMA or flagellin alone.

I sought to investigate whether the activation of TLR7, TLR8 or necroptosis can induce the proteolytic processing of endogenous IL-36γ protein that is induced by TNF and PMA. Western blot data showed that A-431 did not respond to the TLR7 or TLR8 activator. necroptosis stimulus did not induce processing of endogenous IL-36γ. This finding seems to be explained by Kollisch et al., 2005, who showed that HaCaT cells do not express TLR7 and TLR8. This suggests that A-431 also cells do not respond

to TLR7 or TLR8 agonist because these cells, being a keratinocytes cell line also lack these receptors. Furthermore, a necroptosis stimulus did not induce processing of endogenous IL-36γ. *S. aureus* bacteria was also tested to induce expression of endogenous IL-36γ protein in A-431 cells. A western blot showed that *S. aureus* does induce expression of endogenous IL-36γ protein compared with uninfected cells, but proteolytic processing was not apparent.

4.18.3 Using apoptotic stimuli to attempt to induce proteolytic processing of endogenous IL-36γ protein.

Cell damage was induced to see whether proteolytic processing of endogenous IL-36γ protein can be induced. A western blot showed that cycloheximide or staurosporine does induce some proteolytic processing of endogenous IL-36γ protein in A-431 cells, but I could not reproduce this in the primary human keratinocytes. Staurosporine induced proteolytic processing in (A-431) in a time dependent manner. However, the clipped protein appeared to be intermediate in molecular weight between the unprocessed and recombinant n^{18}-IL-36γ which could suggest cleavage other than at n^{17} site. England et al., 2014 showed that proteolytic processing of pro-IL-1α was induced by cycloheximide or staurosporine in bone marrow derived macrophages culture that have been induced by LPS. Although Hayakawa et al., 2009 showed that the IL-33 precursor, which is in the same family of IL-36, is processed into an active form in PMA stimulated human gastric carcinoma cell line culture, when followed by calcium ionophore**,** our western blot data showed that calcium ionophore did not induce proteolytic processing of pro-IL-36γ. However, calcium ionophore increased induction of endogenous pro-IL-36γ protein in A-431 cells after induction of expression by TNF and PMA.

4.19 Conclusion

To summaries, RT-PCR and qPCR data showed that IL-36γ mRNA is the principle IL-36 that is induced in HaCaT and A-431 cells. Expression of endogenous IL-36γ protein is regulated in these cells in response to TNF and PMA, TNF and flagellin or PMA. The TLR7, TLR8 or necroptotic inducers cannot induce processing of the IL-36γ protein. Cycloheximide and staurosporine, which are toxic inducers of cell death both seem to cause a small proteolytic change in the pro IL-36γ protein but the mobility if the product in SDS-PAGE is not the same n^{18}-IL-36γ. control. Staurosporine also did not cause processing of IL-36γ protein in the primary human keratinocytes, although IL-36γ protein is induced in response to PMA and TNF. IL-36γ protein is induced in HaCaT cells after being challenged with *S. aureus*, but it is not processed.

Chapter 6

General Discussion

5. 1 The biological activity of IL-36 on its endogenous receptor

As the first step in exploring the specificity of IL-36 receptor and the specificity of its signalling pathway, I compared the activity of known and new N-terminal variations of IL-36.

To test the biological activity of all IL-36 mutants by an inexpensive and rapid technique, I first cloned single cells to produce a clonal line of HT-29 cells that had been transfected with luciferase reporter gene to achieve high expression of luciferase output. HT-29 cells are one of a minority of cell lines that express IL-36R mRNA (Towne et al., 2004). I selected a single cell from a population of stable reporter gene transfectants, which I named D7 that showed strong expression of luciferase and a 500-fold (see figure 3.20) signal to background ratio in response to IL-36α compared with unstimulated cells. HT-29 and their daughter cell lines also have endogenous receptors for IL-1 and TNF. D7 was used to compare the biological activity of the recombinant proteins that I prepared. Furthermore, if I specifically inactivated the *IL1RL2* gene, which encodes the only known IL-36R, and if that mutation completely inactivates of the response to IL-36, I can conclude that IL-1LR2 is the only receptor for the IL-36, at least on HT-29 cells. A specific mutation in the *IL1RL2* gene should serve to inactivate all the response to IL-36, without inhibiting any other NF-κB activated pathways. The HT-29 clone-κB-*luc* D7 showed strong responsiveness to the TNF, IL-1α and IL-36α. It was arbitrarily chosen for kinetic work and disruption of *IL1RL2*.

A further practical reason was to create a control cell line that was specifically insensitive to IL-36. Hypothetical components of our recombinant protein preparations, such as endotoxin, that activate NF-κB by some other route than through IL-36R would be expected to be unaffected by inactivating IL-36R, and thus the IL-36R deficient cell line could reveal the presence of contaminants.

The signalling pathway of the active form of IL-36α, IL-36β or IL-36γ proteins has an important role in inflammatory diseases through activation of the NF-κB and MAPK pathway. IL-36 proteins expressed by cells are biologically inactive and they require truncation to be activated (Towne et al., 2011). It is assumed that natural truncation results from proteolytic processing of these precursors of inflammatory cytokines, but

the mechanism has not been completely investigated. An in vitro study by (Towne et al., 2011) showed that truncation of five amino acids from IL-36α, four amino acids from IL-36β or 17 amino acids from full length IL-36γ from N terminus raises their biological activity between 1,000-10,000-fold. (Henry et al., 2016) studied the activation of recombinant IL-36 precursors by proteolysis in vitro and reported that neutrophil derived elastase, proteinase 3 and cathepsin G can cleave the N-termini from IL-36 precursors and activate them. The cleavage sites of these enzymes that Henry et al. reported are different from optimal truncation site that observed by Towne et al. For example, Henry et al show that full length IL-36α can be cleaved by cathepsin G and elastase enzymes to activate IL-36α. The recombinant products had Lys^{3} and Ala^{4} as their N-termini specifically rather than Lys^{6}, as suggested by Towne et al. The IL-36β precursor can be processed by cathepsin G before Arg^{5} or non-exclusively at Phe^{53} while IL-36γ precursor can be cleaved by both elastase and proteinase-3 before Val^{15} instead of Ser^{18}, which is the activation site suggested by Towne et al. Henry et al, showed that the biological activity of mixtures of proteins derived from pro-IL-36α contained product whose N-terminal were Ala^{4}, IL-36β at Arg^{5} and IL-36γ at Val^{15} is increased 500-fold compared with unprocessed protein. On the other hand, Towne et al data that showed that N terminus truncation of n^{6} (Lys) IL-36α, n^{5} (Arg) IL-36β and n^{18} (Ser) IL-36γ increased biological activity 3000, 8000 and 1500- fold respectively. If cathepsin G, elastase and proteinase3, which are specifically derived from neutrophils, are required for the processing of pro-IL-36 proteins then IL-36 activation cannot precede neutrophil recruitment. However, IL-36 is reported to have a major role in the recruitment of neutrophils (Foster et al., 2014) because activated IL-36 is recruited the neutrophils into the site of inflammation. This suggests that IL-36 must already be activated before the neutrophil enzymes become available. It could be possible that another signal rather than activated IL-36 can recruit neutrophils, then pro-IL-36 that is released from dead KC as result of apoptosis or another cells death signals can be activated by these enzymes. Neutrophil enzymes then sustain the recruitment of more neutrophils through their activation of IL-36.

(Ainscough et al., 2017) have reported that cathepsin S, which is endogenously activated in human keratinocytes during inflammation, processes IL-36γ precursors in

vitro to yield the same at n^{18}(Ser) IL-36γ that Towne et al showed to be active, and this process, which does not involve neutrophils, has the potential to recruit neutrophils.

I have used our own assays to determine the dose response of endogenous IL-36 receptor into endogenous N-terminal forms of human n^6-IL-36α, n^5-IL-36β and n^{18}-IL-36γ. Firstly, I have shown that n^5-IL-36β and n^{18}-IL-36γ proteins as well as n^6-IL-36α induced luciferase reporter gene expression to the same level that I have seen with TNF (see figure 3.18). The level of induction is consistently at least 5-fold higher compared with induction by IL-1α. recent data from our laboratory has shown the same level of stimulation by IL-1β. Analysis of dose response curves fit well to a curve with the Hill coefficient of 1.5, which implies some cooperativity between receptor for binding IL-36. The EC_{50} of n^6-IL-36α, n^5-IL-36β and n^{18}-IL-36γ were found to be 3.3 nM, 0.12 nM and 18 nM respectively.

The EC_{50} that I found are higher than have been reported before by (Towne et al., 2011). EC_{50} values of IL-36α, n^5-IL-36β and n^{18}-IL-36γ that were published by these authors were 50, 8 and 147-fold lower than have found, were 0.06 nM, 0.015 nM and 0.122 respectively, but they are in the same effective order (IL-36β< IL-36α<IL-36γ). However, the reporter cells that were used by Towne et al were human Jurkat cells, a lymphocyte tumour derived line lacking IL-36R that had been transfected with IL-36R expression vector. I used cells that express endogenous IL-36R, so it might be possible that these differences in EC_{50} result from binding of IL-36α, IL-36β and IL-36γ and recycling of the transfected IL-36R in the Jurkat cells much more slowly than endogenous IL-36R. The differences in response between cells with transfected IL-36R and cells with endogenous IL-36R was previously shown by Foster et al., 2014, who used primary human keratinocytes to assess CCL20 chemokine production protein in response to truncated n^6-IL-36α and n^5-IL-36β or n^{18}-IL-36γ. The EC_{50} that these authors found were much higher than the data reported by Towne et al., 2011 but their EC_{50} are still generally lower than our data except n^5-IL-36β, which is higher than our values but again in the same order (IL-36β (0.465 nM)<IL-36α (0.801)<IL-36γ (1.16 nM) (Foster et al., 2014). The biological activity of n^6-IL-36α or n^{18}-IL-36γ

has been assessed by a third group. (Zhou et al., 2018) that measured secretion of CXCL1 chemokine in HaCaT cells culture after stimulation with these proteins for 24 h. ELISA data showed that the EC_{50} of n^6-IL-36α and n^{18}-IL-36γ are 2 nM and 0.6 nM respectively which are different again from Towne et al., and Foster et al., data. In both experiments, cells were incubated for 24 h (see Table 4.1). In the summary (Table 4.1), the estimated EC_{50} for the three IL-36 ligands differs between all studies. Various factors are different between them which could result in measured differences in the activity of IL-36 cytokines themselves. These factors could include the following. The duration of assay could be a factor since I show that the response to IL-36 is shorter than 24 h of some incubation's periods used by others. The mature of the output measured is another factor. I have used short lived Luc-2p reporter (Leclerc et al., 2000) whereas other groups have measured the accumulation of stable proteins. Different groups have analysed different cell types, and it is possible that other cells specific proteins that modulate the activity of IL-36 signalling and the rate of turnover the receptors may differ between the cells. Finally, there is the differences between using transfected, overexpressed exogenous IL-36R and the endogenously expressed protein, as I have done.

I have examined the duration of the activation of NF-κB in response to IL-36α or IL-36β compared with TNF. I expected that the duration of NF-κB activation in response to n^{18}-IL-36γ protein will not be different from n^6-IL-36α or n^5-IL-36β. I showed that the reporter gene activity shown in response to these cytokines was and to TNF very similar (figure 3.18). I have shown that IL-36β requires 3 hr to reach its maximum response (figure 3.21). The difference in activity is small between 3 h and 6 h while n^6-IL-36α or TNF reach their maximum response in 6 h. The time course data showed that cells largely lost their responsiveness to the n^6-IL-36α, n^5-IL-36β or TNF after 12 h. Towne et al., 2011 incubated their reported cells for 5 h but Foster et al., 2014 incubated primary keratinocytes for 24 h with the n^6-IL-36α and n^5-IL-36β or n^{18}-IL-36γ. It is likely that the response to IL-36 is virtually complete within 18 h.

The response of cells to IL-36α seems to be dependent on the exact structure of N-terminus of the protein. This suggests that the IL-36 receptor can discriminate small

differences. Towne et al. have already shown the importance of the position of N-terminus. I have begun to investigate the effect of changing the N-terminal residue itself. To come to a firm conclusion, I needed to generate the assay by cloning HT-29/luciferase reporter cell line. To start, I cloned single HT-29 cells that had been stably transfected with destabilised luciferase reporter plasmids (pGL4.2, Promega), having made a clonal line (D7), and I created from an IL-36R deficient line (A6) which I have used to test my protein preparations for contamination with NF-κB activators other than IL-36. Figure 3. 21 shows this test and shows that there is no detectable contamination.

The biological activity of the modified IL-36α proteins were then assessed compared with (Lys) n^6-IL-36α. In our lab the Lys^6 N terminus of the biologically active IL-36α that was identified by Towne et al., was replaced with either serine (n^6-K6S-IL-36α) or glycine (n^6-(K6G-IL-36α). I also repeated the biological activity of the pro-protein, n^1-IL-36α or n^4-IL-36α that Henry et al., suggested to be activated. My data showed that n^6-K6S-IL-36α and n^6-K6G-IL-36α induced the NF-κB reporter to the same maximum extent as n^6-IL-36α, but the biological activity of n^6-IL-36α was reduced ~ 9 and ~ 130-fold when lysine residue was replaced with serine or glycine respectively. The molecular masses of these soluble proteins have been determined by mass spectrometry and they corresponded very closely to predicted masses. The only differences between the proteins was the structure of N terminus. These changes in the biological activity, therefore, seem to be related to side chain differences between amino acids. Lysine has an extended side chain containing a positively charged an ε–amino group, while serine is short and has no charge. Glycine, unlike the other two amino acids is conformationally completely free because it has only a hydrogen group side chain consequently its alpha-amino group is not spatially constrained. These differences in the side chain might have a negative way on the binding affinity for endogenous IL-36R. In summary, the data of Towne et al (2011) have suggested to us that the receptor can measure the exact position of the amino terminus of IL-36. My data suggest that the receptor is even sensitive to the structure of the amino terminal residue. In the future, this may further investigate by making mutations in IL-36 and complementary mutation in the IL-36R, which I can now re-introduced into our IL-36R deficient cell line, be explained when a deletion experimental structure is for the IL-36R complex with IL-36.

Henry et al have shown that a tagged pro IL-36α (n^1-IL-36α) can be activated in vitro by neutrophil enzymes and have identified major products in the partially active mixture which inactive, which Towne et al would predict to be inactive. Henry et al., 2016 shows that neutrophils derived enzymes cathepsin G can cleave precursor of IL-36α to produce n^4-IL-36α. We generated n^4-IL-36α by trypsin digestion of His_6-tagged-n^1-IL-36α and I have found it to be inactive although it is stable and soluble. It's identified that was confirmed by mass spectroscopy. I, therefore, conclude that it is not an active product of neutrophil enzymes. I have also shown that the biological activity of n^4-IL-36α is undetectable at the concentration made by (Henry et al., 2016). Since the overall activation of the IL-36α precursor in Henry et al., experiments were small, it seems possible that traces of the n^6-IL-36α that were not detected might account for the activity of the digestion product. In our hands, this n^4-IL-36α is not active and so cannot be the active component in the mixture. It could be argued that our n^4-IL-36α is misfolded even though it is stable. It could be possible to test whether it can be made active by a dipeptidyl peptidase such as cathepsin C this could demonstrate the protein is potentially active in the same way that I have shown that n^1-IL-36α can be fully activated concentration made by chymotrypsin.

I confirmed that n^6-IL-36α is at least 1000-fold more active than n^1-IL-36α, though I cannot measure EC_{50}. By limited chymotrypsin digestions, I have completely activated the n^1-IL-36α precursor, demonstrating that the protein product is activatable though inactive. Mass spectrometry data showed that n^1-IL-36α protein is cleaved by chymotrypsin at three different sites with a major extra cleavage at Iso^{31} (see appendix A.4). Reporter gene showed that digested n^1-IL-36α protein is biologically active as n^6-IL-36α and the product did not induce NF-κB in IL-36R deficient cells, so the activity did not result from contaminant or chymotrypsin. Though these are preliminary findings, it seems that active IL-36α was processed at n^6 but could also be digested at n^{31} without loss the activity.

To see whether NF-κB can be re-activated after declining in the cells after 12 h. I attempted to reactivate the response with IL-36 or TNF. The reporter gene could be reactivated in cells that had been exposed to n^6-IL-36α, n^5-IL-36β. After IL-36 treatment the response to TNF is higher than n^6-IL-36α or n^5-IL-36β. The same is true

to the luciferase expression in the TNF fatigued cells that were reactivated with n^6-IL-36α or n^5-IL-36β (see figure 3.22). The failure of supplemented n^6-IL-36α and n^5-IL-36β to show a major difference indicates that the downregulation of responsiveness to either IL-36 is through the same mechanism.

Table 5.1 Comparison of estimates of EC50 of the n^6-IL-36α, n^5-IL-36β or n^{18}-IL-36γ

Legends	**EC_{50} (nM) Towne et al., 2011**	**EC_{50} (nM) Foster et al., 2014**	**EC_{50} (nM) Zhou et al., 2018**	**EC_{50} (nM) Our proteins**
n^6-IL-36α	0.066	0.8	2	3.3
n^5-IL-36β	0.015	0.46		0.12
n^{18}-IL-36γ	0.122	1.16	0.6	18
n^6-K6S-IL-36α				30
n^6-K6G-IL-36α				435

To summarise, I have confirmed that there is the only one receptor regulating IL-36 cytokine signalling pathway in HT-29 cells. NF-κB reporter gene data showed that n^6-IL-36α, n^5-IL-36β and n^{18}-IL36γ activate a NF-κB reporter gene to a similar extent and time range to TNF and that IL-36 is more potent than IL-1α. In our laboratory we have shown that n^4-IL-36α is not biologically active contrary to what has been previously reported. Moreover, the N-terminal lysine of mature IL-36α is also required for full activity. I also show that the biologically irrelevant proteases chymotrypsin can fully activate the inactive n^1-precursor of IL-36α and that chymotrypsin cleaves before n^6-Lys. To our knowledge, this is the first time that this has been done on a protein of natural sequence.

5.2 Regulation expression of IL-36 mRNA and protein

I have investigated the expression of endogenous IL-36 cytokines for several reasons. Firstly, IL-36 cytokines mRNAs regulation and protein processing are not yet well understood. Secondly, several lines of evidence suggest that these cytokines have important roles in the immune system of epithelia and specifically the skin, gut and airway system. Thirdly, though the IL-36 system is not seen outside the mammals, it is present in every mammalian genome that has been studied so far. In addition to their functional roles in the skin, these cytokines can also regulate the immune system of the skin to mediate inflammatory disorders. Genetic disruption of the system causes disease in mice and natural mutation of IL-36RA is one cause of generalised pustular psoriasis in human. Although IL-36 has a role in the regulation of the inflammatory response, the mechanism of releasing these cytokines is not yet known.

To study the regulation of the expression of IL-36 cytokines at the level of mRNA and protein, I simulated KC, which are currently considered an important source of these cytokines, stimulated with either a single stimulus or a combination of two stimuli. The synergy between TNF and PMA or TNF and flagellin was discovered by chance while I was searching for agents that could induce processing of IL-36γ. I have also sought to discover ways to activated endogenous processing of IL-36γ.

Because the mechanism of processing of IL-36 cytokines has not been clearly identified, different stimulation routes were tried, such as activation of Toll like receptors, necroptosis, apoptosis inducers or bacterial infection, to induce processing of IL-36γ. IL-36γ was specifically chosen because I showed that can be detected reliably by western blotting and because processing causes a relatively large change in mobility. I note that the endogenous IL-36γ from A-431 and HaCaT appears to migrate identically with recombinant pro-L-36γ. I investigated whether TNF and IL-1α, which are the main inflammatory cytokines expressed in the skin during inflammation, can induce expression of IL-36 cytokines. Recombinant IL-36α was also used to assess whether it can activate its own gene and the other IL-36 genes. It has been suggested that IL-36 might activate and regulate itself through an autocrine signalling during inflammation (Carrier et al., 2011). Quantitative assessment of mRNA data

showed that TNF and IL-1α induced expression of IL-36 cytokines but IL-36α in HaCaT cells, had little compared with untreated cells.

It seems that IL-36α weakly regulates expression of its own gene and *IL36B* and *IL36G* genes in HaCaT cells. One explanation may be that the level of expression of IL-36R in HaCaT cells is lower than the level of TNF and IL-1 receptors. ELISA assays of NF-κB responsive chemokine CXCL8 were state used to examine whether IL-36 is less effective than IL-1α or TNF in regulation expression of NF-κB activation in HaCaT cells. In agreement with (Carrier et al., 2011) and (Foster et al., 2014), I found that IL-36α is less potent than IL-1α and much less potent than TNF in activation of NF-κB through assessment of CXCL8 secretion. On the other hand, in the luciferase expressing HT-29 line, D7, IL-36α is much more effective than IL-1 in inducing the κB responsive luciferase reporter gene, and it is as effective as TNF (see figure 3.23). Although Towne et al reported that the EC_{50} of IL36α is 0.066 nM, our own data indicated that the EC_{50} is ~75-fold higher (see Figure 3.18). In this study, different concentrations were used to identify a best dose of IL36α that can induce CXCL8 secretion. I found that IL-36α on HaCaT induces expression of CXCL8 (see figure 4.7), but even at saturation, the activation of CXCL8 expression is relatively weak compared with IL-1 or especially TNF.

My data show that TNF is stronger than IL-1α and much more effective than IL-36α in activation of CXCL8 and that probably NF-κB. I have therefore investigated the optimal condition of IL-36 mRNAs expression in response to TNF. It found that IL-36α mRNA expression is activated by TNF in a dose dependent manner over the range of concentrations used, but IL-36β and IL-36γ mRNAs were not, but the response of IL-36β or IL-36γ were saturated in A-431 cells by 10 ng/ml TNF (figure 4.9). The expression level of IL-36γ mRNA in the A-431 was significantly more strongly induced compared with IL36α and IL-36β in response to TNF. I also demonstrated that expression of IL-36γ mRNA in response to TNF is sustained and is close to maximal at the first time point, 6 h that I investigated. Our experiments on HT-29 D7 also indicate that in the cell lines 6 h is the peak of NF-κB activity in response to TNF (figure 3.21).

RT-qPCR was used in this study to quantify the induction level of IL-36 mRNAs in both HaCaT and A-431 cell lines. TNF and IL-1α strongly induced of IL-36 mRNAs, and the effective dose of IL-36α that was shown by ELISA was also used. I also investigated the effect on IL-36 genes expression of other inflammatory stimuli such as phorbol esters (PMA) and flagellin and combinations of PMA or flagellin with TNF.

PMA induced IL-36β and IL-36γ but not IL-36α mRNAs in a similar manner to TNF and IL-1α. PMA and TNF also showed synergistic induction of IL-36α, IL-36β and IL-36γ mRNAs compared with PMA or TNF alone in HaCaT cells. This is particularly obvious for IL-36γ (see Figure 4.11). In A-431 cells, RT-qPCR data also showed that flagellin and TNF or PMA and TNF synergistically induce expression of IL-36α and IL-36γ but not IL-36β compared with flagellin, TNF or PMA alone (see figure 4.10).

Several studies have observed that IL-36 cytokines are mainly connected with inflammatory skin diseases. (Debets et al., 2001) reported that keratinocytes express IL-36 cytokines and these cytokines are connected with skin diseases. The expression of IL-36α, IL-36β and IL-36γ is increased in the psoriasis (Debets et al., 2001, Blumberg et al., 2007). In allergic contact dermatitis, IL-36α, IL-36β and IL-36γ mRNAs expression is elevated and IL-36α, IL-36β and IL-36γ can be detected in the epidermis (Mattii et al., 2013). I note that my findings suggest that a second signal may be required in vivo to enhance the effect of TNF in the way that I have observed that PMA or flagellin do in vitro. A previous study by Carrier et al showed that IL-36α, IL-36β and IL-36γ are induced in vitro in primary human keratinocytes in response to TNF. (Johnston et al., 2011) also showed that TNF and IL-1α are strong inducers of IL-36α, IL-36β, IL-36γ and IL-36Ra mRNAs in primary human keratinocytes. A study by (Busfield et al., 2000) showed that expression of IL-36γ mRNA is rapidly stimulated in the human primary keratinocytes after stimulation with PMA or TNF. This suggest that regulation of IL-36 genes expression in the skin might be controlled by TNF and IL-1α cytokines, especially as it has been shown that inflammatory responses in the skin are initiated and maintained by TNF through its ability to induce NF-κB pathway that regulates inflammatory genes expression (Aggarwal, 2003, Banno et al., 2004).

Inducing expression of IL-36 mRNAs in response to the synergistic action of stimuli has been shown before. For example, Carrier et al showed that a combination of IL-36α, IL-36β or IL-36γ proteins synergise with IL-17A during regulation of expression of the IL-36 genes themselves in human primary keratinocytes. Furthermore, IL-22 and IL-17A or IL-22 and TNF synergistically induce expression of IL-36α, IL-36β and IL-36γ mRNAs in the primary human keratinocytes in vitro (Carrier et al and Johnston et al).

These data indicate that the expression of IL-36 is under control of NF-κB pathway, and differences between inflammatory stimuli in regulation of IL-36 genes are related to variation between these stimuli in their activation of the NF-κB pathway. This was confirmed by using combination of two NF-κB activators, which leads to enhanced expression of IL-36 genes.

Goel et al., 2007 showed that activation of protein kinase C (PKC) by phorbol esters such as PMA results in an effect on cell differentiation processes, protein synthesis, activities of enzymes, DNA synthesis and gene expression. In keratinocytes, several reports showed that cutaneous inflammation, epidermal tumour stimulation and differentiation are controlled by PKCα (Hansen et al., 1990, Dlugosz et al., 1994, Lee et al., 1997, Wang and Smart, 1999, Mills et al., 1992). PKC Signalling regulates expression of transcription activator protein-1 (AP-1) in the skin (Angel et al., 2001). Chemical carcinogens, cytokines, growth factors and tumours activators can regulate expression of AP-1 (Angel and Karin, 1991, Karin et al., 1997). Epidermal tumour development and progression are induced by PMA through activation of AP-1 (Dekker and Parker 1994). Moreover, TNF receptor signalling can activate AP-1 to regulate expression of genes some of which may have a role in tumour promotion (Baud and Karin, 2001, Balkwill and Mantovani, 2001). My suggest that the expression IL-36 genes are not only NF-κB dependent but also PKC dependent. In particular, there are AP-1 binding sites in the hypersensitivity regions of the IL-36γ promoters. My own findings suggest significant differences in the response of IL-36α, IL-36β and IL-36γ genes to PMA or combination of PMA and TNF in HaCaT and A-431 cells that open up the question, whether all IL-36 agonists have the same level of regulation by NF-κB and AP-1 factors. Secondly, I might ask if PKC is also involved in regulatory IL-36

cytokine expression in airway system and gut in addition to NF-κB signal as in skin or is the NF-κB signal sufficient there.

According to own data, which showed significant expression of IL-36γ mRNA in response to PMA and TNF or flagellin and TNF, I have also shown that IL-36γ protein is clearly expressed in response to these stimuli in HaCaT and A-431 cells. The protein product co-migrates with recombinant n^{1}-IL-36γ (the pro form of the cytokine so far). I have not observed processing of endogenous IL-36γ to produce n^{18}-IL-36γ, which is the form that was identified as active by Towne et al., 2011. In my study, different methods were used to attempt to induce expression and processing of IL-36γ.

I have assessed the induction level of IL-36γ protein in A-431 after stimulation with TNF in different time points. Data showed that IL-36γ protein is induced in a time dependent manner, but the time of induction was reduced when TNF combined with PMA or flagellin in both HaCaT or A-431 cells compared with TNF, PMA or flagellin alone. This generally reflects the effect of TNF and PMA on IL36γ mRNA.

I tested whether a lysosomotropic compound or TLR7 or TLR8 agonists could induce processing of pro-IL-36γ protein after stimulation with PMA and TNF in A-431. I found showed that IL-36γ protein was induced in response to a combination of PMA and TNF but that is not processed even after treating cells with lysosomotropic compound or TLR7 or TLR8 agonists. (Kollisch et al., 2005) have reported that TLR7 and TLR8 mRNAs are not expressed in the HaCaT It is likely that the failure of TLR7 or TLR8 agonists even to induce expression of IL-36γ protein because keratinocytes cell lines do not express TLR7 or TLR8. I showed that when A-431cells were treated with TLR8 agonist by itself, they did not respond to TLR8 agonist. Because A-431 cells are also an immortalised keratinocyte cell line, I would expect that A-431 cells also do not express TLR7 or TLR8.

Since it had become clear that inducers of cell signalling through either the PKC or NF-κB pathways do not induce the expected processing of the IL-36γ protein, I also tried to induce a major damage in the cells to see if pro-IL-36γ could be processed

through using stimuli that cause forms of programmed cell death. To see whether processing of pro-IL-36γ protein processing is might be triggered by activating cytoplasmic calpains, calcium ionophore was used. Though cells clearly died, IL-36γ was not change.

Incubation of A-431 cells with PMA and TNF followed by cycloheximide or staurosporine led to an increase in mobility of a fraction of the IL-36γ presumably because of proteolytic processing of pro-IL-36γ. The processed protein, however, is not as mobile on electrophoresis as recombinant of n^{18}-IL-36γ (see figure 4.26 and 4.27) and would therefore appear to be cleaved close to the N terminus. Staurosporine induced processing of IL-36γ in a time dependent manner (see figure 4.29). (England et al., 2014) showed that cycloheximide or staurosporine induces processing of full-length IL-1α precursor into it's an active form in bone marrow derived macrophages culture that have been induced by LPS. Moreover, pro-IL-36γ protein is not processed after using calcium ionophore, so this means that processing of pro-IL-36γ is not calpain proteases dependent. (Hayakawa et al., 2009) showed that the IL-33 precursor is processed into an active form in PMA stimulated a human gastric carcinoma cell lines culture when followed by calcium ionophore. To see whether processing can be observed or not in primary human keratinocytes, primary human keratinocytes were treated with PMA and TNF followed by staurosporine. Western blot data showed that IL-36γ protein is notably induced in treated cells compared with untreated cells, but induced IL-36γ protein is not processed (see figure 4.30). A study by (Henseleit et al., 1996) reported that calcium ionophore induces morphological changes in the HaCaT cells but these changes are not similar to apoptotic programmed cells death. An apoptotic pattern can be induced in keratinocytes, but it has been reported that it might not be complete as other types of cells Henseleit et al., 1996. Moreover, I infected HaCaT cells with living *Staphylococcus aureus* strain (SH1000) to examine whether pathogen infection could induce processing of IL-36γ protein. I observed that precursor IL-36γ protein is induced compared with uninfected cells, but bacterial infection does not induce proteolytic processing of IL-36γ precursor. Therefore, I would only hypothesise that other signals from skin resident cells, such as T cells or Langerhans cells might have a role either directly through inducing apoptosis in the keratinocytes cells to allow release pro-IL-36 proteins and then proteolytically processing pro-IL-36

proteins by these other cells. Henseleit et al reported that IFNγ and UV light are much more effective than cycloheximide, staurosporine, calcium ionophore, TNF or PMA in inducing apoptosis in HaCaT cells. Alternatively, LCs or T cells might regulate expression of proteolytic enzymes that are required by KCs to process pro-IL-36 proteins within KCs themselves. In this connection, (Ainscough et al., 2017) have shown that the cysteine proteases cathepsin S is induced in KC in response to inflammatory stimuli and it can process a recombinant IL-36γ precursor to produce n^{18}-IL-36γ. These authors have proposed that cathepsin S functions outside the cell. However, it seems possible that it could also process pro IL-36γ inside the cell that and mature protein could be released during cell death.

(Schonefuss et al., 2010) reported that cathepsin S proteolytic enzyme is detected in Langerhans but not keratinocytes in normal skin. However, in skin psoriasis, KCs express cathepsin S and its expression is activated in KCs by T cells. Another in vitro study by (Schwarz et al., 2002), showed that IFNγ upregulates expression of cathepsin S in both primary human keratinocytes and HaCaT cells. (Schonefuss et al., 2010) showed that incubation of HaCAT cells with T cells upregulated expression of cathepsin S in HaCaT cells through secretion of TNF or IFNγ, and the source of these cytokines is T cells. However, it is clear from my experiments that even 24 h treatment of HaCaT cells with TNF, on its own, is not sufficient to activate IL-36γ processing, thus other extracellular signal must also be needed, and these might come from T cells.

In conclusion, my results have shown that different stimuli can regulate expression of IL-36 cytokines in keratinocytes, and expression of IL-36 cytokines is not only under control of the NF-κB pathway because activators of the NF-κB pathway alone do not maximally induce IL-36γ. Synergy with PMA suggests the involvement of PKC and other factors that could naturally induce PKC. Although my data have shown significant induction of pro-IL-36γ protein in the HaCaT and A-431 cells in response to PMA and TNF, TNF and flagellin or bacterial infection, this pro-IL-36γ protein is not processed. Staurosporine and cycloheximide can induce processing of pro-IL-36γ but

the product is not at the same molecular weight and it will be necessary to test the product for possible activity.

5.3 Limitation of these studies

Primary keratinocytes (KC) can be difficult to work with because of long isolation procedure and extremely sensitive cells. Their short life span makes in vitro manipulation difficult and genetic manipulation is not practical. Moreover, there are suitable keratinocyte cell line that resembles primary keratinocyte which are available. In this study, a human keratinocyte cell line (HaCaT) and a skin carcinoma cell line (A-431) were used as models because I expected that these cells could produce IL-36 cytokines in a similar way to the keratinocytes from which they are derived. Human cell lines are more affordable and easier to manipulate than primary cells. However, other signalling pathways are provided by immune cells that surround keratinocytes in vivo and these signals might be required to regulate proteolytic processing of IL-36 proteins while these signalling pathways might be provided to cell lines.

The activation and expression of endogenous IL-36γ protein by either TNF and PMA or TNF and flagellin was induced in HaCaT and A-431 cell lines and was only assessed in cell lysates. However, detection of IL-36γ protein would need to be assessed in the supernatants by ELISA or by western blot in response to these stimuli to identify rapid transportation of the cytokine. Ainscough et al showed that IL-36γ can be activated in vitro by cathepsin S. Cathepsin S was shown in another study to be activated in keratinocytes in response to TNF or IFNγ from T cells. Although TNF was used as an inflammatory stimulus to induce expression of IL-36γ protein at different time points and concentrations, no proteolysis was detected in the induced pro-IL-36γ. For this to be conclusive, I would need evidence that cathepsin S is expressed required to be assessed in A-431 cells.

The proteolytic processing of endogenous IL-36γ protein was observed in A-431 cells, when cells were treated with either cycloheximide or staurosporine after induction of expression by TNF and PMA. The same proteolytic processing was shown in HaCat cells (data not shown). However, the clipped protein appeared to be intermediate in molecular weight between the unprocessed and recombinant n^{18}-IL-36γ, which is

known to be an active form. However, the biological activity of processed IL-36γ protein would need to be assessed.

5.4 Future work

Data from chapter 3 showed that there are differences between my own EC_{50} data for IL-36 proteins which were derived from cells that express the endogenous IL-36 reporter and the work of Towne et al (2011), who used transfected, overexpressed exogenous IL-36R. Future work, comparing transfected and endogenous IL-36R in the same cell line could resolve this issue. It would be interesting to employ the IL-36R deficient cell line (A6).

In addition, future work should focus on the role of NF-κB and PKCα in the regulation of IL-36 genes. Targeting of the NF-κB pathway might be an attractive approach. It would be interesting to investigate role of AP-1 transcription factor in IL-36 genes in response to TNF and PMA or other inflammatory stimuli that can regulate expression of IL-36 genes this could be by using an AP-1 responsive reporter gene. Moreover, investigation which isoform of PKC is involved in regulation of IL-36 cytokines would be important.

Ainscough et al showed that cathepsin S can cleave IL-36γ at the same site (n^{18}) that suggested by Towne et al (2011). Moreover, Schonefuss et al 2010 showed that cathepsin S is expressed in psoriasis associated keratinocytes but not in normal skin. However, in vitro, incubation of primary human keratinocytes and HaCaT cells with TNF or IFNγ, which are produced by T cells, induce expression of cathepsin S. It would be interesting to investigate the role of resident skin cells and the role of resident cells in lungs and the gut system in proteolytic processing of IL-36 precursors through using an animal model and targeting signals of these resident cells.

Chapter 6

Bibliography

AGGARWAL, B. B. 2003. Signalling pathways of the TNF superfamily: a double-edged sword. *Nat Rev Immunol,* 3**,** 745-56.

AGIUS, E., LACY, K. E., VUKMANOVIC-STEJIC, M., JAGGER, A. L., PAPAGEORGIOU, A. P., HALL, S., REED, J. R., CURNOW, S. J., FUENTES-DUCULAN, J., BUCKLEY, C. D., SALMON, M., TAAMS, L. S., KRUEGER, J., GREENWOOD, J., KLEIN, N., RUSTIN, M. H. & AKBAR, A. N. 2009. Decreased TNF-alphasynthesis by macrophages restricts cutaneous immunosurveillance by memory CD4+ T cells during aging. *J Exp Med,* 206**,** 1929-40.

AHMADZADEH, M., FELIPE-SILVA, A., HEEMSKERK, B., POWELL, D. J., JR., WUNDERLICH, J. R., MERINO, M. J. & ROSENBERG, S. A. 2008. FOXP3 expression accurately defines the population of intratumoral regulatory T cells that selectively accumulate in metastatic melanoma lesions. *Blood,* 112**,** 4953-60.

AHSAN, F., MOURA-ALVES, P., GUHLICH-BORNHOF, U., KLEMM, M., KAUFMANN, S. H. & MAERTZDORF, J. 2016. Role of Interleukin 36gamma in Host Defense Against Tuberculosis. *J Infect Dis,* 214**,** 464-74.

AINSCOUGH, J. S., MACLEOD, T., MCGONAGLE, D., BRAKEFIELD, R., BARON, J. M., ALASE, A., WITTMANN, M. & STACEY, M. 2017. Cathepsin S is the major activator of the psoriasis-associated proinflammatory cytokine IL-36gamma. *Proc Natl Acad Sci U S A,* 114**,** E2748-e2757.

ALBANESI, C., SCARPONI, C., GIUSTIZIERI, M. L. & GIROLOMONI, G. 2005. Keratinocytes in inflammatory skin diseases. *Curr Drug Targets Inflamm Allergy,* 4**,** 329-34.

ANGEL, C. E., LALA, A., CHEN, C. J., EDGAR, S. G., OSTROVSKY, L. L. & DUNBAR, P. R. 2007. CD14+ antigen-presenting cells in human dermis are less mature than their CD1a+ counterparts. *Int Immunol,* 19**,** 1271-9.

ANGEL, P. & KARIN, M. 1991. The role of Jun, Fos and the AP-1 complex in cell-proliferation and transformation. *Biochim Biophys Acta,* 1072**,** 129-57.

ANGEL, P., SZABOWSKI, A. & SCHORPP-KISTNER, M. 2001. Function and regulation of AP-1 subunits in skin physiology and pathology. *Oncogene,* 20**,** 2413-23.

AOYAGI, T., NEWSTEAD, M. W., ZENG, X., KUNKEL, S. L., KAKU, M. & STANDIFORD, T. J. 2017a. IL-36 receptor deletion attenuates lung injury and decreases mortality in murine influenza pneumonia. *Mucosal Immunol,* 10**,** 1043-1055.

AOYAGI, T., NEWSTEAD, M. W., ZENG, X., NANJO, Y., PETERS-GOLDEN, M., KAKU, M. & STANDIFORD, T. J. 2017b. Interleukin-36gamma and IL-36 receptor Signalling mediate impaired host immunity and lung injury in cytotoxic Pseudomonas aeruginosa pulmonary infection: Role of prostaglandin E2. *PLoS Pathog,* 13**,** e1006737.

AREND, W. P. 1993. Interleukin-1 receptor antagonist. *Adv Immunol,* 54**,** 167-227.

AREND, W. P., PALMER, G. & GABAY, C. 2008. IL-1, IL-18, and IL-33 families of cytokines. *Immunol Rev,* 223**,** 20-38.

BACHMANN, M., SCHEIERMANN, P., HARDLE, L., PFEILSCHIFTER, J. & MUHL, H. 2012. IL-36gamma/IL-1F9, an innate T-bet target in myeloid cells. *J Biol Chem,* 287**,** 41684-96.

BALKWILL, F. & MANTOVANI, A. 2001. Inflammation and cancer: back to Virchow? *Lancet,* 357**,** 539-45.

BALS, R. & HIEMSTRA, P. S. 2004. Innate immunity in the lung: how epithelial cells fight against respiratory pathogens. *Eur Respir J,* 23**,** 327-33.

BANNO, T., GAZEL, A. & BLUMENBERG, M. 2004. Effects of tumor necrosis factor-alpha (TNF alpha) in epidermal keratinocytes revealed using global transcriptional profiling. *J Biol Chem,* 279**,** 32633-42.

BARTON, J. L., HERBST, R., BOSISIO, D., HIGGINS, L. & NICKLIN, M. J. 2000. A tissue specific IL-1 receptor antagonist homolog from the IL-1 cluster lacks IL-1, IL-1ra, IL-18 and IL-18 antagonist activities. *Eur J Immunol,* 30**,** 3299-308.

BAUD, V. & KARIN, M. 2001. Signal transduction by tumor necrosis factor and its relatives. *Trends Cell Biol,* 11**,** 372-7.

BEDOUI, S., WHITNEY, P. G., WAITHMAN, J., EIDSMO, L., WAKIM, L., CAMINSCHI, I., ALLAN, R. S., WOJTASIAK, M., SHORTMAN, K., CARBONE, F. R., BROOKS, A. G. & HEATH, W. R. 2009. Cross-presentation of viral and self antigens by skin-derived CD103+ dendritic cells. *Nat Immunol,* 10**,** 488-95.

BLANCO, P., PALUCKA, A. K., GILL, M., PASCUAL, V. & BANCHEREAU, J. 2001. Induction of dendritic cell differentiation by IFN-alpha in systemic lupus erythematosus. *Science,* 294**,** 1540-3.

BLUMBERG, H., DINH, H., DEAN, C., JR., TRUEBLOOD, E. S., BAILEY, K., SHOWS, D., BHAGAVATHULA, N., ASLAM, M. N., VARANI, J., TOWNE, J. E. & SIMS, J. E. 2010. IL-1RL2 and its ligands contribute to the cytokine network in psoriasis. *J Immunol,* 185**,** 4354-62.

BLUMBERG, H., DINH, H., TRUEBLOOD, E. S., PRETORIUS, J., KUGLER, D., WENG, N., KANALY, S. T., TOWNE, J. E., WILLIS, C. R., KUECHLE, M. K., SIMS, J. E. & PESCHON, J. J. 2007. Opposing activities of two novel members of the IL-1 ligand family regulate skin inflammation. *J Exp Med,* 204**,** 2603-14.

BOCHKOV, Y. A., HANSON, K. M., KELES, S., BROCKMAN-SCHNEIDER, R. A., JARJOUR, N. N. & GERN, J. E. 2010. Rhinovirus-induced modulation of gene expression in bronchial epithelial cells from subjects with asthma. *Mucosal Immunol,* 3**,** 69-80.

BOUTET, M. A., BART, G., PENHOAT, M., AMIAUD, J., BRULIN, B., CHARRIER, C., MOREL, F., LECRON, J. C., ROLLI-DERKINDEREN, M., BOURREILLE, A., VIGNE, S., GABAY, C., PALMER, G., LE GOFF, B. & BLANCHARD, F. 2016. Distinct expression of interleukin (IL)-36alpha, beta and gamma, their antagonist IL-36Ra and IL-38 in psoriasis, rheumatoid arthritis and Crohn's disease. *Clin Exp Immunol,* 184**,** 159-73.

BRIDGEWOOD, C., FEARNLEY, G. W., BEREKMERI, A., LAWS, P., MACLEOD, T., PONNAMBALAM, S., STACEY, M., GRAHAM, A. & WITTMANN, M. 2018. IL-36gamma Is a Strong Inducer of IL-23 in Psoriatic Cells and Activates Angiogenesis. *Front Immunol,* 9**,** 200.

BUSFIELD, S. J., COMRACK, C. A., YU, G., CHICKERING, T. W., SMUTKO, J. S., ZHOU, H., LEIBY, K. R., HOLMGREN, L. M., GEARING, D. P. & PAN, Y. 2000. Identification and gene organization of three novel members of the IL-1 family on human chromosome 2. *Genomics,* 66**,** 213-6.

CAO, Z., HENZEL, W. J. & GAO, X. 1996a. IRAK: a kinase associated with the interleukin-1 receptor. *Science,* 271**,** 1128-31.

CAO, Z., XIONG, J., TAKEUCHI, M., KURAMA, T. & GOEDDEL, D. V. 1996b. TRAF6 is a signal transducer for interleukin-1. *Nature,* 383**,** 443-6.

CARMODY, R. J. & CHEN, Y. H. 2007. Nuclear factor-kappaB: activation and regulation during toll-like receptor signaling. *Cell Mol Immunol,* 4**,** 31-41.

CARRIER, Y., MA, H. L., RAMON, H. E., NAPIERATA, L., SMALL, C., O'TOOLE, M., YOUNG, D. A., FOUSER, L. A., NICKERSON-NUTTER, C., COLLINS, M., DUNUSSI-JOANNOPOULOS, K. & MEDLEY, Q. G. 2011. Inter-regulation of Th17 cytokines and the IL-36 cytokines in vitro and in vivo: implications in psoriasis pathogenesis. *J Invest Dermatol,* 131**,** 2428-37.

CHIANG, C. Y., ULRICH, R. L., ULRICH, M. P., EATON, B., OJEDA, J. F., LANE, D. J., KOTA, K. P., KENNY, T. A., LADNER, J. T., DICKSON, S. P., KUEHL, K., RAYCHAUDHURI, R., SUN, M., BAVARI, S., WOLCOTT, M. J., COVELL, D. & PANCHAL, R. G. 2015. Characterization of the murine macrophage response to infection with virulent and avirulent Burkholderia species. *BMC Microbiol,* 15**,** 259.

CHIRICOZZI, A., GUTTMAN-YASSKY, E., SUAREZ-FARINAS, M., NOGRALES, K. E., TIAN, S., CARDINALE, I., CHIMENTI, S. & KRUEGER, J. G. 2011. Integrative responses to IL-17 and TNF-alpha in human keratinocytes account for key inflammatory pathogenic circuits in psoriasis. *J Invest Dermatol,* 131**,** 677-87.

CHU, D. H. 2008. *Overview of biology, development, and structure of skin,* New York: McGraw-Hill., In K. Wolff, L.A. Goldsmith, S.I. Katz, B.A. Gilchrest, A.S. Paller, & D.J. Leffell (Eds.).

CHUSTZ, R. T., NAGARKAR, D. R., POPOSKI, J. A., FAVORETO, S., JR., AVILA, P. C., SCHLEIMER, R. P. & KATO, A. 2011. Regulation and function of the IL-1 family cytokine IL-1F9 in human bronchial epithelial cells. *Am J Respir Cell Mol Biol,* 45**,** 145-53.

CLARK, R. A., CHONG, B., MIRCHANDANI, N., BRINSTER, N. K., YAMANAKA, K., DOWGIERT, R. K. & KUPPER, T. S. 2006. The vast majority of CLA+ T cells are resident in normal skin. *J Immunol,* 176**,** 4431-9.

CLARK, R. A., HUANG, S. J., MURPHY, G. F., MOLLET, I. G., HIJNEN, D., MUTHUKURU, M., SCHANBACHER, C. F., EDWARDS, V., MILLER, D. M., KIM, J. E., LAMBERT, J. & KUPPER, T. S. 2008. Human squamous cell carcinomas evade the immune response by down-regulation of vascular E-selectin and recruitment of regulatory T cells. *J Exp Med,* 205**,** 2221-34.

CROSTON, G. E., CAO, Z. & GOEDDEL, D. V. 1995. NF-kappa B activation by interleukin-1 (IL-1) requires an IL-1 receptor-associated protein kinase activity. *J Biol Chem,* 270**,** 16514-7.

DEBETS, R., TIMANS, J. C., HOMEY, B., ZURAWSKI, S., SANA, T. R., LO, S., WAGNER, J., EDWARDS, G., CLIFFORD, T., MENON, S., BAZAN, J. F. & KASTELEIN, R. A. 2001. Two novel IL-1 family members, IL-1 delta and IL-1 epsilon, function as an antagonist and agonist of NF-kappa B activation through the orphan IL-1 receptor-related protein 2. *J Immunol,* 167**,** 1440-6.

DENG, L., WANG, C., SPENCER, E., YANG, L., BRAUN, A., YOU, J., SLAUGHTER, C., PICKART, C. & CHEN, Z. J. 2000. Activation of the IkappaB kinase complex by TRAF6 requires a dimeric ubiquitin-conjugating enzyme complex and a unique polyubiquitin chain. *Cell,* 103**,** 351-61.

DERER, A., GROETSCH, B., HARRE, U., BOHM, C., TOWNE, J., SCHETT, G., FREY, S. & HUEBER, A. J. 2014. Blockade of IL-36 receptor Signalling does not prevent from TNF-induced arthritis. *PLoS One,* 9**,** e101954.

DEVOTI, J. A., ROSENTHAL, D. W., WU, R., ABRAMSON, A. L., STEINBERG, B. M. & BONAGURA, V. R. 2008. Immune dysregulation and tumor-associated gene changes in recurrent respiratory papillomatosis: a paired microarray analysis. *Mol Med,* 14**,** 608-17.

DI CESARE, A., DI MEGLIO, P. & NESTLE, F. O. 2008. A role for Th17 cells in the immunopathogenesis of atopic dermatitis? *J Invest Dermatol,* 128**,** 2569-71.

DI CESARE, A., DI MEGLIO, P. & NESTLE, F. O. 2009. The IL-23/Th17 axis in the immunopathogenesis of psoriasis. *J Invest Dermatol,* 129**,** 1339-50.

DI MEGLIO, P., PERERA, G. K. & NESTLE, F. O. 2011. The multitasking organ: recent insights into skin immune function. *Immunity,* 35**,** 857-69.

DLUGOSZ, A. A., CHENG, C., WILLIAMS, E. K., DHARIA, A. G., DENNING, M. F. & YUSPA, S. H. 1994. Alterations in murine keratinocyte differentiation induced by activated rasHa genes are mediated by protein kinase C-alpha. *Cancer Res,* 54**,** 6413-20.

Donoghue, P.C. and Benton, M.J., 2007. Rocks and clocks: calibrating the Tree of Life using fossils and molecules. *Trends in ecology & evolution*, *22*(8), pp.424-431.

DUNN, E., SIMS, J. E., NICKLIN, M. J. & O'NEILL, L. A. 2001. Annotating genes with potential roles in the immune system: six new members of the IL-1 family. *Trends Immunol,* 22**,** 533-6.

ENGLAND, H., SUMMERSGILL, H. R., EDYE, M. E., ROTHWELL, N. J. & BROUGH, D. 2014. Release of interleukin-1alpha or interleukin-1beta depends on mechanism of cell death. *J Biol Chem,* 289**,** 15942-50.

FELDMEYER, L., KELLER, M., NIKLAUS, G., HOHL, D., WERNER, S. & BEER, H. D. 2007. The inflammasome mediates UVB-induced activation and secretion of interleukin-1beta by keratinocytes. *Curr Biol,* 17**,** 1140-5.

FOSTER, A. M., BALIWAG, J., CHEN, C. S., GUZMAN, A. M., STOLL, S. W., GUDJONSSON, J. E., WARD, N. L. & JOHNSTON, A. 2014. IL-36 promotes myeloid cell infiltration, activation, and inflammatory activity in skin. *J Immunol,* 192**,** 6053-61.

FOSTER, C. A., YOKOZEKI, H., RAPPERSBERGER, K., KONING, F., VOLC-PLATZER, B., RIEGER, A., COLIGAN, J. E., WOLFF, K. & STINGL, G. 1990. Human epidermal T cells predominantly belong to the lineage expressing alpha/beta T cell receptor. *J Exp Med,* 171**,** 997-1013.

FREY, S., DERER, A., MESSBACHER, M. E., BAETEN, D. L., BUGATTI, S., MONTECUCCO, C., SCHETT, G. & HUEBER, A. J. 2013. The novel cytokine interleukin-36alpha is expressed in psoriatic and rheumatoid arthritis synovium. *Ann Rheum Dis,* 72**,** 1569-74.

FUCHS, E. 2008. Skin stem cells: rising to the surface. *J Cell Biol,* 180**,** 273-84.

FUKUNAGA, A., KHASKHELY, N. M., SREEVIDYA, C. S., BYRNE, S. N. & ULLRICH, S. E. 2008. Dermal dendritic cells, and not Langerhans cells, play an essential role in inducing an immune response. *J Immunol,* 180**,** 3057-64.

GABAY, C. & TOWNE, J. E. 2015. Regulation and function of interleukin-36 cytokines in homeostasis and pathological conditions. *J Leukoc Biol,* 97**,** 645-52.

Gibson, M.S., Kaiser, P. and Fife, M., 2014. The chicken IL-1 family: evolution in the context of the studied vertebrate lineage. *Immunogenetics*, *66*(7-8), pp.427-438.

GILLIET, M. & LANDE, R. 2008. Antimicrobial peptides and self-DNA in autoimmune skin inflammation. *Curr Opin Immunol,* 20**,** 401-7.

GREENFEDER, S. A., NUNES, P., KWEE, L., LABOW, M., CHIZZONITE, R. A. & JU, G. 1995. Molecular cloning and characterization of a second subunit of the interleukin 1 receptor complex. *J Biol Chem,* 270**,** 13757-65.

GRESNIGT, M. S., ROSLER, B., JACOBS, C. W., BECKER, K. L., JOOSTEN, L. A., VAN DER MEER, J. W., NETEA, M. G., DINARELLO, C. A. & VAN DE VEERDONK, F. L. 2013. The IL-36 receptor pathway regulates Aspergillus fumigatus-induced Th1 and Th17 responses. *Eur J Immunol,* 43**,** 416-26.

GRIFFITHS, C. E. & NICKOLOFF, B. J. 1989. Keratinocyte intercellular adhesion molecule-1 (ICAM-1) expression precedes dermal T lymphocytic infiltration in allergic contact dermatitis (Rhus dermatitis). *Am J Pathol,* 135**,** 1045-53.

GROVES, R. W., MIZUTANI, H., KIEFFER, J. D. & KUPPER, T. S. 1995. Inflammatory skin disease in transgenic mice that express high levels of interleukin 1 alpha in basal epidermis. *Proc Natl Acad Sci U S A,* 92**,** 11874-8.

GUTTMAN-YASSKY, E., LOWES, M. A., FUENTES-DUCULAN, J., WHYNOT, J., NOVITSKAYA, I., CARDINALE, I., HAIDER, A., KHATCHERIAN, A., CARUCCI, J. A., BERGMAN, R. & KRUEGER, J. G. 2007. Major differences in inflammatory dendritic cells and their products distinguish atopic dermatitis from psoriasis. *J Allergy Clin Immunol,* 119**,** 1210-7.

HANSEN, L. A., MONTEIRO-RIVIERE, N. A. & SMART, R. C. 1990. Differential down-regulation of epidermal protein kinase C by 12-O-tetradecanoylphorbol-13-acetate and diacylglycerol: association with epidermal hyperplasia and tumor promotion. *Cancer Res,* 50**,** 5740-5.

HARDER, J., BARTELS, J., CHRISTOPHERS, E. & SCHRODER, J. M. 1997. A peptide antibiotic from human skin. *Nature,* 387**,** 861.

HASHIGUCHI, Y., YABE, R., CHUNG, S. H., MURAYAMA, M. A., YOSHIDA, K., MATSUO, K., KUBO, S., SAIJO, S., NAKAMURA, Y., MATSUE, H. & IWAKURA, Y. 2018. IL-36alpha from Skin-Resident Cells Plays an Important Role in the Pathogenesis of Imiquimod-Induced Psoriasiform Dermatitis by Forming a Local Autoamplification Loop. *J Immunol,* 201**,** 167-182.

HAYAKAWA, M., HAYAKAWA, H., MATSUYAMA, Y., TAMEMOTO, H., OKAZAKI, H. & TOMINAGA, S. 2009. Mature interleukin-33 is produced by calpain-mediated cleavage in vivo. *Biochem Biophys Res Commun,* 387**,** 218-22.

HENRY, C. M., SULLIVAN, G. P., CLANCY, D. M., AFONINA, I. S., KULMS, D. & MARTIN, S. J. 2016. Neutrophil-Derived Proteases Escalate Inflammation through Activation of IL-36 Family Cytokines. *Cell Rep,* 14**,** 708-722.

HENSELEIT, U., ROSENBACH, T. & KOLDE, G. 1996. Induction of apoptosis in human HaCaT keratinocytes. *Arch Dermatol Res,* 288**,** 676-83.

HESSAM, S., SAND, M., GAMBICHLER, T., SKRYGAN, M., RUDDEL, I. & BECHARA, F. G. 2018. Interleukin-36 in hidradenitis suppurativa: evidence for a distinctive proinflammatory role and a key factor in the development of an inflammatory loop. *Br J Dermatol,* 178**,** 761-767.

HUANG, J., GAO, X., LI, S. & CAO, Z. 1997. Recruitment of IRAK to the interleukin 1 receptor complex requires interleukin 1 receptor accessory protein. *Proc Natl Acad Sci U S A,* 94**,** 12829-32.

JAMES, W. D., BERGER, T. G., & ELSTON, D. M. 2006. *Andrews' diseases of the skin:,* Philadelphia: Elsevier Saunders.

JANEWAY, C. A., JR. 1989. Approaching the asymptote? Evolution and revolution in immunology. *Cold Spring Harb Symp Quant Biol,* 54 Pt 1**,** 1-13.

JENSEN, L. E. 2017. Interleukin-36 cytokines may overcome microbial immune evasion strategies that inhibit interleukin-1 family signaling. *Sci Signal,* 10.

JOHNSTON, A., XING, X., GUZMAN, A. M., RIBLETT, M., LOYD, C. M., WARD, N. L., WOHN, C., PRENS, E. P., WANG, F., MAIER, L. E., KANG, S., VOORHEES, J. J., ELDER, J. T. & GUDJONSSON, J. E. 2011. IL-1F5, -F6, -F8, and -F9: a novel IL-1 family Signalling system that is active in psoriasis and promotes keratinocyte antimicrobial peptide expression. *J Immunol,* 186**,** 2613-22.

JOHNSTON, A., XING, X., WOLTERINK, L., BARNES, D. H., YIN, Z., REINGOLD, L., KAHLENBERG, J. M., HARMS, P. W. & GUDJONSSON, J. E. 2017. IL-1 and IL-36 are dominant cytokines in generalized pustular psoriasis. *J Allergy Clin Immunol,* 140**,** 109-120.

JONES, P. H. 1996. Isolation and characterization of human epidermal stem cells. *Clin Sci (Lond),* 91**,** 141-6.

KALALI, B. N., KOLLISCH, G., MAGES, J., MULLER, T., BAUER, S., WAGNER, H., RING, J., LANG, R., MEMPEL, M. & OLLERT, M. 2008. Double-stranded RNA induces an antiviral defense status in epidermal keratinocytes through TLR3-, PKR-, and MDA5/RIG-I-mediated differential signaling. *J Immunol,* 181**,** 2694-704.

KANDA, T., NISHIDA, A., TAKAHASHI, K., HIDAKA, K., IMAEDA, H., INATOMI, O., BAMBA, S., SUGIMOTO, M. & ANDOH, A. 2015. Interleukin(IL)-36alpha and IL-36gamma Induce Proinflammatory Mediators from Human Colonic Subepithelial Myofibroblasts. *Front Med (Lausanne),* 2**,** 69.

KANITAKIS, J. 2002. Anatomy, histology and immunohistochemistry of normal human skin. *Eur J Dermatol,* 12**,** 390-9; quiz 400-1.

KARIN, M., LIU, Z. & ZANDI, E. 1997. AP-1 function and regulation. *Curr Opin Cell Biol,* 9**,** 240-6.

KASHEM, S. W., IGYARTO, B. Z., GERAMI-NEJAD, M., KUMAMOTO, Y., MOHAMMED, J. A., JARRETT, E., DRUMMOND, R. A., ZURAWSKI, S. M., ZURAWSKI, G., BERMAN, J., IWASAKI, A., BROWN, G. D. & KAPLAN, D. H. 2015. Candida albicans morphology and dendritic cell subsets determine T helper cell differentiation. *Immunity,* 42**,** 356-366.

KELLER, M., RUEGG, A., WERNER, S. & BEER, H. D. 2008. Active caspase-1 is a regulator of unconventional protein secretion. *Cell,* 132**,** 818-31.

KENT, W. J., SUGNET, C. W., FUREY, T. S., ROSKIN, K. M., PRINGLE, T. H., ZAHLER, A. M. & HAUSSLER, D. 2002. The human genome browser at UCSC. *Genome Res,* 12**,** 996-1006.

KISSENPFENNIG, A., HENRI, S., DUBOIS, B., LAPLACE-BUILHE, C., PERRIN, P., ROMANI, N., TRIPP, C. H., DOUILLARD, P., LESERMAN, L., KAISERLIAN, D., SAELAND, S., DAVOUST, J. & MALISSEN, B. 2005. Dynamics and function of Langerhans cells in vivo: dermal dendritic cells colonize lymph node areas distinct from slower migrating Langerhans cells. *Immunity,* 22**,** 643-54.

KLECHEVSKY, E., MORITA, R., LIU, M., CAO, Y., COQUERY, S., THOMPSON-SNIPES, L., BRIERE, F., CHAUSSABEL, D., ZURAWSKI, G., PALUCKA, A. K., REITER, Y., BANCHEREAU, J. & UENO, H. 2008. Functional specializations of human epidermal Langerhans cells and CD14+ dermal dendritic cells. *Immunity,* 29**,** 497-510.

KOLLISCH, G., KALALI, B. N., VOELCKER, V., WALLICH, R., BEHRENDT, H., RING, J., BAUER, S., JAKOB, T., MEMPEL, M. & OLLERT, M. 2005. Various members of the Toll-like receptor family contribute to the innate immune response of human epidermal keratinocytes. *Immunology,* 114**,** 531-41.

KORHERR, C., HOFMEISTER, R., WESCHE, H. & FALK, W. 1997. A critical role for interleukin-1 receptor accessory protein in interleukin-1 signaling. *Eur J Immunol,* 27**,** 262-7.

KOVACH, M. A., SINGER, B., MARTINEZ-COLON, G., NEWSTEAD, M. W., ZENG, X., MANCUSO, P., MOORE, T. A., KUNKEL, S. L., PETERS-GOLDEN, M., MOORE, B. B. & STANDIFORD, T. J. 2017. IL-36gamma is a crucial proximal component of protective type-1-mediated lung mucosal immunity in Gram-positive and -negative bacterial pneumonia. *Mucosal Immunol,* 10**,** 1320-1334.

KUMAR, S., MCDONNELL, P. C., LEHR, R., TIERNEY, L., TZIMAS, M. N., GRISWOLD, D. E., CAPPER, E. A., TAL-SINGER, R., WELLS, G. I., DOYLE, M. L. & YOUNG, P. R. 2000. Identification and initial

characterization of four novel members of the interleukin-1 family. *J Biol Chem,* 275**,** 10308-14.

KUPPER, T. S., BALLARD, D. W., CHUA, A. O., MCGUIRE, J. S., FLOOD, P. M., HOROWITZ, M. C., LANGDON, R., LIGHTFOOT, L. & GUBLER, U. 1986. Human keratinocytes contain mRNA indistinguishable from monocyte interleukin 1 alpha and beta mRNA. Keratinocyte epidermal cell-derived thymocyte-activating factor is identical to interleukin 1. *J Exp Med,* 164**,** 2095-100.

LAI, Y. & GALLO, R. L. 2009. AMPed up immunity: how antimicrobial peptides have multiple roles in immune defense. *Trends Immunol,* 30**,** 131-41.

LANDE, R., GREGORIO, J., FACCHINETTI, V., CHATTERJEE, B., WANG, Y. H., HOMEY, B., CAO, W., WANG, Y. H., SU, B., NESTLE, F. O., ZAL, T., MELLMAN, I., SCHRODER, J. M., LIU, Y. J. & GILLIET, M. 2007. Plasmacytoid dendritic cells sense self-DNA coupled with antimicrobial peptide. *Nature,* 449**,** 564-9.

LAVKER, R. M. & SUN, T. T. 1982. Heterogeneity in epidermal basal keratinocytes: morphological and functional correlations. *Science,* 215**,** 1239-41.

LEBRE, M. C., VAN DER AAR, A. M., VAN BAARSEN, L., VAN CAPEL, T. M., SCHUITEMAKER, J. H., KAPSENBERG, M. L. & DE JONG, E. C. 2007. Human keratinocytes express functional Toll-like receptor 3, 4, 5, and 9. *J Invest Dermatol,* 127**,** 331-41.

LECLERC, G. M., BOOCKFOR, F. R., FAUGHT, W. J. & FRAWLEY, L. S. 2000. Development of a destabilized firefly luciferase enzyme for measurement of gene expression. *Biotechniques,* 29**,** 590-1, 594-6, 598 passim.

LEE, P., LEE, D. J., CHAN, C., CHEN, S. W., CH'EN, I. & JAMORA, C. 2009. Dynamic expression of epidermal caspase 8 simulates a wound healing response. *Nature,* 458**,** 519-23.

LEE, Y. S., DLUGOSZ, A. A., MCKAY, R., DEAN, N. M. & YUSPA, S. H. 1997. Definition by specific antisense oligonucleotides of a role for protein kinase C alpha in expression of differentiation markers in normal and neoplastic mouse epidermal keratinocytes. *Mol Carcinog,* 18**,** 44-53.

LIAN, L. H., MILORA, K. A., MANUPIPATPONG, K. K. & JENSEN, L. E. 2012. The double-stranded RNA analogue polyinosinic-polycytidylic acid induces keratinocyte pyroptosis and release of IL-36gamma. *J Invest Dermatol,* 132**,** 1346-53.

LIANG, S. C., TAN, X. Y., LUXENBERG, D. P., KARIM, R., DUNUSSI-JOANNOPOULOS, K., COLLINS, M. & FOUSER, L. A. 2006. Interleukin (IL)-22 and IL-17 are coexpressed by Th17 cells and cooperatively enhance expression of antimicrobial peptides. *J Exp Med,* 203**,** 2271-9.

LIU, H., ARCHER, N. K., DILLEN, C. A., WANG, Y., ASHBAUGH, A. G., ORTINES, R. V., KAO, T., LEE, S. K., CAI, S. S., MILLER, R. J., MARCHITTO, M. C., ZHANG, E., RIGGINS, D. P., PLAUT, R. D., STIBITZ, S., GEHA, R. S. & MILLER, L. S. 2017. Staphylococcus aureus Epicutaneous Exposure Drives Skin Inflammation via IL-36-Mediated T Cell Responses. *Cell Host Microbe,* 22**,** 653-666.e5.

LOWES, M. A., CHAMIAN, F., ABELLO, M. V., FUENTES-DUCULAN, J., LIN, S. L., NUSSBAUM, R., NOVITSKAYA, I., CARBONARO, H., CARDINALE, I., KIKUCHI, T., GILLEAUDEAU, P., SULLIVAN-WHALEN, M., WITTKOWSKI, K. M., PAPP, K., GAROVOY, M., DUMMER, W., STEINMAN, R. M. & KRUEGER, J. G. 2005. Increase in TNF-alpha and inducible nitric oxide synthase-expressing dendritic cells in psoriasis and reduction with efalizumab (anti-CD11a). *Proc Natl Acad Sci U S A,* 102**,** 19057-62.

MAGNE, D., PALMER, G., BARTON, J. L., MEZIN, F., TALABOT-AYER, D., BAS, S., DUFFY, T., NOGER, M., GUERNE, P. A., NICKLIN, M. J. & GABAY, C. 2006. The new IL-1 family member IL-1F8 stimulates production of inflammatory mediators by synovial fibroblasts and articular chondrocytes. *Arthritis Res Ther,* 8**,** R80.

MARRAKCHI, S., GUIGUE, P., RENSHAW, B. R., PUEL, A., PEI, X. Y., FRAITAG, S., ZRIBI, J., BAL, E., CLUZEAU, C., CHRABIEH, M., TOWNE, J. E., DOUANGPANYA, J., PONS, C., MANSOUR, S., SERRE, V., MAKNI, H., MAHFOUDH, N., FAKHFAKH, F., BODEMER, C., FEINGOLD, J., HADJ-RABIA, S., FAVRE, M., GENIN, E., SAHBATOU, M., MUNNICH, A., CASANOVA, J. L., SIMS, J. E.,

TURKI, H., BACHELEZ, H. & SMAHI, A. 2011. Interleukin-36-receptor antagonist deficiency and generalized pustular psoriasis. *N Engl J Med,* 365**,** 620-8.
MARTIN, U., SCHOLLER, J., GURGEL, J., RENSHAW, B., SIMS, J. E. & GABEL, C. A. 2009. Externalization of the leaderless cytokine IL-1F6 occurs in response to lipopolysaccharide/ATP activation of transduced bone marrow macrophages. *J Immunol,* 183**,** 4021-30.
MARTINON, F., MAYOR, A. & TSCHOPP, J. 2009. The inflammasomes: guardians of the body. *Annu Rev Immunol,* 27**,** 229-65.
MATEJUK, A. 2018. Skin Immunity. *Arch Immunol Ther Exp (Warsz),* 66**,** 45-54.
MATTII, M., AYALA, F., BALATO, N., FILOTICO, R., LEMBO, S., SCHIATTARELLA, M., PATRUNO, C., MARONE, G. & BALATO, A. 2013. The balance between pro- and anti-inflammatory cytokines is crucial in human allergic contact dermatitis pathogenesis: the role of IL-1 family members. *Exp Dermatol,* 22**,** 813-9.
MEDINA-CONTRERAS, O., HARUSATO, A., NISHIO, H., FLANNIGAN, K. L., NGO, V., LEONI, G., NEUMANN, P. A., GEEM, D., LILI, L. N., RAMADAS, R. A., CHASSAING, B., GEWIRTZ, A. T., KOHLMEIER, J. E., PARKOS, C. A., TOWNE, J. E., NUSRAT, A. & DENNING, T. L. 2016. Cutting Edge: IL-36 Receptor Promotes Resolution of Intestinal Damage. *J Immunol,* 196**,** 34-8.
MEHLING, A., LOSER, K., VARGA, G., METZE, D., LUGER, T. A., SCHWARZ, T., GRABBE, S. & BEISSERT, S. 2001. Overexpression of CD40 ligand in murine epidermis results in chronic skin inflammation and systemic autoimmunity. *J Exp Med,* 194**,** 615-28.
MILLER, L. S. & MODLIN, R. L. 2007. Human keratinocyte Toll-like receptors promote distinct immune responses. *J Invest Dermatol,* 127**,** 262-3.
MILLS, K. J., BOCCKINO, S. B., BURNS, D. J., LOOMIS, C. R. & SMART, R. C. 1992. Alterations in protein kinase C isozymes alpha and beta 2 in activated Ha-ras containing papillomas in the absence of an increase in diacylglycerol. *Carcinogenesis,* 13**,** 1113-20.
MURPHY, G. F. 1997. *Histology of the skin,* Philadelphia: Lippincott Williams & Wilkins., In D. Elder, R. Elenitsas, C. Jaworsky, & B. Johnson Jr.
MUZIO, M., NI, J., FENG, P. & DIXIT, V. M. 1997. IRAK (Pelle) family member IRAK-2 and MyD88 as proximal mediators of IL-1 signaling. *Science,* 278**,** 1612-5.
NANJO, Y., NEWSTEAD, M. W., AOYAGI, T., ZENG, X., TAKAHASHI, K., YU, F. S., TATEDA, K. & STANDIFORD, T. J. 2019. Overlapping Roles for Interleukin-36 Cytokines in Protective Host Defense against Murine Legionella pneumophila Pneumonia. *Infect Immun,* 87.
NERLICH, A., RUANGKIATTIKUL, N., LAARMANN, K., JANZE, N., DITTRICH-BREIHOLZ, O., KRACHT, M. & GOETHE, R. 2015. C/EBPbeta is a transcriptional key regulator of IL-36alpha in murine macrophages. *Biochim Biophys Acta,* 1849**,** 966-78.
NESTLE, F. O., CONRAD, C., TUN-KYI, A., HOMEY, B., GOMBERT, M., BOYMAN, O., BURG, G., LIU, Y. J. & GILLIET, M. 2005. Plasmacytoid predendritic cells initiate psoriasis through interferon-alpha production. *J Exp Med,* 202**,** 135-43.
NESTLE, F. O., DI MEGLIO, P., QIN, J. Z. & NICKOLOFF, B. J. 2009. Skin immune sentinels in health and disease. *Nat Rev Immunol,* 9**,** 679-91.
NGO, V. L., ABO, H., MAXIM, E., HARUSATO, A., GEEM, D., MEDINA-CONTRERAS, O., MERLIN, D., GEWIRTZ, A. T., NUSRAT, A. & DENNING, T. L. 2018. A cytokine network involving IL-36gamma, IL-23, and IL-22 promotes antimicrobial defense and recovery from intestinal barrier damage. *Proc Natl Acad Sci U S A,* 115**,** E5076-e5085.
NGUYEN, T. T., NIYONSABA, F., USHIO, H., AKIYAMA, T., KIATSURAYANON, C., SMITHRITHEE, R., IKEDA, S., OKUMURA, K. & OGAWA, H. 2012. Interleukin-36 cytokines enhance the production of host defense peptides psoriasin and LL-37 by human keratinocytes through activation of MAPKs and NF-kappaB. *J Dermatol Sci,* 68**,** 63-6.
NICKLIN, M. J. 2011. Finally, function for "IL-1Fs". *Blood,* 118**,** 5713-4.
NICKLIN, M. J., BARTON, J. L., NGUYEN, M., FITZGERALD, M. G., DUFF, G. W. & KORNMAN, K. 2002. A sequence-based map of the nine genes of the human interleukin-1 cluster. *Genomics,* 79**,** 718-25.

NINOMIYA-TSUJI, J., KISHIMOTO, K., HIYAMA, A., INOUE, J., CAO, Z. & MATSUMOTO, K. 1999. The kinase TAK1 can activate the NIK-I kappaB as well as the MAP kinase cascade in the IL-1 signalling pathway. *Nature,* 398**,** 252-6.

NISHIDA, A., HIDAKA, K., KANDA, T., IMAEDA, H., SHIOYA, M., INATOMI, O., BAMBA, S., KITOH, K., SUGIMOTO, M. & ANDOH, A. 2016. Increased Expression of Interleukin-36, a Member of the Interleukin-1 Cytokine Family, in Inflammatory Bowel Disease. *Inflamm Bowel Dis,* 22**,** 303-14.

ODAKA, M., FURUTA, T., KOBAYASHI, Y. & IWAMURA, M. 1995. Synthesis of caged compounds of L-leucyl-L-leucine methyl ester, an apoptosis inducer, and their cytotoxic activity. *Biochem Biophys Res Commun,* 213**,** 652-6.

PARSANEJAD, R., FIELDS, W. R., STEICHEN, T. J., BOMBICK, B. R. & DOOLITTLE, D. J. 2008. Distinct regulatory profiles of interleukins and chemokines in response to cigarette smoke condensate in normal human bronchial epithelial (NHBE) cells. *J Interferon Cytokine Res,* 28**,** 703-12.

PASPARAKIS, M., COURTOIS, G., HAFNER, M., SCHMIDT-SUPPRIAN, M., NENCI, A., TOKSOY, A., KRAMPERT, M., GOEBELER, M., GILLITZER, R., ISRAEL, A., KRIEG, T., RAJEWSKY, K. & HAASE, I. 2002. TNF-mediated inflammatory skin disease in mice with epidermis-specific deletion of IKK2. *Nature,* 417**,** 861-6.

PENHA, R., HIGGINS, J., MUTAMBA, S., BARROW, P., MAHIDA, Y. & FOSTER, N. 2016. IL-36 receptor is expressed by human blood and intestinal T lymphocytes and is dose-dependently activated via IL-36beta and induces CD4+ lymphocyte proliferation. *Cytokine,* 85**,** 18-25.

PERIC, M., KOGLIN, S., KIM, S. M., MORIZANE, S., BESCH, R., PRINZ, J. C., RUZICKA, T., GALLO, R. L. & SCHAUBER, J. 2008. IL-17A enhances vitamin D3-induced expression of cathelicidin antimicrobial peptide in human keratinocytes. *J Immunol,* 181**,** 8504-12.

RAMADAS, R. A., EWART, S. L., IWAKURA, Y., MEDOFF, B. D. & LEVINE, A. M. 2012. IL-36alpha exerts pro-inflammatory effects in the lungs of mice. *PLoS One,* 7**,** e45784.

RAMADAS, R. A., EWART, S. L., MEDOFF, B. D. & LEVINE, A. M. 2011. Interleukin-1 family member 9 stimulates chemokine production and neutrophil influx in mouse lungs. *Am J Respir Cell Mol Biol,* 44**,** 134-45.

RAMADAS, R. A., LI, X., SHUBITOWSKI, D. M., SAMINENI, S., WILLS-KARP, M. & EWART, S. L. 2006. IL-1 Receptor antagonist as a positional candidate gene in a murine model of allergic asthma. *Immunogenetics,* 58**,** 851-5.

RAN, F. A., HSU, P. D., WRIGHT, J., AGARWALA, V., SCOTT, D. A. & ZHANG, F. 2013. Genome engineering using the CRISPR-Cas9 system. *Nat Protoc,* 8**,** 2281-2308.

RANA, A. A., LUCS, A. V., DEVOTI, J., BLANC, L., PAPOIN, J., WU, R., PAPAYANNAKOS, C. J., ABRAMSON, A., BONAGURA, V. R. & STEINBERG, B. M. 2015. Poly(I:C) induces controlled release of IL-36gamma from keratinocytes in the absence of cell death. *Immunol Res,* 63**,** 228-35.

Rivers-Auty, J., Daniels, M.J., Colliver, I., Robertson, D.L. and Brough, D., 2018. Redefining the ancestral origins of the interleukin-1 superfamily. *Nature communications*, *9*(1), p.1156.

ROMANI, N., EBNER, S., TRIPP, C. H., FLACHER, V., KOCH, F. & STOITZNER, P. 2006. Epidermal Langerhans cells--changing views on their function in vivo. *Immunol Lett,* 106**,** 119-25.

RUSSELL, S. E., HORAN, R. M., STEFANSKA, A. M., CAREY, A., LEON, G., AGUILERA, M., STATOVCI, D., MORAN, T., FALLON, P. G., SHANAHAN, F., BRINT, E. K., MELGAR, S., HUSSEY, S. & WALSH, P. T. 2016. IL-36alpha expression is elevated in ulcerative colitis and promotes colonic inflammation. *Mucosal Immunol,* 9**,** 1193-204.

SANO, S., CHAN, K. S., CARBAJAL, S., CLIFFORD, J., PEAVEY, M., KIGUCHI, K., ITAMI, S., NICKOLOFF, B. J. & DIGIOVANNI, J. 2005. Stat3 links activated keratinocytes and immunocytes required for development of psoriasis in a novel transgenic mouse model. *Nat Med,* 11**,** 43-9.

SANZ, L., DIAZ-MECO, M. T., NAKANO, H. & MOSCAT, J. 2000. The atypical PKC-interacting protein p62 channels NF-kappaB activation by the IL-1-TRAF6 pathway. *Embo j,* 19**,** 1576-86.

SCHAUBER, J., DORSCHNER, R. A., CODA, A. B., BUCHAU, A. S., LIU, P. T., KIKEN, D., HELFRICH, Y. R., KANG, S., ELALIEH, H. Z., STEINMEYER, A., ZUGEL, U., BIKLE, D. D., MODLIN, R. L. & GALLO, R. L. 2007. Injury enhances TLR2 function and antimicrobial peptide expression through a vitamin D-dependent mechanism. *J Clin Invest,* 117**,** 803-11.

SCHEIBE, K., BACKERT, I., WIRTZ, S., HUEBER, A., SCHETT, G., VIETH, M., PROBST, H. C., BOPP, T., NEURATH, M. F. & NEUFERT, C. 2017. IL-36R signalling activates intestinal epithelial cells and fibroblasts and promotes mucosal healing in vivo. *Gut,* 66**,** 823-838.

SCHOLZ, G. M., HEATH, J. E., AW, J. & REYNOLDS, E. C. 2018a. Regulation of the Peptidoglycan Amidase PGLYRP2 in Epithelial Cells by Interleukin-36gamma. *Infect Immun,* 86.

SCHOLZ, G. M., HEATH, J. E., WALSH, K. A. & REYNOLDS, E. C. 2018b. MEK-ERK Signalling diametrically controls the stimulation of IL-23p19 and EBI3 expression in epithelial cells by IL-36gamma. *Immunol Cell Biol,* 96**,** 646-655.

SCHONEFUSS, A., WENDT, W., SCHATTLING, B., SCHULTEN, R., HOFFMANN, K., STUECKER, M., TIGGES, C., LUBBERT, H. & STICHEL, C. 2010. Upregulation of cathepsin S in psoriatic keratinocytes. *Exp Dermatol,* 19**,** e80-8.

SCHWARZ, A. & SCHWARZ, T. 2010. UVR-induced regulatory T cells switch antigen-presenting cells from a stimulatory to a regulatory phenotype. *J Invest Dermatol,* 130**,** 1914-21.

SCHWARZ, G., BOEHNCKE, W. H., BRAUN, M., SCHROTER, C. J., BURSTER, T., FLAD, T., DRESSEL, D., WEBER, E., SCHMID, H. & KALBACHER, H. 2002. Cathepsin S activity is detectable in human keratinocytes and is selectively upregulated upon stimulation with interferon-gamma. *J Invest Dermatol,* 119**,** 44-9.

SHIRAKABE, K., YAMAGUCHI, K., SHIBUYA, H., IRIE, K., MATSUDA, S., MORIGUCHI, T., GOTOH, Y., MATSUMOTO, K. & NISHIDA, E. 1997. TAK1 mediates the ceramide Signalling to stress-activated protein kinase/c-Jun N-terminal kinase. *J Biol Chem,* 272**,** 8141-4.

SMITH, D. E., RENSHAW, B. R., KETCHEM, R. R., KUBIN, M., GARKA, K. E. & SIMS, J. E. 2000. Four new members expand the interleukin-1 superfamily. *J Biol Chem,* 275**,** 1169-75.

SOUMELIS, V., RECHE, P. A., KANZLER, H., YUAN, W., EDWARD, G., HOMEY, B., GILLIET, M., HO, S., ANTONENKO, S., LAUERMA, A., SMITH, K., GORMAN, D., ZURAWSKI, S., ABRAMS, J., MENON, S., MCCLANAHAN, T., DE WAAL-MALEFYT RD, R., BAZAN, F., KASTELEIN, R. A. & LIU, Y. J. 2002. Human epithelial cells trigger dendritic cell mediated allergic inflammation by producing TSLP. *Nat Immunol,* 3**,** 673-80.

STUDIER, F. W. 2005. Protein production by auto-induction in high density shaking cultures. *Protein Expr Purif,* 41**,** 207-34.

SUAREZ-FARINAS, M., UNGAR, B., CORREA DA ROSA, J., EWALD, D. A., ROZENBLIT, M., GONZALEZ, J., XU, H., ZHENG, X., PENG, X., ESTRADA, Y. D., DILLON, S. R., KRUEGER, J. G. & GUTTMAN-YASSKY, E. 2015. RNA sequencing atopic dermatitis transcriptome profiling provides insights into novel disease mechanisms with potential therapeutic implications. *J Allergy Clin Immunol,* 135**,** 1218-27.

SUZUKI, N., SUZUKI, S., DUNCAN, G. S., MILLAR, D. G., WADA, T., MIRTSOS, C., TAKADA, H., WAKEHAM, A., ITIE, A., LI, S., PENNINGER, J. M., WESCHE, H., OHASHI, P. S., MAK, T. W. & YEH, W. C. 2002. Severe impairment of interleukin-1 and Toll-like receptor signalling in mice lacking IRAK-4. *Nature,* 416**,** 750-6.

TAKAESU, G., KISHIDA, S., HIYAMA, A., YAMAGUCHI, K., SHIBUYA, H., IRIE, K., NINOMIYA-TSUJI, J. & MATSUMOTO, K. 2000. TAB2, a novel adaptor protein, mediates activation of TAK1 MAPKKK by linking TAK1 to TRAF6 in the IL-1 signal transduction pathway. *Mol Cell,* 5**,** 649-58.

TAKAHASHI, K., NISHIDA, A., SHIOYA, M., IMAEDA, H., BAMBA, S., INATOMI, O., SHIMIZU, T., KITOH, K. & ANDOH, A. 2015. Interleukin (IL)-1beta Is a Strong Inducer of IL-36gamma Expression in Human Colonic Myofibroblasts. *PLoS One,* 10**,** e0138423.

TAO, X., SONG, Z., WANG, C., LUO, H., LUO, Q., LIN, X., ZHANG, L., YIN, Y. & CAO, J. 2017. Interleukin 36alpha Attenuates Sepsis by Enhancing Antibacterial Functions of Macrophages. *J Infect Dis,* 215**,** 321-332.

THOMI, R., KAKEDA, M., YAWALKAR, N., SCHLAPBACH, C. & HUNGER, R. E. 2017. Increased expression of the interleukin-36 cytokines in lesions of hidradenitis suppurativa. *J Eur Acad Dermatol Venereol,* 31**,** 2091-2096.

THORNBERRY, N. A., BULL, H. G., CALAYCAY, J. R., CHAPMAN, K. T., HOWARD, A. D., KOSTURA, M. J., MILLER, D. K., MOLINEAUX, S. M., WEIDNER, J. R., AUNINS, J. & ET AL. 1992. A novel heterodimeric cysteine protease is required for interleukin-1 beta processing in monocytes. *Nature,* 356**,** 768-74.

TIEMESSEN, M. M., JAGGER, A. L., EVANS, H. G., VAN HERWIJNEN, M. J., JOHN, S. & TAAMS, L. S. 2007. CD4+CD25+Foxp3+ regulatory T cells induce alternative activation of human monocytes/macrophages. *Proc Natl Acad Sci U S A,* 104**,** 19446-51.

TOMURA, M., HONDA, T., TANIZAKI, H., OTSUKA, A., EGAWA, G., TOKURA, Y., WALDMANN, H., HORI, S., CYSTER, J. G., WATANABE, T., MIYACHI, Y., KANAGAWA, O. & KABASHIMA, K. 2010. Activated regulatory T cells are the major T cell type emigrating from the skin during a cutaneous immune response in mice. *J Clin Invest,* 120**,** 883-93.

TORTOLA, L., ROSENWALD, E., ABEL, B., BLUMBERG, H., SCHAFER, M., COYLE, A. J., RENAULD, J. C., WERNER, S., KISIELOW, J. & KOPF, M. 2012. Psoriasiform dermatitis is driven by IL-36-mediated DC-keratinocyte crosstalk. *J Clin Invest,* 122**,** 3965-76.

TOWNE, J. E., GARKA, K. E., RENSHAW, B. R., VIRCA, G. D. & SIMS, J. E. 2004. Interleukin (IL)-1F6, IL-1F8, and IL-1F9 signal through IL-1Rrp2 and IL-1RAcP to activate the pathway leading to NF-kappaB and MAPKs. *J Biol Chem,* 279**,** 13677-88.

TOWNE, J. E., RENSHAW, B. R., DOUANGPANYA, J., LIPSKY, B. P., SHEN, M., GABEL, C. A. & SIMS, J. E. 2011. Interleukin-36 (IL-36) ligands require processing for full agonist (IL-36alpha, IL-36beta, and IL-36gamma) or antagonist (IL-36Ra) activity. *J Biol Chem,* 286**,** 42594-602.

TOWNE, J. E. & SIMS, J. E. 2012. IL-36 in psoriasis. *Curr Opin Pharmacol,* 12**,** 486-90.

VAN DE VEERDONK, F. L. & NETEA, M. G. 2013. New Insights in the Immunobiology of IL-1 Family Members. *Front Immunol,* 4**,** 167.

VERMA, A. H., RICHARDSON, J. P., ZHOU, C., COLEMAN, B. M., MOYES, D. L., HO, J., HUPPLER, A. R., RAMANI, K., MCGEACHY, M. J., MUFAZALOV, I. A., WAISMAN, A., KANE, L. P., BISWAS, P. S., HUBE, B., NAGLIK, J. R. & GAFFEN, S. L. 2017. Oral epithelial cells orchestrate innate type 17 responses to Candida albicans through the virulence factor candidalysin. *Sci Immunol,* 2.

VIGNE, S., PALMER, G., LAMACCHIA, C., MARTIN, P., TALABOT-AYER, D., RODRIGUEZ, E., RONCHI, F., SALLUSTO, F., DINH, H., SIMS, J. E. & GABAY, C. 2011. IL-36R ligands are potent regulators of dendritic and T cells. *Blood,* 118**,** 5813-23.

VIGNE, S., PALMER, G., MARTIN, P., LAMACCHIA, C., STREBEL, D., RODRIGUEZ, E., OLLEROS, M. L., VESIN, D., GARCIA, I., RONCHI, F., SALLUSTO, F., SIMS, J. E. & GABAY, C. 2012. IL-36 Signalling amplifies Th1 responses by enhancing proliferation and Th1 polarization of naive CD4+ T cells. *Blood,* 120**,** 3478-87.

VOLPE, F., CLATWORTHY, J., KAPTEIN, A., MASCHERA, B., GRIFFIN, A. M. & RAY, K. 1997. The IL1 receptor accessory protein is responsible for the recruitment of the interleukin-1 receptor associated kinase to the IL1/IL1 receptor I complex. *FEBS Lett,* 419**,** 41-4.

VOS, J. B., VAN STERKENBURG, M. A., RABE, K. F., SCHALKWIJK, J., HIEMSTRA, P. S. & DATSON, N. A. 2005. Transcriptional response of bronchial epithelial cells to Pseudomonas aeruginosa: identification of early mediators of host defense. *Physiol Genomics,* 21**,** 324-36.

VUKMANOVIC-STEJIC, M., AGIUS, E., BOOTH, N., DUNNE, P. J., LACY, K. E., REED, J. R., SOBANDE, T. O., KISSANE, S., SALMON, M., RUSTIN, M. H. & AKBAR, A. N. 2008. The kinetics of CD4+Foxp3+ T cell accumulation during a human cutaneous antigen-specific memory response in vivo. *J Clin Invest,* 118**,** 3639-50.

WANG, H. Q. & SMART, R. C. 1999. Overexpression of protein kinase C-alpha in the epidermis of transgenic mice results in striking alterations in phorbol ester-induced inflammation and COX-2, MIP-2 and TNF-alpha expression but not tumor promotion. *J Cell Sci,* 112 (Pt 20)**,** 3497-506.

WATANABE, H., GAIDE, O., PETRILLI, V., MARTINON, F., CONTASSOT, E., ROQUES, S., KUMMER, J. A., TSCHOPP, J. & FRENCH, L. E. 2007. Activation of the IL-1beta-processing inflammasome is involved in contact hypersensitivity. *J Invest Dermatol,* 127**,** 1956-63.

WEIN, A. N., DUNBAR, P. R., MCMASTER, S. R., LI, Z. T., DENNING, T. L. & KOHLMEIER, J. E. 2018. IL-36gamma Protects against Severe Influenza Infection by Promoting Lung Alveolar Macrophage Survival and Limiting Viral Replication. *J Immunol,* 201**,** 573-582.

WESCHE, H., KORHERR, C., KRACHT, M., FALK, W., RESCH, K. & MARTIN, M. U. 1997. The interleukin-1 receptor accessory protein (IL-1RAcP) is essential for IL-1-induced activation of interleukin-1 receptor-associated kinase (IRAK) and stress-activated protein kinases (SAP kinases). *J Biol Chem,* 272**,** 7727-31.

WINKLE, S. M., THROOP, A. L. & HERBST-KRALOVETZ, M. M. 2016. IL-36gamma Augments Host Defense and Immune Responses in Human Female Reproductive Tract Epithelial Cells. *Front Microbiol,* 7**,** 955.

WOLLENBERG, A., MOMMAAS, M., OPPEL, T., SCHOTTDORF, E. M., GUNTHER, S. & MODERER, M. 2002. Expression and function of the mannose receptor CD206 on epidermal dendritic cells in inflammatory skin diseases. *J Invest Dermatol,* 118**,** 327-34.

YAO, J., KIM, T. W., QIN, J., JIANG, Z., QIAN, Y., XIAO, H., LU, Y., QIAN, W., GULEN, M. F., SIZEMORE, N., DIDONATO, J., SATO, S., AKIRA, S., SU, B. & LI, X. 2007. Interleukin-1 (IL-1)-induced TAK1-dependent Versus MEKK3-dependent NFkappaB activation pathways bifurcate at IL-1 receptor-associated kinase modification. *J Biol Chem,* 282**,** 6075-89.

ZABA, L. C., FUENTES-DUCULAN, J., STEINMAN, R. M., KRUEGER, J. G. & LOWES, M. A. 2007. Normal human dermis contains distinct populations of CD11c+BDCA-1+ dendritic cells and CD163+FXIIIA+ macrophages. *J Clin Invest,* 117**,** 2517-25.

ZHANG, J., YIN, Y., LIN, X., YAN, X., XIA, Y., ZHANG, L. & CAO, J. 2017. IL-36 induces cytokine IL-6 and chemokine CXCL8 expression in human lung tissue cells: Implications for pulmonary inflammatory responses. *Cytokine,* 99**,** 114-123.

ZHOU, L., TODOROVIC, V., KAKAVAS, S., SIELAFF, B., MEDINA, L., WANG, L., SADHUKHAN, R., STOCKMANN, H., RICHARDSON, P. L., DIGIAMMARINO, E., SUN, C. & SCOTT, V. 2018. Quantitative ligand and receptor binding studies reveal the mechanism of interleukin-36 (IL-36) pathway activation. *J Biol Chem,* 293**,** 403-411.

Appendices

Appendix I- Predicted details of pET-IL1RN plasmid

T7 promoter XbaI

taatacgactcactatagggagaccacaacggtttccctctagaaataatttgtttaac

NdeI His_6 Tag

tttaagaaggagatatacatatggctagcatgactggtggtcaccatcaccatcaccatt

Acc65I M A S M T G G H H H H H H

ctggtacc

S G T…

XhoI

ctcgagatccggctgctaacaaagcccgaaaggaagctgagttggctgctgccaccgctgagcaataactagcataacccccttggggcctctaaacgggtct
tgaggggttttttgctgaaaggaggaactatatccggatatccacaggacgggtgtggtcgccatgatcgcgtagtcgatagtggctccaagtagcgaagcg
agcaggactgggcggcggccaaagcggtcggacagtgctccgagaacgggtgcgcatagaaattgcatcaacgcatatagcgctagcagcacgccatagtga
ctggcgatgctgtcggaatggacgatatcccgcaagaggcccggcagtaccggcataaccaagcctatgcctacagcatccagggtgacggtgccgaggatg
acgatgagcgcattgttagatttcatacacggtgcctgactgcgttagcaatttaactgtgataaactaccgcattaaagcttatcgatgataagctgtcaa
acatgagaattcttgaagacgaaagggcctcgtgatacgcctatttttataggttaatgtcatgataataatggtttcttagacgtcaggtggcacttttcg
gggaaatgtgcgcggaacccctatttgtttatttttctaaatacattcaaatatgtatccgctcatgagacaataaccctgataaatgcttcaataatattg
aaaaaggaagagtatgagtattcaacatttccgtgtcgcccttattcccttttttgcggcattttgccttcctgtttttgctcacccagaaacgctggtgaa
agtaaaagatgctgaagatcagttgggtgcacgagtgggttacatcgaactggatctcaacagcggtaagatccttgagagttttcgccccgaagaacgttt
tccaatgatgagcacttttaaagttctgctatgtggcgcggtattatcccgtgttgacgccgggcaagagcaactcggtcgccgcatacactattctcagaa
tgacttggttgagtactcaccagtcacagaaaagcatcttacggatggcatgacagtaagagaattatgcagtgctgccataaccatgagtgataacactgc
ggccaacttacttctgacaacgatcggaggaccgaaggagctaaccgcttttttgcacaacatgggggatcatgtaactcgccttgatcgttgggaaccgga
gctgaatgaagccataccaaacgacgagcgtgacaccacgatgcctgcagcaatggcaacaacgttgcgcaaactattaactggcgaactacttactctagc
ttcccggcaacaattaatagactggatggaggcggataaagttgcaggaccacttctgcgctcggcccttccggctggctggtttattgctgataaatctgg
agccggtgagcgtgggtctcgcggtatcattgcagcactggggccagatggtaagccctcccgtatcgtagttatctacacgacggggagtcaggcaactat
ggatgaacgaaatagacagatcgctgagataggtgcctcactgattaagcattggtaactgtcagaccaagtttactcatatatactttagattgatttaaa
acttcatttttaatttaaaaggatctaggtgaagatccttttgataatctcatgaccaaaatcccttaacgtgagttttcgttccactgagcgtcagaccc
cgtagaaaagatcaaaggatcttcttgagatcctttttttctgcgcgtaatctgctgcttgcaaacaaaaaaaccaccgctaccagcggtggtttgtttgcc
ggatcaagagctaccaactctttttccgaaggtaactggcttcagcagagcgcagataccaaatactgtccttctagtgtagccgtagttaggccaccactt
caagaactctgtagcaccgcctacatacctcgctctgctaatcctgttaccagtggctgctgccagtggcgataagtcgtgtcttaccgggttggactcaag
acgatagttaccggataaggcgcagcggtcgggctgaacgggggttcgtgcacacagcccagcttggagcgaacgacctacaccgaactgagatacctaca
gcgtgagctatgagaaagcgccacgcttcccgaagggagaaaggcggacaggtatccggtaagcggcagggtcggaacaggagagcgcacgagggagcttcc
agggggaaacgcctggtatctttatagtcctgtcgggtttcgccacctctgacttgagcgtcgatttttgtgatgctcgtcaggggggcggagcctatggaa
aaacgccagcaacgcggcctttttacggttcctggccttttgctggccttttgctcacatgttctttcctgcgttatcccctgattctgtggataaccgtat
taccgcctttgagtgagctgataccgctcgccgcagccgaacgacgagcgcagcgagtcagtgagcgaggaagcggaagagcgcctgatgcggtattttctc
cttacgcatctgtgcggtatttcacaccgcatatatggtgcactctcagtacaatctgctctgatgccgcatagttaagccagtatacactccgctatcgct
acgtgactgggtcatggctgcgccccgacacccgccaacacccgctgacgcgccctgacgggcttgtctgctcccggcatccgcttacagacaagctgtgac
cgtctccgggagctgcatgtgtcagaggttttcaccgtcatcaccgaaacgcgaggcagctgcggtaaagctcatcagcgtggtcgtgaagcgattcacaga
tgtctgcctgttcatccgcgtccagctcgttgagtttctccagaagcgttaatgtctggcttctgataaagcgggccatgttaagggcggttttttcctgtt
tggtcactgatgcctccgtgtaagggggatttctgttcatgggggtaatgataccgatgaaacgagagaggatgctcacgatacgggttactgatgatgaac
atgcccggttactggaacgttgtgagggtaaacaactggcggtatggatgcggcgggaccagagaaaaatcactcagggtcaatgccagcgcttcgttaata
cagatgtaggtgttccacagggtagccagcagcatcctgcgatgcagatccggaacataatggtgcagggcgctgacttccgcgtttccagactttacgaaa
cacggaaaccgaagaccattcatgttgttgctcaggtcgcagacgttttgcagcagcagtcgcttcacgttcgctcgcgtatcggtgattcattctgctaac
cagtaaggcaaccccgccagcctagccgggtcctcaacgacaggagcacgatcatgcgcacccgtggccaggacccaacgctgcccgagatgcgccgcgtgc
ggctgctggagatggcggacgcgatggatatgttctgccaagggttggtttgcgcattcacagttctccgcaagaattgattggctccaattcttggagtgg
tgaatccgttagcgaggtgccgccggcttccattcaggtcgaggtggcccggctccatgcaccgcgacgcaacgcggggaggcagacaaggtatagggcggc
gcctacaatccatgccaacccgttccatgtgctcgccgaggcggcataaatcgccgtgacgatcagcggtccagtgatcgaagttaggctggtaagagccgc
gagcgatccttgaagctgtccctgatggtcgtcatctacctgcctggacagcatggcctgcaacgcgggcatcccgatgccgccggaagcgagaagaatcat
aatggggaaggccatccagcctcgcgtcgcgaacgccagcaagacgtagcccagcgcgtcggccgccatgccggcgataatggcctgcttctcgccgaaacg
tttggtggcgggaccagtgacgaaggcttgagcgagggcgtgcaagattccgaataccgcaagcgacaggccgatcatcgtcgcgctccagcgaaagcggtc
ctcgccgaaaatgacccagagcgctgccggcacctgtcctacgagttgcatgataaagaagacagtcataagtgcggcgacgatagtcatgccccgcgccca
ccggaaggagctgactgggttgaaggctctcaagggcatcggtcgacgctctcccttatgcgactcctgcattaggaagcagcccagtagtaggttgaggcc
gttgagcaccgccgccgcaaggaatggtgcatgcaaggagatggcgcccaacagtcccccggccacggggcctgccaccatacccacgccgaaacaagcgct
catgagcccgaagtggcgagcccgatcttccccatcggtgatgtcggcgatataggcgccagcaaccgcacctgtggcgccggtgatgccggccacgatgcg
tccggcgtagaggatcgagatctcgatcccgcgaaat

Figure A.1 Sequence of pET-IL1RN plasmid. pET-IL1RN is the designed sequence including the T7 promoter (grey) and the entire open reading frame (bright green ATG). The yellow and red hexanucleotides correspond to the Acc65I and XhoI sites, respectively.

Appendix II Mass spectroscopy of digested and purified IL-36β protein

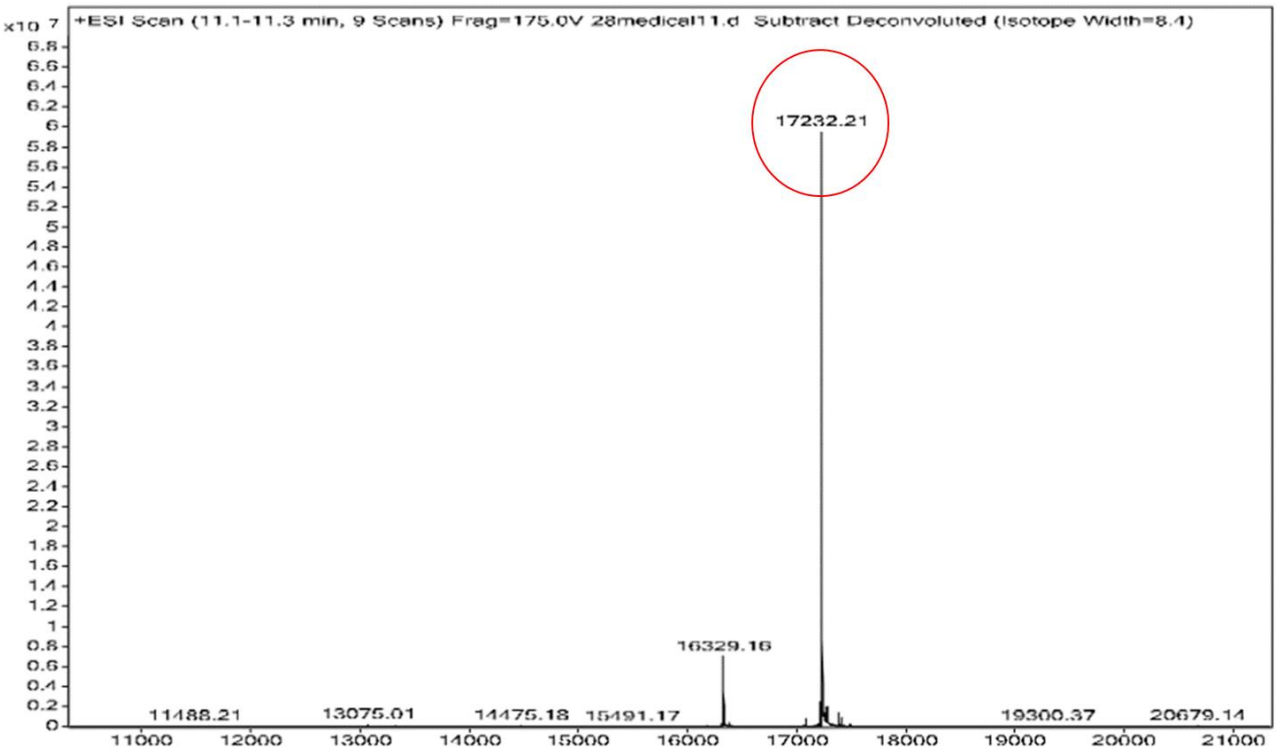

Figure A.2. Mass spectrometry of n^5-IL-36β protein that digested by chymotrypsin and purified by FPLC. Red circle indicates the expected molecular weight of n^5-IL-36β protein.

Appendix III- Mass spectrometry of digested and purified n^{18}-IL-36γ protein

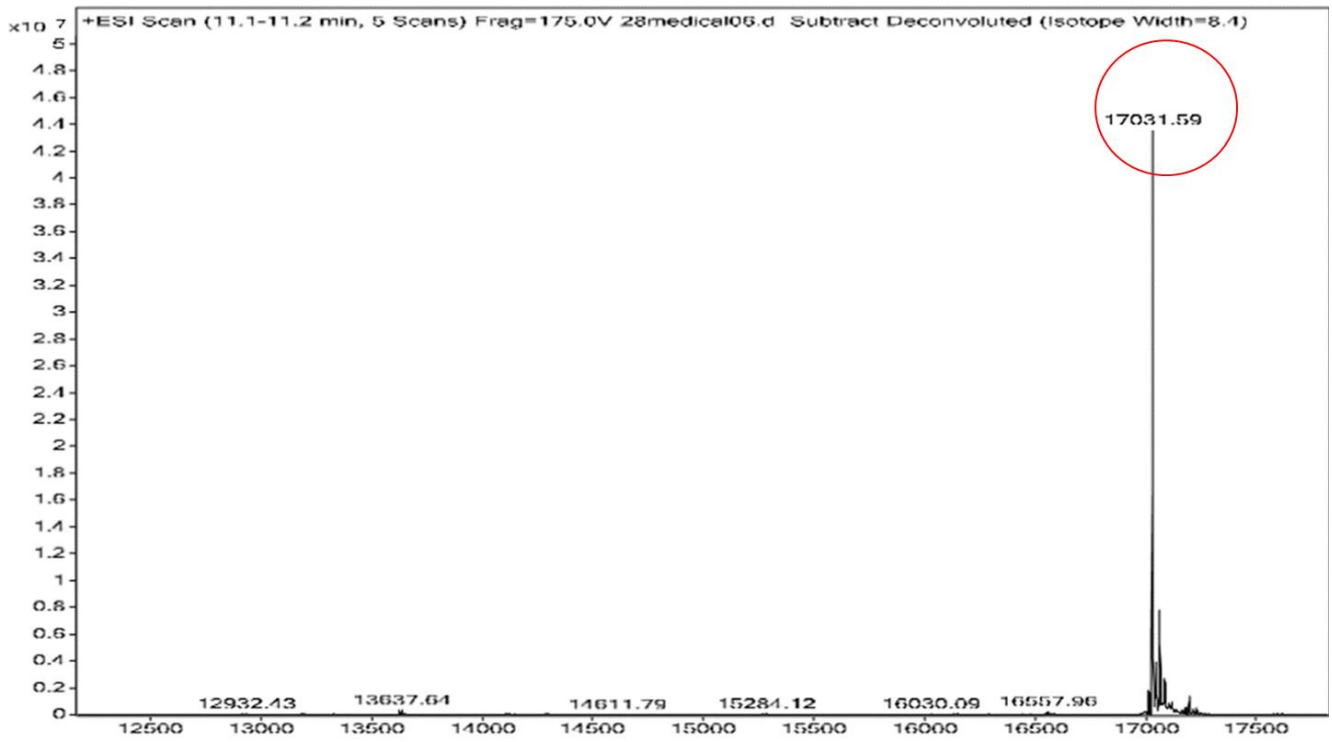

Figure A.3. Mass spectrometry of n^{18}-IL-36γ protein that digested by thrombin and purified by FPLC. Red circle indicates the expected molecular weight of n^{18}-IL-36γ protein.

Appendix IV Mass spectroscopy of digested n^1-IL-36α..

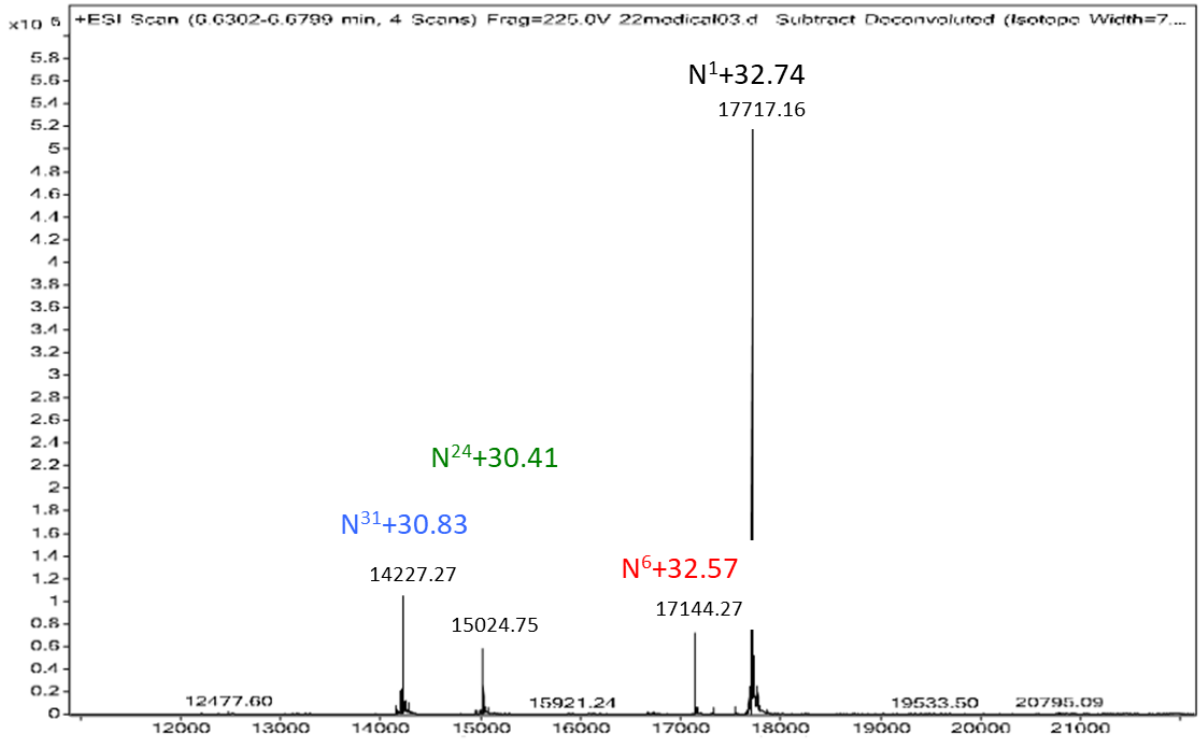

Figure A.4 Mass spectroscopy data of n^1-IL-36α that digested by chymotrypsin. n^1-IL-36α is shown to be cleaved at three different sites from N-terminus. Protein appears to be modified, most probably through the addition of two oxygen atoms.

Appendix V- Table A.2 Successful qPCR determination of IL36, IL36R and controls cDNAs in A-431

Treatment	N_0	IL36A	IL36B	IL36G	IL36R	B2M	HPRT	PPIA	ABL
Control	11 [33]	8 [20]	5 [12]	11 [32]	11 [33]	11 [33]	11 [33]	11 [32]	11 [32]
10 ng/ml TNF	3 [9]	3 [6]	3 [9]	3 [9]	3 [9]	3 [9]	3 [9]	3 [9]	3 [9]
20 ng/ml TNF	8 [24]	8 [24]	8 [20]	8 [24]	8 [24]	8 [24]	8 [24]	8 [24]	8 [24]
40 ng/ml TNF	3 [9]	3 [8]	3 [9]	3 [9]	3 [9]	3 [9]	3 [9]	3 [9]	3 [9]
Time control	3 [9]	ND	2 [3]	3 [9]	3 [9]	3 [9]	3 [9]	3 [9]	3 [9]
6 h TNF	3 [9]	ND	3 [9]	3 [9]	3 [9]	3 [9]	3 [9]	3 [9]	3 [9]
9 h TNF	3 [9]	ND	3 [9]	3 [9]	3 [9]	3 [9]	3 [9]	3 [9]	3 [9]
12 h TNF	3 [9]	ND	3 [9]	3 [9]	3 [9]	3 [9]	3 [9]	3 [9]	3 [9]
PMA	3 [9]	3 [9]	3 [9]	3 [9]	3 [8]	3 [9]	3 [9]	3 [9]	3 [9]
Flagellin	3 [9]	3 [9]	3 [9]	3 [9]	3 [9]	3 [9]	3 [8]	3 [9]	3 [9]
TNF+ Flagellin	3 [9]	3 [9]	3 [9]	3 [9]	3 [9]	3 [9]	3 [9]	3 [9]	3 [9]
TNF+ PMA	3 [9]	3 [9]	3 [9]	3 [9]	3 [9]	3 [9]	3 [9]	3 [9]	3 [9]

Each biological replicate (RNA sample derived from a well in tissue culture) was analysed three times for each cDNA target. N_0 is the total number of biological replicates that were analysed, N is the total number of biological replicated where the Cq estimate was successful [Σm] is the total number of successful Cq measurement.

Appendix VI- Table A.1 Successful qPCR determination of IL36, IL36R and controls cDNAs in HaCaT cells.

Treatment	N_0	IL36A	IL36B	IL36G	IL36R	B2M	HPRT	PPIA	ABL
Control	6	4 [5]	6 [18]	6 [18]	6 [18]	6 [18]	6 [18]	6 [18]	6 [18]
IL-1α	3	3 [9]	3 [9]	3 [9]	3 [9]	3 [9]	3 [9]	3 [9]	3 [9]
IL-36α	3	3 [9]	3 [9]	3 [9]	3 [9]	3 [9]	3 [9]	3 [9]	3 [9]
PMA	3	3 [5]	3 [9]	3 [9]	3 [9]	3 [9]	3 [9]	3 [9]	3 [9]
TNF	3	3 [9]	3 [9]	3 [9]	3 [9]	3 [9]	3 [9]	3 [9]	3 [9]
TNF+PMA	6	6 [18]	6 [18]	6 [18]	6 [18]	6 [18]	6 [18]	6 [18]	6 [18]

Each biological replicate (RNA samples derived from a well in tissue culture) was analysed three times for each cDNA target. N_0 is the total number of biological replicates that were analysed, N is the total number of biological replicated where the Cq estimate was successful [Σm] is the total number of successful Cq measurement.

Appendix VII- Gel electrophoresis of RT-qPCR products

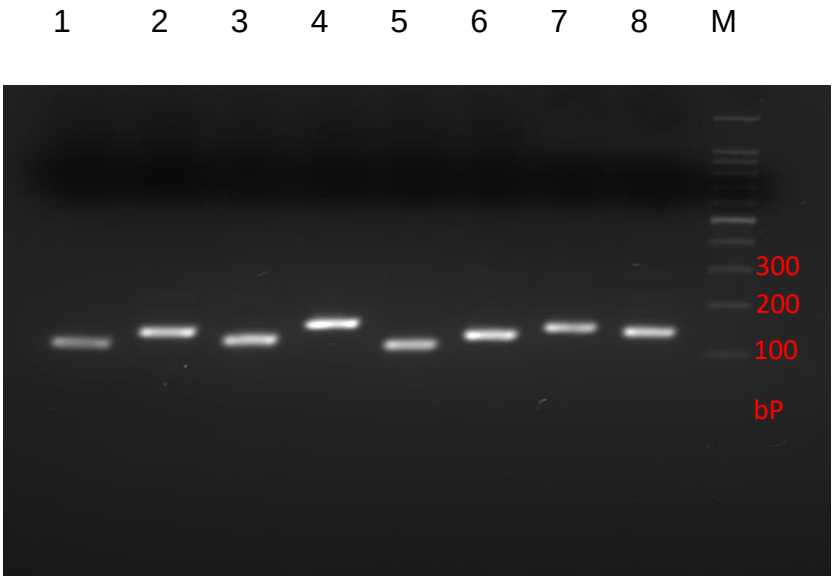

Figure A.5 Gel electrophoresis of RT-qPCR products of HaCAT cells: Lane 1: IL-36α (**128 bp**), Lane 2: IL-36β (**150 bp**), Lane 3: IL-36γ (**135 bp**), Lane 4: IL-36R (**162 bp**), Lane 5: β2 microglobulin (**120 bp**), Lane 6: Hypoxanthine phosphoribosyltransferase (**136 bp**), Lane 7: Peptidyl proline isomerase (PPIA) (**148 bp**), Lane 8: Abelson murine leukemia viral oncogene homolog (ABL1) (**140 bp**).

Appendix VIII- pSpCas9(BB)-2A-Puro (PX459) V2.0 plasmid structure (9175bps)

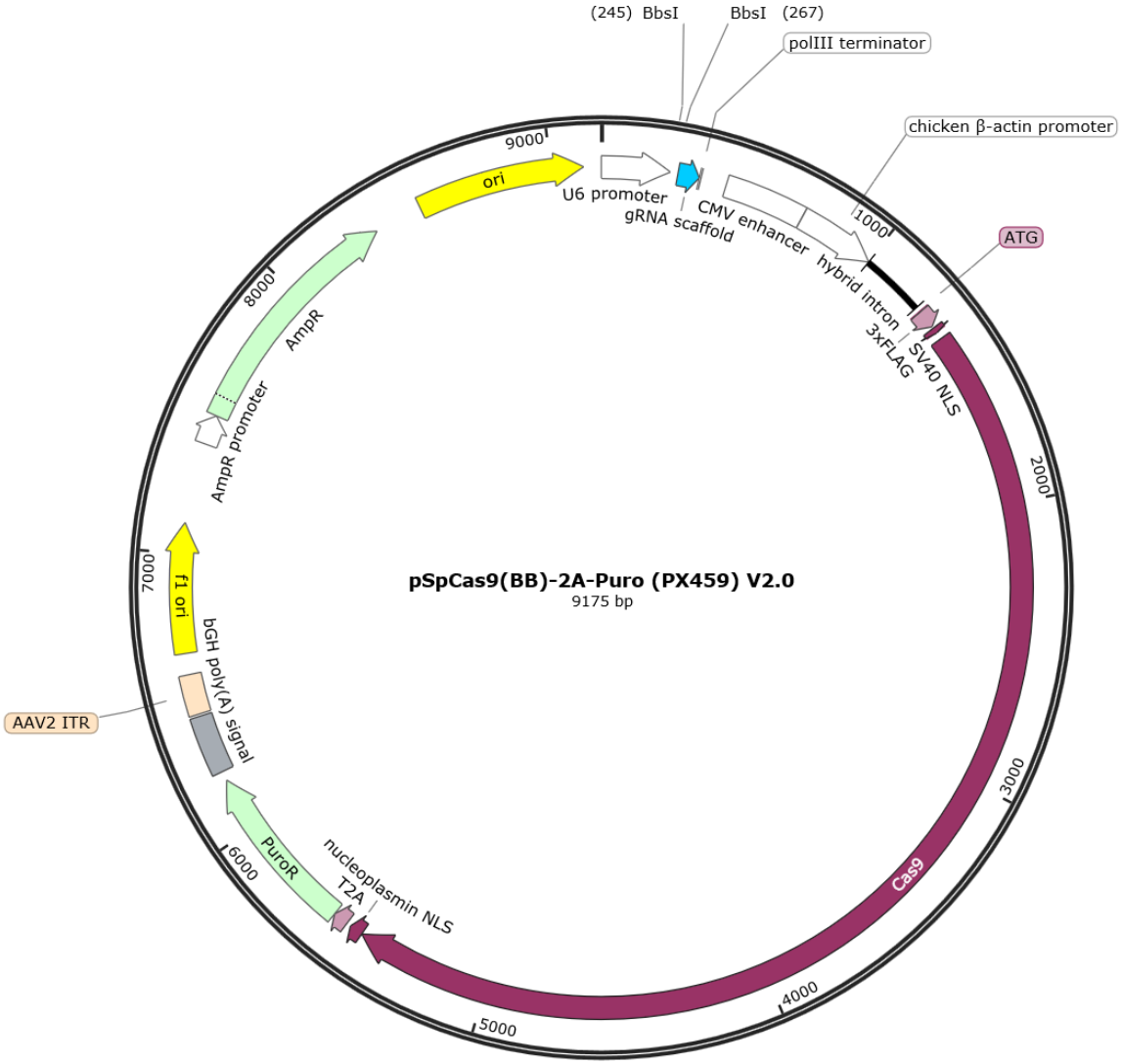

Figure A.6 The puromycin resistance plasmid pX459. Two oligonucleotides (**GGTGAGCAATGTCTCGGCAG**) or (**AGGGGAGCGGTTCACTGTTT**) were synthesised. Synthesised oligonucleotides were hybridised and ligated into the open (double) *Bbs* I site.